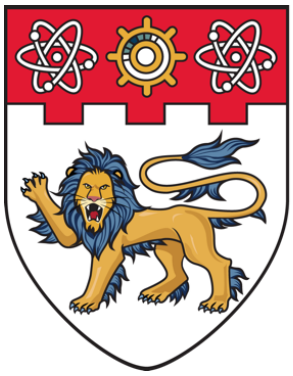

NANYANG TECHNOLOGICAL UNIVERSITY
SINGAPORE

SYNTHESES AND APPLICATIONS OF PHOSPHINE-*N*-HETEROCYCLIC CARBENE METAL COMPLEXES *VIA* CATALYTIC ASYMMETRIC HYDROPHOSPHINATION

SEAH WEE KIONG JEFFERY

SCHOOL OF PHYSICAL AND MATHEMATICAL SCIENCES

2021

SYNTHESES AND APPLICATIONS OF PHOSPHINE-*N*-HETEROCYCLIC CARBENE METAL COMPLEXES *VIA* CATALYTIC ASYMMETRIC HYDROPHOSPHINATION

SEAH WEE KIONG JEFFERY

SCHOOL OF PHYSICAL AND MATHEMATICAL SCIENCES

A thesis submitted to the Nanyang Technological University in partial fulfilment of the requirement for the degree of Doctor of Philosophy

2021

Statement of Originality

I hereby certify that the work embodied in this thesis is the result of original research done by me except where otherwise stated in this thesis. The thesis work has not been submitted for a degree or professional qualification to any other university or institution. I declare that this thesis is written by myself and is free of plagiarism and of sufficient grammatical clarity to be examined. I confirm that the investigations were conducted in accord with the ethics policies and integrity standards of Nanyang Technological University and that the research data are presented honestly and without prejudice.

.....05-08-2021.....
Date

.....
Seah Wee Kiong Jeffery

Supervisor Declaration Statement

I have reviewed the content and presentation style of this thesis and declare it of sufficient grammatical clarity to be examined. To the best of my knowledge, the thesis is free of plagiarism and the research and writing are those of the candidate's except as acknowledged in the Author Attribution Statement. I confirm that the investigations were conducted in accord with the ethics policies and integrity standards of Nanyang Technological University and that the research data are presented honestly and without prejudice.

5-8-2021
Date

Sumod A. Pullarkat

5/8/2021
Date

Leung Pak-Hing

Authorship Attribution Statement

This thesis contains material from two papers, published and submitted, in the following peer-reviewed journals where I was the first author.

Chapters 2 and 3 are published as Seah, J. W. K.; Li, Y.; Pullarkat, S. A.; Leung, P.-H., Access to a Chiral Phosphine–NHC Palladium(II) Complex *via* the Asymmetric Hydrophosphination of Achiral Vinyl Azoles. *Organometallics* **2021,** *40* (13), 2118-2122. DOI: 10.1021/acs.organomet.1c00262.

The contributions of the co-authors are as follows:

- Dr Li, Y. collected and resolved the X-ray crystallographic data,
- Dr. Pullarkat, S. A. revised the manuscript draft and assisted in idea generation,
- Prof. Leung, P.-H. revised the manuscript draft and assisted in idea generation,
- I designed the study, performed the experiments, collected the Nuclear Magnetic Resonance (^{1}H, ^{13}C and $^{31}P\{^{1}H\}$), High Resolution Mass Spectroscopy, High Performance Liquid Chromatography, optical rotation data, and
- I prepared the manuscript draft and Supporting Information.

Chapters 3 and 4 have been submitted as Seah, J. W. K.; Lee, J. X. T.; Li, Y.; Pullarkat, S. A,; Tan, N. S.; and Leung, P.-H., Novel Chelating Phosphine-NHC Platinum Complexes *via* Catalytic Asymmetric Hydrophosphination and their Cytotoxicity Towards MKN74 and MCF7 Cancer Cell Lines.

The contributions of the co-authors are as follows:

- Dr Li, Y. collected and resolved the X-ray crystallographic data,
- Dr. Pullarkat, S. A. revised the manuscript draft and assisted in idea generation,
- Prof. Tan, N. S. revised the manuscript draft and assisted in idea generation,
- Prof. Leung, P.-H. revised the manuscript draft and assisted in idea generation,
- I designed the chemical syntheses and collected the Nuclear Magnetic Resonance (^{1}H, ^{13}C and $^{31}P\{^{1}H\}$), High Resolution Mass Spectroscopy, High Performance Liquid Chromatography, optical rotation data,
- Lee, J. X. T conducted the biological testing on the cancer cell lines, and
- I prepared the manuscript draft and Supporting Information.

. . . . .05-08-2021. . . . .
Date

. . . . . .
Seah Wee Kiong Jeffery

Abstract

Chiral hybrid phosphine- *N*-heterocyclic carbenes form a unique class of bidentate ligands which finds extensive uses as privileged ligands in homogeneous transition metal catalysis. The current methodologies associated with their syntheses suffer from significant drawbacks and the diversity of the structural backbones of these ligands has hence been limited. Catalytic asymmetric hydrophosphination was contrived as a solution to address the abovementioned problem as it is arguably one of the most efficient methods of generating chiral phosphines with high enantiopurities and simultaneously, offering additional advantages such as a 100% atom economy, mild reaction conditions and a diverse substrate scope. Catalytic asymmetric hydrophosphination was employed in the syntheses of novel chiral phosphine- *N*- heterocyclic carbene precursors and these precursors were subsequently transformed into chiral novel phosphine- *N*- heterocyclic carbene metal complexes. The structures of the complexes were elucidated *via* X-ray crystallography and their catalytic and biological applications were explored.

Acknowledgements

I would like to express my sincere gratitude to my supervisor, Prof. Leung Pak-Hing, whose passion for Chemistry has motivated me in numerous ways during the course of my project; for his encouragement that made challenging situations seem simpler; for the freedom he has given me to pursue my own directions; and for his trust and support he has placed in me. My gratitude also extends to my co-supervisor, Dr. Sumod A. Pullarkat, for his unwavering support and guidance provided to me way before I began my postgraduate journey. I would also like to thank Prof. Andrew Tan and Prof. Leong Weng Kee for being my academic mentors over the years and providing valuable insights which proved to be greatly helpful in my research. In addition, I would like to thank Jeannie from the Lee Kong Chian School of Medicine for her contributions towards the biological applications of the novel platinum complexes on cancer cells.

Special appreciation goes to my lab mates and friends Ronald, Shafiq, Ce Qing, Jeremy, Jia Sheng, Po Kai, Sadeer, Wee Shan and Wen Qian for being my lunch buddies and rendering help unconditionally whenever I needed. I would also like to thank my parents for their constant encouragement, confidence and trust placed in me for the past 29 years.

Lastly, I would also like to acknowledge the kind assistance provided by Dr. Li Yongxin, Ms. Goh Eeling and Ms. Seow Ai Hua in terms of X-ray crystallography, NMR, teaching lab facilities respectively and thank the Division of Chemistry and Biological Chemistry, School of Physical and Mathematical Sciences and Nanyang Technological University, for supporting my research as well as the award of the prestigious Nanyang President's Graduate Scholarship.

Table of Contents

Nomenclature

The nomenclature used throughout the thesis conforms to the format adopted by Chemical Abstracts (Chemical Abstracts, 13th Collective Index, Index Guide, 1992-1996).

Abbreviations and Symbols

Ar	aryl group
BINAP	2,2′-*bis*(diphenylphosphino)-1,1′-binaphthyl
Bn	benzyl
Bp	boiling point
br	broad
calcd.	calculated
$CDCl_3$	chloroform-d1
$CHCl_3$	chloroform
conc.	concentrated
d	doublet (NMR)
DCM	dichloromethane
dec.	decomposed
de	diastereomeric excess
DIOP	2,3-*O*-isopropylidene-2,3-dihydroxy-1,4-*bis*(diphenylphosphino)butane
DIPAMP	1,2-*bis*((2-methoxyphenyl)phenylphosphino)ethane
dm	decimetre(s)
DMF	*N*,*N*-dimethylformamide
ee	enantiomeric excess
equiv.	equivalence

ESI-MS	electrospray ionization mass spectrometry
Et	ethyl
g	gram(s)
h	hour(s)
^{i}Pr	isopropyl
Hz	hertz
m	multiplet (NMR)
Me	methyl
min	minute(s)
mL	millilitre(s)
mmol	millimole(s)
Mp	melting point
NMR	Nuclear Magnetic Resonance
Ph	phenyl
ppm	parts per million
Pr	propyl
R	rectus (Latin right absolute configuration)
rt	room temperature
S	sinister (Latin left absolute configuration)
s	singlet (NMR)
t	triplet (NMR)
t	time
T	temperature
^{t}Bu	*tert*-butyl
THF	tetrahydrofuran

TMS	tetramethylsilane
TOF	turn over frequency
TON	turn over number
δ	NMR chemical shift in ppm
°	degree (angles)
Å	angstrom(s)
°C	degree Celsius
$[\alpha]_D$	specific rotation measured at sodium D line (589 nm)

Summary

In Chapter 1, an overview of chiral phosphines and chiral NHC precursors is given. Recent developments pertaining to the syntheses of chiral phosphines and chiral NHC precursors, along with their limitations, will be discussed. In addition, the research gap will be introduced and the aims of this thesis will be stated.

In Chapter 2, the viability of catalytic asymmetric hydrophosphination in the syntheses of structurally varied chiral NHC precursors, specifically phosphine-functionalized ones, from carefully designed achiral substrates will be studied and discussed. The scope of this chapter will primarily be focused on the importance of combinational phosphine-NHC ligands and the formulation and optimization of a new methodology to access such chiral hybrid precursors.

In Chapter 3, the transformation of chiral phosphine-NHC precursors to the respective phosphine-NHC complexes will be discussed. In addition to the discussions made on the post-functionalization of selected phosphine-NHC metal complexes and the challenges encountered in the complexation process, the solution- and solid-state structures of the phosphine-NHC metal complexes will also be discussed. Lastly, attempts at applying these metal complexes as homogeneous catalysts will be mentioned.

In Chapter 4, the syntheses of a series of selected functionalized phosphine-NHC platinum complexes bearing different aryl functionalities and their uses as potential anti-cancer drugs in two cancer cell lines, MKN74 and MCF7 will be discussed briefly.

In Chapter 5, the conclusions of this thesis will be given and the possibility of future work will be mentioned briefly.

Chapter 1

Introduction

1.1 Chirality

Chirality, derived from the word *handedness* in ancient Greek, is an intrinsic geometric property of a chemical species and an individual species which exhibits chirality is said to have at least one mirror image which is non-superimposable on itself. Together, the object and mirror images form what is known as a pair of enantiomers that differ only in their spatial orientation. Chirality plays an important role in nature, particularly in the field of biochemistry. Classes of biological molecules such as carbohydrates,[1] amino acids,[2] steroids, hormones,[3] nuclei acids,[4] enzymes[5] and pheromones[6] are predominantly homochiral and exist only in one enantiomeric form. Besides microscopic discrete biomolecules, macrostructures such as receptors and membranes also possess chirality so as to effect specific interactions such as binding and recognition of other chiral agents.[7] Notoriously, the lack of attention paid to the idea of chirality in living systems has led to one of the most infamous chiral drugs-related incidents in history- the thalidomide incident. In that incident, a racemic mixture of thalidomide initially prescribed and administered as a drug for morning sickness due to pregnancy subsequently induced birth defects in new-borns due to the presence of the malignant enantiomer of thalidomide.[8] As the relevance of chirality gains recognition over the years, issues pertaining to the syntheses, properties, characterizations, and applications of chiral compounds have also become a prominent topic, especially in chemical, biological and pharmaceutical industries.

Broadly speaking, chirality can be classified into four distinct classes. Central chirality, also known as point chirality, is a type of chirality that occurs in molecules which bear a set of

ligands whose mirror image is not superimposable on itself around a centrally located atom. Planar chirality refers to the out-of-plane arrangement of groups with respect to a mirror plane and axial chirality refers to a combination of four atoms which are spatially different with respect to a central axis of rotation. Lastly, helical chirality refers to the unidirectional orientation of groups in a spiral fashion, akin to that of a screw.

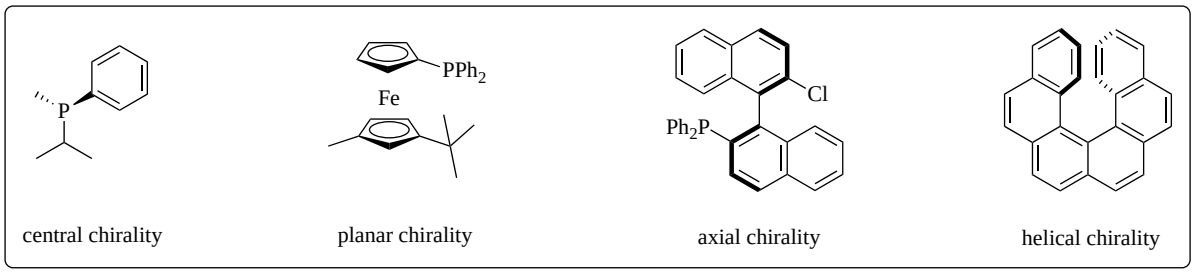

Figure 1.1 Chiral phosphines displaying various forms of chirality.

1.2 Chiral Phosphines

As enantiopure chemicals continue to find increasingly important applications in applied fields such as fragrances, flavours, drugs, cosmetics, pesticides and materials around the world, the market of demand for enantiopure chemicals continues to expand. This has in turn provided the motivation for synthetic chemists to develop new methodologies to gain access to these coveted chiral chemicals. Generally, enantiopure chemicals can be obtained using four different approaches- resolution of racemates, syntheses from materials from the chiral pool, biocatalytic (enzymes and antibodies) syntheses and asymmetric catalysis using artificial reagents.

Out of all chiral chemicals, chiral phosphines have unequivocally established a pivotal role in various fields such as transition metal catalysis,[9] agrochemicals, fine chemicals and organocatalysis.[10] In this aspect, optically active phosphine ligands may also bear more than

one type of chirality and the incorporated chiral moieties in turn help to transmit chiral information throughout the molecular structure so as to produce desirable stereochemical changes in chemical reactions. Since the 1970s, numerous chiral phosphine ligands with varying denticities and modes of chirality have been synthesized.[11] Amongst the phosphines, notable examples which have found applications in metal-catalysed reactions with remarkable successes include DIOP with *C*-stereogenic centres, DIPAMP with *P*-stereogenic centres, BIPHEP with axial chirality, PHANEPHOS with planar chirality and Josiphos with a combination of different chiralities.[12]

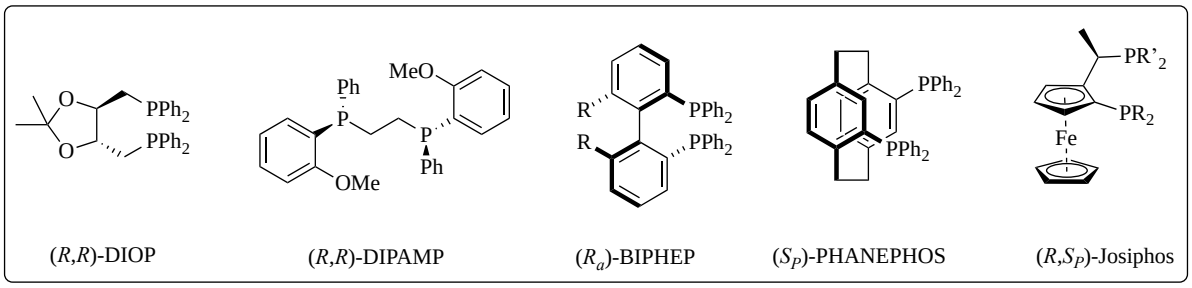

Figure 1.2 Diphosphines exhibiting different modes of chirality.

Particularly in the field of transition metal catalysis, chiral phosphines play an unsurmountable role as privileged ligands in asymmetric catalysis as asymmetric catalysis promises unprecedented improvements over other traditional methods of syntheses in terms of its versatility, efficiency, and environmental friendliness. Chiral phosphines have also shown to be an indispensable tool in a myriad of reactions including hydrogenation,[13] hydrosilylation,[14] allylic alkylation,[15] heterofunctionalization,[16] cross coupling,[17] cycloisomerization,[18] cycloaddition[19] and many others. Due to the large amount of literature on the preparation of chiral phosphines, only selected examples will be given and discussed to illustrate the concepts behind the synthetic techniques. Lastly, the term *phosphines* will be used to refer to only compounds containing a phosphorus atom covalently bonded to carbon and

hydrogen and other phosphorus-heteroatom (P-O, P-N, P-S etc.) species will be excluded in the discussion.

1.2.1 Resolution and Syntheses of Chiral Phosphines

In contrast to amines which undergo rapid pyramidal inversion at room temperature, phosphines containing three dissimilar substituents are generally chiral at room temperature and their enantiomers can be separated. The cause for the chirality in phosphines is the higher inversion barrier due to the mixing of the highest occupied molecular orbital (HOMO) and the lowest unoccupied molecular orbital (LUMO) mediated by a coupled vibrational mode in a second-order *Jahn-Teller* distortion.[20] (Figure 1.3)

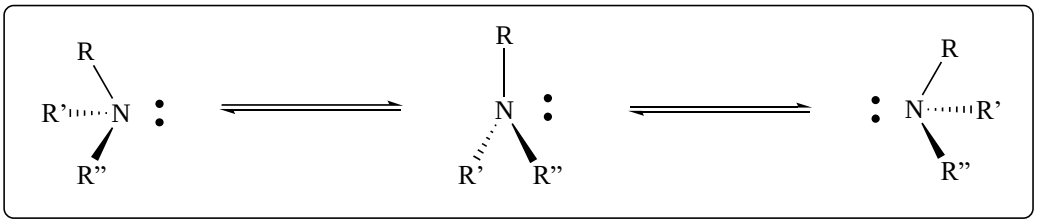

Figure 1.3 Pyramidal (and chirality) inversion of amines *via* a trigonal planar transition state.

The inversion barrier of phosphines depends on the steric bulk and electronic properties of the substituents but in general, the risk of inversion limits the handling of phosphines at elevated temperatures. In addition, electron-rich phosphines are air-sensitive and hence react quickly with oxygen and other oxidizing agents, making their handling even more cumbersome. As a result, phosphines are usually treated as their derivatives in the form of phosphine oxides,[21] sulfide,[22] boranes and metal phosphine complexes due to the relative ease of usage and storage of these configurationally stable derivatives.[16b, 23] While numerous protocols pertaining to the deprotection of phosphine derivatives have been developed, the methods frequently suffer from disadvantages such as incompatibility with reactive functional groups,

harsh reagents and conditions, a poor atom economy, diminished yields, loss of chirality through racemization and low chemoselectivities.[24]

The first example of synthesis and resolution of enantiopure BINAP by Noyori involved the coordination of a racemic mixture of BINAP **1c** to a chiral auxiliary **2** to afford diastereomers **1d**.[25] Due to the difference in solubilities of the two diastereomers, individual diastereomers could be obtained through a laborious process of recrystallization. Once the phosphine-metal derivatives **1d** were separated, the phosphine was liberated from the template *via* reduction with lithium aluminium hydride. From the viewpoint of environmental friendliness, this synthetic protocol unavoidably violated many of the principles advocated by green chemists.[26] (Scheme 1.1)

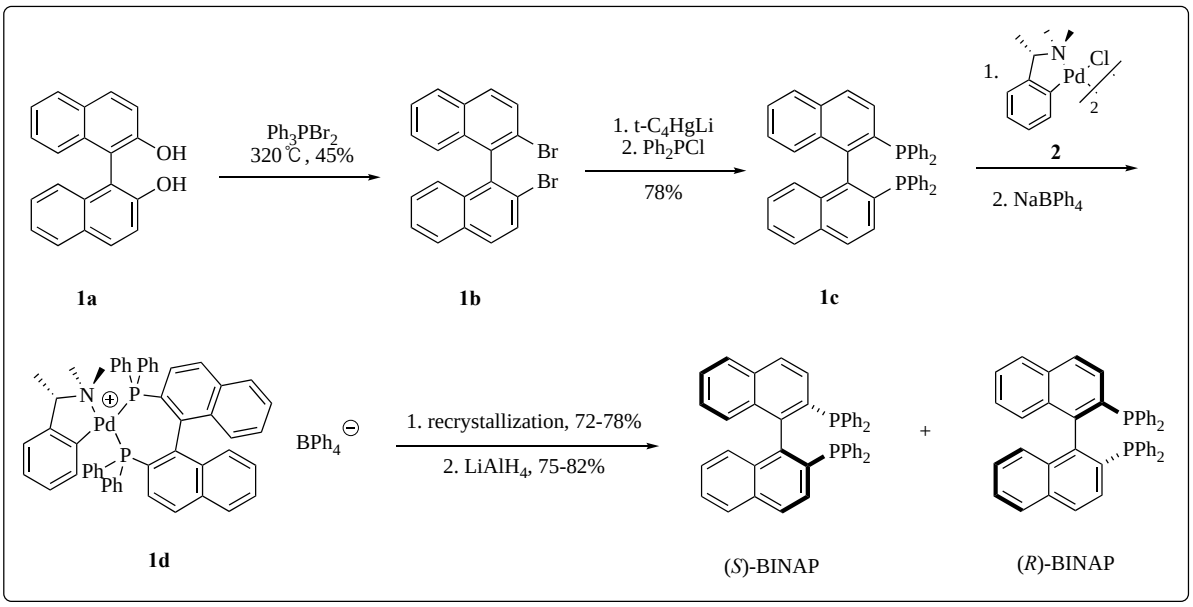

Scheme 1.1 Synthesis and resolution of enantiopure BINAP reported by Noyori.

Besides exploiting the nucleophilic nature of the phosphorus atom in the utility of *Lewis* acidic chiral metal complexes as resolving agents, the weakly basic behaviour of phosphines

also allows the use of chiral acids and chiral counterions as resolving agents. Some of the widely utilized resolving agents are given in Figure 1.4.

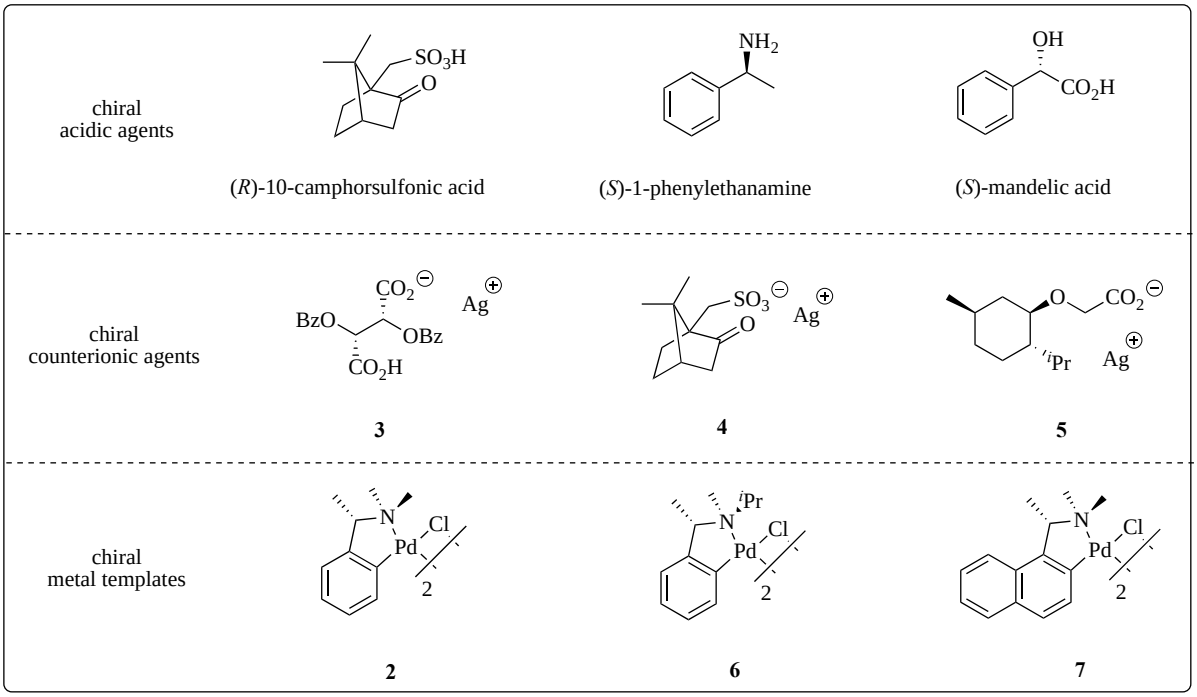

Figure 1.4 Classes of resolving agents.

Phosphine oxide **8** was directly resolved into its enantiomers through the use of (+)-bromocamphorsulfonic acid and subsequent recrystallization from ethyl acetate.[27] Similarly, phosphine oxide **9** could be obtained using camphorsulfonic acid.[28] The use of sulfonic acid greatly relies on the protonation of the weakly basic phosphoryl oxygen and thus, this reagent has impeded the resolution of other simple *P*-chiral phosphine oxides.[29] Phosphine oxides **12** and **13** were resolved using binapthol through the formation of intermolecular hydrogen bonds[30] while free thiophosphine **15** and quinolinephosphine **16** were resolved using metal template **7** by virtue of their bidentate chelating propensity.[31] In addition to the above methods, other prominent means of obtaining enantiopure phosphines include resolution *via* covalent diastereomers, self-resolving systems and kinetic resolution. For instance, phosphine oxide **17**

could be obtained using camphanyl chloride as the esterification reagent.[32] followed by diastereomeric separation and hydrolysis.

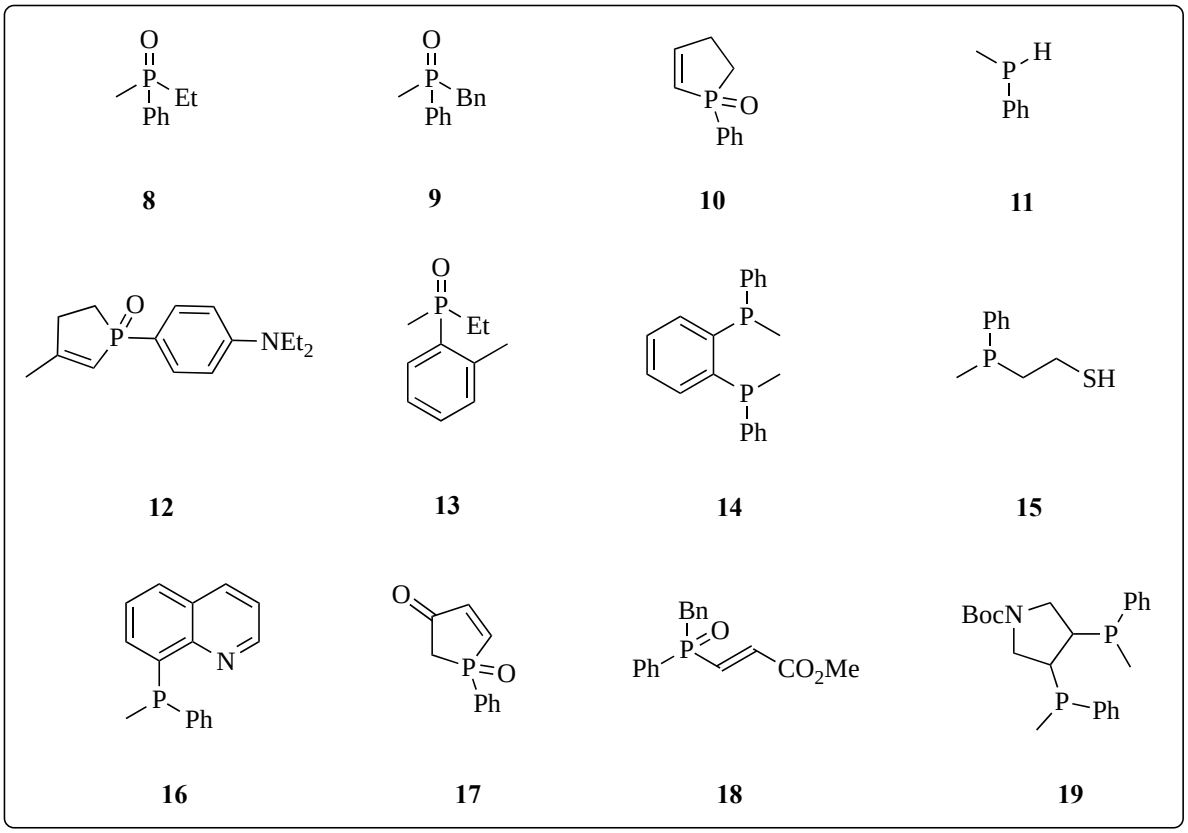

Figure 1.5 Examples of chiral phosphines obtained through resolution.

Despite the successes of the abovementioned methods of exploiting diastereomers for the purpose of resolution, modern technology has promoted other novel methods such as enantioselective chromatography and biocatalytic syntheses as alternative efficient routes to access chiral phosphines. One notable example is the synthesis of phosphine **22** from a racemic mixture of ferrocenyl ethanol **20** using chiral lipase from living organisms.[33]

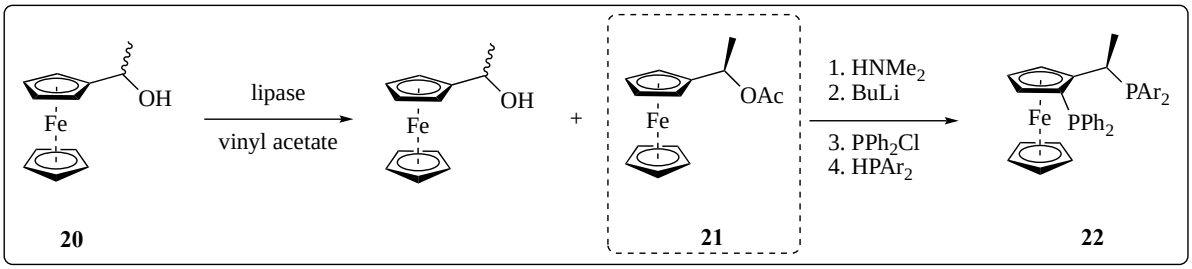

Scheme 1.2 Enzymatic synthesis of chiral diphosphine **22**.

Several enzymatic systems using pig liver esterase and cholesterol esterase have also been employed to furnish ligands **23** and **24** although a variety of drawbacks such as a) moderate to high enantioselectivities, b) typical resolution of only one of the two enantiomers, c) enzymatic action being a highly dependent function on the molecular structure of the substrate since docking of the substrate in the active site of the enzyme is required, d) generally narrow substrate scope and e) additional issues associated with the recovery of enzyme and maintenance of a constant pH working condition for proper reaction are commonly encountered.[34]

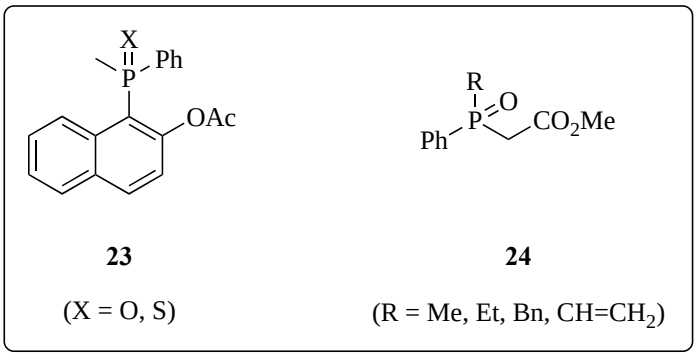

Figure 1.6 Phosphine oxides and sulfide obtained from enzymatic systems.

1.2.2 Chiral Auxiliary-Mediated Syntheses of Chiral Phosphines

The quest for increased flexibility and applicability of generating chiral phosphines from resolved phosphines, obtained previously from the methods described in section 1.2.1,

eventually led to the development of other facile methods to access chiral phosphines. Several chiral auxiliaries derived from optically active secondary alcohols (e.g. (-)-menthol, *endo*-borneol),[35] amines (e.g. (*S*)-1-phenylethanamine),[36] amino acid derivatives (e.g. SAMP, RAMP),[37] and ephedrine[38] have been utilized. Due to the great number of examples available in the literature, only some representative protocols illustrating the use of chiral auxiliaries in the syntheses of phosphines bearing 1) *P*-stereogenic, 2) *C*-stereogenic, 3) axial and 4) planar chiralities will be given.

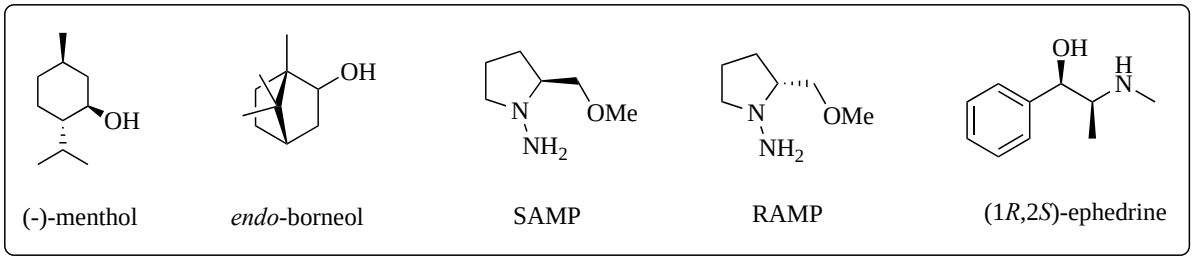

Figure 1.7 Naturally occurring chiral auxiliaries.

Pioneering works by Cram and Mislow showed that unsymmetrically substituted menthylphosphinates **25**, derived from incorporation of the (-)-menthol leaving group into phosphinates, could be separated cleanly into their diastereomeric forms *via* crystallization from hexane.[39] Besides monophosphine monoxides, tertiary diphosphine oxides could also be prepared using the resolved phosphinates and organometallic reagents with inversion of configuration at phosphorus. The phosphine oxides could then be reduced to furnish the desired chiral diphosphines. The DIPAMP diphosphine ligand was prepared according to scheme 1.3.

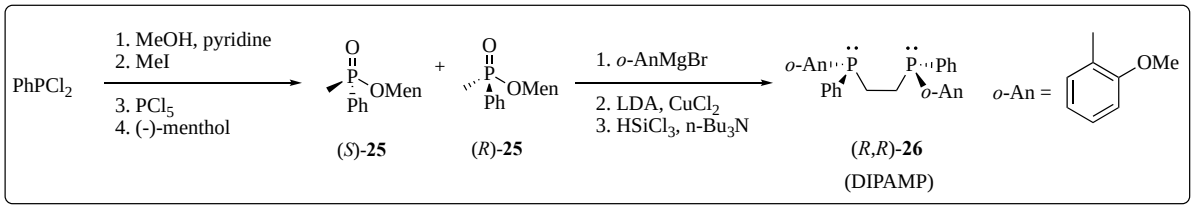

Scheme 1.3 Synthesis of DIPAMP.

Despite the high level of flexibility and stereoselectivity associated with the above protocol, an excess of the organometallic reagent under stringent conditions is usually needed and the reaction has been shown to be sensitive to variation of substituents at the phosphorus, oxygen and magnesium centres.[35c] Frequently, only one diastereomer is obtained pure and unsuccessful attempts have also been reported.[40]

In a similar vein, *C*-stereogenic phosphines can also be synthesized using materials directly from the chiral pool, if the latter are available. Alternatively, resolution using the abovementioned methods is another viable route. In 1971, Kagan reported the synthesis of an enantiopure bidentate *P*-chiral diphosphine from naturally occurring (*R*,*R*)-tartaric acid.[11, 41] Tartaric acid was esterified before being reduced and attached a leaving tosylate group, which was subsequently displaced by the nucleophilic diphenylphosphide anion in the last step to furnish the DIOP ligand.

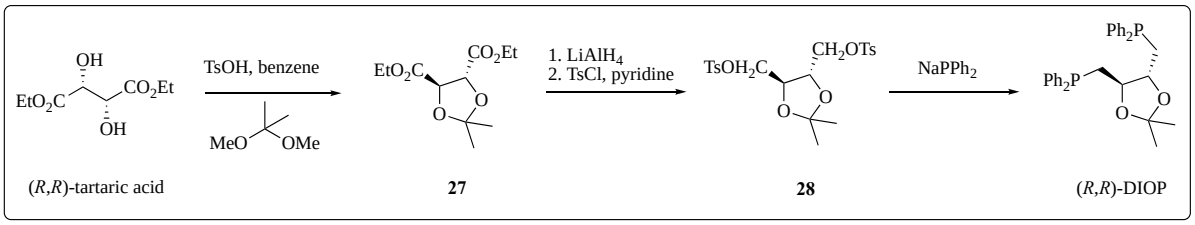

Scheme 1.4 Synthesis of (*R*,*R*)-DIOP from naturally occurring (*R*,*R*)-tartaric acid.

Using starting materials form the chiral pool is common in the syntheses of other chiral phosphines bearing axial and planar chiralities. Besides the resolution-based synthesis of BINAP derivatives, Lipshutz utilized (*S*,*S*)-2,4-pentanediol as the enantiopure starting reagent in a series of transformation to afford the axially chiral diphosphine **32**.[42]

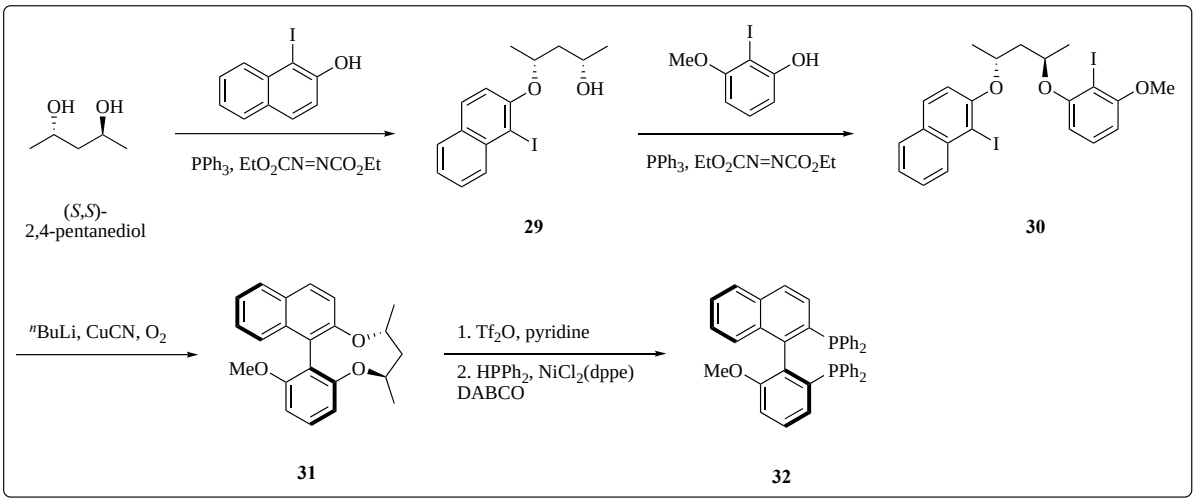

Scheme 1.5 Synthesis of chiral BINAP derivative from (*S*,*S*)-2,4-pentanediol.

Another general synthetic method reported by Kagan made use of (*S*)-butane-1,2,4-triol **34** as a chiral *ortho*-directing group that guided the installation of lithium and the subsequent phosphine moiety from chlorodiphenylphosphine. The directing group was then hydrolysed to return the aldehyde group in the final planarly chiral ferrocene phosphine **36**.[43]

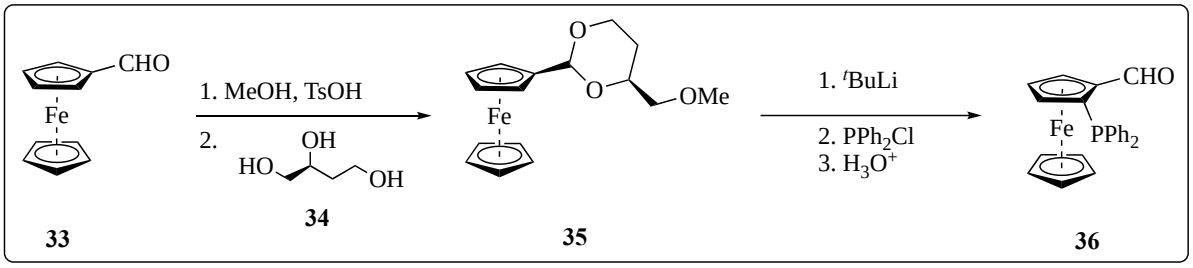

Scheme 1.6 Utility of chiral *ortho*-directing (*S*)-triol **34** in the synthesis of ferrocenyl phosphine **36**.

Other than organic chiral auxiliaries, chiral metal templates can also serve as effective auxiliaries in the generation of chiral phosphines. In the last decade, our group has reported numerous chiral metal template-promoted asymmetric hydrophosphination with great successes.[44] A few examples are illustrated below.

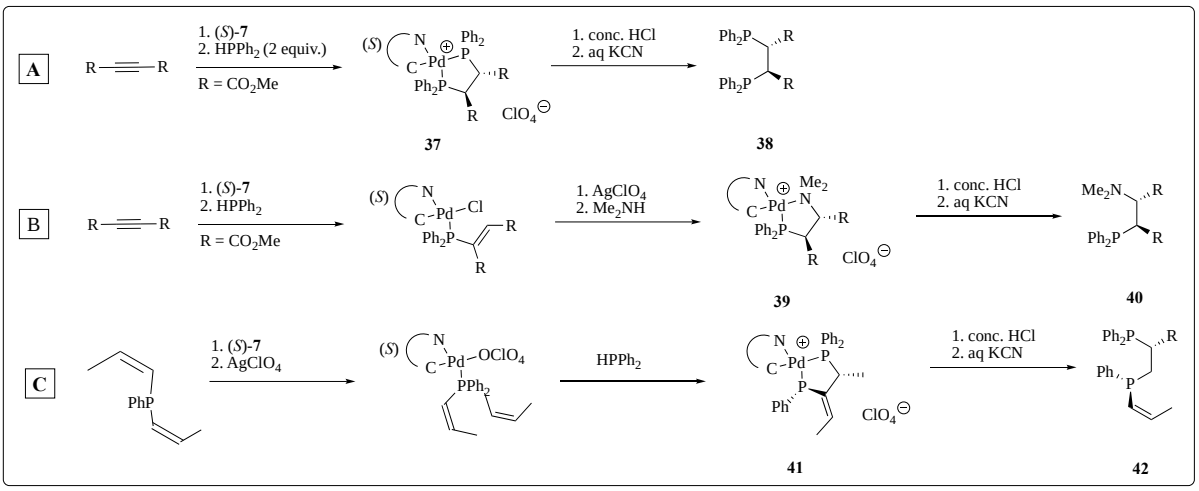

Scheme 1.7 Selected electrophiles employed in chiral metal-mediated asymmetric hydrophosphination by **7**.

Hydrophosphination of an unsaturated moiety bound to a chiral metal template allows the synthesis of enantioenriched diphosphines and P,N-products. The phosphine products could be liberated from the metal template through treatments with concentrated hydrochloric acid followed by aqueous potassium cyanide. It is interesting to note that in example B, the P,N-product was formed from a sequential asymmetric hydrophosphination and asymmetric hydroamination. Other chiral phosphines have also been prepared using similar methodologies; while most were prepared *via* monohydrophosphination, some were prepared *via* dihydrophosphination. (Scheme 1.7)

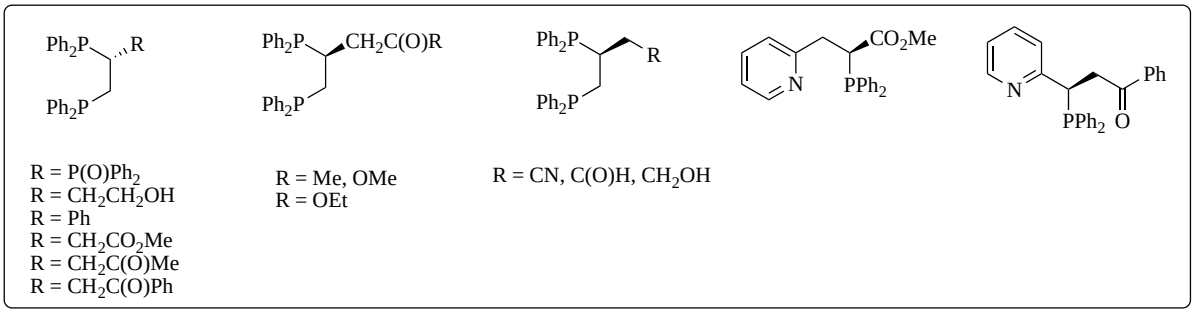

Figure 1.8 Chiral diphosphines and P,N-chelates obtained through chiral metal template asymmetric hydrophosphination.

Chiral auxiliary-mediated syntheses, both organic and metal-based, of chiral phosphines, while being able to afford variably substituted phosphines with high selectivities, exhibit some significant drawbacks: 1) a stoichiometric amount of chiral auxiliary is needed and sometimes, only one enantiomer of the auxiliary is available, 2) chiral auxiliaries are costly, 3) removal of the auxiliaries is tedious and energy-consuming, 4) chiral auxiliaries can be highly substrate dependent and 5) undesirable by-products are produced from the reagents used to introduce and eliminate the auxiliaries.[45] In an attempt to address these unfavourable disadvantages associated with chiral auxiliary-mediated syntheses, catalytic asymmetric syntheses emerged as a new solution.

1.2.3 Catalytic Asymmetric Syntheses of Chiral Phosphines

Obtaining chiral phosphines through the post-functionalization of chiral alcohols or chiral alkanes obtained from asymmetric hydrogenation and aryl triflates and aryl halides through phosphine displacement represents a major method of accessing chiral phosphines and many catalysts have since been developed in the fields of asymmetric hydrogenation and asymmetric C-C coupling reactions.[17, 46]

Fryzuk reported the first self-breeding catalytic system involving acrylates.[47] A rhodium-catalyzed asymmetric hydrogenation of the acrylate yielded chiral compound **43** in 81% *ee*. The ester groups were then reduced by lithium aluminum hydride to afford a diol with a small drop in *ee* of 1%. The diol was then transposed with tosylate and substituted by lithium diphenylphosphide to furnish the final bidentate chiral diphosphines **45**.

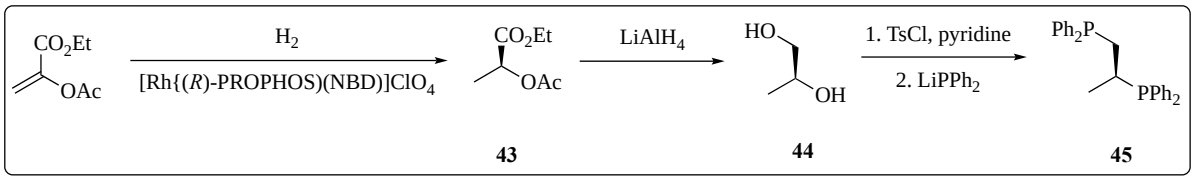

Scheme 1.8 Synthesis of chiral diphosphine **45** *via* asymmetric hydrogenation.

In another example, the coupling of Grignard reagents with aryl triflates in the presence of a palladium catalyst **49** produced **47** with high enantioselectivity. Compound **47** was then coupled to diphenylphosphine oxide by the use of palladium(II) acetate with dppp as the supporting ligand, followed by reduction of the oxide using trichlorosilane, to give the final axially chiral phosphine **48**.[48]

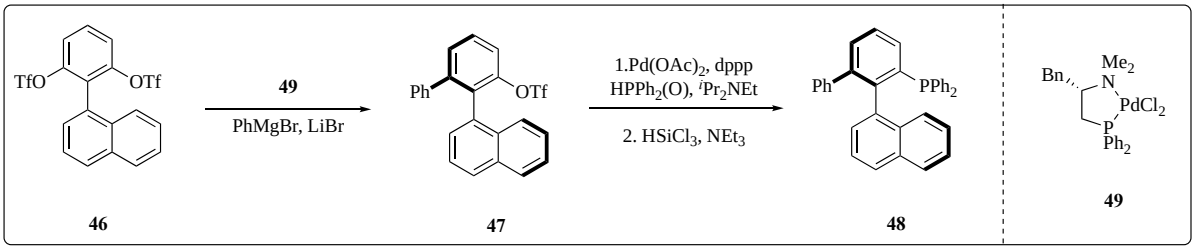

Scheme 1.9 Synthesis of axially chiral phosphine catalyzed by chiral palladium complex **49**.

The other major class of generating chiral phosphines involves a more elegant way of directly cross coupling benzyl or alkyl halides with racemic secondary phosphines in the presence of a metal complexes such as palladium, platinum and ruthenium bearing chiral ligands. The enantioselectivity of these phosphination and hydrophosphination depends on dynamic kinetic resolution. When a secondary phosphine coordinates to the metal centre bearing a chiral ligand and undergoes a deprotonation due to its enhanced acidity, diastereomeric phosphido-metal complexes are formed. The inversion barrier of these phosphido-metal complexes is low and the diastereomers interconvert rapidly. The diastereomers then react with electrophiles such as alkyl halides, alkenes and aryl iodides at

different rates, giving rise to phosphine-metal complexes from which the free phosphine can be liberated after dissociation from the metal centre. Kinetically, if the individual rates of P-C bond formation between the phosphido ligand and electrophile are vastly different and simultaneously, slower than the inversion rate, enantioenriched phosphines can be obtained.[49] (Scheme 1.10)

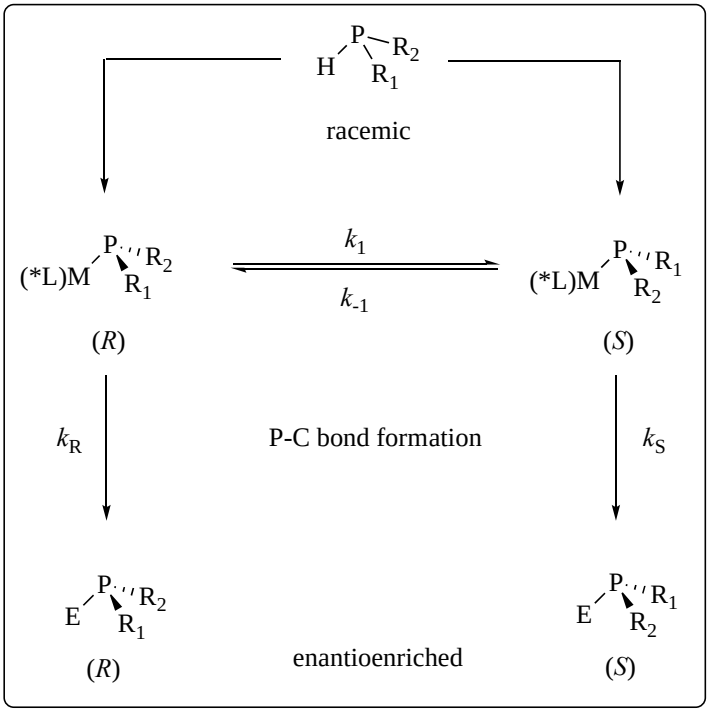

Scheme 1.10 Kinetic resolution as a method to access chiral phosphines.

Glueck reported the asymmetric alkylation of racemic secondary phosphines by means of the chiral platinum complex **50**.[50] Substrate scope was broad and encompassed benzylic bromides and different phosphines and high enantioselectivities were observed. Moving on, Glueck also developed a similar methodology for the alkylation/arylation of primary phosphines using another platinum catalyst to give numerous enantioenriched phosphaacenaphtalenes.[49b]

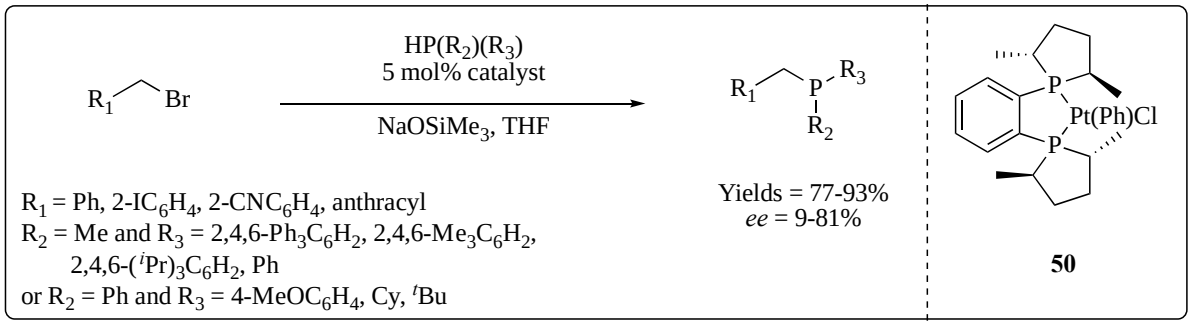

Scheme 1.11 Asymmetric phosphination catalyzed by chiral platinum complex **50**.

Hydrophosphination involves the direct addition of P-H across an unsaturated C-C bond. In this class of reactions, silylphosphines,[51] phosphine-borane complexes and phosphines can serve as useful substrates to react with both inactivated and activated alkenes, dienes and alkynes. Depending on the electronic effects of the substrates, the addition of P-H can give rise to both Markovnikov and *anti*-Markovnikov's products.[52] The stereoselectivity of this reaction determines the conformation at the newly formed chiral centres. This method of synthesizing phosphines has gained much attention as a milder alternative to classical syntheses as the reaction occurs under generally mild conditions and is compatible with a large variety of functional groups. In addition, the reaction is 100% atom economical and hence more environmentally friendly than methods that involve chiral auxiliaries. Most importantly in recent years, much progress has been made in metal complex-catalyzed hydrophosphination and several metals have been shown to act as catalysts for the addition of secondary phosphines to alkenes by activation of the *C*-electrophile.[53] Due to the large number of examples in the literature, only selected systems based on commonly available metals such as nickel,[54] palladium,[55] platinum[50, 56] will be covered. In addition, this section will be heavily focused on recent works by our group in the field of catalytic asymmetric hydrophosphination.

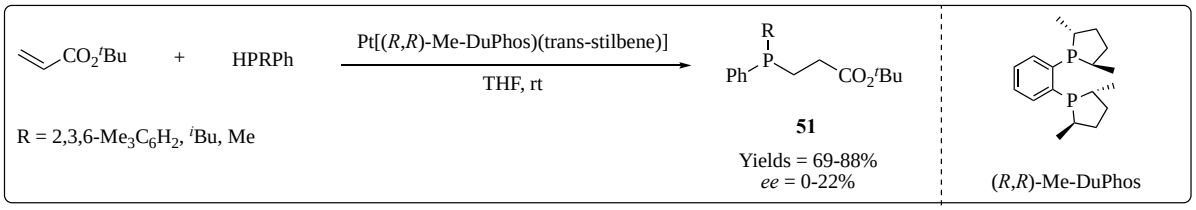

Scheme 1.12 Enantioselective synthesis of chiral phosphine catalyzed by chiral diphosphine-ligated platinum catalyst.

Glueck reported the synthesis of *P*-stereogenic phosphines from racemic secondary phosphines and Michael acceptors such as acrylonitrile, acrylate esters and associated derivatives in the presence of a platinum catalyst with (*R*,*R*)-Me-DuPhos as the chiral ligand.[57] The proposed mechanism includes the activation of the phosphine nucleophile through the oxidative addition of the P-H bond across the electron rich platinum(0) centre, giving rise to the active phosphido-platinum complex which the served as the phosphinating agent to furnish **51**. The asymmetric hydrophosphination gave low enantioselectivities, however.

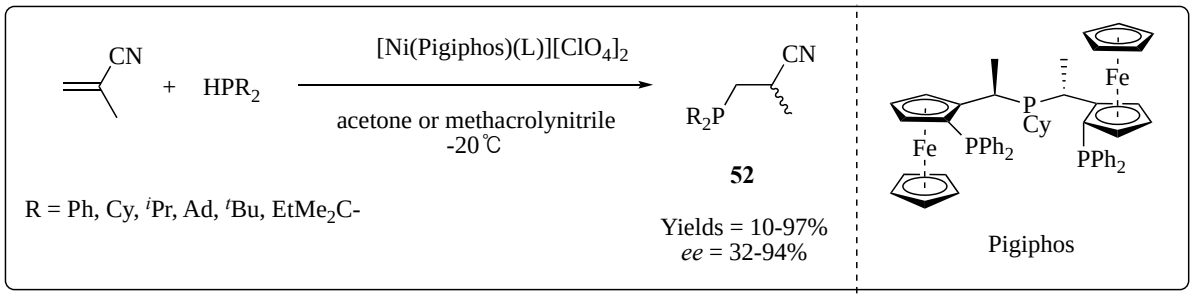

Scheme 1.13 Asymmetric hydrophosphination of olefins activated by nitrile.

In addition to the platinum catalyst developed by Glueck, Togni also developed an asymmetric hydrophosphination protocol involving a nickel complex bearing Pigiphos as the chiral ligand. The method, however, was based on the activation of the electrophile by the coordination of the nitrile to the *Lewis* acidic nickel centre. The enantioselectivities of this reaction were generally moderate.[58]

Within our group, we have also developed a few palladium-based catalytic systems which were efficient catalysts in asymmetric hydrophosphination in the generation of chiral phosphines. Besides the conspicuous benefits such as a 100% atom economy, mild reaction conditions and modest to excellent stereoselectivities, a wide range of functional groups was also tolerated by this methodology.

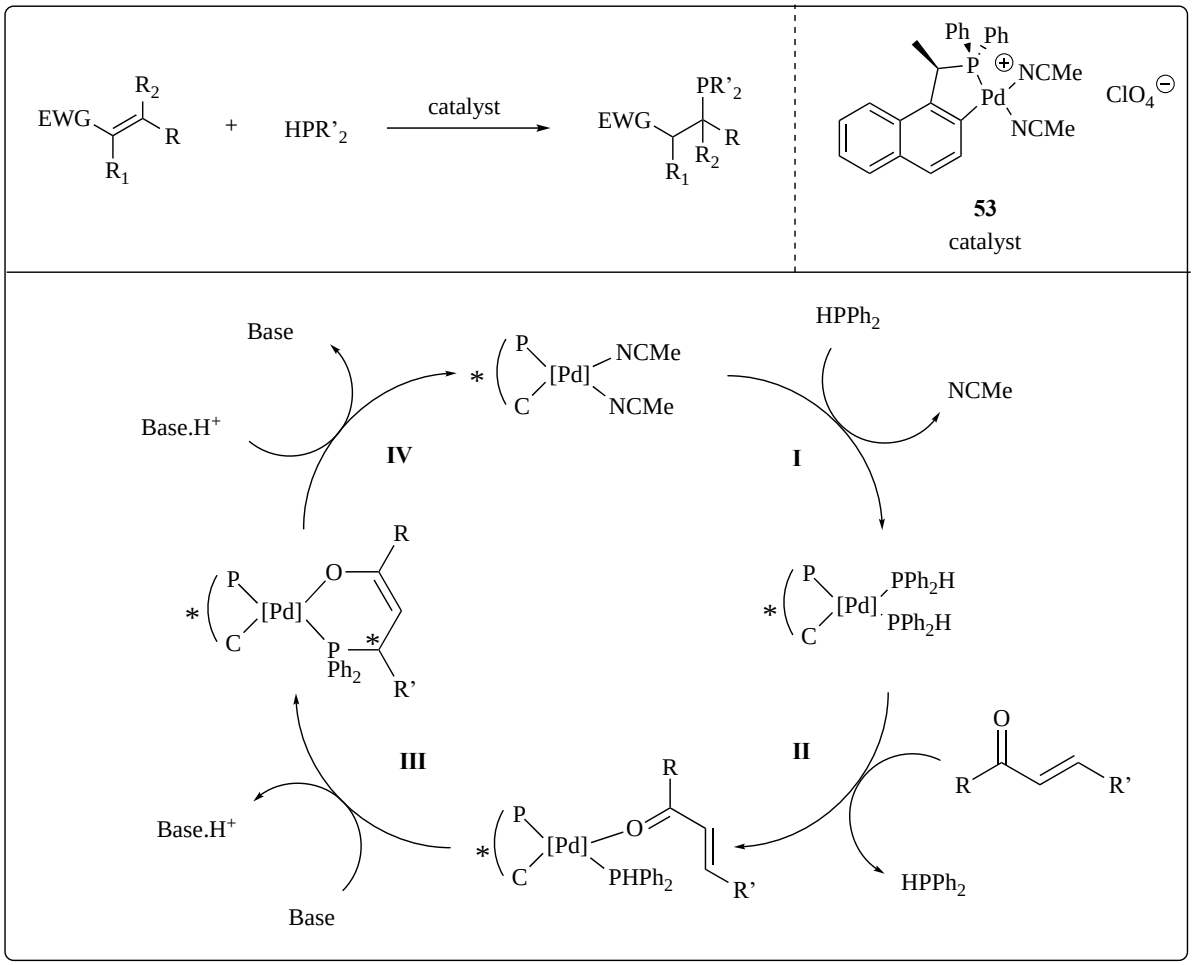

Figure 1.9 Putative mechanism of hydrophosphination (R' = Ph) catalyzed by **53**.

Mechanistically, step **I** involves the displacement of the two bound labile acetonitrile ligands in complex **53** by two equivalents of diphenylphosphine. In step **II**, ligand exchange between the phosphine *trans* to the chelating aryl carbon and the incoming enone occurs and subsequently, due to the intensified acidity of the bound phosphine, deprotonation by a weak

base and the conjugate addition to the β- carbon of the enone takes place intramolecularly in step **III**. This step has been determined to be the rate-determining step and the chirality induction step. Lastly, the coordinated P,O product dissociates from the palladium centre to regenerate the catalytic active species (step **IV**).[59] From a mechanistic standpoint, it is important to note that before the product elimination process, both the P,O product and the C,P chiral auxiliary simultaneously chelate the palladium(II) centre. While the electronically unfavorable *trans* P-Pd-P orientation renders both P-Pd bonds kinetically labile, the chemoselective liberation of the P,O product, rather than the alternative departure of C,P auxiliary is itself an interesting observation that could be attributed to the anionic aryl carbon within the C,P chelate being attracted more strongly to the palladium(II) cation additionally through charge stabilization as compared to the electrically neutral P,O product. Furthermore, while the C,P auxiliary remains as a five-membered chelate ring throughout the reaction, the addition reaction produces the six-membered P,O chelate product. The effect of ring size on the stability of chelate rings has been previously established; while both five- and six-membered metal chelates were stable, the five-membered rings were observably more stable than their larger counterparts. To date, the expanded substrate scope (non-exhaustive) includes bis(enones),[60] and activated enones,[61] β , γ - unsaturated α - ketoesters,[62] *N*-tosyl α , β - unsaturated ketimines,[63] *N*-enoyl phthalimides,[64] isoxazoles,[65] quinoline malonates,[66] activated alkenes[67] and vinyl azoles.[68]

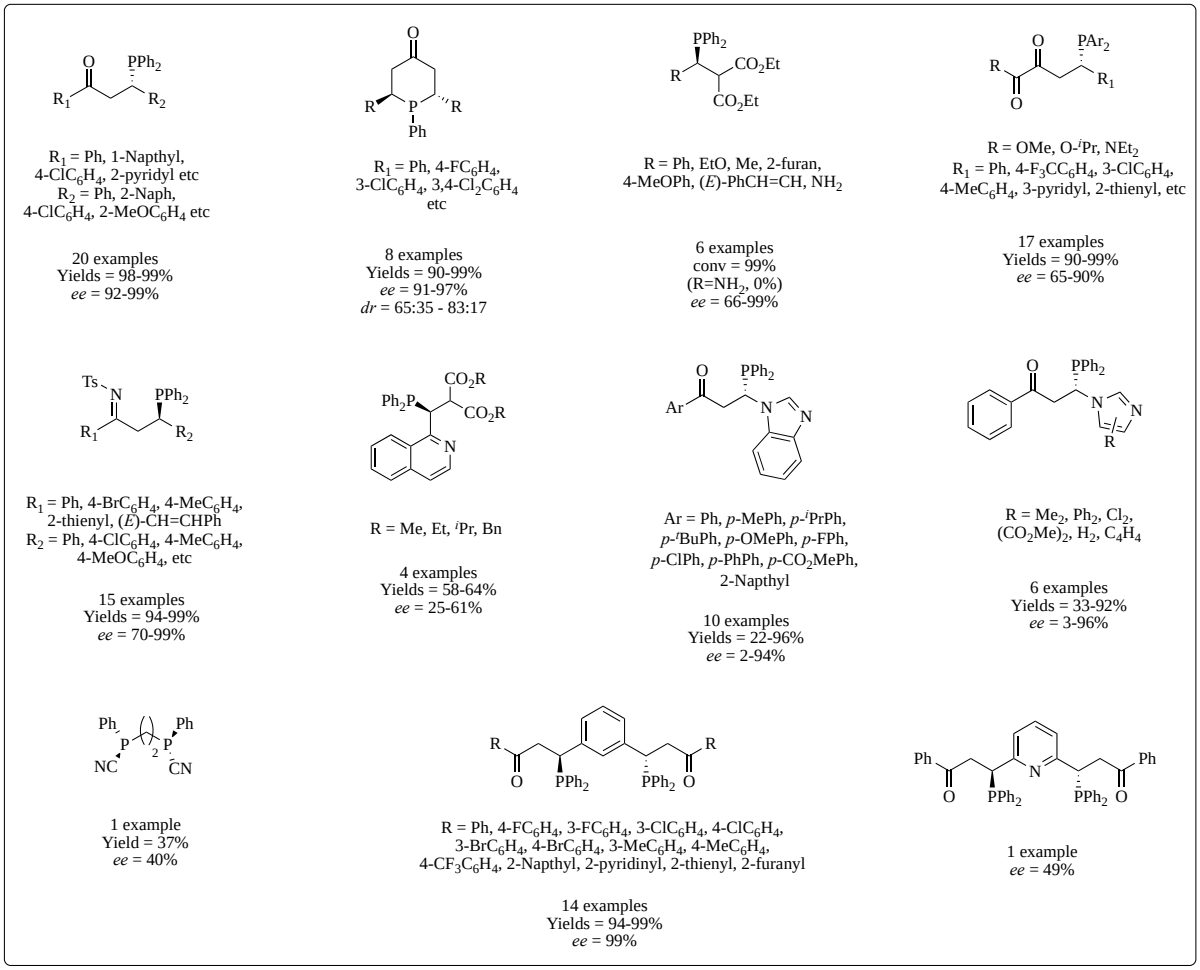

Figure 1.10 Functional groups tolerated in hydrophosphination by **53**.

While catalyst **53** remains effective in the catalytic asymmetric hydrophosphination of a large variety of substrates in most hydrophosphination reactions, severe poisoning was nonetheless observed in some special situations in which stable five-membered P,N-chelate products were generated from the addition reaction, or O,O-chelates were formed with the substrates prior to the catalytic reaction. Since oxygen is an efficient π - donor, the corresponding trans P-Pd-O and trans C-Pd-O bonds were stable to ligand redistribution reactions. In such circumstances, catalyst poisoning could be inhibited by raising the steric bulk of the substituents on the *N*- and *O*- termini.[60b]

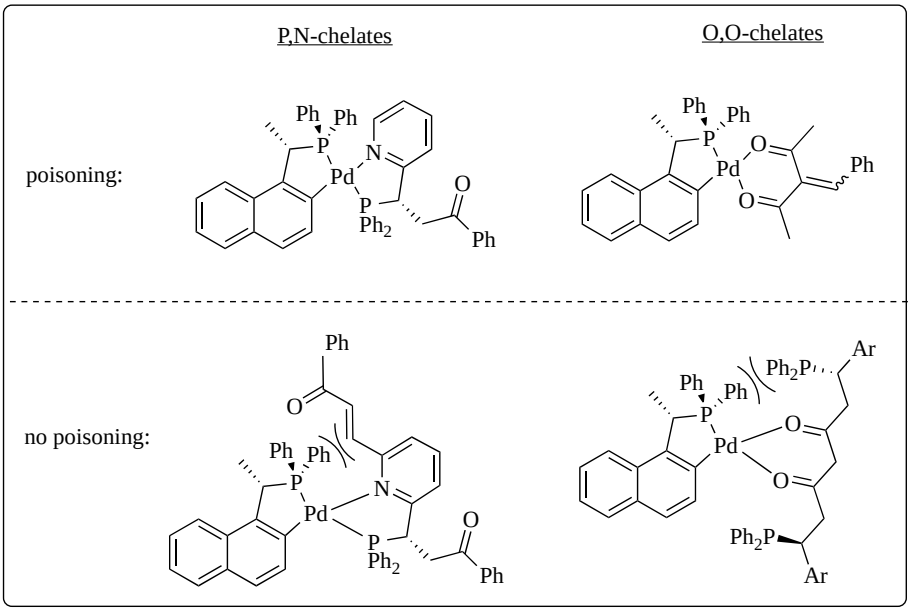

Figure 1.11 Illustrations of steric influence in catalyst poisoning.

Alternatively, the reduction in the number of active sites in the coordination sphere of the metal could also circumvent the issue of poisoning. As such, another class of four palladacycle catalysts featuring only a vacant site *trans* to an aryl anionic carbon donor flanked by two phosphine ligands, together with different supporting anionic ligands and backbones of varied steric bulk, was developed from the catalytic asymmetric hydrophosphination of *bis*(enone) and *bis*(malonate) by **53**.[69] The ligands produced were coordinated directly *in situ* to give the desired novel catalysts **54a-d**. This set of improved catalysts proved to be more versatile than complex **53** in situations where the bidentate phosphine product is a strong chelating agents, especially P,N-and O,O-chelates with unhindered substituents.

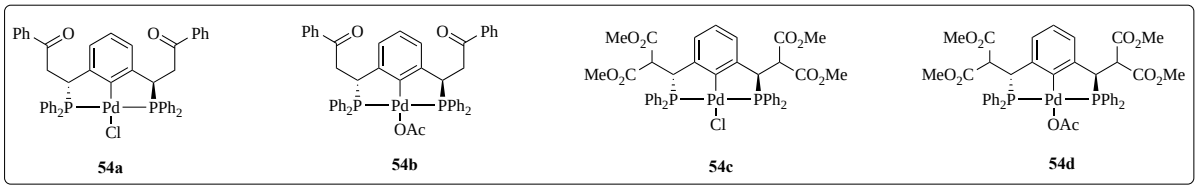

Figure 1.12 Tridentate pincer-type ligands with different structural backbones and supporting anionic ligands.

Notably, catalyst **54c** showed impressive activity in the dihydrophosphination of activated olefins in the presence of diisopropylamine in acetonitrile followed by sulfurization to afford *P*-stereogenic diphosphine sulfides.[67]

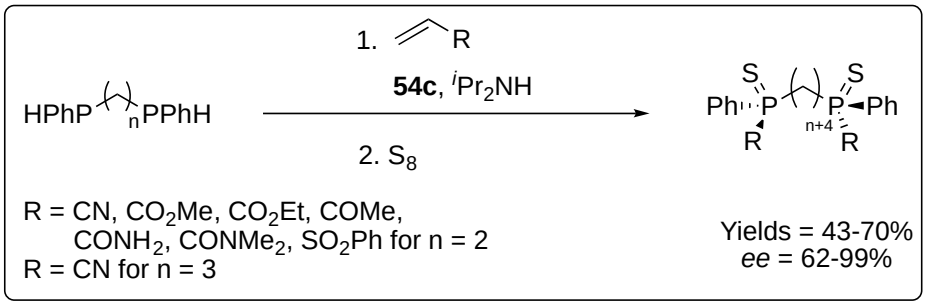

Scheme 1.14 Catalytic asymmetric dihydrophosphination catalyzed by **54c**.

Catalyst **54d** also avoided the issue of poisoning as diarylpyridine and derivatives were subjected to dihydrophosphination in the absence of an external base to afford chiral diphosphines bearing a central pyridine donor atom; the products constitute a special class of versatile chiral P-N-P tridentate ligands.[60b]

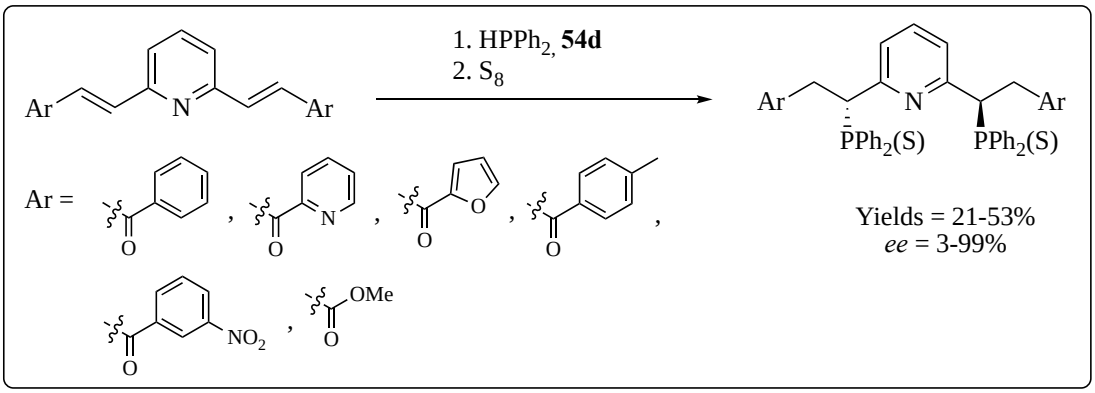

Scheme 1.15 Asymmetric hydrophosphination by **54d** to furnish chiral P-N-P pincer ligands.

1.3 Chiral *N*-Heterocyclic Carbenes (NHCs)

N-Heterocyclic carbenes (NHCs) are defined as singlet carbenes in which a divalent central carbon atom is bonded to at least one nitrogen atom within a heterocycle. As there exists a wide variety of NHCs, both achiral and chiral, in the literature, only chiral NHCs bearing *two adjacent* nitrogen atoms, in addition to the *absence* of other heteroatoms in the *cyclic* backbone, to the central carbon will be discussed in this thesis.

In as early as the 1960s, Wanzlick suggested the existence of NHCs and proposed a practical way to generate them *in situ*.[70] This pioneering work paved the way to their utility as inert ligands in organometallic chemistry ever since. Even though NHCs are generally considered to be highly elusive and reactive, Arduengo, in 1991, isolated and fully characterized the first free NHC, 1,3-di(adamantly)imidazole-2-ylidene (IAd), from its protonated precursor **55**.[71]

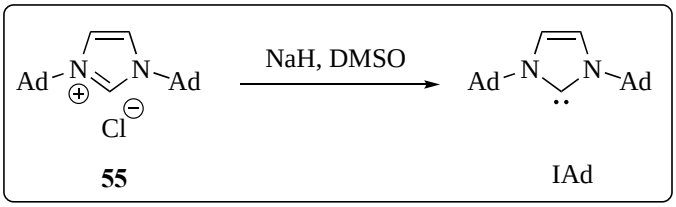

55 IAd

Scheme 1.16 Deprotonation of **55** by a strong base, NaH, to give IAd.

Contrary to other carbenes which are generally electrophilic, NHCs are electron-rich nucleophiles in which the carbon benefits from the σ- withdrawing and π- donating character of the nitrogen atoms.[72] Electronically, NHCs have a high energy HOMO and a high energy LUMO due to the combined electronic effects of the push-pull mechanism exerted by the flanking nitrogen atoms in a bent geometry about the carbon. Due to the polarized lone pair (HOMO) on carbon, NHCs form stronger bonds than classical phosphines, generating NHC-

complexes which are more resistant to decomposition.[72c] In addition, in accordance with the high LUMO, computational studies have also confirmed little to no π- accepting character in NHCs and that the metal-NHC bonds have been reported to exhibit low rotational barriers.[73]

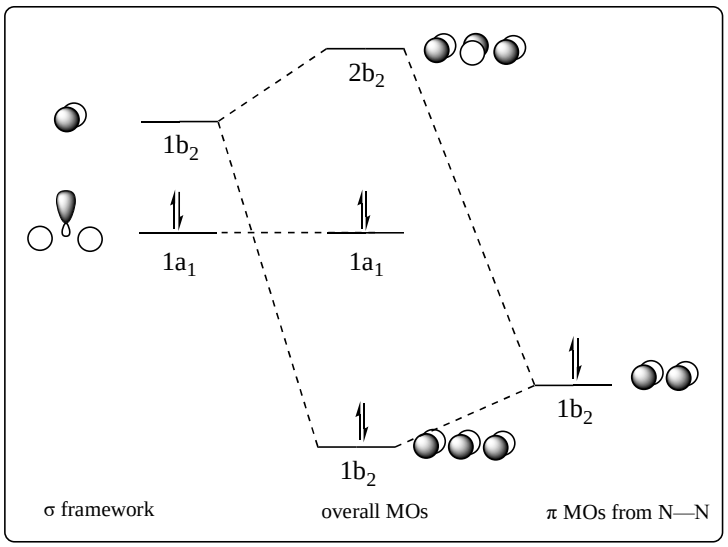

Figure 1.13 MO diagram illustrating the HOMO and LUMO of NCN moiety in NHC.

Sterically, the substituents on the nitrogen atoms can be functionalized readily, giving rise to NHCs with variable fan-like steric attributes. The steric influence imparted by NHCs is spatially different from that imparted by phosphines as in the former, the substituents point towards the metal into the coordination sphere, unlike in the latter where substituents point away from the sphere. The difference in steric properties has since motivated the development of NHCs with different steric properties for applications in fields such as catalysis,[74] materials and medicinal chemistry[75] and organocatalysis.[76]

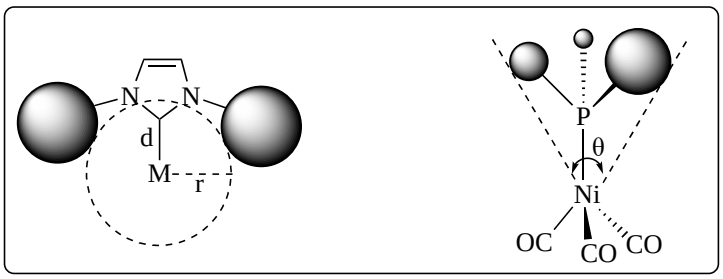

Figure 1.14 Difference in steric influence exerted by NHC and phosphine ligands.

While NHCs are more stable than other classes of carbenes lacking the electronic and steric stabilization provided by the nitrogen atoms, not all NHCs are stable enough for long term storage as free NHCs are highly basic and nucleophilic and require stringent conditions for storage. Thus, it has become pertinent for chemists to develop a range of synthetic methodologies to access precursors of NHCs, which are usually air- and moisture-stable solids easy to work with in a laboratory. Structurally, chiral NHC precursors can be seen as an amalgamation of three different smaller subunits: a carbon backbone, an amino unit, and a pre-carbenic unit with at least one of the former two moieties bearing the chirality component. Assembly of these units sequentially furnishes the final chiral NHC precursors, and upon deprotonation, yields the desired active chiral NHCs.

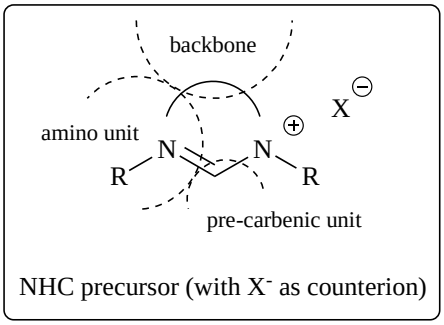

Figure 1.15 Breakdown of the three major components of a NHC precursor.

1.3.1 Syntheses of Chiral NHC Precursors from Chiral Pool

Introduction of the C_1 moiety in the final stage of cyclisation represents the most widely utilized strategy to NHC precursors since the method generally gives high yields and tolerates various substituents. Depending on the desired core of the NHC precursors, several reagents

have been identified. In 1991, Saba reported the trialkyl orthoformate ($HC(OR)_3$) as a versatile pre-carbenic unit in the syntheses of NHC precursors.[77]

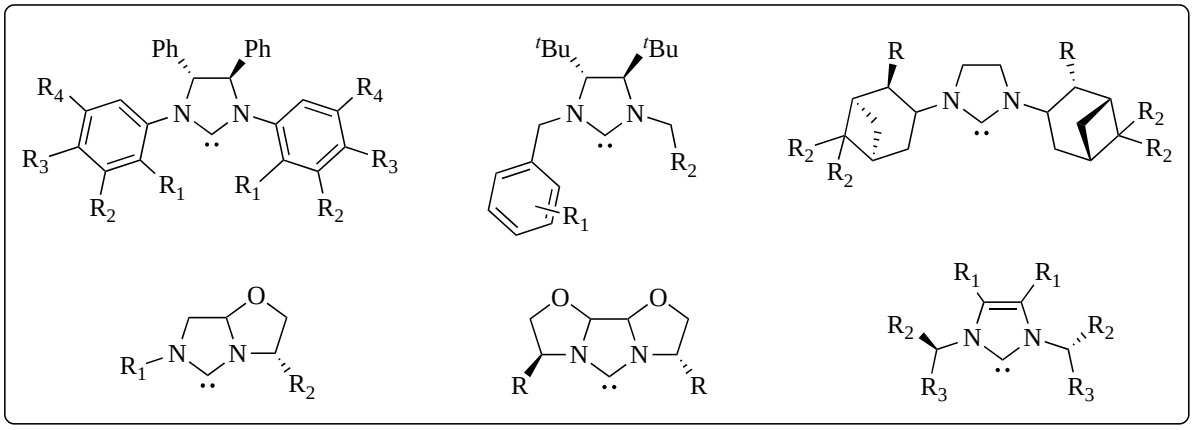

Figure 1.16 Examples of chiral NHC ligands obtained from naturally occurring chiral amines.

As this step does not introduce chirality into the structure, trialkyl orthoformate is usually used to simply cyclize a chiral *N,N*'-disubstituted tethered diamine backbone. Chiral *N,N'*-disubstituted tethered diamines are frequently obtained from chiral diamine or chiral amino acid cores and these diamines and amino acids can be coupled to achiral electrophilic substrates such as α- halogenoacyl, glyoxal and *bis*-electrophilic cores to give the desired *N,N'*-disubstituted tethered diamines.

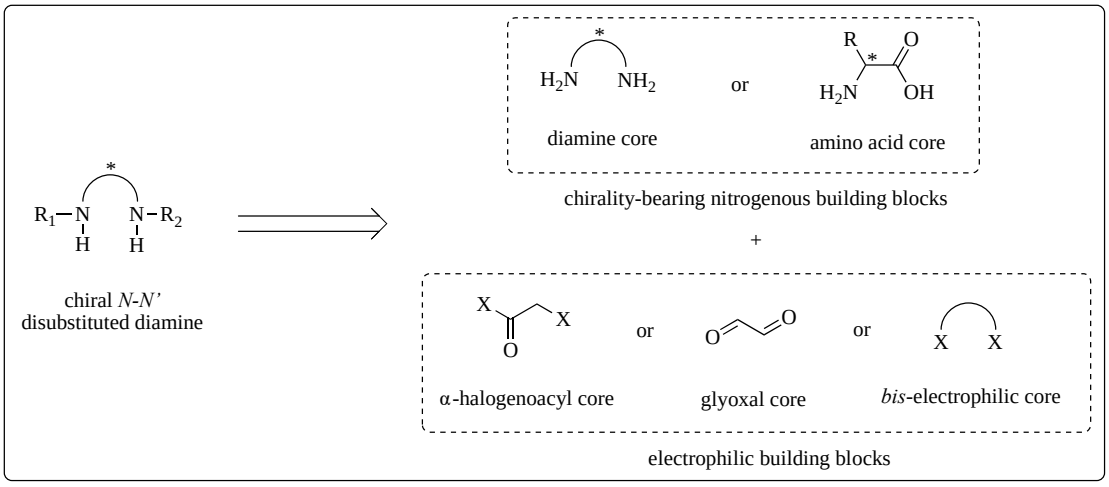

Figure 1.17 Retrosynthetic analysis of chiral *N-N'* disubstituted diamine.

Starting from the most reactive electrophilic building block, α- halogenoacyl cores have been shown to react with chiral primary amines in the presence of a weak base to furnish amino-amide compounds such as **56** which can then be reduced and ring-closed to give NHC precursors such as **57a** and **b**.[78]

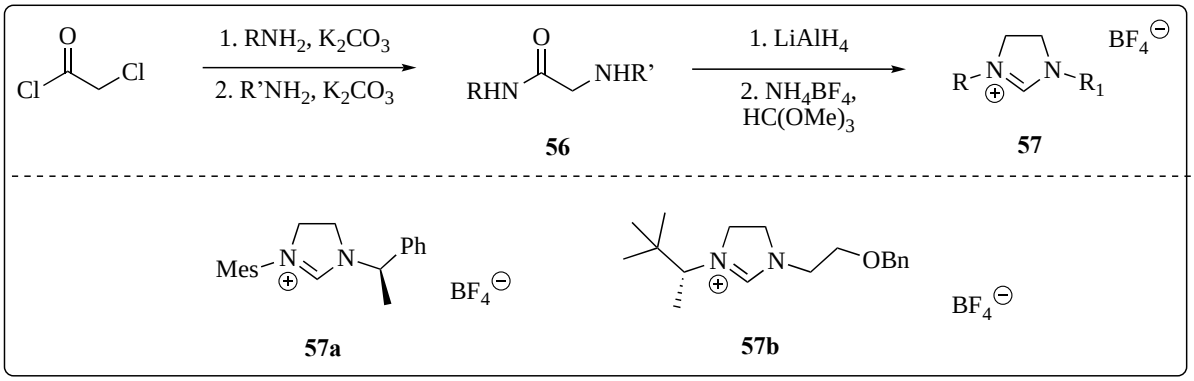

Scheme 1.17 Synthesis of NHC precursors **57a** and **b** from α- halogenoacyl cores and chiral primary amines.

In the glyoxal method, Hoveyda transformed (*S*)-NOBIN into the chiral diamine core **58** by coupling it with an aldehyde in a reductive amination reaction and then converted **58** to the final NHC precursor **59** using triethyl orthoformate.[79]

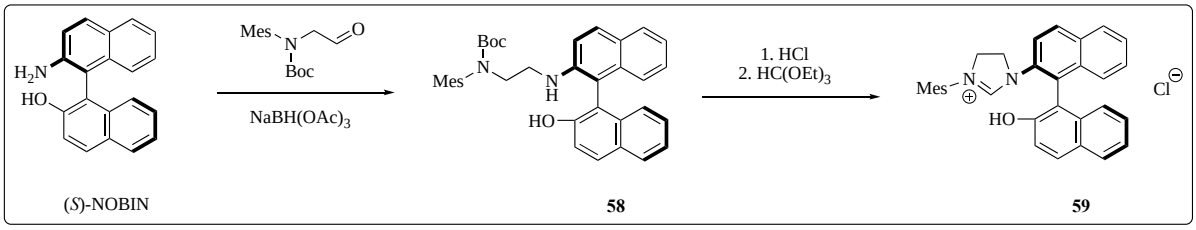

Scheme 1.18 Synthesis of axially chiral NHC precursor **59** from enantiopure (*S*)-NOBIN.

Alternatively, chiral *N*,*N*'-dialkylhydrazines **60** and **62** could also be used as 'masked' diamine cores which could be further transformed either by reduction or nucleophilic addition

by a Grignard reagent to give chiral diamine cores, which could then be cyclized using triethyl orthoformate to furnish the final chiral NHC precursors **61** and **63**.[80]

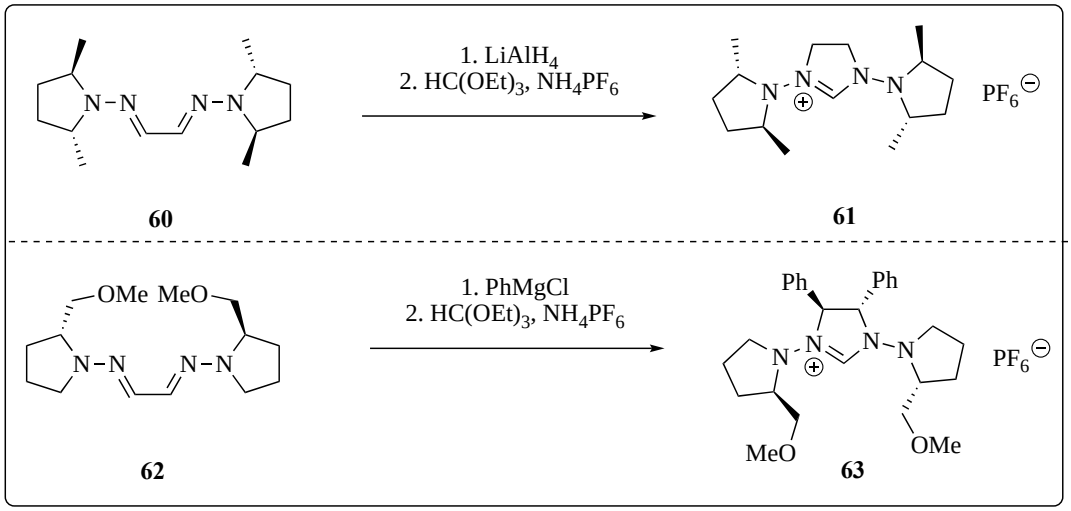

Scheme 1.19 Synthesis of symmetrical chiral NHC precursors **62** and **63** from chiral *N*,*N*'-dialkylhydrazines.

Aryl groups on pendant nitrogen atoms could be introduced *via* the Buchwald-Hartwig coupling reaction using a chiral diamine core. (1*R*,2*R*)-1,2-diaminocyclohexane derived from the chiral pool could be coupled to 2-bromotoluene in the presence of palladium(II) acetate to give the chiral diamine core **64**, which was then cyclized using triethyl orthoformate to yield the desired diaryl-functionalized NHC precursor **65**.[81]

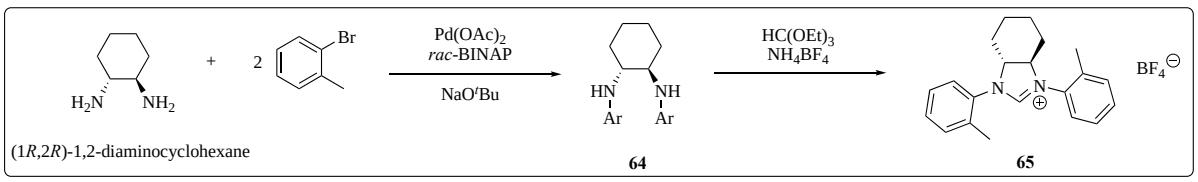

Scheme 1.20 Buchwald-Hartwig coupling between chiral cyclic diamines with aryl bromides.

In the event two different aryl groups were desired, sequential addition of aryl halides in a Buchwald-Hartwig reaction could be accomplished to afford dissimilar diaryl-functionalized NHC precursor **66**.[82]

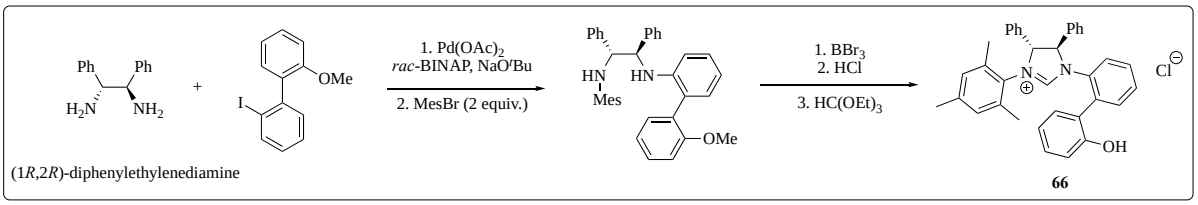

Scheme 1.21 Sequential C-N coupling with chiral diamines to give diaryl NHC precursor **66**.

Besides α- halogenoacyl and glyoxal cores, *bis*-electrophilic cores could also be used as coupling agents with chiral amines to furnish chiral diamines which could then be ring-closed by trimethyl orthoformate to give chiral NHC precursors **67a** to **67d**.[83]

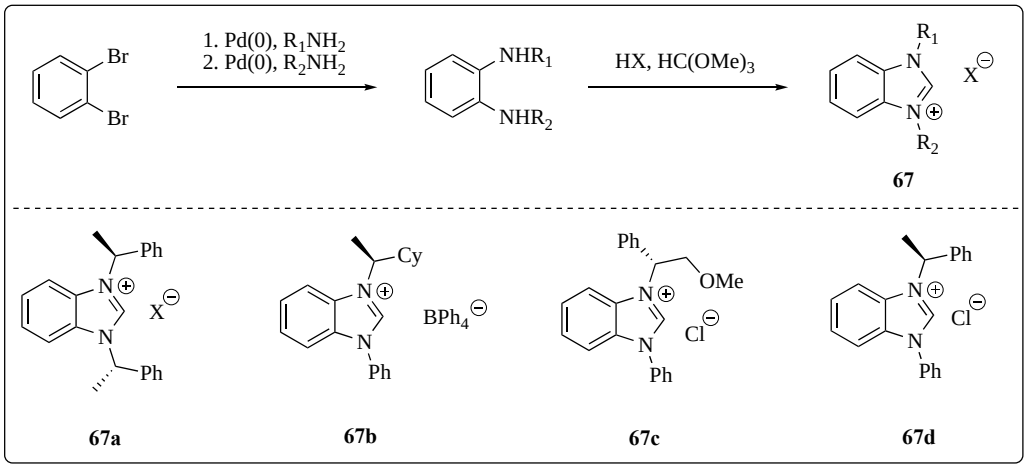

Scheme 1.22 Combinational alkyl/aryl and diaryl chiral NHC precursors from sequential coupling with chiral diamines.

Lastly, using chiral amino acids as chiral starting materials, sulfamidate **69** was obtained from the nucleophilic ring closure of **68**, before being coupled to another secondary amine HN(Boc)Mes with the expulsion of the sulfone group to give NHC precursor **70**.[84]

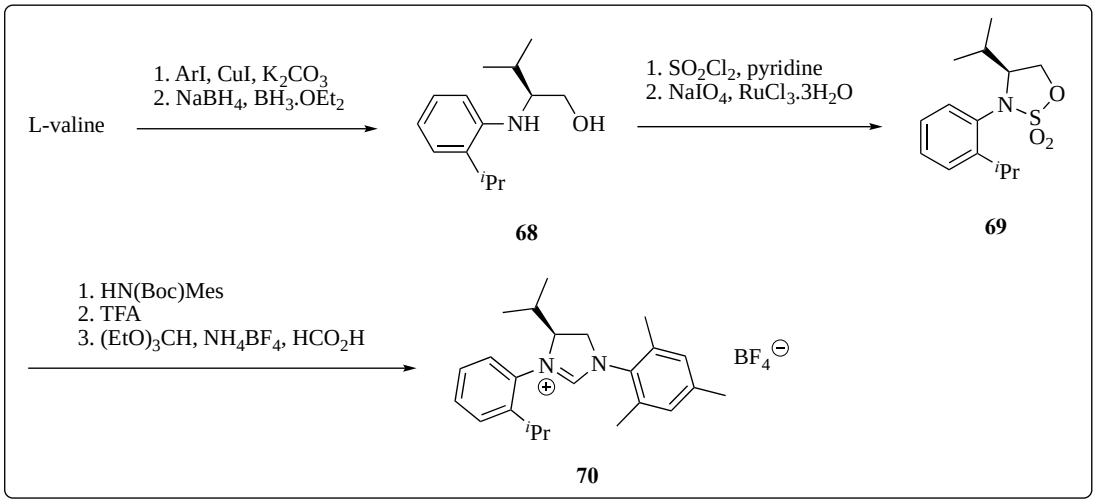

Scheme 1.23 Synthesis of chiral NHC precursor **70** from enantiopure L-valine.

While the chiral pool of amines and amino acids allows in several cases the syntheses of chiral NHC precursors, the reliance on the chiral pool for enantiopure starting materials has posed significant limitations in the syntheses of other structurally different chiral NHC precursors. As such, there exists a strong impetus to expand the methodologies associated with the syntheses of structurally varied chiral NHC precursors and the corresponding NHC metal complexes.

1.4 Research Objectives

In view of the ongoing efforts of our group in advancing the utility of catalytic asymmetric hydrophosphination and the limitation associated with the syntheses of structurally varied chiral NHC precursors and their corresponding metal complexes, an unprecedented pursuit of introducing catalytic asymmetric hydrophosphination as a feasible tool in the syntheses of chiral NHC precursors bearing multivariate ligand backbones and their metal complexes will be disclosed. Challenges and solutions to the problems encountered with this protocol will be described. Lastly, attempted catalytic and biological applications of the complexes will also be presented.

References

(1) Hollingsworth, R. I.; Wang, G., *Toward a Carbohydrate-Based Chemistry: Progress in the Development of General-Purpose Chiral Synthons from Carbohydrates, Chem. Rev.* **2000,** *100*, 4267-4282.

(2) Kim, H.; Im, S. W.; Kim, R. M.; Cho, N. H.; Lee, H.-E.; Ahn, H.-Y.; Nam, K. T., *Chirality control of inorganic materials and metals by peptides or amino acids, Mater. Adv.* **2020,** *1*, 512-524.

(3) Hanashima, S.; Yano, Y.; Murata, M., *Enantiomers of phospholipids and cholesterol: A key to decipher lipid-lipid interplay in membrane, Chirality* **2020,** *32*, 282-298.

(4) D'Alonzo, D.; Guaragna, A.; Palumbo, G., *Exploring the role of chirality in nucleic acid recognition, Chem Biodivers* **2011,** *8*, 373-413.

(5) Margolin, A. L., *Enzymes in the synthesis of chiral drugs, Enzyme Microb. Technol.* **1993,** *15*, 266-280.

(6) Mori, K., *Significance of chirality in pheromone science, Biorg. Med. Chem.* **2007,** *15*, 7505-7523.

(7) Bentley, R., Chirality in Biology. In *Reviews in Cell Biology and Molecular Medicine*.

(8) Tokunaga, E.; Yamamoto, T.; Ito, E.; Shibata, N., *Understanding the Thalidomide Chirality in Biological Processes by the Self-disproportionation of Enantiomers, Sci. Rep.* **2018,** *8*, 17131.

(9) Pignolet, L. M., *Homogeneous Catalysis with Metal Phosphine Complexes*. 1 ed.; Springer US: 1983; p 489.

(10) (a) Guo, H.; Fan, Y. C.; Sun, Z.; Wu, Y.; Kwon, O., *Phosphine Organocatalysis, Chem. Rev.* **2018,** *118*, 10049-10293; (b) Ni, H.; Chan, W.-L.; Lu, Y., *Phosphine-Catalyzed Asymmetric Organic Reactions, Chem. Rev.* **2018,** *118*, 9344-9411.

(11) Kagan, H. B.; Dang, T.-P., *Asymmetric catalytic reduction with transition metal complexes. I. Catalytic system of rhodium(I) with (-)-2,3-0-isopropylidene-2,3-dihydroxy-1,4-bis(diphenylphosphino)butane, a new chiral diphosphine, J. Am. Chem. Soc.* **1972,** *94*, 6429-6433.

(12) Brunner, H., VCH (January 1, 1993): p 947.

(13) Imamoto, T.; Tamura, K.; Zhang, Z.; Horiuchi, Y.; Sugiya, M.; Yoshida, K.; Yanagisawa, A.; Gridnev, I. D., *Rigid P-Chiral Phosphine Ligands with tert-Butylmethylphosphino Groups for Rhodium-Catalyzed Asymmetric Hydrogenation of Functionalized Alkenes, J. Am. Chem. Soc.* **2012,** *134*, 1754-1769.

(14) Yamamoto, K.; Hayashi, T.; Kumada, M., *Asymmetric homogeneous hydrosilylation with platinum(II) complexes of chiral phosphines, J. Am. Chem. Soc.* **1971,** *93*, 5301-5302.

(15) Cao, Z.; Liu, Y.; Liu, Z.; Feng, X.; Zhuang, M.; Du, H., *Pd-Catalyzed Asymmetric Allylic Alkylation of Indoles and Pyrroles by Chiral Alkene-Phosphine Ligands, Org. Lett.* **2011,** *13*, 2164-2167.

(16) (a) Hannedouche, J.; Schulz, E., *Asymmetric Hydroamination: A Survey of the Most Recent Developments, Chem. Eur. J.* **2013,** *19*, 4972-4985; (b) Feng, J.-J.; Chen, X.-F.; Shi, M.; Duan, W.-L., *Palladium-Catalyzed Asymmetric Addition of Diarylphosphines to Enones toward the Synthesis of Chiral Phosphines, J. Am. Chem. Soc.* **2010,** *132*, 5562-5563; (c) Kawamoto, T.; Hirabayashi, S.; Guo, X.-X.; Nishimura, T.; Hayashi, T., *Rhodium-catalyzed asymmetric hydroalkoxylation and hydrosulfenylation of diphenylphosphinylallenes, Chem. Commun.* **2009**, 3528-3530.

(17) Cherney, A. H.; Kadunce, N. T.; Reisman, S. E., *Enantioselective and Enantiospecific Transition-Metal-Catalyzed Cross-Coupling Reactions of Organometallic Reagents To Construct C–C Bonds, Chem. Rev.* **2015,** *115*, 9587-9652.

(18) Nishimura, T.; Maeda, Y.; Hayashi, T., *Chiral Diene-Phosphine Tridentate Ligands for Rhodium-Catalyzed Asymmetric Cycloisomerization of 1,6-Enynes, Org. Lett.* **2011,** *13*, 3674-3677.

(19) Wang, C.; Chen, Y.; Li, J.; Zhou, L.; Wang, B.; Xiao, Y.; Guo, H., *Phosphine-Catalyzed Asymmetric Cycloaddition Reaction of Diazenes: Enantioselective Synthesis of Chiral Dihydropyrazoles, Org. Lett.* **2019,** *21*, 7519-7523.

(20) Gilheany, D. G., *No d Orbitals but Walsh Diagrams and Maybe Banana Bonds: Chemical Bonding in Phosphines, Phosphine Oxides, and Phosphonium Ylides, Chem. Rev.* **1994,** *94*, 1339-1374.

(21) (a) Ingle, G. K.; Liang, Y.; Mormino, M. G.; Li, G.; Fronczek, F. R.; Antilla, J. C., *Chiral Magnesium BINOL Phosphate-Catalyzed Phosphination of Imines: Access to Enantioenriched α-Amino Phosphine Oxides, Org. Lett.* **2011,** *13*, 2054-2057; (b) Zhao, D.; Mao, L.; Wang, L.; Yang, D.; Wang, R., *Catalytic asymmetric construction of tetrasubstituted carbon stereocenters by conjugate addition of dialkyl phosphine oxides to β,β-disubstituted α,β-unsaturated carbonyl compounds, Chem. Commun.* **2012,** *48*, 889-891.

(22) (a) Malysheva, S. F.; Gusarova, N. K.; Artem'ev, A. V.; Belogorlova, N. A.; Albanov, A. I.; Borodina, T. N.; Smirnov, V. I.; Trofimov, B. A., *Facile Non-Catalyzed Synthesis of Tertiary Phosphine Sulfides by Regioselective Addition of Secondary Phosphine Sulfides to Alkenes, Eur. J. Org. Chem.* **2014,** *2014*, 2516-2521; (b) Artem'ev, A.; Malysheva, S.; Gusarova, N.; Belogorlova, N.; Shagun, V.; Albanov, A.; Trofimov, B., *Catalyst- and Solvent-Free Stereoselective Addition of Secondary Phosphine Chalcogenides to Alkynes, Synthesis* **2015,** *47*, 263-271.

(23) (a) Hao, X.-Q.; Huang, J.-J.; Wang, T.; Lv, J.; Gong, J.-F.; Song, M.-P., *PCN Pincer Palladium(II) Complex Catalyzed Enantioselective Hydrophosphination of Enones: Synthesis of Pyridine-Functionalized Chiral Phosphine Oxides as NCsp3O Pincer Preligands, J. Org.*

Chem. **2014,** *79*, 9512-9530; (b) Du, D.; Lin, Z.-Q.; Lu, J.-Z.; Li, C.; Duan, W.-L., *Palladium-catalyzed Asymmetric 1,4-Addition of Diarylphosphines to α,β-Unsaturated Carboxylic Esters, Asian J. Org.Chem.* **2013,** *2*, 392-394; (c) Chen, Y.-R.; Feng, J.-J.; Duan, W.-L., *NHC–copper-catalyzed asymmetric 1,4-addition of diarylphosphines to α,β-unsaturated ketones, Tetrahedron Lett.* **2014,** *55*, 595-597.

(24) Hérault, D.; Nguyen, D. H.; Nuel, D.; Buono, G., *Reduction of secondary and tertiary phosphine oxides to phosphines, Chem. Soc. Rev.* **2015,** *44*, 2508-2528.

(25) Miyashita, A.; Yasuda, A.; Takaya, H.; Toriumi, K.; Ito, T.; Souchi, T.; Noyori, R., *Synthesis of 2,2'-bis(diphenylphosphino)-1,1'-binaphthyl (BINAP), an atropisomeric chiral bis(triaryl)phosphine, and its use in the rhodium(I)-catalyzed asymmetric hydrogenation of .alpha.-(acylamino)acrylic acids, J. Am. Chem. Soc.* **1980,** *102*, 7932-7934.

(26) Anastas, P.; Eghbali, N., *Green Chemistry: Principles and Practice, Chem. Soc. Rev.* **2010,** *39*, 301-312.

(27) Meisenheimer, J. L., *L. Chem. Ber.* **1911,** *44*.

(28) Meisenheimer, J. C., J.; Horing, M.; Lauter, W.; Lichtenstadt,; L.; Samuel, W. J., *Liebigs Ann. Chem.* **1926,** *449*.

(29) Kříž, O. Č. a. O., *Asymmetric reactions. X. Configuration on asymmetric nitrogen and phosphorus, Collect. Czeck. Chem. Commun.* **1966,** *31*, 1910-1913.

(30) (a) Toda, F.; Mori, K.; Stein, Z.; Goldberg, I., *Optical resolution of phosphinates and phosphine oxides by complex formation with optically active 2,2'-dihydroxy-1,1'-binaphthyl and crystallographic study of two diastereomeric complexes with methyl methylphenylphosphinate, J. Org. Chem.* **1988,** *53*, 308-312; (b) Ostrogovich, G.; Kerek, F., *An Optically Active Phospholene Oxide, Angew. Chem. Int. Ed.* **1971,** *10*, 498-498.

(31) (a) Martin, J. W. L.; Palmer, J. A. L.; Wild, S. B., *Resolutions involving metal complexation. Resolution of (.+-.)-1-amino-2-(methylphenylarsino)ethane and its phosphorus*

analog. Stereochemistry and stability of square-planar bis(bidentate) complexes of bivalent palladium and platinum, Inorg. Chem. **1984,** *23*, 2664-2668; (b) Leung, P. H.; Willis, A. C.; Wild, S. B., *Resolutions involving metal complexation. Optical resolution and photochemical rearrangement of (.+-.)-(2-mercaptoethyl)methylphenylphosphine, Inorg. Chem.* **1992,** *31*, 1406-1410.

(32) Bodalski, R.; Janecki, T.; Gałdecki, Z.; Główka, M., *SYNTHESIS OF OPTICALLY ACTIVE 4-OXO-1-PHENYL-2-PHOSPHOLENE-1-OXIDE AND THE DETERMINATION OF ITS CONFIGURATION, Phosphorus Sulfur Silicon Relat. Elem.* **1982,** *14*, 15-21.

(33) A. Wickli, E., Schmidt, J. R. Bourne, *1992, Biocatalysis in Non-Conventional Media (Ed.: J. Tramper), Elsevier, Amsterdam 577*.

(34) (a) Kiełbasiński, P.; Omelańczuk, J.; Mikołajczyk, M., *Lipase-promoted kinetic resolution of racemic, P-chiral hydroxymethylphosphonates and phosphinates, Tetrahedron: Asymmetry* **1998,** *9*, 3283-3287; (b) Serreqi, A. N.; Kazlauskas, R. J., *Kinetic Resolution of Phosphines and Phosphine Oxides with Phosphorus Stereocenters by Hydrolases, J. Org. Chem.* **1994,** *59*, 7609-7615; (c) Fogassy, E.; Nógrádi, M.; Kozma, D.; Egri, G.; Pálovics, E.; Kiss, V., *Optical resolution methods*, *Org. Biomol. Chem.* **2006,** *4*, 3011-3030; (d) Faulconbridge, S. J.; Holt, K. E.; Garcia Sevillano, L.; Lock, C. J.; Tiffin, P. D.; Tremayne, N.; Winter, S., *Preparation of enantiomerically enriched aromatic β-amino acids via enzymatic resolution, Tetrahedron Lett.* **2000,** *41*, 2679-2681.

(35) (a) Korpiun, O.; Lewis, R. A.; Chickos, J.; Mislow, K., *Synthesis and absolute configuration of optically active phosphine oxides and phosphinates, J. Am. Chem. Soc.* **1968,** *90*, 4842-4846; (b) Hoge, G., *Synthesis of Both Enantiomers of a P-Chirogenic 1,2-Bisphospholanoethane Ligand via Convergent Routes and Application to Rhodium-Catalyzed Asymmetric Hydrogenation of CI-1008 (Pregabalin), J. Am. Chem. Soc.* **2003,** *125*, 10219-10227; (c) Vineyard, B. D.; Knowles, W. S.; Sabacky, M. J.; Bachman, G. L.; Weinkauff, D.

J., *Asymmetric hydrogenation. Rhodium chiral bisphosphine catalyst, J. Am. Chem. Soc.* **1977,** *99*, 5946-5952.

(36) (a) Kolodiazhnyi, O. I.; Gryshkun, E. V.; Andrushko, N. V.; Freytag, M.; Jones, P. G.; Schmutzler, R., *Asymmetric synthesis of chiral N-(1-methylbenzyl)aminophosphines, Tetrahedron: Asymmetry* **2003,** *14*, 181-183; (b) Gryshkun, E. V.; Andrushko, N. V.; Kolodiazhnyi, O. I., *STEREOSELECTIVE REACTIONS OF CHIRAL AMINES WITH RACEMIC CHLOROPHOSPHINES, Phosphorus Sulfur Silicon Relat. Elem.* **2004,** *179*, 1027-1046.

(37) (a) Juge, S.; Stephan, M.; Laffitte, J. A.; Genet, J. P., *Efficient asymmetric synthesis of optically pure tertiary mono and diphosphine ligands, Tetrahedron Lett.* **1990,** *31*, 6357-6360; (b) Juge, S.; Genet, J. P., *Asymmetric synthesis of phosphinates, phosphine oxides and phosphines by Michaelis Arbuzov rearrangement of chiral oxazaphospholidine, Tetrahedron Lett.* **1989,** *30*, 2783-2786.

(38) Jugé, S., *Enantioselective Synthesis of P-Chirogenic Phosphorus Compounds via the Ephedrine-Borane Complex Methodology, Phosphorus Sulfur Silicon Relat. Elem.* **2008,** *183*, 233-248.

(39) (a) Nudelman, A.; Cram, D. J., *The stereochemical course of ester-amide interchange leading to optically active phosphinic and sulfinic amides, J. Am. Chem. Soc.* **1968,** *90*, 3869-3870; (b) Korpiun, O.; Mislow, K., *New route to the preparation and configurational correlation of optically active phosphine oxides, J. Am. Chem. Soc.* **1967,** *89*, 4784-4786.

(40) (a) Horner, L.; Simons, G., *PHOSPHORORGANISCHE VERBINDUNGEN 1061 DIE SYNTHESE OPTISCH AKTIVER TERTIÄRER PHOSPHINE UND PHOSPHINOXIDE MIT ORTHO-SUBSTITUIERTEN ARYLLIGANDEN, Phosphorus Sulfur Silicon Relat. Elem.* **1984,** *19*, 77-89; (b) Wolfe, B. H. New methods for preparing scalemic P-chiral secondary

phosphine -boranes and enantiomerically pure phosphine ligand precursors. Ph.D., Montana State University, Ann Arbor, 2000.

(41) Dang, T. P.; Kagan, H. B., *The asymmetric synthesis of hydratropic acid and amino-acids by homogeneous catalytic hydrogenation, J. Chem. Soc. D* **1971**, 481-481.

(42) Michaud, G.; Bulliard, M.; Ricard, L.; Genêt, J.-P.; Marinetti, A., *A Strategy for the Stereoselective Synthesis of Unsymmetric Atropisomeric Ligands: Preparation of NAPhePHOS, a New Biaryl Diphosphine, Chem. Eur. J.* **2002,** *8*, 3327-3330.

(43) Riant, O.; Samuel, O.; Kagan, H. B., *A general asymmetric synthesis of ferrocenes with planar chirality, J. Am. Chem. Soc.* **1993,** *115*, 5835-5836.

(44) (a) Yuan, M.; Zhang, N.; Pullarkat, S. A.; Li, Y.; Liu, F.; Pham, P.-T.; Leung, P.-H., *Asymmetric Synthesis of Functionalized 1,3-Diphosphines via Chiral Palladium Complex Promoted Hydrophosphination of Activated Olefins, Inorg. Chem.* **2010,** *49*, 989-996; (b) Yuan, M.; Pullarkat, S. A.; Li, Y.; Leung, P.-H., *Palladacycle mediated synthesis of cyano-functionalized chiral 1,2-diphosphine and subsequent functional group transformations, J. Organomet. Chem.* **2011,** *696*, 905-912; (c) Huang, Y.; Pullarkat, S. A.; Yuan, M.; Ding, Y.; Li, Y.; Leung, P.-H., *Palladium Template Promoted Asymmetric Synthesis of 1,2-Diphosphines by Hydrophosphination of Functionalized Allenes, Organometallics* **2010,** *29*, 536-542; (d) Chen, S.; Ng, J. K.-P.; Pullarkat, S. A.; Liu, F.; Li, Y.; Leung, P.-H., *Asymmetric Synthesis of New Diphosphines and Pyridylphosphines via a Kinetic Resolution Process Promoted and Controlled by a Chiral Palladacycle, Organometallics* **2010,** *29*, 3374-3386; (e) Chen, K.; Pullarkat, S. A.; Ma, M.; Li, Y.; Leung, P.-H., *Chiral cyclopalladated complex promoted asymmetric synthesis of diester-substituted P,N-ligands via stepwise hydrophosphination and hydroamination reactions, Dalton Trans.* **2012,** *41*, 5391-5400.

(45) Gnas, Y.; Glorius, F., *Chiral Auxiliaries — Principles and Recent Applications, ChemInform* **2006,** *37*.

(46) (a) Wen, J.; Wang, F.; Zhang, X., *Asymmetric hydrogenation catalyzed by first-row transition metal complexes, Chem. Soc. Rev.* **2021,** *50*, 3211-3237; (b) Verendel, J. J.; Pàmies, O.; Diéguez, M.; Andersson, P. G., *Asymmetric Hydrogenation of Olefins Using Chiral Crabtree-type Catalysts: Scope and Limitations, Chem. Rev.* **2014,** *114*, 2130-2169; (c) Yang, L.; Huang, H., *Asymmetric catalytic carbon–carbon coupling reactions via C–H bond activation, Catal. Sci. Technol.* **2012,** *2*, 1099-1112.

(47) Fryzuk, M. D.; Bosnich, B., *Asymmetric synthesis. An asymmetric homogeneous hydrogenation catalyst which breeds its own chirality, J. Am. Chem. Soc.* **1978,** *100*, 5491-5494.

(48) Hayashi, T.; Niizuma, S.; Kamikawa, T.; Suzuki, N.; Uozumi, Y., *Catalytic asymmetric synthesis of axially chiral biaryls by palladium-catalyzed enantioposition-selective cross-coupling, J. Am. Chem. Soc.* **1995,** *117*, 9101-9102.

(49) (a) Glueck, D. S., *Metal-catalyzed asymmetric synthesis of P-stereogenic phosphines, Synlett* **2007,** *2007*, 2627-2634; (b) Anderson, B. J.; Guino-o, M. A.; Glueck, D. S.; Golen, J. A.; DiPasquale, A. G.; Liable-Sands, L. M.; Rheingold, A. L., *Platinum-catalyzed enantioselective tandem alkylation/arylation of primary phosphines. Asymmetric synthesis of P-stereogenic 1-phosphaacenaphthenes, Org. Lett.* **2008,** *10*, 4425-4428.

(50) Scriban, C.; Glueck, D. S., *Platinum-catalyzed asymmetric alkylation of secondary phosphines: enantioselective synthesis of P-stereogenic phosphines, J. Am. Chem. Soc.* **2006,** *128*, 2788-2789.

(51) (a) Hayashi, M.; Matsuura, Y.; Watanabe, Y., *Fluoride-catalyzed three-component coupling reaction of a silylphosphine, activated alkenes and aldehydes, Tetrahedron Lett.* **2005,** *46*, 5135-5138; (b) Hayashi, M.; Matsuura, Y.; Watanabe, Y., *Fluoride-mediated phosphination of alkenes and alkynes by silylphosphines, Tetrahedron Lett.* **2004,** *45*, 9167-9169.

(52) (a) Baillie, C.; Xiao, J., *Catalytic synthesis of phosphines and related compounds, Curr. Org. Chem.* **2003,** *7*, 477-514; (b) Delacroix, O.; Gaumont, A., *Hydrophosphination of unactivated alkenes, dienes and alkynes: a versatile and valuable approach for the synthesis of phosphines, Curr. Org. Chem.* **2005,** *9*, 1851-1882.

(53) Chew, R. J.; Leung, P.-H., *Our Odyssey with Functionalized Chiral Phosphines: From Optical Resolution to Asymmetric Synthesis to Catalysis, Chem. Rec.* **2016,** *16*, 141-158.

(54) (a) Ganushevich, Y. S.; Miluykov, V. A.; Polyancev, F. M.; Latypov, S. K.; Lönnecke, P.; Hey-Hawkins, E.; Yakhvarov, D. G.; Sinyashin, O. G., *Nickel Phosphanido Hydride Complex: An Intermediate in the Hydrophosphination of Unactivated Alkenes by Primary Phosphine, Organometallics* **2013,** *32*, 3914-3919; (b) Shulyupin, M. O.; Kazankova, M. A.; Beletskaya, I. P., *Catalytic hydrophosphination of styrenes, Org. Lett.* **2002,** *4*, 761-763; (c) Kazankova, M. A.; Shulyupin, M. O.; Beletskaya, I. P., *Catalytic hydrophosphination of alkenylalkyl ethers, Synlett* **2003,** *2003*, 2155-2158.

(55) (a) Trepohl, V. T.; Mori, S.; Itami, K.; Oestreich, M., *Palladium (II)-Catalyzed Conjugate Phosphination of Electron-Deficient Acceptors, Org. Lett.* **2009,** *11*, 1091-1094; (b) Nagel, U.; Rieger, B.; Bublewitz, A., *Enantioselektive katalyse: VII. Komplexe von (P (R, S), 3R, 4R, P'(R, S))-3, 4-bis (phenylphosphino) pyrrolidinen. Die darstellung optisch reiner 1, 2-bisphosphanliganden mit vier stereozentren, die zusätzliche funktionnelle gruppen enthalten, J. Organomet. Chem.* **1989,** *370*, 223-239.

(56) (a) Pringle, P. G.; Smith, M. B., *Platinum (0)-catalysed hydrophosphination of acrylonitrile, J. Chem. Soc., Chem. Commun.* **1990**, 1701-1702; (b) Scriban, C.; Kovacik, I.; Glueck, D. S., *A Protic Additive Suppresses Formation of Byproducts in Platinum-Catalyzed Hydrophosphination of Activated Olefins. Evidence for P− C and C− C Bond Formation by Michael Addition, Organometallics* **2005,** *24*, 4871-4874; (c) Wicht, D. K.; Kourkine, I. V.; Lew, B. M.; Nthenge, J. M.; Glueck, D. S., *Platinum-Catalyzed Acrylonitrile*

Hydrophosphination via Olefin Insertion into a Pt− P Bond, J. Am. Chem. Soc. **1997,** *119*, 5039-5040; (d) Wicht, D. K.; Kourkine, I. V.; Kovacik, I.; Glueck, D. S.; Concolino, T. E.; Yap, G. P.; Incarvito, C. D.; Rheingold, A. L., *Platinum-Catalyzed Acrylonitrile Hydrophosphination. P− C Bond Formation via Olefin Insertion into a Pt− P Bond, Organometallics* **1999,** *18*, 5381-5394.

(57) Kovacik, I.; Wicht, D. K.; Grewal, N. S.; Glueck, D. S.; Incarvito, C. D.; Guzei, I. A.; Rheingold, A. L., *Pt (Me-Duphos)-catalyzed asymmetric hydrophosphination of activated olefins: enantioselective synthesis of chiral phosphines, Organometallics* **2000,** *19*, 950-953.

(58) (a) Sadow, A. D.; Togni, A., *Enantioselective addition of secondary phosphines to methacrylonitrile: catalysis and mechanism, J. Am. Chem. Soc.* **2005,** *127*, 17012-17024; (b) Sadow, A. D.; Haller, I.; Fadini, L.; Togni, A., *Nickel (II)-catalyzed highly enantioselective hydrophosphination of methacrylonitrile, J. Am. Chem. Soc.* **2004,** *126*, 14704-14705.

(59) Huang, Y.; Pullarkat, S. A.; Li, Y.; Leung, P.-H., *Palladacycle-Catalyzed Asymmetric Hydrophosphination of Enones for Synthesis of C*- and P*-Chiral Tertiary Phosphines, Inorg. Chem.* **2012,** *51*, 2533-2540.

(60) (a) Huang, Y.; Pullarkat, S. A.; Teong, S.; Chew, R. J.; Li, Y.; Leung, P.-H., *Palladacycle-catalyzed asymmetric intermolecular construction of chiral tertiary P-heterocycles by stepwise addition of H–P–H bonds to bis (enones), Organometallics* **2012,** *31*, 4871-4875; (b) Foo, C. Q.; Sadeer, A.; Li, Y.; Pullarkat, S. A.; Leung, P.-H., *Access to C-Stereogenic PN(sp2)P Pincer Ligands via Phosphapalladacycle Catalyzed Asymmetric Hydrophosphination, Organometallics* **2021,** *40*, 682-692.

(61) (a) Huang, Y.; Pullarkat, S. A.; Li, Y.; Leung, P.-H., *Palladium (II)-catalyzed asymmetric hydrophosphination of enones: efficient access to chiral tertiary phosphines, Chem. Commun.* **2010,** *46*, 6950-6952; (b) Xu, C.; Jun Hao Kennard, G.; Hennersdorf, F.; Li, Y.; Pullarkat, S. A.; Leung, P.-H., *Chiral Phosphapalladacycles as Efficient Catalysts for the*

Asymmetric Hydrophosphination of Substituted Methylidenemalonate Esters: Direct Access to Functionalized Tertiary Chiral Phosphines, Organometallics **2012,** *31*, 3022-3026.

(62) Chew, R. J.; Teo, K. Y.; Huang, Y.; Li, B.-B.; Li, Y.; Pullarkat, S. A.; Leung, P.-H., *Enantioselective phospha-Michael addition of diarylphosphines to β, γ-unsaturated α-ketoesters and amides, Chem. Commun.* **2014,** *50*, 8768-8770.

(63) Huang, Y.; Chew, R. J.; Pullarkat, S. A.; Li, Y.; Leung, P.-H., *Asymmetric synthesis of enaminophosphines via palladacycle-catalyzed addition of Ph2PH to α, β-unsaturated imines, J. Org. Chem.* **2012,** *77*, 6849-6854.

(64) Chew, R. J.; Lu, Y.; Jia, Y. X.; Li, B. B.; Wong, E. H. Y.; Goh, R.; Li, Y.; Huang, Y.; Pullarkat, S. A.; Leung, P. H., *Palladacycle Catalyzed Asymmetric P- H Addition of Diarylphosphines to N-Enoyl Phthalimides, Chem. Eur. J.* **2014,** *20*, 14514-14517.

(65) Chew, R. J.; Huang, Y.; Li, Y.; Pullarkat, S. A.; Leung, P. H., *Enantioselective Addition of Diphenylphosphine to 3-Methyl-4-nitro-5-alkenylisoxazoles, Adv. Synth. Catal.* **2013,** *355*, 1403-1408.

(66) Katona, D.; Lu, Y.; Li, Y.; Pullarkat, S. A.; Leung, P.-H., *Catalytic Approach toward Chiral P,N-Chelate Complexes Utilizing the Asymmetric Hydrophosphination Protocol, Inorg. Chem.* **2020,** *59*, 3874-3886.

(67) Teo, R. H. X.; Chen, H. J.; Li, Y.; Pullarkat, S. A.; Leung, P.-H., *Asymmetric Catalytic 1,2-Dihydrophosphination of Secondary 1,2-Diphosphines – Direct Access to Free P*- and P*,C*-Diphosphines, Adv. Synth. Catal.* **2020,** *362*, 2373-2378.

(68) Seah, J. W. K.; Li, Y.; Pullarkat, S. A.; Leung, P.-H., *Access to a Chiral Phosphine–NHC Palladium(II) Complex via the Asymmetric Hydrophosphination of Achiral Vinyl Azoles, Organometallics* **2021,** *40*, 2118-2122.

(69) Huang, Y.; Chew, R. J.; Li, Y.; Pullarkat, S. A.; Leung, P.-H., *Direct Synthesis of Chiral Tertiary Diphosphines via Pd(II)-Catalyzed Asymmetric Hydrophosphination of Dienones, Org. Lett.* **2011,** *13*, 5862-5865.

(70) Wanzlick, H., *Aspects of nucleophilic carbene chemistry, Angew. Chem. Int. Ed.* **1962,** *1*, 75-80.

(71) Arduengo III, A. J.; Harlow, R. L.; Kline, M., *A stable crystalline carbene, J. Am. Chem. Soc.* **1991,** *113*, 361-363.

(72) (a) Dröge, T.; Glorius, F., *The measure of all rings—N-heterocyclic carbenes, Angew. Chem. Int. Ed.* **2010,** *49*, 6940-6952; (b) Clavier, H.; Nolan, S. P., *Percent buried volume for phosphine and N-heterocyclic carbene ligands: steric properties in organometallic chemistry, Chem. Commun.* **2010,** *46*, 841-861; (c) Kühl, O., *Sterically induced differences in N-heterocyclic carbene transition metal complexes, Coord. Chem. Rev.* **2009,** *253*, 2481-2492; (d) Díez-González, S.; Nolan, S. P., *Stereoelectronic parameters associated with N-heterocyclic carbene (NHC) ligands: A quest for understanding, Coord. Chem. Rev.* **2007,** *251*, 874-883.

(73) Lee, H. M.; Zeng, J. Y.; Hu, C.-H.; Lee, M.-T., *A New Tridentate Pincer Phosphine/N-Heterocyclic Carbene Ligand: Palladium Complexes, Their Structures, and Catalytic Activities, Inorg. Chem.* **2004,** *43*, 6822-6829.

(74) (a) Jalal, M.; Hammouti, B.; Touzani, R.; Aouniti, A.; Ozdemir, I., *Metal-NHC heterocycle complexes in catalysis and biological applications: Systematic review, Materials Today: Proceedings* **2020,** *31*, S122-S129; (b) Glorius, F., *N-Heterocyclic Carbenes in Transition Metal Catalysis*. Springer-Verlag Berlin Heidelberg: 2007; p 232.

(75) Mercs, L.; Albrecht, M., *Beyond catalysis: N-heterocyclic carbene complexes as components for medicinal, luminescent, and functional materials applications, Chem. Soc. Rev.* **2010,** *39*, 1903-1912.

(76) Nair, V.; Vellalath, S.; Babu, B. P., *Recent advances in carbon–carbon bond-forming reactions involving homoenolates generated by NHC catalysis, Chem. Soc. Rev.* **2008,** *37*, 2691-2698.

(77) Saba, S.; Brescia, A.; Kaloustian, M. K., *One-pot synthesis of cyclic amidinium tetrafluoroborates and hexafluorophosphates; the simplest models of N5, N100methenyltetrahydrofolate coenzyme, Tetrahedron Lett.* **1991,** *32*, 5031-5034.

(78) Paczal, A.; Bényei, A. C.; Kotschy, A., *Modular synthesis of heterocyclic carbene precursors, J. Org. Chem.* **2006,** *71*, 5969-5979.

(79) Van Veldhuizen, J. J.; Garber, S. B.; Kingsbury, J. S.; Hoveyda, A. H., *A recyclable chiral Ru catalyst for enantioselective olefin metathesis. Efficient catalytic asymmetric ring-opening/cross metathesis in air, J. Am. Chem. Soc.* **2002,** *124*, 4954-4955.

(80) (a) Alcarazo, M.; Roseblade, S. J.; Alonso, E.; Fernández, R.; Alvarez, E.; Lahoz, F. J.; Lassaletta, J. M., *1, 3-Bis (N, N-dialkylamino) imidazolin-2-ylidenes: Synthesis and reactivity of a new family of stable N-heterocyclic carbenes, J. Am. Chem. Soc.* **2004,** *126*, 13242-13243; (b) Enders, D.; Meiers, M., *Diastereo-and Enantioselective Syntheses of C2-Symmetric 1, n-Diamines by Nucleophilic Addition to Dialdehyde-SAMP-Hydrazones, Synthesis* **2002,** *2002*, 2542-2560.

(81) Seiders, T. J.; Ward, D. W.; Grubbs, R. H., *Enantioselective ruthenium-catalyzed ring-closing metathesis, Org. Lett.* **2001,** *3*, 3225-3228.

(82) Van Veldhuizen, J. J.; Campbell, J. E.; Giudici, R. E.; Hoveyda, A. H., *A readily available chiral Ag-based N-heterocyclic carbene complex for use in efficient and highly enantioselective Ru-catalyzed olefin metathesis and Cu-catalyzed allylic alkylation reactions, J. Am. Chem. Soc.* **2005,** *127*, 6877-6882.

(83) (a) Rivas, F. M.; Riaz, U.; Giessert, A.; Smulik, J. A.; Diver, S. T., *A versatile synthesis of substituted benzimidazolium salts by an amination/ring closure sequence, Org.*

Lett. **2001,** *3*, 2673-2676; (b) Rivas, F. M.; Riaz, U.; Diver, S. T., *Synthesis of chiral N, N′-disubstituted 1, 2-benzenediamines from o-dibromobenzene, Tetrahedron: Asymmetry* **2000,** *11*, 1703-1707.

(84) Tiede, S.; Berger, A.; Schlesiger, D.; Rost, D.; Lühl, A.; Blechert, S., *Highly Active Chiral Ruthenium-Based Metathesis Catalysts through a Monosubstitution in the N-Heterocyclic Carbene, Angew. Chem. Int. Ed.* **2010,** *49*, 3972-3975.

Chapter 2

Asymmetric Hydrophosphination of Achiral Vinyl Azoles

2.1 General Introduction to Phosphine-Azolium Salts

Since the introduction of *N*-heterocyclic carbenes (NHC) from Wanzlick[1] , Lappert[2] , and Arduengo[3] , NHCs have adopted a ubiquitous position of significance in the fields of homogeneous catalysis, organocatalysis and in medical applications.[4] In homogeneous catalysis in particular, NHCs have proven to be a valuable asset in terms of the electronic and steric tunability they offer. While NHCs have been commonly compared to traditional phosphine ligands, important differences exist between these two ligand systems. Electronically, NHCs are stronger σ-donors but weaker π-acceptors than phosphines and are thought to form stronger bonds with metals.[5] The strong bonds between NHCs and metals limit ligand dissociation and subsequently complex decomposition during the catalytic cycle. This is especially beneficial as phosphine ligands, especially electron-rich ones, once dissociated form the metal centre, tend to get oxidized rapidly in the presence of oxidants.[6] Sterically, the substituents on the nitrogen pendant arms in NHCs point towards the coordination sphere of the metal while those on the phosphorus donor atom in phosphines point away from the coordination sphere of the metal.[7] The stark differences between these two systems provide novel and promising opportunities in the fine-tuning of the electronic and steric parameters around a metal centre in a catalytically active complex. Following this idea, several groups have developed synthetic protocols to produce ligand systems bearing both NHC and phosphine moieties.[8]

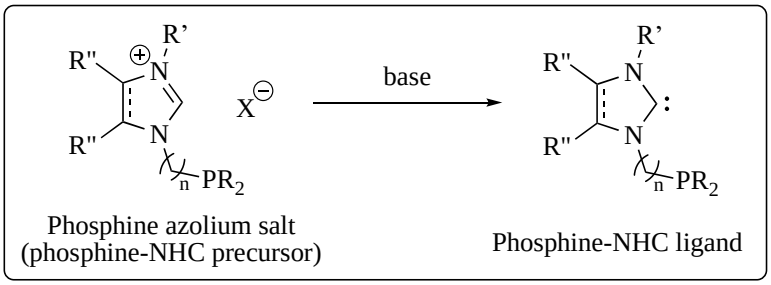

Scheme 2.1 Deprotonation of acidic NC(*H*)N to liberate free NHC.

N-tethered phosphino-azolium salts or phosphine-NHC precursors are also known as the protonated analogues of phosphine-NHC (P-NHC or NHC-P) ligands and this class of salts also happens to be the most widely represented amongst phosphine-containing azolium salts. (Scheme 2.1) Structurally, phosphino-azolium salts contain a phosphine moiety attached to the nitrogen atoms in NHCs *via* at least one carbon linker. These precursors can be deprotonated by a suitable base to give a chelating P-NHC ligand. Due to the increasing interest in such novel chelating ligands, several methodologies have been developed over the years.

2.1.1 Traditional Method of Synthesis *via* Nucleophilic Substitution

Structurally, the overall motif of a phosphino-azolium salt can be obtained from two molecular fragments in a nucleophilic substitution reaction. In this synthetic method, both the phosphine and azole fragments can bifunctionally serve as complementary nucleophile and electrophile. (Scheme 2.2)

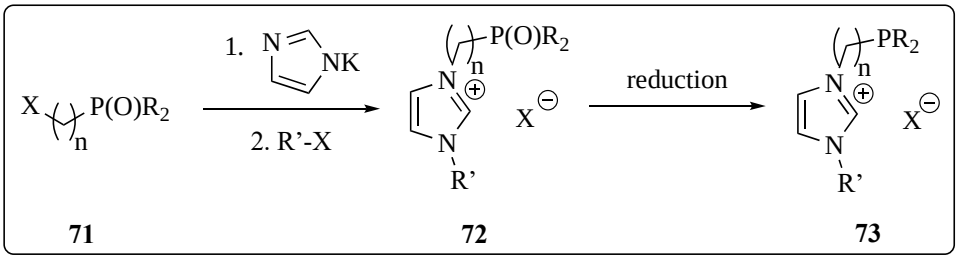

Scheme 2.2 Nucleophilic displacement of halide followed by C-N coupling and reduction of phosphine oxide to furnish phosphine-azolium salt **73**.

Imidazoles can be deprotonated by a strong base to generate the highly nucleophilic anionic imidazolide species which then attacks a phosphine or phosphine oxide species (a subsequent reduction by silanes can be achieved in the latter) bearing a leaving group such as a halide or a hydroxyl group.[9] To avoid harsh reaction conditions for the reduction step, a more generic approach leading to a two- or three-carbon linker-tethered phosphine can be achieved using the following method. Starting from benzimidazole, the nitrogen is first alkylated to give an azole with a leaving group which is subsequently displaced by the lithium salt of a phosphine derivative or a secondary phosphine in the presence of a base to give the final phosphino-azolium salt.[10] (Scheme 2.3)

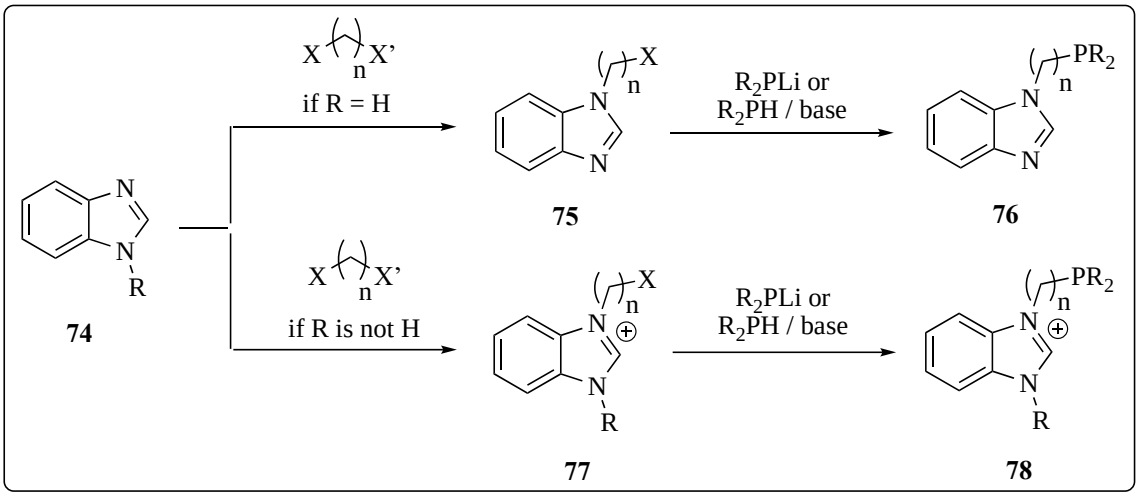

Scheme 2.3 Sequential nucleophilic displacement of halides in a dihalide to afford neutral phosphine-azole **76** and phosphine-azolium salt **78**. Counterion associated with the cation not shown for clarity.

The introduction of chirality can be done using optically pure diamines[11] which are commercially available or a chiral phosphine electrophile. (Scheme 2.4)

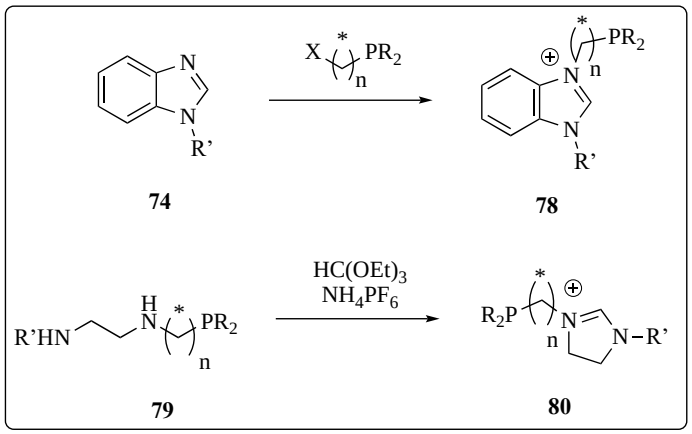

Scheme 2.4 Nucleophilic displacement of halide in a halo-phosphine bearing a chiral element (**78**) and ring closure of a chiral diamine with trialkyl orthoformate (**80**). Counterion associated with the cation not shown for clarity.

Pfaltz and Nanchen made use of a chiral epoxide as the electrophile in the synthesis of a phosphinooxy-NHC salt.[12] *N*-alkylation of imidazole with (*S*)-phenyloxirane followed by quaternization using isopropyliodide and counterion exchange afforded a hydroxy-imidazolium cation. The hydroxyl group was then swapped out with diphenylphosphine-diethylamine in the presence of a base to yield the final phosphinooxy-azolium salt. (Scheme 2.5)

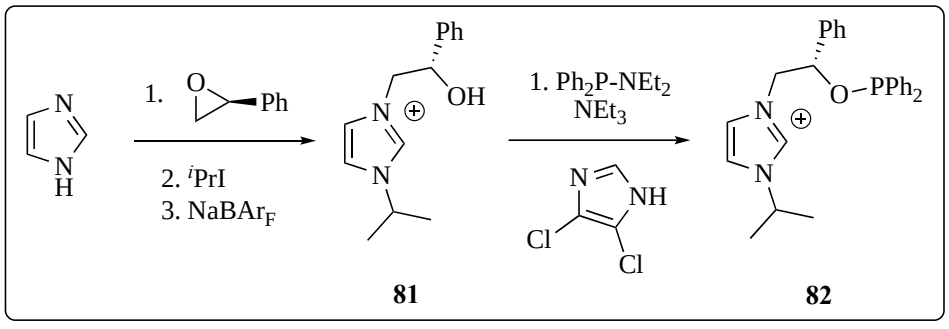

Scheme 2.5 Pfaltz's synthesis of phosphinooxy-azolium salt **82**. Counterion associated with the cation not shown for clarity.

Chiral diamines obtained from the chiral pool can also be alkylated with phosphine or phosphine oxide, followed by a reduction for the latter before the ring is closed to give the desired chiral phosphino-azolium salt.[13] (Scheme 2.6)

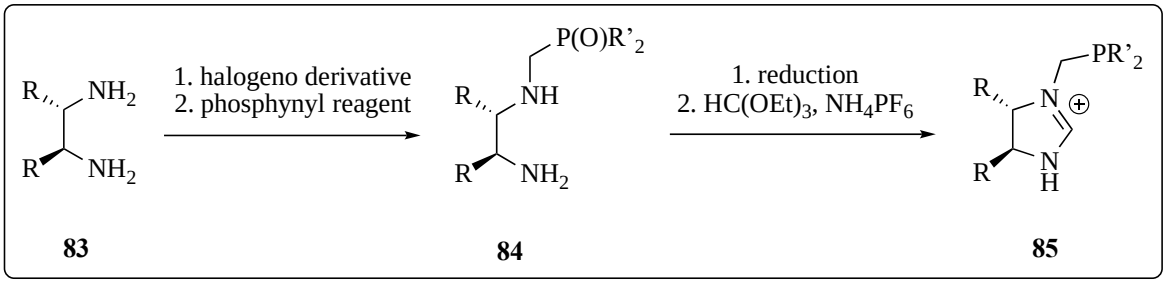

Scheme 2.6 Versatility of chiral diamines as coupling agents to halogen derivatives and phosphynyl agents. Ring closure in subsequent step was achieved using orthoformate ester to give **85**. Counterion associated with the cation not shown for clarity.

Other novel phosphino-azolium salts have also been synthesized by Hodgson and Douthwaite. In those cases, the phosphoramidite was the donating moiety instead of the usual phosphino group.[14] (Scheme 2.7)

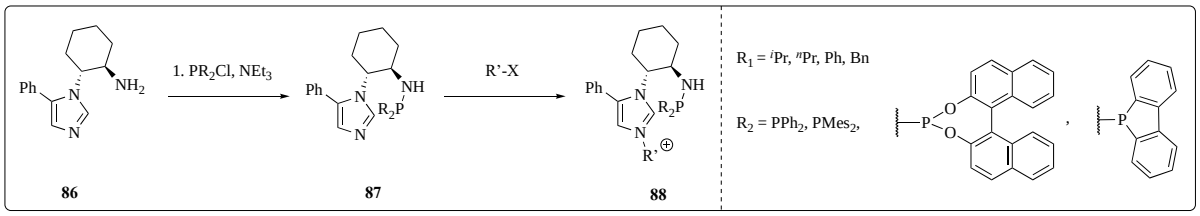

Scheme 2.7 Chiral cyclic diamines as useful tools in the synthesis of phosphine-azolium salt **88**. Counterion associated with the cation not shown for clarity.

Phosphino-azolium salts bearing planar chirality instead of the abovementioned central chirality have also been synthesized using chiral ferrocenyl derivatives.[13a, b, 15] As this form of chirality is not of interest to this project, examples of such planarly chiral salts will not be discussed. Besides bidentate phosphino-azolium salts, analogous achiral and chiral tridentate

bis(phosphine)-azolium salts can also be prepared using the abovementioned methods.[10b, 15-16] (Figure 2.1)

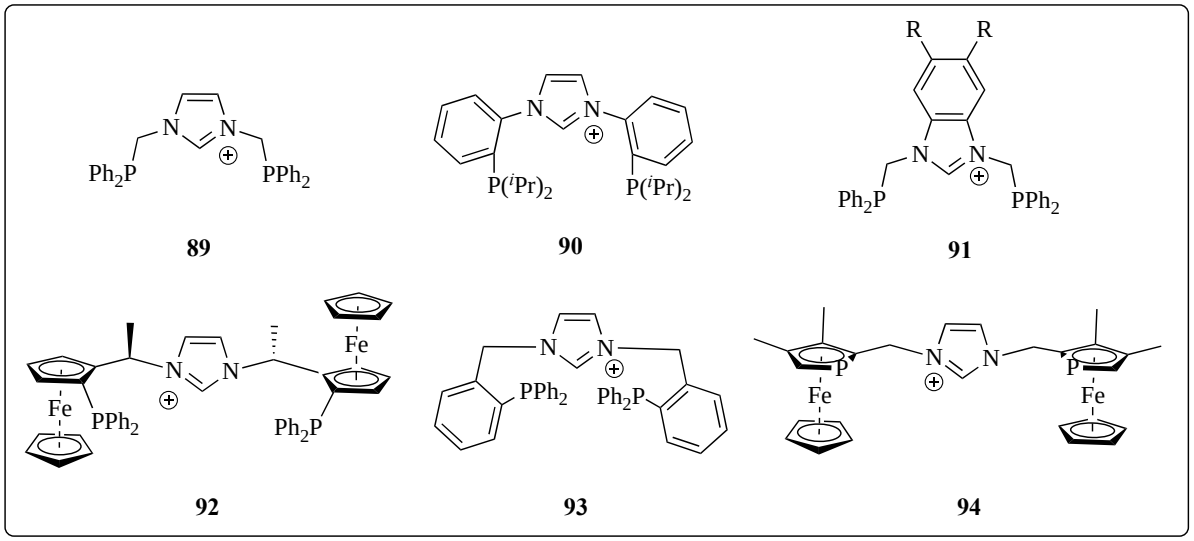

Figure 2.1 Examples of chiral tridentate P-NHC(H)-P systems. Counterion associated with the cation not shown for clarity.

In spite of the successes associated with these methods of accessing phosphino-azolium salts, substitution reactions generally generate a considerable amount of side products and are not atom-economical. In addition, the syntheses of chiral analogues require starting materials from the chiral pool, and this drawback limits the potential to expand the structural diversity of phosphino-azolium salts.

2.1.2 Proposed Novel Method of Synthesis *via* Catalytic Asymmetric Hydrophosphination

Employing catalytic asymmetric hydrophosphination as a valuable methodology described in Chapter 1, it was envisioned that hybrid chiral phosphino-azolium salts could be synthesized from enone-bearing substrate containing an azole group. The general method involves an initial asymmetric hydrophosphination of the enone moiety in the substrate

followed by functionalization at the *N*-terminal to give the desired enantioenriched phosphino-azolium salts. (Scheme 2.8)

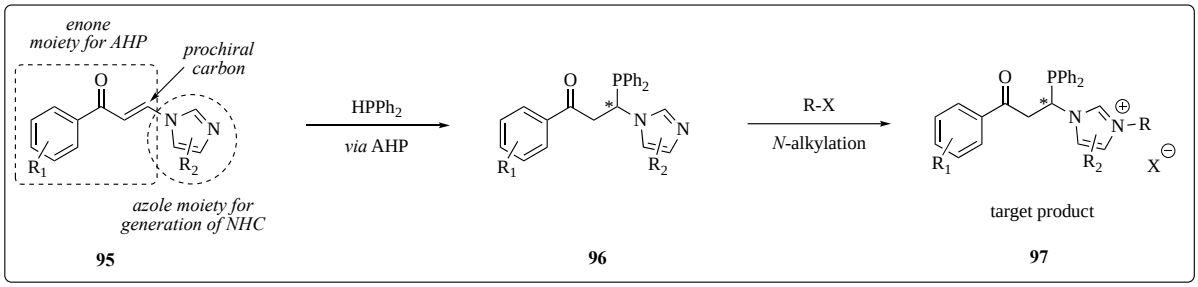

Scheme 2.8 Proposed synthetic method to access chiral phosphine azolium salt **97**.

2.2 Results and Discussion

2.2.1 Substrate Design & Catalytic Asymmetric Hydrophosphination

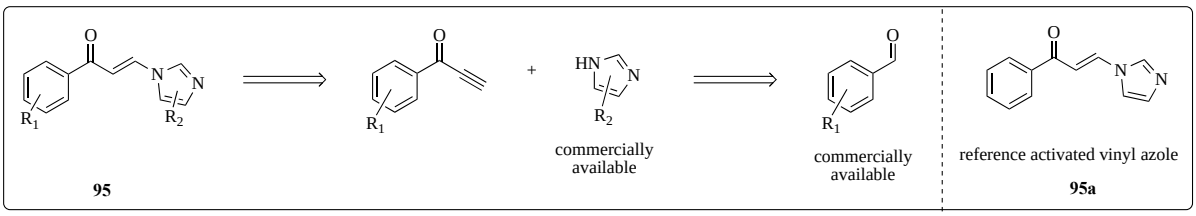

Scheme 2.9 Retrosynthetic analysis of substrate **95** and reference substrate **95a**.

An enone-bearing substrate incorporating an azole group capable of being transformed in further steps into an NHC functional group and a prochiral β-carbon was carefully designed. Reference substrate **95a** was synthesized by combining individual molecular fragments of an azole with an alkyne ketone in a Michael addition reaction. The standard azole and alkyne ketone used were imidazole and 1-phenylprop-2-yn-1-one (R_1 = R_2 = H) respectively. The alkyne ketone could in turn be obtained in a few steps from the commercially available benzaldehyde. (Scheme 2.9)

An initial hydrophosphination of **95a** was attempted using potassium hydroxide in methanol at room temperature. Upon the addition of pulverized potassium hydroxide, the colorless solution turned intense red immediately, indicating the presence of a high concentration of the diphenylphosphine anion, PPh_2^- (*step 1*). The highly nucleophilic PPh_2^- subsequently attacked the β-carbon in **95a** to form the intermediatory phosphino-enolate anion (*step 2*) before reforming the C=O double bond by a proton transfer from water (*step 3*). However, due to the high concentration of the nucleophilic PPh_2^-, an additional undesirable nucleophilic substitution and displacement of the imidazolide leaving group occurred to give the unexpected diphosphine product **98** (*step 4a*). Alternatively, the phosphine azole **96** could also undergo an E1cb mechanism in the presence of a strong base, OH^-, to give an intermediary vinyl phosphine before a final hydrophosphination converted the former to the observed diphosphine **98** (*step 4b*). Due to insufficient experimental data, both mechanisms were deemed possible. Diphosphine **98** was insoluble in the protic methanolic solvent and precipitated out as a highly air-sensitive white solid. Diphosphine **98** was identified *via* recrystallization from tetrahydrofuran and methanol under a protective atmosphere of nitrogen at room temperature over one week. (Scheme 2.10)

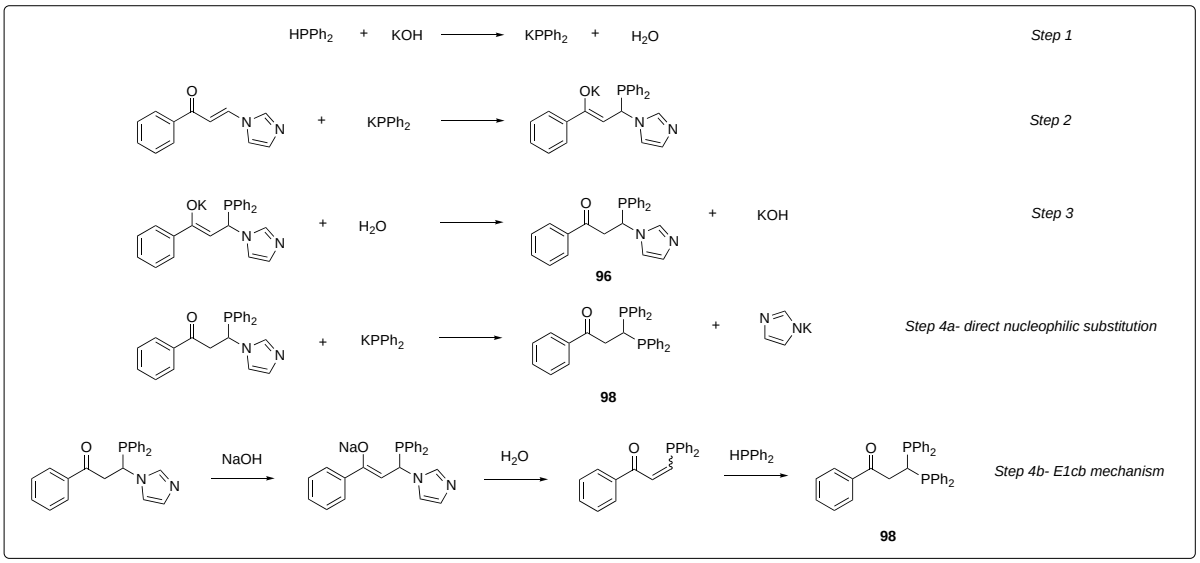

Scheme 2.10 Proposed mechanisms of the formation of **96** and **98** from **95a**.

Initially, to allow step 3 but prevent step 4 from occurring in the proposed mechanism, a weaker base such as triethylamine was substituted for the strongly basic potassium hydroxide. This step was taken in hope that the concentration of PPh_2^- would remain low and hopefully, terminate the hydrophosphination reaction at step 3. However, even with the use of a less basic catalyst, the sole product of the reaction was found to still be the diphosphine.

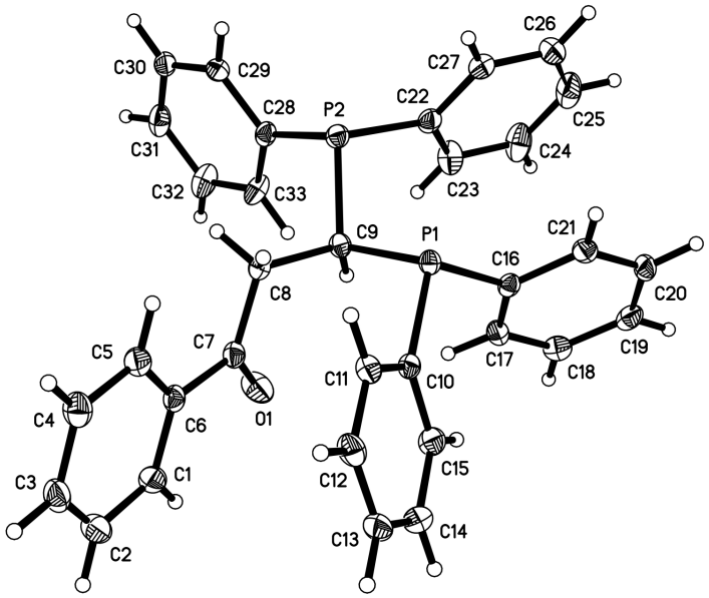

Figure 2.2 Molecular structure of achiral diphosphine **98** with thermal ellipsoids shown at 50% probability.

To obtain the desired phosphine azole intermediate **96** in step 3, attention was then turned to modifying the electrophilicity of the vinyl azole. The main idea was to shut down the rapid and competing step 4 by preventing the formation of the diphenylphosphide anion. Specifically, the nucleophilicity of the phosphine species was reduced while the electrophilicity of the vinyl azole was enhanced; *Brønsted* acid-mediated and several chiral *Lewis*-acidic palladacycles-mediated phosphinations were investigated since their modes of electrophile

activation were believed to be largely similar, that is, *via* the interaction between the hard carbonyl oxygen in the vinyl azole with the acid. (Scheme 2.11)

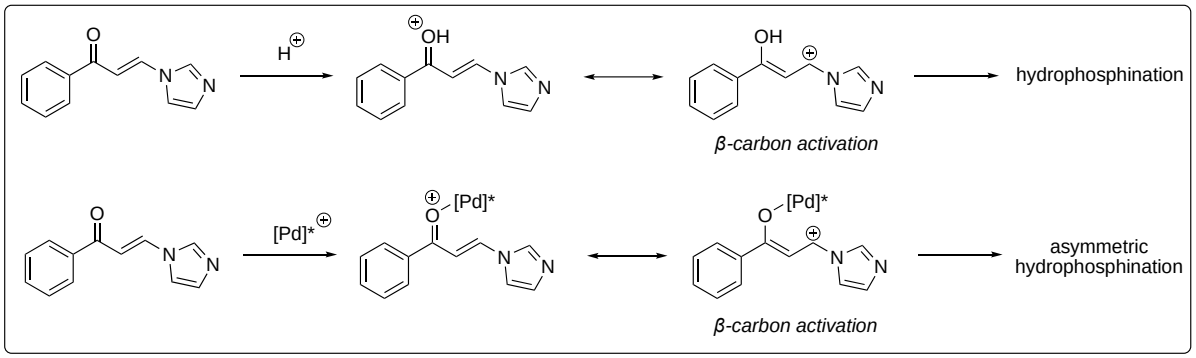

Scheme 2.11 Analogous modes of electrophile activation of **95a** using *Brønsted* and *Lewis* acids.

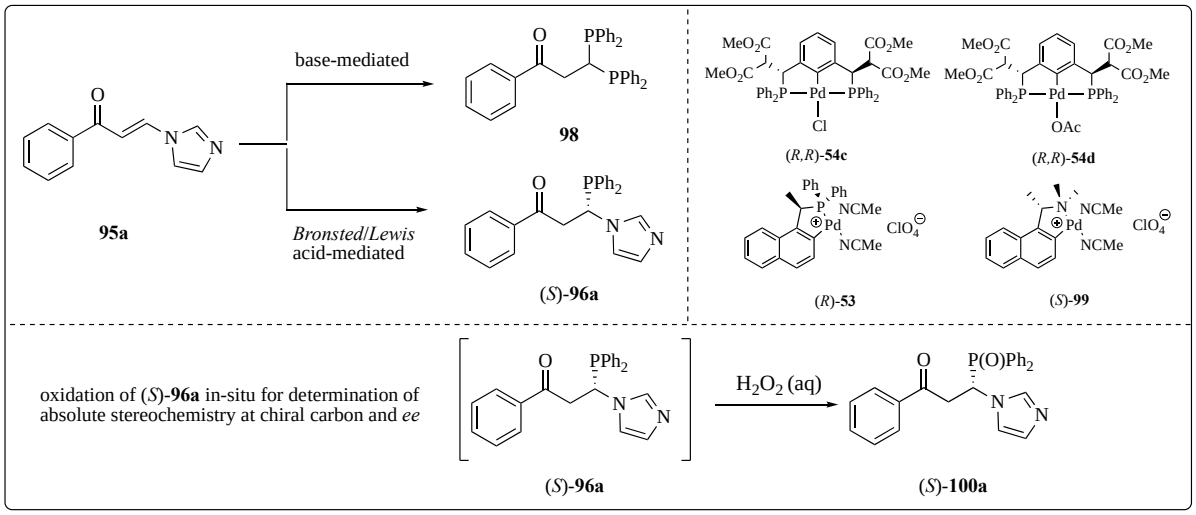

Table 2.1 Divergent pathways of (hydro)phosphination of **95a** and protocol for post analysis of product **96a**.

S/N[a]	Catalyst	Solvent	T/°C	*t*/h	Product	Yield[b]/%	*ee*[c]/%
1	KOH	MeOH	25	8	**98**	>99	0
2	NEt_3	MeOH	25	8	**98**	>99	0
3	$TsOH.H_2O$	MeOH	25	8	**96a**[d]	>99	0

4[e]	(*R*,*R*)-**54c**	THF	25	8	**96a**[f]	35	3
5	(*R*,*R*)-**54d**	THF	25	8	**96a**[f]	93	25
6[e]	(*R*)-**53**	THF	25	8	**96a**[f]	>99	78
7[e]	(*S*)-**99**	THF	25	8	**96a**[f]	75	45[g]

[a] Reactions were carried out with diphenylphosphine (0.0575 mmol), **95a** (0.0575 mmol), catalyst (0.0575 mmol for entries 1-3, and 5 mol% of catalyst for entries 4-7) in the stated solvent (575 μL) at the respective temperature for 8 h. [b] $^{31}P\{^{1}H\}$ NMR yield. [c] Determined by chiral HPLC based on (*S*)-**100a** after a small sample of (*S*)-**96a** was oxidized by 30% w/w aqueous hydrogen peroxide. [d] Racemic **96a** obtained. [e] An external base, NEt_3 (1 equiv.) was required. [f] Enantioenriched **96a** obtained. [g] (*R*)-**100a** was the major enantiomer.

Firstly, the results confirmed the previous hypothesis that the highly nucleophilic PPh_2^- was indeed responsible for the expulsion of the leaving imidazolide group to give the diphosphine product **98** as under highly acidic condition, only the phosphine azole was isolated (entry 3). This shows that while the nucleophilicity of the attacking phosphine was diminished greatly, the β-carbon remained sufficiently activated by the binding of the proton from the tosic acid hydrate to the carbonyl moiety of the vinyl azole. With the chemoselectivity of the hydrophosphination reaction controlled, attention was then shifted towards the utilization of chiral *Lewis*-acidic palladacycles bearing chiral auxiliary ligands in place of tosic acid hydrate to produce enantioenriched **96a** (entries 4-7). Delightfully, all four chiral palladacycles examined were not only able to catalyze the hydrophosphination of the vinyl azole, the phosphine azoles **96a** obtained were also enantioenriched, albeit to different extent. To quantify the enantioselectivity of the hydrophosphination catalyzed by the four chiral palladacycles, a small sample of the phosphine azole **96a** from each trial was oxidized with 30% w/w aqueous hydrogen peroxide to give air-stable phosphine oxide **100a**. Phosphine oxide **100a** was then

purified using silica gel column chromatography to give a pure white solid which were then analyzed spectroscopically for determination of enantiomeric excesses. From the results, palladacycles containing two vacant sites yielded higher enantioselectivity (entries 6 and 7). For tridentate palladacycles, the yield and enantioselectivity were higher when the anionic ligand was acetate instead of chloride (entries 4 and 5). The catalyst which gave the poorest performance was (*R*,*R*)-**54c**, which can be explained by the less labile Pd-Cl bond. Consequentially, catalyst (*R*)-**53** was deemed as the best catalyst for the asymmetric hydrophosphination of vinyl azole **95a** as it afforded the highest yield and enantioselectivity.

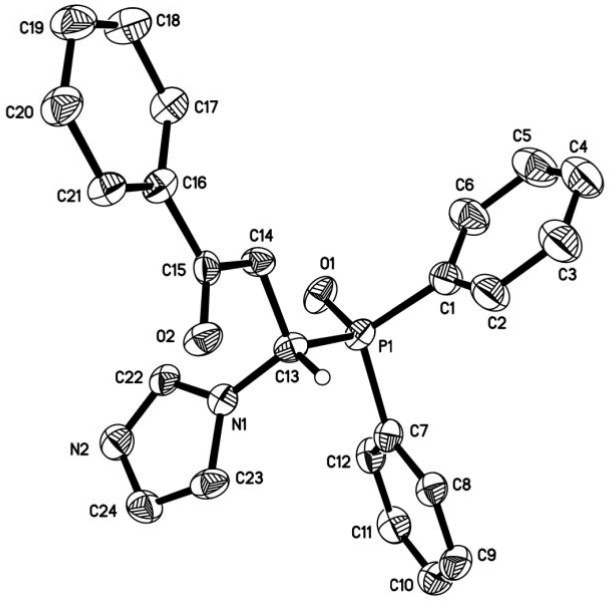

Figure 2.3 Molecular structure of (*S*)-**100a** with thermal ellipsoids shown at 50% probability.

Enantiomerically pure colourless crystals of **100a** were grown *via* evaporation crystallization from a saturated solution of product in a mixture of dichloromethane and hexane at room temperature. The absolute stereochemistry of the chiral carbon centre in the phosphine oxide was determined to be (*S*) *via* X-ray crystallography in the solid state. As oxidation did not alter the stereochemistry at the chiral carbon in **100a**, the absolute stereochemistry of the

chiral carbon in **96a** was determined to be also (*S*), identical to that of the chiral carbon in the oxidized product **100a**.

2.2.2 Optimization of Catalytic Asymmetric Hydrophosphination Conditions

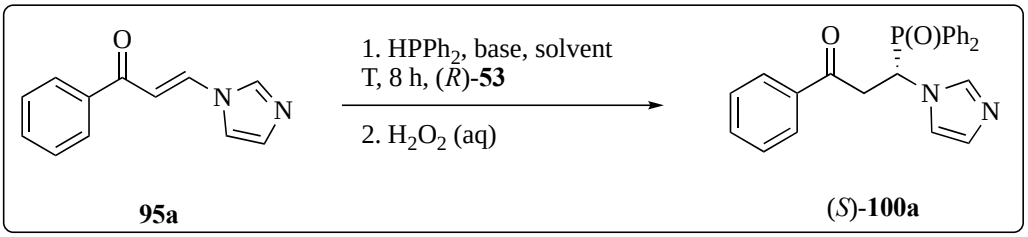

Table 2.2 Asymmetric hydrophosphination and oxidation of vinyl azole **95a**.

S/N[a]	Base	Base/equiv.	(*R*)-**53**/mol%	Solvent	T/°C	Conv.[b]/%	*ee*[c]/%
1	NEt_3	1	5	THF	25	>99	78
2	NEt_3	1	5	CH_2Cl_2	25	>99	80
3	NEt_3	1	5	Me_2CO	25	>99	51
4	NEt_3	1	5	NCMe	25	>99	65
5	NEt_3	1	5	EtOH	25	>99	13
6	NEt_3	1	5	$CHCl_3$	25	>99	75
7	NEt_3	1	5	EtOAc	25	>99	59
8	$^{i}Pr_2NH$	1	5	CH_2Cl_2	25	>99	51
9	TMEDA	1	5	CH_2Cl_2	25	>99	82
10	DBU	1	5	CH_2Cl_2	25	>99	2
11	pyridine	1	5	CH_2Cl_2	25	>99	n.d.[d]
12	NaOAc	1	5	CH_2Cl_2	25	>99	73
13	Na_2CO_3	1	5	CH_2Cl_2	25	>99	69
14	TMEDA	1	5	CH_2Cl_2	0	>99	92
15	TMEDA	1	5	CH_2Cl_2	-40	>99	93
16	TMEDA	1	5	CH_2Cl_2	-78	>99	96

17	TMEDA	1	10	CH_2Cl_2	-78	>99	96
18	TMEDA	1	2.5	CH_2Cl_2	-78	>99	96
19	TMEDA	1	1	CH_2Cl_2	-78	40	96
20	TMEDA	2	2.5	CH_2Cl_2	-78	>99	96
21	TMEDA	1	-	CH_2Cl_2	-78	0	n.d.[e]

[a] Reactions were carried out using vinyl azole **95a** (0.0575 mmol, 1 equiv.) with the stated equivalence of diphenylphosphine, (*R*)-**53** and respective base in the listed solvent (575 µL) at stated temperature for 8 h before being oxidized with one drop of 30% w/w aqueous hydrogen peroxide at the stated temperature. [b] $^{31}P\{^1H\}$ NMR yield. [c] Determined by chiral HPLC. [d] Phosphine oxide **100a** was not formed and side product could not be isolated. [e] No reaction.

Reaction yields with (*R*)-**53** were excellent in all the solvents screened with conversion >99% as deduced from the $^{31}P\{^1H\}$ NMR spectra of the crude mixtures. Enantioselectivities were superior when moderately polar solvents were used (entries 1, 2 and 6) and slightly inferior when highly polar solvents were used (entries 3,4 and 7). In addition, protic ethanol resulted in the lowest enantioselectivity (entry 5). Next, a series of bases were screened, and it was found that in general, the enantioselectivity was not greatly affected by the steric bulk of base (entries 8 and 9). Inorganic bases such as sodium acetate and sodium carbonate suffered from a marginally reduced enantioselectivity possibly due to their poor solubilities in dichloromethane while the strongly basic 1,8-diazabicyclo(5.4.0)undec-7-ene (DBU) resulted in an extremely low enantioselectivity with *ee* of just 2% (entries 10, 12 and 13). When the reaction temperature was gradually reduced, a consistent increase in enantioselectivity was observed alongside no adverse impact to the conversion and reaction rate (entries 14-16). For catalyst loading, a heightened loading of 10 mol% did not further enhance enantioselectivity while a lower loading below 2.5 mol% significantly diminished the reaction rate even though the corresponding enantioselectivity was not compromised (entries 17-19) Base loading did

not influence the conversion and the enantioselectivity significantly (entry 20). Lastly, it should be noted that in the absence of (*R*)-**53**, the vinzyl azole failed to react with diphenylphosphine at -78 °C (entry 21), hence the asymmetric hydrophosphination catalysed by (*R*)-**53** produced a true enantioselective effect in which no background reaction occurred to lower the enantioselectivity of the asymmetric hydrophosphination reaction.

2.2.3 Expansion and Screening of Substrate Scope

Upon optimization of the reaction conditions for the asymmetric hydrophosphination of the reference vinyl azole, a series of vinyl azoles bearing electronically and sterically varied substituents on both the *C*- and *N*-termini were synthesized as shown below. (Scheme 2.12)

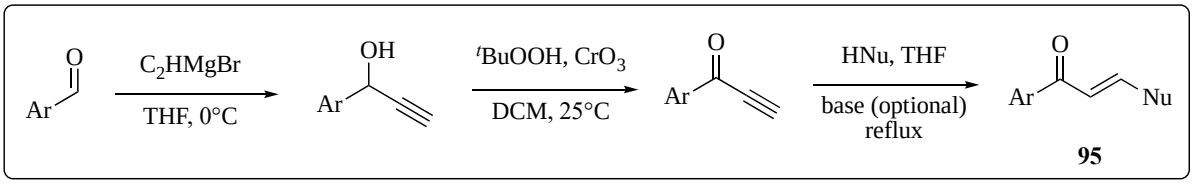

Scheme 2.12 Detailed overall synthetic scheme of vinyl azole derivatives **95** from benzaldehyde derivatives.

Commercially available benzaldehyde and its derivatives were reacted with acetylide Grignard reagent in tetrahydrofuran in the cold before the reaction was raised to room temperature and stirred overnight to furnish the propargylic alcohols. The alcohols were then purified by vacuum distillation before being oxidized by *tert*-butyl hydroperoxide in the presence of a catalytic amount of chromium(VI) oxide to yield the alkyne ketones. The alkyne ketones were then purified using silica gel chromatography before being reacted with a suitable azole in refluxing tetrahydrofuran overnight, in the presence of triethylamine as the catalyst for weakly nucleophilic azoles, to give the final series of functionalized *trans* vinyl azoles **95**. The

vinyl azoles could be easily crystallized from boiling ethanol to give fluffy pale yellow to colorless crystals of analytical purity.

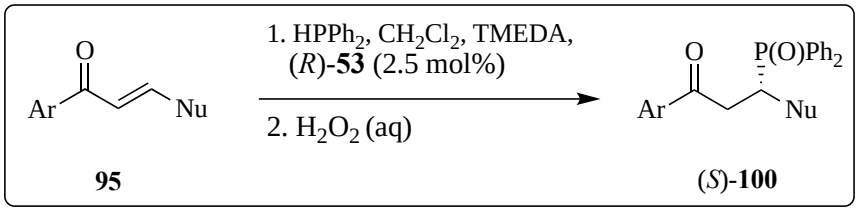

Table 2.4 Asymmetric hydrophosphination of vinyl azole derivatives **95** using the optimized condition.

S/N[a]	substrate	Ar	Nu	T/°C	*t*/h	Yield[c]/%	*ee*[d]/%
1	**95a**	Ph		-78	8	92	96
2[b]	**95b**	Ph		-78	8	78	81
3	**95c**	Ph	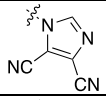	-78	8	0	n.d.[f]
4	**95d**	Ph	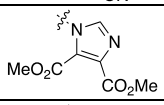	-78	8	76	90
5[b]	**95e**	Ph	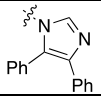	-40	8	89	91
6	**95f**	Ph		-78	8	33	3
7	**95g**	Ph		-78	8	0	n.d.[f]
8[b]	**95h**	Ph	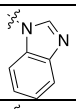	-78	8	81	94
9[g]	**95i**	4-MeC$_6$H$_4$	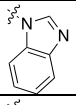	-20	14	87	69
10[g]	**95j**	4-^{i}PrC$_6$H$_4$	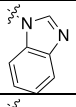	-20	14	77	69
11[g]	**95k**	4-^{t}BuC$_6$H$_4$	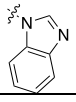	-20	14	88	70

12[g]	**95l**	4-FC_6H_4	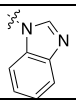	-20	14	88	65
13[g]	**95m**	4-ClC_6H_4	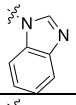	-20	14	96	69
14[g]	**95n**	4-$CO_2MeC_6H_4$	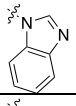	-20	14	79	2
15[g]	**95o**	4-$OMeC_6H_4$	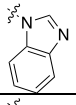	-20	14	22	65
16[g]	**95p**	4-PhC_6H_4	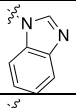	-20	14	70	71
17[g]	**95q**	2-Napthyl	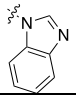	-20	14	88	71

[a] Reactions were carried out with diphenylphosphine (0.0575 mmol), (*R*)-**53** (2.5 mol%) and base (0.0575 mmol) in CH_2Cl_2 (575 µL) and the listed vinyl azoles **95a** to **q** (0.0575 mmol) at stated temperature for the stated duration before being oxidized with 30% w/w aqueous hydrogen peroxide at the stated temperature. [b} 1150 µL of CH_2Cl_2 was used. [c] Isolated yield of phosphine oxide. [d] Determined by chiral HPLC based on (*S*)-**100a** to **q**. [e] Reaction was halted after 96 h. [f] Phosphine oxide product not formed. [g] 2000 µL of CH_2Cl_2 was used.

For the azolyl-functionalized (*N*-functionalized) substrates, the results show that for electronically, electron-withdrawing substituents generally had an accelerated rate and better enantioselectivity as compared to electron-donating substituents. This was expected as electron-withdrawing groups lower the LUMO of the electrophile so the attacking phosphine could interact more strongly with its HOMO. The highly electron-rich **95f** was so weakly electrophilic that it only managed to give a yield of 33% after 96 h. Notably, highly electron-withdrawing substituents on the activated olefins such as the dicyano and triazolyl groups led to no formation of product. The crude reaction mixtures containing the dicyano and triazolyl substrates showed the lack of the characteristic diastereotopic proton peaks present in the desired phosphine oxide products. This might be due to the cleavage of the C-N bond favored

by the highly electronic-deficient leaving groups. The side products of these reactions were not identified and isolated. Sterically, bulky substituent such as diphenyl on the activated olefin gave roughly the same enantioselectivity (*ee* of 91%) as those olefins with a less bulky substituent such as hydrogen (*ee* of 96%), signaling that the enantioselectivity and rate of the asymmetric hydrophosphination of such activated olefins was more sensitive towards the electronic structure than the steric bulk of the substrates.

For the aryl-functionalized (*C*-functionalized) substrates, the observed trend in reactivity, enantioselectivity and yield paralleled that of the azolyl-functionalized analogues. However, due to the significantly reduced solubilities of the azolyl-functionalized substrates at extremely low temperatures, the reaction temperature and time had to be increased from -78 °C to -20 °C and from 8 h to 14 h respectively and more solvent had to be used in the asymmetric hydrophosphination reaction. Even though the enantioselectivities of the reaction diminished slightly due to the higher reaction temperature, the *ee* values were still considerably good, ranging from 65 to 71% across a broad spectrum of electron-rich and electron-deficient substrates except **95n**, whose extremely low *ee* might be attributed to a lack of stereochemical differentiation in the chirality induction step and not a background reaction as confirmed in a separate control reaction. These *ee* values were absolute as it was also determined in a separate experiment that the asymmetric hydrophosphination of substrate **95a** did not proceed at -20 °C.

2.2.4 *N*-alkylation of Phosphine Azoles

Next, *N*-alkylation of the enantioenriched phosphine azole, after removal of the solvent and base under an inert atmosphere of nitrogen, was attempted using different alkylating agents. (*S*)-**96a** was used as the reference standard in this section.

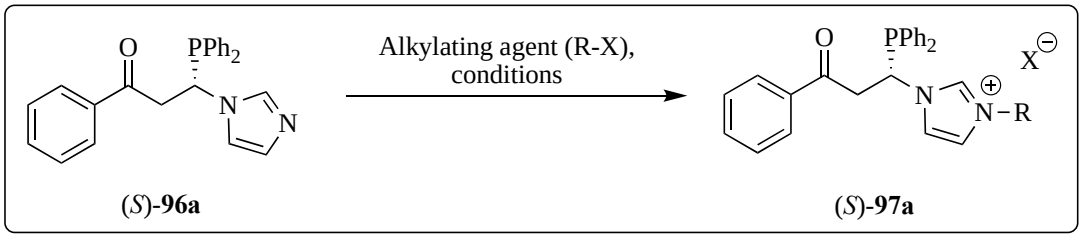

Table 2.5 *N*-alkylation of standard enantioenriched phosphine azole (*S*)-**96a** to give phosphine azolium salt (*S*)-**97a**.

S/N	R-X	Additive (1 equiv.)	Reaction conditions	Results
1	1-Adamantyl iodide	AgOTf	25 °C, dark, CH_2Cl_2, 6 h	n.r.
2	Trityl chloride	AgOTf	25 °C, dark, CH_2Cl_2, 6 h	Messy
3	Benzyl bromide	AgOTf	25 °C, dark, CH_2Cl_2, 6 h	n.r.
4	Methyl iodide	AgOTf	25 °C, dark, CH_2Cl_2, 6 h	n.r.
5	Methyl triflate	-	25 °C, CH_2Cl_2, 5 h	New $^{31}P\{^1H\}$ resonance signals at -4 ppm and 27 ppm
6	Methyl triflate	-	-40 °C, CH_2Cl_2, 5 h	New $^{31}P\{^1H\}$ resonance signal at -4 ppm

Generally, the alkylation process of the phosphine azole (*S*)-**96a** presented two significant issues. Firstly, the need for selective alkylation at both nucleophilic *N*- and *P*-termini was crucial and secondly, for alkylation at the *N*-terminal to occur, a strongly electrophilic alkylating agent had to be used since the nitrogen in the azole moiety was weakly nucleophilic by virtue of its lone pair of electrons in a low energy sp^2 hybrid orbital. In the optimization step of the alkylation process, relatively bulky alkylating agents did not produce the intended product even with the inclusion of a halide abstracting agent, silver(I) triflate. (entries 1-3) Subsequently, attention was turned to more electrophilic alkylating agents such as methyl iodide and methyl triflate. Methyl iodide was not useful as the alkylating agent, unlike

methyl triflate which featured an excellent leaving group. Methylation using methyl triflate at room temperature led to a small amount of phosphonium salt being formed due to the extreme reactivity of methyl triflate. The $^{31}P\{^{1}H\}$ resonance signals at -4 ppm and 27 ppm observed in the crude mixture from entry 5 corresponded to the methylated nitrogen in (*S*)-**97a** and methylated phosphine species respectively. To increase the selectivity of the methylation step, the reaction temperature was reduced to -40 °C, and fortunately, only the methylated nitrogen species was obtained as the sole product. Spectroscopically, the ^{1}H spectrum of the crude mixture exhibited a new resonance signal at 10.6 ppm after methylation, which corresponded to the NC(*H*)N proton and another signal at 4.17 ppm, which corresponded to the methyl group on the nitrogen pendant arm. The set of three protons corresponding to the pair of diastereotopic protons and the proton adjacent to the phosphine functional group was also detected. The *N*-methylated phosphine azole (*S*)-**97a** was a highly air-sensitive sticky solid that could not be isolated in pure form but it could be used directly *in situ* for further transformations. (see Chapter 3)

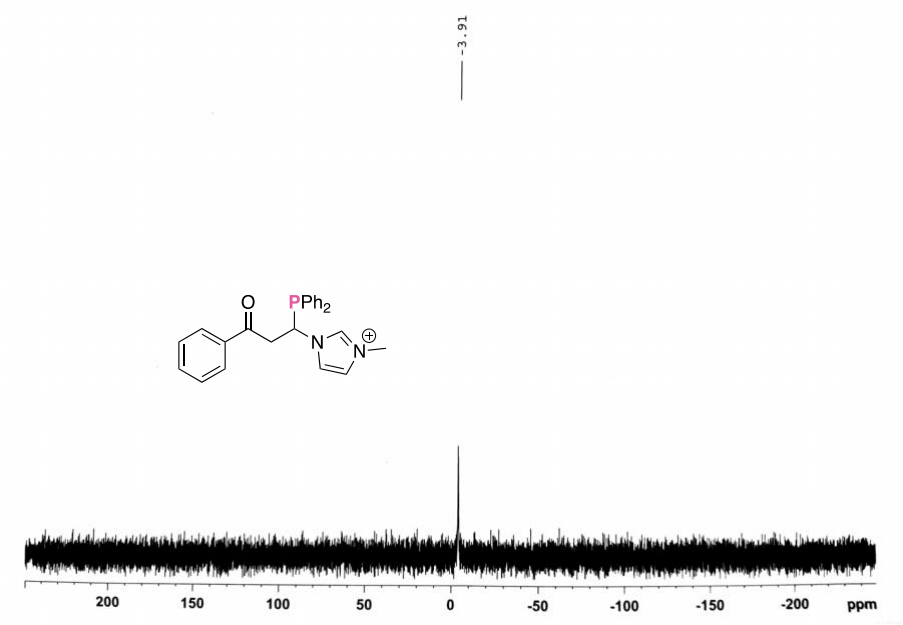

Figure 2.6 $^{31}P\{^{1}H\}$ NMR spectrum of (*S*)-**97a**.

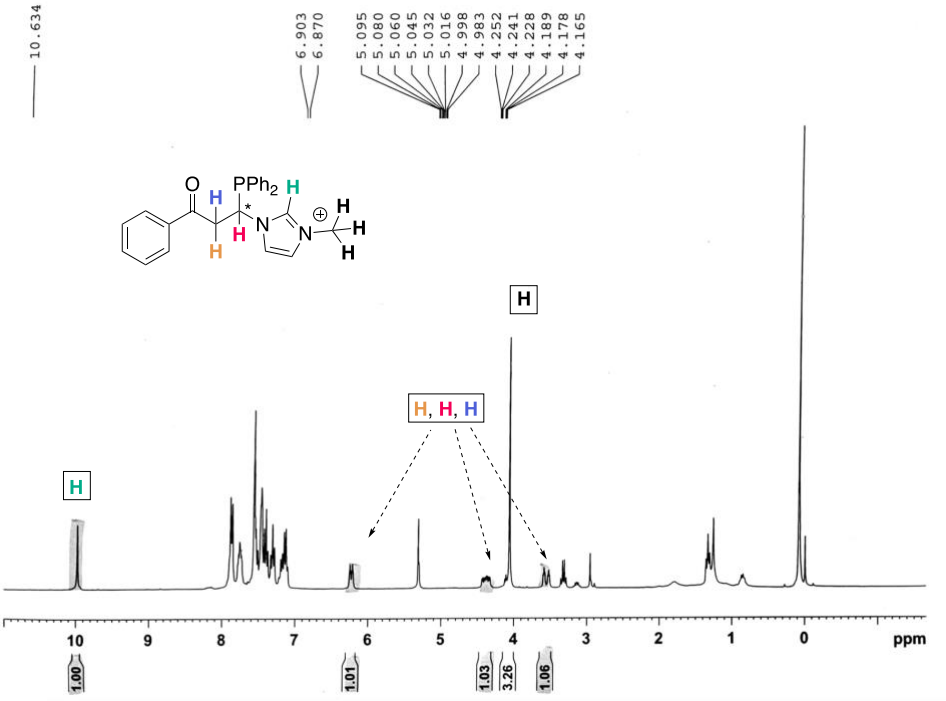

Figure 2.7 ^{1}H NMR spectrum of (*S*)-**97a**.

2.3 Conclusion

In conclusion, the effects of base, acid and a *Lewis*-acidic palladacycle on the chemoselectivity of the hydrophosphination of a series of activated vinyl azoles were discussed. The mechanisms of the hydrophosphination and diphosphination were also illustrated. A myriad of chiral palladacycles and substrates, both *N*- and *C*-functionalized, were synthesized and the effects of steric bulk and electronics of the substrates on the rate and enantioselectivity of the asymmetric hydrophosphination were mentioned. Challenges associated with the alkylation at the *N*-terminal of the resulting phosphine azoles were also overcome using a highly electrophilic methylating agent. The final highly enantioenriched phosphino-azolium salt was synthesized with excellent yield even though it could not be purified and isolated. Crude $^{31}P\{^{1}H\}$ and ^{1}H NMR spectral evidence to support the formation of the phosphino-azolium salt were instead provided.

Experimental Section

Unless otherwise stated, all reactions were carried out under a positive pressure of nitrogen using standard Schlenk techniques. Solvents were purchased from their respective companies (MeOH: Fulltime Reagent, DCM, EA: Fisher Chemicals, Toluene, n-hexane: Avantor, THF: Schedelco, Acetone: VWR Chemicals) and used as supplied. Prior to use, all solvents intended for air sensitive reactions were dried and distilled or degassed where necessary. A PSL-1820 Low Temp Pairstirrer was used for conducting low temperature reactions. Thin layer chromatography (TLC) was done using Merck silica gel 60 F254 aluminium supported plates. Flash column chromatography was performed using Merck silica gel 60. NMR spectra were obtained using Bruker AV 300 (^{1}H at 300 MHz, ^{13}C{^{1}H} at 75 MHz, ^{31}P{^{1}H} at 121 MHz); AV 400 (^{1}H at 400 MHz, ^{13}C{^{1}H} at 100 MHz, ^{31}P{^{1}H} at 162 MHz), AV 500 (^{1}H at 500 MHz, ^{13}C{^{1}H} at 125 MHz, ^{31}P{^{1}H} at 202 MHz) and BBFO (^{1}H at 400 MHz, ^{13}C{^{1}H} at 100 MHz, ^{31}P{^{1}H} at 161 MHz) spectrometers. Chemical shifts were reported in ppm and referenced to an internal $SiMe_4$ standard at δ 0 ppm, or to the residual proton signals of the respective deuterated solvents for ^{1}H and ^{13}C{^{1}H} NMR. Melting points were measured using an SRS Optimelt Automated Point System SRS MPA100m machine. Chiral high-performance liquid chromatography (HPLC) data were acquired using an Agilent Technologies 1200 Series HPLC machine with Daicel CHIRALPAK I-series columns. Optical rotations were measured with a JASCO P-1030 Polarimeter in the specified solvent and concentration in a 0.1 dm cell at 25.0^{o}C unless otherwise stated.

General synthesis of substrates **95a** to **h**

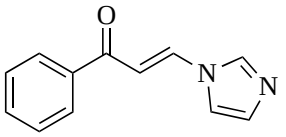

Adapted from literature and procedure was modified slightly.[17] A 50 mL round-bottomed flask was charged with phenyl propargyl ketone (0.5 g, 3.84 mmol) and THF (30 mL). After which, imidazole (0.314 g, 4.61 mmol, 1.2 equiv.) was added. The reaction was heated under reflux overnight. Volatiles were removed under reduced pressure and the crude product was purified using silica gel chromatography (4 DCM:1 EA) to give pure **95a**.

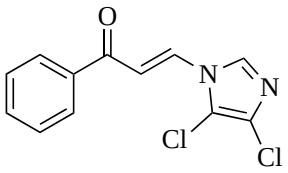

A 50 mL round-bottomed flask was charged with phenyl propargyl ketone (0.5 g, 3.84 mmol) and THF (30 mL). After which, 4,5-dichloroimidazole (0.631 g, 4.61 mmol, 1.2 equiv.) and triethylamine (0.26 mL, 1.92 mmol, 0.5 equiv.) were added. The reaction was heated under reflux overnight. Volatiles were removed under reduced pressure and the crude product was purified using silica gel chromatography (4 DCM:1 EA) to give pure **95b**.

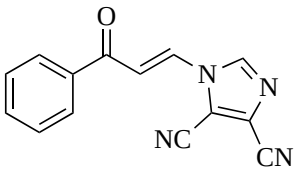

A 50 mL round-bottomed flask was charged with phenyl propargyl ketone (0.5 g, 3.84 mmol) and THF (30 mL). After which, 4,5-dicyano-1H-imidazole (0.544 g, 4.61 mmol, 1.2 equiv.)

and triethylamine (0.26 mL, 1.92 mmol, 0.5 equiv.) were added. The reaction was heated under reflux overnight. Volatiles were removed under reduced pressure and the crude product was purified using silica gel chromatography (4 DCM:1 EA) to give pure **95c**.

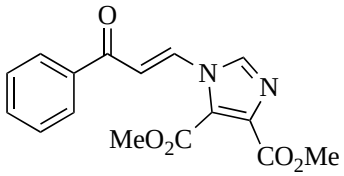

A 50 mL round-bottomed flask was charged with phenyl propargyl ketone (0.5 g, 3.84 mmol) and THF (30 mL). After which, dimethyl imidazole-4,5-dicarboxylate (0.849 g, 4.61 mmol, 1.2 equiv.) and triethylamine (0.26 mL, 1.92 mmol, 0.5 equiv.) were added. The reaction was heated under reflux overnight. Volatiles were removed under reduced pressure and the crude product was purified using silica gel chromatography (4 DCM:1 EA) to give pure **95d**.

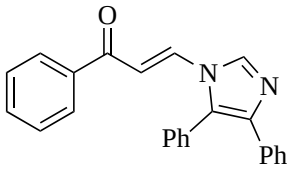

A 50 mL round-bottomed flask was charged with phenyl propargyl ketone (0.5 g, 3.84 mmol) and THF (30 mL). After which, 4,5-diphenyl-1H-imidazole (1.015 g, 4.61 mmol, 1.2 equiv.) was added. The reaction was heated under reflux overnight. Volatiles were removed under reduced pressure and the crude product was purified using silica gel chromatography (4 DCM:1 EA) to give pure **95e**.

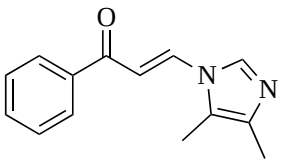

A 50 mL round-bottomed flask was charged with phenyl propargyl ketone (0.5 g, 3.84 mmol) and THF (30 mL). After which, 4,5-dimethylimidazole (0.443 g, 4.61 mmol, 1.2 equiv.) was added. The reaction was heated under reflux overnight. Volatiles were removed under reduced pressure and the crude product was purified using silica gel chromatography (4 DCM:1 EA) to give pure **95f**.

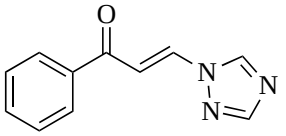

A 50 mL round-bottomed flask was charged with phenyl propargyl ketone (0.5 g, 3.84 mmol) and THF (30 mL). After which, 1,2,4-triazole (0.381 g, 4.61 mmol, 1.2 equiv.) and triethylamine (0.26 mL, 1.92 mmol, 0.5 equiv.) were added. The reaction was heated under reflux overnight. Volatiles were removed under reduced pressure and the crude product was purified using silica gel chromatography (4 DCM:1 EA) to give pure **95g**.

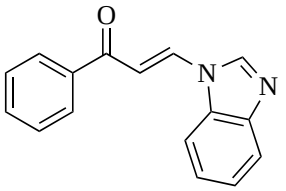

A 50 mL round-bottomed flask was charged with phenyl propargyl ketone (0.5 g, 3.84 mmol) and THF (30 mL). After which, benzimidazole (0.544 g, 4.61 mmol, 1.2 equiv.) and triethylamine (0.26 mL, 1.92 mmol, 0.5 equiv.) were added. The reaction was heated under

reflux overnight. Volatiles were removed under reduced pressure and the crude product was purified using silica gel chromatography (4 DCM:1 EA) to give pure **95h**.

General synthesis of substrates **95i** to **q**

A 50 mL round-bottomed flask was charged with the respective alkyne ketone (3.5 mmol) and THF (30 mL). After which, benzimidazole (0.455 g, 3.85 mmol, 1.1 equiv.) and triethylamine (0.24 mL, 1.75 mmol, 0.5 equiv.) were added. The reaction was heated under reflux for 4 h. Volatiles were removed under reduced pressure and the crude product was purified using silica gel chromatography (4 DCM:1 EA) to give pure substrates **95i** to **q**.

Characterisation of substrates **95a** to **q**

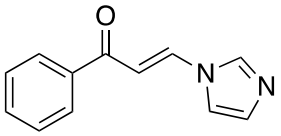

95a. Pale yellow solid. Yield: 0.457 g, 2.30 mmol, 60%. ^{1}H NMR (CD_2Cl_2, 500 MHz): δ 7.17, 7.21 (m, 2H), 7.41 (s, 1H), 7.53 (t, 2H, J_{HH} = 7.4 Hz), 7.63 (t, 1H, J_{HH} 7.0 = Hz), 7.86 (s, 1H), 7.99 (d, 2H, J_{HH} = 7.4 Hz), 8.04 (d, 1H, J_{HH} = 14 Hz); ^{13}C{^{1}H} NMR ($CDCl_3$, 75 MHz): δ 110., 116.3, 128.3, 128.8, 132.0, 133.4, 136.7, 137.6, 138.4, 188.9; HRMS (+ESI) m/z: (M + H)+ calcd for $C_{12}H_{11}N_2O$, 199.0871; found, 199.0871.

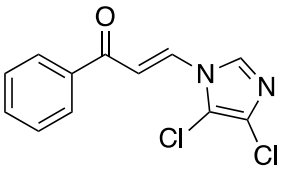

95b. Off-white solid. Yield: 0.563 g, 2.11 mmol, 55%. ^{1}H NMR (CD_2Cl_2, 500 MHz): δ 7.44 (d, 1H, J_{HH} = 14 Hz), 7.55 (t, 2H, J_{HH} = 7.3 Hz), 7.66 (t, 1H, J_{HH} = 7.1 Hz), 7.92 - 7.96 (m, 2H), 8.01 (d, 2H, J_{HH} = 7.4 Hz); ^{13}C{^{1}H} NMR (CD_2Cl_2, 125 MHz): δ 113.1, 114.6, 128.7, 129.1, 129.3, 133.6, 133.8, 134.0, 137.6, 188.4; HRMS (+ESI) m/z: (M + H)+ calcd for $C_{12}H_9N_2OCl_2$, 267.0092; found, 267.0093.

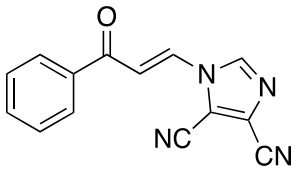

95c. Yellow solid. Yield: 0.315 g, 1.27 mmol, 33%. ^{1}H NMR (CD_2Cl_2, 500 MHz): δ 7.58 (t, 2H, J_{HH} = 7.6 Hz), 7.69 - 7.76 (m, 2H), 7.96 - 8.02 (m, 3H), 8.14 (s, 1H); ^{13}C{^{1}H} NMR ($CDCl_3$, 75 MHz): δ 107.8, 110.7, 116.9, 125.6, 128.6, 129.2, 132.5, 134.5, 136.3, 140.4, 140.7, 186.9; HRMS (+ESI) m/z: (M + H)+ calcd for $C_{14}H_9N_4O$, 249.0776; found, 249.0775.

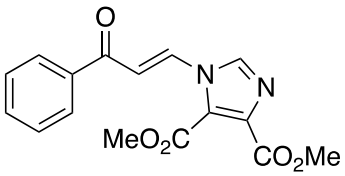

95d. White solid. Yield: 0.761 g, 2.42 mmol, 63%. ^{1}H NMR (CD_2Cl_2, 500 MHz): δ 3.90 (s, 3H, CO_2Me), 3.95 (s, 3H, CO_2Me), 7.33 (d, 1H, J_{HH} =14.4 Hz), 7.55 (t, 2H, J_{HH} = 7.4 Hz), 7.64 (d, 1H, J_{HH} = 6.8 Hz), 7.98 (d, 2H, J_{HH} = 7.5 Hz), 8.10 (s, 1H), 8.29 (d, 1H, J_{HH} = 14.5 Hz); ^{13}C{^{1}H} NMR ($CDCl_3$, 75 MHz): δ 52.6, 53., 115.7, 125.2, 128.5, 128.9, 133.7, 135.5,

136.7, 137.0, 137.9, 159.7, 162.0, 188.3; HRMS (+ESI) m/z: (M + H)+ calcd for $C_{16}H_{15}N_2O_5$, 315.0981; found, 315.0981.

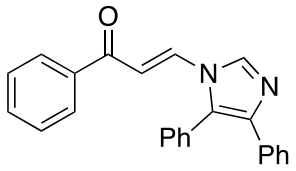

95e. White solid. Yield: 0.673 g, 1.92 mmol, 50%. ^{1}H NMR (CD_2Cl_2, 500 MHz): δ 7.10 (d, 1H, J_{HH} = 14 Hz), 7.11-7.42 (m, 3H), 7.48 -7.61 (m, 10H), 7.70 (d, 1H, J_{HH} = 14 Hz), 7.86 (d, 2H, J_{HH} = 7.6 Hz), 8.17 (s, 1H); ^{13}C{^{1}H} NMR (CD_2Cl_2, 125 MHz): δ 110.8, 126.8, 127.1, 128.1, 128.1, 128.1, 128.7, 129.3 129. 4, 129.5, 131.2, 133.1, 133.6, 135.3, 135.7, 137.6, 139.9, 188.5; HRMS (+ESI) m/z: (M + H)+ calcd for $C_{24}H_{19}N_2O$, 351.1491; found, 351.1494.

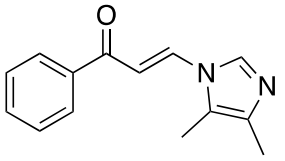

95f. Yellow solid. Yield: 0.200 g, 0.883 mmol, 23%. ^{1}H NMR (CD_2Cl_2, 500 MHz): δ 2.15 (s, 3H), 2.28 (s, 3H), 7.22 (d, 1H, J_{HH} = 14 Hz), 7.53 (t, 2H, J_{HH} = 7.8 Hz), 7.62 (m, 1H), 7.90 (m, 2H), 7.97 (d, 2H, J_{HH} = 7.5 Hz); ^{13}C{^{1}H} NMR ($CDCl_3$, 75 MHz): δ 8.9, 12.6, 109.1, 122.8 (s), 128.3, 128.8, 133.2, 133.5, 135.9, 136.4, 137.8, 189.0; HRMS (+ESI) m/z: (M + H)+ calcd for $C_{14}H_{15}N_2O$, 227.1184; found, 227.1177.

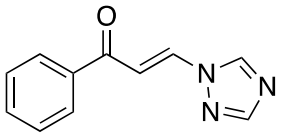

95g. White solid. Yield: 0.275 g, 1.38 mmol, 36%. ^{1}H NMR (CD_2Cl_2, 500 MHz): δ 7.54 (t, 2H J_{HH} = 7.5 Hz), 7.63 (t, 1H, J_{HH} = 7.2 Hz), 7.75 (d, 1H, J_{HH} = 13.5 Hz), 8.03-8.15 (m, 4H), 8.43 (s, 1H); ^{13}C{^{1}H} NMR ($CDCl_3$, 75 MHz): δ 113.3, 128.6, 128.9, 133.6, 134.8, 137.3, 145.1, 153.6, 188.8; HRMS (+ESI) m/z: (M + H)+ calcd for $C_{11}H_{10}N_3O$, 200.0824; found, 200.0824.

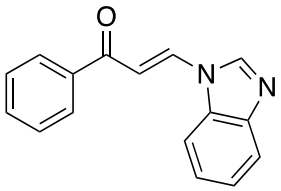

95h. White solid. Yield: 0.467 g, 1.96 mmol, 51%. ^{1}H NMR (CD_2Cl_2, 500 MHz): δ 7.40-7.47 (m, 3H), 7.56 (t, 2H, J_{HH} = 7.3 Hz), 7.64 (t, 1H, J_{HH} = 6.8 Hz), 7.78 (d, 1H, J_{HH} = 8 Hz), 7.83 (d, 1H, J_{HH} = 8 Hz), 8.05 (d, 2H, J_{HH} = 7.4 Hz), 8.33 (d, 2H, J_{HH} = 12 Hz); ^{13}C{^{1}H} NMR ($CDCl_3$, 75 MHz): δ 109.0, 111.3, 121.3, 124.5, 125.1, 128.3, 128.9, 132.4, 133.3, 135.7, 137.8, 141.7, 144.7, 189.0; HRMS (+ESI) m/z: (M + H)+ calcd for $C_{16}H_{13}N_2O$, 249.1028; found, 249.1036.

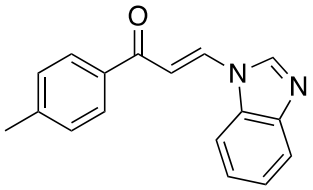

95i. White solid. Yield: 0.376 g, 1.44 mmol, 41%. ^{1}H NMR (CD_2Cl_2, 400 MHz): δ 2.45 (s, 3H), 7.35-7.48 (m, 5H), 7.77 (d, 1H, J_{HH} = 7.9 Hz), 7.82 (d, 1H, J_{HH} = 8 Hz), 7.95 (d, 2H, J_{HH} = 8.2 Hz), 8.29-8.32 (m, 2H); ^{13}C{^{1}H} NMR (CD_2Cl_2, 100 MHz): δ 21.8, 109.5, 111.8, 121.3, 124.6,

125.2, 128.7, 129.9, 132.5, 132.9, 135.7, 142.3, 144.7, 145.1, 188.7; HRMS (+ESI) m/z: (M + H)+ calcd for $C_{17}H_{15}N_2O$, 263.1184; found, 263.1185.

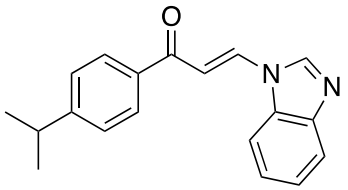

95j. White solid. Yield: 0.528 g, 1.82 mmol, 52%. ^{1}H NMR (CD_2Cl_2, 400 MHz): δ 1.30 (d, 6H, J_{HH} = 6.8 Hz), 3.02 (sep, 1H, J_{HH} = 6.9 Hz), 7.38-7.48 (m, 5H), 7.77 (d, 1H, J_{HH} = 8 Hz), 7.82 (d, 1H, J_{HH} = 7.8 Hz), 7.99 (d, 2H, J_{HH} = 8.2 Hz), 8.30-8.33 (m, 2H); ^{13}C{^{1}H} NMR (CD_2Cl_2, 100 MHz): δ 23.8, 34.7, 109.5, 111.8, 121.3, 124.6, 125.2, 127.3, 128.9, 132.9, 135.7, 136.0, 142.4, 145.1, 155.4, 188.7; HRMS (+ESI) m/z: (M + H)+ calcd for $C_{19}H_{19}N_2O$, 291.1497; found, 291.1497.

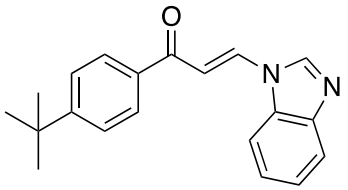

95k. White solid. Yield: 0.479 g, 1.58 mmol, 45%. ^{1}H NMR (CD_2Cl_2, 400 MHz): δ 1.37 (s, 9H), 7.38-7.49 (m, 3H), 7.58 (d, 2H, J_{HH} = 8.6 Hz), 7.77 (d, 1H, J_{HH} = 7.9 Hz), 7.82 (d, 1H, J_{HH} = 8.0 Hz), 7.99 (d, 2H, J_{HH} = 8.6 Hz), 8.30-8.33 (m, 2H); ^{13}C{^{1}H} NMR (CD_2Cl_2, 100 MHz): δ 31.2, 35.5, 109.5, 111.8, 121.4, 124.6, 125.2, 126.2, 128.6, 132.9, 135.6, 135.6, 142.4, 145.2, 157.5, 188.7; HRMS (+ESI) m/z: (M + H)+ calcd for $C_{20}H_{21}N_2O$, 305.1654; found, 305.1647.

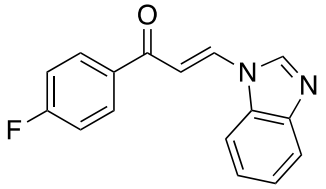

95l. Pale yellow solid. Yield: 0.419 g, 1.58 mmol, 45%. ^{1}H NMR (CD_2Cl_2, 400 MHz): δ 7.24 (t, 2H, J_{HH} = 8.7 Hz), 7.39-7.49 (m, 3H), 7.77 (d, 1H, J_{HH} = 8.0 Hz), 7.83 (d, 1H, J_{HH} = 7.7 Hz), 8.07-8.11 (m, 2H), 8.31-8.35 (m, 2H); ^{13}C{^{1}H} NMR (CD_2Cl_2, 100 MHz): δ 108.9, 111.8, 116.1, 116.4, 121.4, 124.7, 125.3, 131.3, 131.4, 134.7, 136.2, 142.3, 145.2, 187.6; HRMS (+ESI) m/z: (M + H)+ calcd for $C_{16}H_{12}N_2OF$, 267.0934; found, 267.0937.

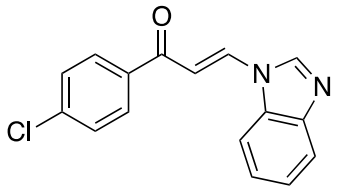

95m. Pale yellow solid. Yield: 0.366 g, 1.30 mmol, 37%. ^{1}H NMR (CD_2Cl_2, 400 MHz): δ 7.39-7.49 (m, 3H), 7.54 (d, 2H, J_{HH} = 8.6 Hz), 7.76 (d, 1H, J_{HH} = 8.1 Hz), 7.83 (d, 1H, J_{HH} = 7.8 Hz), 8.00 (d, 2H, J_{HH} = 8.6 Hz), 8.32-8.35 (m, 2H); ^{13}C{^{1}H} NMR (CD_2Cl_2, 100 MHz): δ 108.8, 111.8, 114.0, 121.4, 124.8, 125.3, 129.5, 130.1, 136.4, 136.7, 138.5, 139.8, 142.4, 187.7; HRMS (+ESI) m/z: (M + H)+ calcd for $C_{16}H_{12}N_2Ocl$, 283.0638; found, 283.0641.

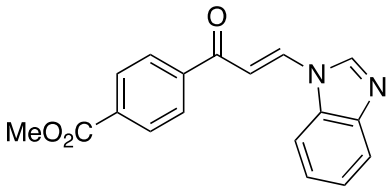

95n. White solid. Yield: 0.204 g, 0.67 mmol, 19%. ^{1}H NMR (CD_2Cl_2, 400 MHz): δ 3.95 (s, 3H), 7.40-7.50 (m, 3H), 7.77 (d, 1H, J_{HH} = 8.1 Hz), 7.83 (d, 1H, J_{HH} = 8.0 Hz), 8.09 (d, 2H, J_{HH}

= 7.5 Hz), 8.19 (d, 2H, J_{HH} = 7.6 Hz), 8.33-8.37 (m, 2H); $^{13}C\{^{1}H\}$ NMR (CD_2Cl_2, 100 MHz): δ 52.8, 109.1, 111.8, 121.5, 124.8, 125.4, 128.6, 130.3, 132.8, 134.5, 136.6, 141.6, 142.4, 145.2, 166.5, 188.8; HRMS (+ESI) m/z: (M + H)+ calcd for $C_{18}H_{15}N_2O_3$, 307.1083; found, 307.1080.

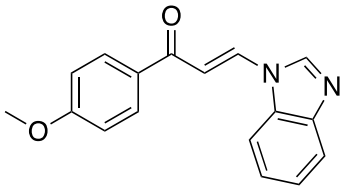

95o. Yellow solid. Yield: 0.302 g, 1.09 mmol, 31%. ^{1}H NMR (CD_2Cl_2, 400 MHz): δ 3.90 (s, 3H), 7.03 (d, 2H, J_{HH} = 8.9 Hz), 7.38-7.48 (m, 3H), 7.77 (d, 1H, J_{HH} = 8.1 Hz), 7.82 (d, 1H, J_{HH} = 7.8 Hz), 8.05 (d, 2H, J_{HH} = 9.0 Hz), 8.28-8.32 (m, 2H); $^{13}C\{^{1}H\}$ NMR (CD_2Cl_2, 100 MHz): δ 56.0, 109.4, 111.8, 114.4, 121.3, 124.5, 125.2, 130.9, 131.1, 132.9, 135.3, 142.3, 145.1, 164.2, 187.4; HRMS (+ESI) m/z: (M + H)+ calcd for $C_{17}H_{15}N_2O_2$, 279.1134; found, 279.1134.

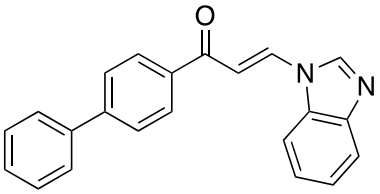

95p. Yellow solid. Yield: 0.170 g, 0.53 mmol, 15%. ^{1}H NMR (CD_2Cl_2, 400 MHz): δ 7.40-7.45 (m, 2H), 7.48-7.53 (m, 4H), 7.69-7.71 (m, 2H), 7.79-7.85 (m, 4H), 8.13-8.15 (m, 2H), 8.34-8.38 (m, 2H); $^{13}C\{^{1}H\}$ NMR (CD_2Cl_2, 100 MHz): δ 109.4, 111.8, 121.4, 124.7, 125.3, 127.6, 127.8, 128.7, 129.3, 129.4, 132.9, 135.9, 136.9, 140.1, 142.4, 145.2, 146.2, 188.6; HRMS (+ESI) m/z: (M + H)+ calcd for $C_{22}H_{17}N_2O$, 325.1341; found, 325.1330.

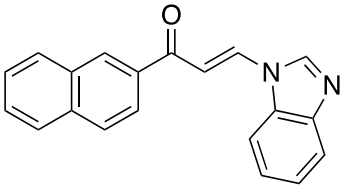

95q. White solid. Yield: 0.470 g, 1.58 mmol, 45%. ^{1}H NMR (DMSO-d6, 400 MHz): δ 7.41 (td, 1H, J_{HH} = 1.0 Hz, 11.2 Hz), 7.46 (td, 1H, J_{HH} = 1.0 Hz, 11.3 Hz), 7.66 (dq, 2H, J_{HH} = 1.3 Hz, 13.3 Hz), 7.80 (d, 1H, J_{HH} = 7.7 Hz), 8.03-8.10 (m, 3H), 8.16-8.20 (m, 3H), 8.52 (d, 1H, J_{HH} = 14.0 Hz), 8.93 (s, 1H), 9.08 (s, 1H); ^{13}C{^{1}H} NMR (DMSO-d6, 100 MHz): δ 109.3, 112.3, 120.2, 124.0, 124.0, 124.6, 127.0, 127.8, 128.5, 128.8, 129.6, 130.3, 132.1, 132.3, 134.8, 135.1, 135.9, 143.6, 144.1, 188.5; HRMS (+ESI) m/z: (M + H)+ calcd for $C_{20}H_{15}N_2O$, 299.1184; found, 299.1183.

Synthesis of enantioenriched *N*-methylated phosphine azole (*S*)-**97a**

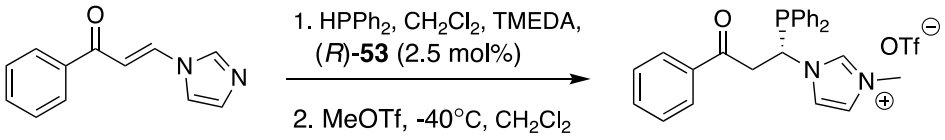

Diphenylphosphine (10 µL, 0.0575 mmol, 1 equiv.), CH_2Cl_2 (1150 µL) and (*R*)-**53** (0.0009 g, 2.5 mol%) were added to an oven-dried 10 mL storage tube and cooled to - 78 °C. Substrate **95a** (0.0575 mmol, 1 equiv.) and tetramethylethylenediamine (8.6 µL, 1 equiv.) were added sequentially into the mixture and the reaction mixture was stirred at - 78 °C for the stipulated time. After which, the reaction mixture was filtered through a short plug of celite to give (*S*)-**96a.** Solvent and base were fully removed by heating the mixture to 50 °C under strong vacuum for 1 hr. CH_2Cl_2 (1150 µL) was then added and the reaction mixture was cooled back to -40 °C. MeOTf (6.5 µL, 0.0590 mmol) was added and the mixture was left to stir for 5 hrs to give (*S*)-**97a** which was not isolated due to difficulty in purifying the air sensitive sticky compound.

General synthesis of enantioenriched phosphine oxides **100a** to **q**

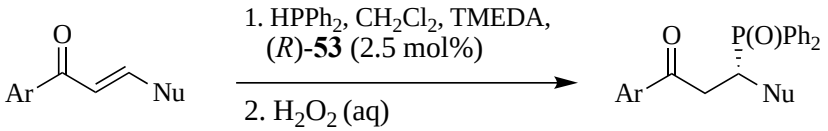

Diphenylphosphine (10 µL, 0.0575 mmol, 1 equiv.), CH_2Cl_2 (1150 µL for **95b**, **e** and **h**, 2000 µL for **95i** to **q** and 575 µL for the rest) and (*R*)-**53** (0.0009 g, 2.5 mol%) were added to an oven-dried 10 mL storage tube and cooled to the respective temperature (-78°C for **95a** to **h** and -20 °C for **95i** to **q**). The respective substrate (0.0575 mmol, 1 equiv.) and tetramethylethylenediamine (8.6 µL, 1 equiv.) were added sequentially into the mixture. The reaction mixture was then stirred at the respective temperature for the stipulated time. After which, 30% w/w aqueous hydrogen peroxide (1 drop) was added to the mixture and after 5 minutes, the reaction was allowed to warm to room temperature. Volatiles were then removed under reduced pressure and the crude mixture was purified by silica gel chromatography (90 EtOAc:10 MeOH) to afford the corresponding pure enantioenriched phosphine oxide.

Characterization of enantioenriched phosphine oxides **100a** to **q**

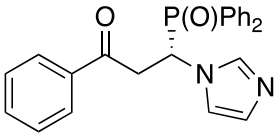

100a. White solid. Yield: 0.0212 g, 0.0529 mmol, 92%. $[\alpha]_D$ (21 °C) = -57.2°; ^{1}H NMR (CD_2Cl_2, 500 MHz): δ 3.42 (ddd, 1H, J_{HH} = 18.3 Hz, 2.4 Hz, J_{HP} = 7.2 Hz), 4.06 (ddd, 1H, J_{HH} = 18.3 Hz, 10.3 Hz, J_{HP} = 4.1 Hz), 5.80 (ddd, 1H, J_{HH} = 10.4 Hz, 2.5 Hz, J_{HP} = 3.5 Hz), 6.85 (s, 1H), 7.26 (s, 1H), 7.42-7.48 (m, 4H), 7.53-7.66 (m, 8H), 7.88-7.90 (m, 2H), 7.96-8.00 (m, 2H); ^{13}C{^{1}H} NMR (CD_2Cl_2, 125 MHz): δ 118.9, 128.1, 128.7, 128.7, 128.7, 128.9 (d, J = 9.7 Hz),

129.0, 129.2, 129.3, 129.7 (d, J = 13.9 Hz), 130.6 (d, J = 9.2 Hz), 131.1 (d, J = 9.0 Hz), 132.5 (d, J = 2.8 Hz), 132.8 (d, J = 2.6 Hz), 133.9, 135.8, 137.8, 194.8 (d, J = 11.2 Hz); $^{31}P\{^{1}H\}$ NMR (CH_2Cl_2, 121 MHz): δ 30.63; HRMS (+ESI) m/z: (M + H)+ calcd for $C_{24}H_{22}N_2O_2P$, 401.1419; found, 401.1420.

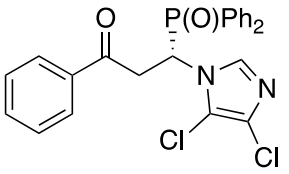

100b. White solid. Yield: 0.0211 g, 0.0449 mmol, 78%. $[\alpha]_D$ (21 °C) = -169.2°; ^{1}H NMR (CD_2Cl_2, 300 MHz): δ 3.50 (ddd, 1H, J_{HH} = 18.5 Hz, 2.8 Hz, J_{HP} = 6.7 Hz), 4.06 (ddd, 1H, J_{HH} = 18.4 Hz, 10.3 Hz, J_{HP} = 5.0 Hz), 5.75 (ddd, 1H, J_{HH} = 10.2 Hz, 2.7 Hz, J_{HP} = 3.0 Hz), 7.41-7.65 (m, 11H), 7.83-8.01 (m, 5H); $^{13}C\{^{1}H\}$ NMR ($CDCl_3$, 100 MHz): δ 38.6 (d, J = 4.9 Hz), 50.6, 51.3, 114.6 (d, J = 2.0 Hz), 125.9, 127.7 (d, J = 3.3 Hz), 128.3, 128.7 (d, J = 8.3 Hz), 129.0, 129.0 (d, J = 12.2 Hz), 129.6 (d, J = 11.7 Hz), 130.8 (d, J = 9.6 Hz), 131.6 (d, J = 8.8 Hz), 133.3 (dd, J = 2.9 Hz, 23.1 Hz), 133.9, 134.3, 135.5, 194.1 (d, J = 10.5); $^{31}P\{^{1}H\}$ NMR (CH_2Cl_2, 121 MHz): δ 31.88; HRMS (+ESI) m/z: (M + H)+ calcd for $C_{24}H_{20}N_2O_2PCl_2$, 469.0639; found, 469.0639.

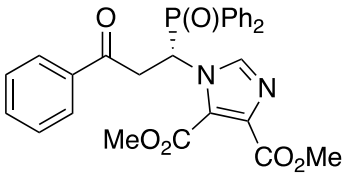

100d. White solid. Yield: 0.0226 g, 0.0437 mmol, 76%.$[\alpha]_D$ (21 °C) = -131.8°; ^{1}H NMR (CD_2Cl_2, 300 MHz): δ 3.46 (ddd, 1H, J_{HH} = 18.5 Hz, 2.6 Hz, J_{HP} = 5.9 Hz), 3.78 (s, 3H), 3.91 (s, 3H), 4.08 (ddd, 1H, J_{HH} = 18.4 Hz, 11.0 Hz, J_{HP} = 5.0 Hz), 6.67 (ddd, 1H, J_{HH} = 10.9 Hz, 2.6 Hz, J_{HP} = 3.9 Hz), 7.36-7.76 (m, 13H), 8.00-8.06 (m, 2H), 8.15 (s, 1H); $^{13}C\{^{1}H\}$ NMR

($CDCl_3$, 100 MHz): δ 39.3 (d, J = 4.2 Hz), 50.4, 51.1, 52.3, 52.6, 52.9, 126.4, 127.7, 128.3, 128.4, 128.8, 128.9, 129.5 (d, J = 11.8 Hz), 131.2 (dd, J = 26.4 Hz, 9.4 Hz), 133.0 (dd, J = 34.0 Hz, 2.6 Hz), 134.1, 135.6, 135.7, 138.4, 161.5, 162.4, 194.5 (d, J = 11.5 Hz); $^{31}P\{^1H\}$ NMR (CH_2Cl_2, 121 MHz): δ 32.53; HRMS (+ESI) m/z: (M + H)+ calcd for $C_{28}H_{26}N_2O_6P$, 517.1529; found, 517.1528.

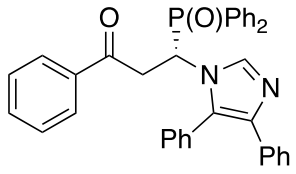

100e. White solid. Yield: 0.0283 g, 0.0512 mmol, 89%. $[\alpha]_D$ (21 °C) = -83.6°; ^1H NMR (CD_2Cl_2, 300 MHz): δ 3.50 (ddd, 1H, J_{HH} = 18.1 Hz, 3.6 Hz, J_{HP} = 8.1 Hz), 4.11 (ddd, 1H, J_{HH} = 18.0 Hz, 9.4 Hz, J_{HP} = 6.7 Hz), 5.46 (ddd, 1H, J_{HH} = 9.2 Hz, 3.5 Hz, J_{HP} = 2.7 Hz), 7.10-7.85 (m, 25H), 8.23 (s, 1H); $^{13}C\{^1H\}$ NMR ($CDCl_3$, 100 MHz): δ 39.2 (d, J = 5.0 Hz), 50.2, 50.9, 126.5, 126.8, 127.3, 127.9, 128.0, 128.2 (d, J = 23.5 Hz), 128.8 (d, J = 17.8 Hz), 128.8, 128.9, 129.0, 129.3 (d, J = 11.6 Hz), 129.4, 129.5, 129.6, 129.7, 131.5, 131.6 (q, J = 8.8 Hz), 132.9 (d, J = 2.8 Hz), 133.1 (d, J = 2.5 Hz), 134.0, 134.4, 135.9, 136.0, 137.8, 194.8 (d, J =10.3 Hz); $^{31}P\{^1H\}$ NMR (CH_2Cl_2, 121 MHz): δ 31.44; HRMS (+ESI) m/z: (M + H)+ calcd for $C_{36}H_{30}N_2O_2P$, 553.2045; found, 553.2045.

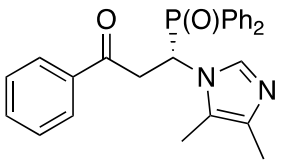

100f. White solid. Yield: 0.0081 g, 0.0190 mmol, 33%. $[\alpha]_D$ (21 °C) = -3.1°; ^1H NMR (CD_2Cl_2, 300 MHz): δ 1.84 (s, 3H), 1.93 (s, 3H), 3.42 (ddd, 1H, J_{HH} = 18.3 Hz, 2.5 Hz, J_{HP} = 7.1 Hz), 4.04 (ddd, 1H, J_{HH} = 18.3 Hz, 10.3 Hz, J_{HP} = 4.4 Hz), 5.45 (ddd, 1H, J_{HH} = 10.2 Hz, 2.6 Hz,

J_{HP} = 3.6 Hz), 7.35-7.62 (m, 11H), 7.76-7.95 (m, 5H); $^{13}C\{^{1}H\}$ NMR ($CDCl_3$, 100 MHz): δ 7.94, 11.0, 39.4, 50.6, 51.3, 124.8, 127.2, 128.3, 128.9, 129.0, 129.5, 129.6, 130.7 (d, J = 9.6 Hz), 131.4 (d, J = 8.6 Hz), 133.1, 133.4, 134.3, 135.3, 137.2, 194.5 (d, J = 11.0 Hz); $^{31}P\{^{1}H\}$ NMR (CH_2Cl_2, 121 MHz): δ 34.18; HRMS (+ESI) m/z: (M + H)+ calcd for $C_{26}H_{26}N_2O_2P$, 429.1732; found, 429.1736.

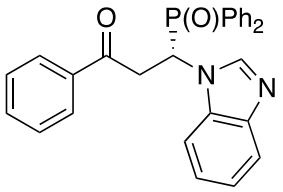

100h. White solid. Yield: 0.0210 g, 0.0466 mmol, 81%. $[\alpha]_D$ (21 °C) = 7.6°; ^{1}H NMR (CD_2Cl_2, 300 MHz): δ 3.61 (ddd, 1H, J_{HH} = 18.5 Hz, 2.3 Hz, J_{HP} = 7.5 Hz), 4.19 (ddd, 1H, J_{HH} = 18.5 Hz, 9.7 Hz, J_{HP} = 4.2 Hz), 6.09 (ddd, 1H, J_{HH} = 9.5 Hz, 2.4 Hz, J_{HP} = 4.0 Hz), 7.13-7.41 (m, 7H), 7.50-7.65 (m, 7H), 7.74-7.83 (m, 3H), 8.02 (t, 2H, J_{HH} = 9.3 Hz), 8.28 (s, 1H); $^{13}C\{^{1}H\}$ NMR ($CDCl_3$, 100 MHz): δ 38.3, 50.3, 51.1, 110.8, 120.3, 122.4, 122.8, 123.3, 128.3, 128.7 (d, J = 11.9 Hz), 128.9, 129.5 (d, J = 11.6 Hz), 130.6 (d, J = 9.7 Hz), 131.4 (d, J = 8.9 Hz), 132.7 (d, J = 2.6 Hz), 133.1 (d, J = 2.3 Hz), 133.8, 134.1, 135.6, 142.7, 143.1, 194.9 (d, J = 10.3 Hz); $^{31}P\{^{1}H\}$ NMR (CH_2Cl_2, 121 MHz): δ 31.32; HRMS (+ESI) m/z: (M + H)+ calcd for $C_{28}H_{24}N_2O_2P$, 451.1575; found, 451.1575.

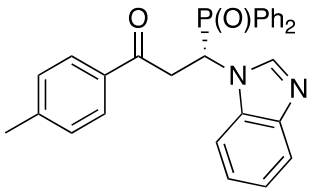

100i. White solid. Yield: 0.0232 g, 0.0499 mmol, 87%. $[\alpha]_D$ (21 °C) = -49°; ^{1}H NMR (CD_2Cl_2, 300 MHz): δ 2.34 (3H), 3.56 (ddd, 1H, J_{HH} = 18.4 Hz, 2.6 Hz, J_{HP} = 7.6 Hz), 4.16 (ddd, 1H,

J_{HH} = 18.3 Hz, 9.8 Hz, J_{HP} = 4.2 Hz), 6.09 (ddd, 1H, J_{HH} = 9.7 Hz, 2.8 Hz, J_{HP} = 4.0 Hz), 7.12-7.33 (m, 7H), 7.48-7.76 (m, 9H), 7.98-8.05 (m, 2H), 8.27 (s, 1H); $^{13}C\{^{1}H\}$ NMR (CD_2Cl_2, 100 MHz): δ 21.8, 38.3, 50.6, 51.4, 111.3, 120.2, 122.5, 123.3, 128.6, 128.9 (d, J = 11.8 Hz), 129.2 (d, J = 10.3 Hz), 129.4 (d, J = 12.6 Hz), 129.7 (d, J = 11.4 Hz), 129.7, 130.9 (d, J = 9.5 Hz), 131.6 (d, J = 8.9 Hz), 132.8 (d, J = 2.4 Hz), 133.3 (d, J = 2.4 Hz), 133.5, 143.0, 143.3, 145.5, 194.7 (d, J = 10.7 Hz); $^{31}P\{^{1}H\}$ NMR (CH_2Cl_2, 121 MHz): δ 31.03; HRMS (+ESI) m/z: (M + H)+ calcd for $C_{29}H_{26}N_2O_2P$, 465.1732; found, 465.1732.

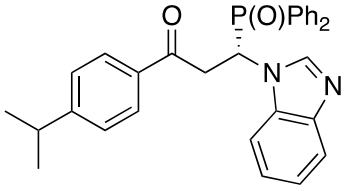

100j. White solid. Yield: 0.0218 g, 0.0443 mmol, 77%. $[\alpha]_D$ (21 °C) = -35°; ^{1}H NMR (CD_2Cl_2, 300 MHz): δ 1.20 (d, 6H, J_{HH} = 6.9 Hz), 2.90 (sep, 1H, J_{HH} = 6.9 Hz), 3.56 (ddd, 1H, J_{HH} = 18.4 Hz, 2.5 Hz, J_{HP} = 7.6 Hz), 4.17 (ddd, 1H, J_{HH} = 18.4 Hz, 9.8 Hz, J_{HP} = 4.2 Hz), 6.09 (ddd, 1H, J_{HH} = 9.7 Hz, 2.8 Hz, J_{HP} = 3.9 Hz), 7.12-7.33 (m, 7H), 7.49-7.61 (m, 6H), 7.73-7.76 (m, 3H), 7.98-8.05 (m, 2H), 8.27 (s, 1H); $^{13}C\{^{1}H\}$ NMR (CD_2Cl_2, 100 MHz): δ 23.7, 34.6, 38.3, 50.6, 111.3, 120.2, 122.4, 123.3, 127.2, 128.7, 128.9 (d, J = 11.9 Hz), 129.2 (d, J = 20.2 Hz), 129.7 (d, J = 11.6 Hz), 130.2 (d, J = 15.2 Hz), 130.9 (d, J = 9.5 Hz), 131.6 (d, J = 8.8 Hz), 132.8 (d, J = 2.8 Hz), 133.3 (d, J = 2.6 Hz), 133.9, 134.2, 143.0, 143.4, 156.1, 194.7 (d, J = 10.8 Hz); $^{31}P\{^{1}H\}$ NMR (CH_2Cl_2, 121 MHz): δ 30.92; HRMS (+ESI) m/z: (M + H)+ calcd for $C_{31}H_{30}N_2O_2P$, 493.2045; found, 493.2047.

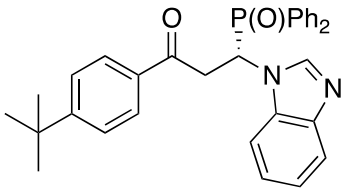

100k. White solid. Yield: 0.0256 g, 0.0506 mmol, 88%. $[\alpha]_D$ (21 °C) = -114°; ^{1}H NMR (CD_2Cl_2, 300 MHz): δ 1.27 (s, 9H), 3.56 (ddd, 1H, J_{HH} = 18.4 Hz, 2.5 Hz, J_{HP} = 7.5 Hz), 4.18 (ddd, 1H, J_{HH} = 18.3 Hz, 9.8 Hz, J_{HP} = 4.1 Hz), 6.10 (ddd, 1H, J_{HH} = 9.7 Hz, 2.7 Hz, J_{HP} = 4.0 Hz), 7.12-7.34 (m, 5H), 7.39-7.42 (m, 2H), 7.49-7.61 (m, 6H), 7.74-7.77 (m, 3H), 7.98-8.05 (m, 2H), 8.27 (s, 1H); ^{13}C{^{1}H} NMR (CD_2Cl_2, 100 MHz): δ 31.1, 35.4, 38.4, 50.7, 51.4, 111.3, 120.2, 122.4, 123.3, 126.1, 128.4, 128.9 (d, J = 12.2 Hz), 129.2, 129.7 (d, J = 11.6 Hz), 130.9 (d, J = 9.2 Hz), 131.6 (d, J = 9.0 Hz), 132.8, 133.3, 133.5, 134.2, 143.1, 143.4, 158.3, 194.8 (d, J = 10.6 Hz); ^{31}P{^{1}H} NMR (CH_2Cl_2, 121 MHz): δ 30.86; HRMS (+ESI) m/z: (M + H)+ calcd for $C_{32}H_{32}N_2O_2P$, 507.2201; found, 507.2203.

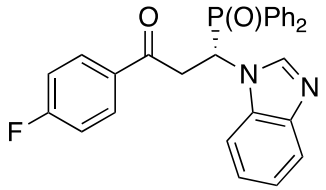

100l. White solid. Yield: 0.0237 g, 0.0506 mmol, 88%. $[\alpha]_D$ (21 °C) = -23°; ^{1}H NMR (CD_2Cl_2, 300 MHz): δ 3.59 (ddd, 1H, J_{HH} = 18.3 Hz, 2.5 Hz, J_{HP} = 7.4 Hz), 4.14 (ddd, 1H, J_{HH} = 18.4 Hz, 9.7 Hz, J_{HP} = 4.3 Hz), 6.07 (ddd, 1H, J_{HH} = 9.4 Hz, 3.0 Hz, J_{HP} = 4.0 Hz), 7.04-7.09 (m, 2H), 7.12-7.34 (m, 5H), 7.49-7.61 (m, 6H), 7.73-7.76 (m, 1H), 7.83-7.87 (m, 2H), 7.98-8.04 (m, 2H), 8.27 (s, 1H); ^{13}C{^{1}H} NMR (CD_2Cl_2, 100 MHz): δ 38.5, 111.2, 116.1, 116.3, 120.3, 122.5, 123.3, 128.9 (d, J = 11.9 Hz), 129.0, 129.3 (d, J = 12.3 Hz), 129.7 (d, J = 11.6 Hz), 130.3, 130.9 (d, J = 9.4 Hz), 131.3 (d, J = 9.6 Hz), 131.7 (d, J = 8.9 Hz), 132.1 (d, J = 8.3 Hz), 132.6, 132.8 (d, J = 2.9 Hz), 133.3 (d, J = 3.2 Hz), 143.0, 143.5, 193.7 (d, J = 11.0 Hz); ^{31}P{^{1}H} NMR

(CH_2Cl_2, 121 MHz): δ 30.70; HRMS (+ESI) m/z: (M + H)+ calcd for $C_{28}H_{23}N_2O_2PF$, 469.1481; found, 469.1458.

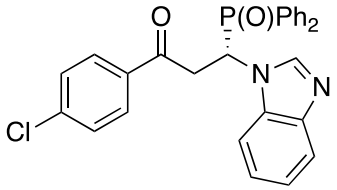

100m. White solid. Yield: 0.0268 g, 0.0552 mmol, 96%. $[\alpha]_D$ (21 °C) = -27°; ^{1}H NMR (CD_2Cl_2, 300 MHz): δ 3.54-3.63 (m, 1H), 4.08-4.19 (m, 1H), 6.04-6.07 (m, 1H), 7.13-7.38 (m, 7H), 7.49-7.60 (m, 6H), 7.74-7.77 (m, 3H), 7.98-8.03 (m, 2H), 8.27 (s, 1H); ^{13}C{^{1}H} NMR (CD_2Cl_2, 100 MHz): δ 51.3, 111.3, 113.1, 120.3, 120.3, 122.5, 123.3, 128.7, 128.9 (d, J = 12.1 Hz), 129.4, 129.6, 129.7 (d, J = 11.5 Hz), 130.0, 130.9 (d, J = 9.5 Hz), 131.5, 131.7 (d, J = 8.7 Hz), 132.0 (d, J = 4.5 Hz), 132.9 (d, J = 2.7 Hz);, 133.4 (d, J = 3.0 Hz), 134.4, 140.7,194.2 (d, J = 10.9 Hz); ^{31}P{^{1}H} NMR (CH_2Cl_2, 121 MHz): δ 30.65; HRMS (+ESI) m/z: (M + H)+ calcd for $C_{28}H_{23}N_2O_2PCl$, 485.1186; found, 485.1162.

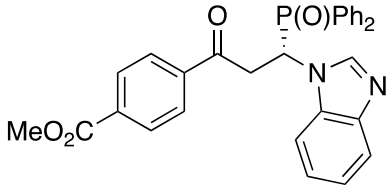

100n. White solid. Yield: 0.0231 g, 0.0454 mmol, 79%. $[\alpha]_D$ (21 °C) = -6.9°; ^{1}H NMR (CD_2Cl_2, 400 MHz): δ 3.65 (ddd, 1H, J_{HH} = 19.0 Hz, 3.0 Hz, J_{HP} = 7.0 Hz), 3.89 (s, 3H), 4.20 (ddd, 1H, J_{HH} = 19.0 Hz, 10.0 Hz, J_{HP} = 5.0 Hz), 6.05-6.09 (m, 1H), 7.14-7.34 (m, 6H), 7.50-7.64 (m, 8H), 7.86 (d, 2H, J_{HH} = 8.0 Hz), 8.02 (d, 2H, J_{HH} = 8.0 Hz), 8.29 (s, 1H); ^{13}C{^{1}H} NMR (CD_2Cl_2, 100 MHz): δ 38.9, 52.8, 111.2, 120.3, 122.5, 123.0, 123.4, 128.5, 128.9 (d, J = 11.8 Hz), 129.3 (d, J = 12.6 Hz), 129.7 (d, J = 11.6 Hz), 130.1, 130.2 (d, J = 11.0 Hz), 130.9 (d, J = 9.4 Hz),

131.6 (d, J = 10.0 Hz), 131.7 (d, J = 8.9 Hz), 132.8 (d, J = 2.7 Hz), 133.4 (d, J = 2.9 Hz), 135.1, 139.0, 143.0, 143.4, 166.2, 195.0 (d, J = 17.7 Hz),; $^{31}P\{^{1}H\}$ NMR (CH_2Cl_2, 121 MHz): δ 30.68; HRMS (+ESI) m/z: (M + H)+ calcd for $C_{30}H_{26}N_2O_4P$, 509.1630; found, 509.1629.

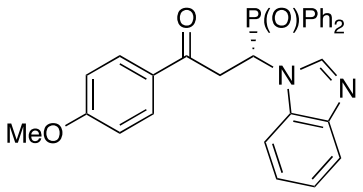

100o. White solid. Yield: 0.0061 g, 0.0126 mmol, 22%. $[\alpha]_D$ (21 °C) = -32°; ^{1}H NMR (CD_2Cl_2, 300 MHz): δ 3.53 (ddd, 1H, J_{HH} = 18.3 Hz, 2.6 Hz, J_{HP} = 7.7 Hz), 3.81 (s, 3H), 4.13 (ddd, 1H, J_{HH} = 18.3 Hz, 9.7 Hz, J_{HP} = 4.2 Hz), 6.09 (ddd, 1H, J_{HH} = 9.7 Hz, 2.7 Hz, J_{HP} = 4.0 Hz), 6.84-6.87 (m, 2H), 7.12-7.33 (m, 5H), 7.48-7.61 (m, 6H), 7.73-7.81 (m, 3H), 7.97-8.04 (m, 2H), 8.27 (s, 1H); $^{13}C\{^{1}H\}$ NMR (CD_2Cl_2, 100 MHz): δ 55.9, 111.3, 114.2, 120.2, 122.4, 122.7 (d, J = 3.2 Hz), 122.8 (d, J = 2.5 Hz), 123.2, 128.9 (d, J = 12.2 Hz), 129.1, 129.3, 129.5, 129.7 (d, J = 11.6 Hz), 130.3, 130.8, 130.8 (d, J = 9.5 Hz), 131.2, 131.5 (d, J = 7.3 Hz), 131.7 (d, J = 8.9 Hz), 132.7 (d, J = 3.3 Hz), 133.3 (d, J = 3.0 Hz), 164.6, 193.4 (d, J = 11.1 Hz); $^{31}P\{^{1}H\}$ NMR (CH_2Cl_2, 121 MHz): δ 30.79; HRMS (+ESI) m/z: (M + H)+ calcd for $C_{29}H_{26}N_2O_3P$, 481.1681; found, 481.1666.

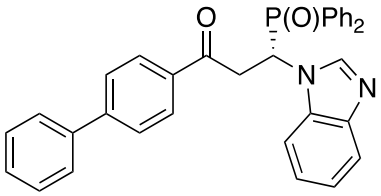

100p. White solid. Yield: 0.0212 g, 0.0402 mmol, 70%. $[\alpha]_D$ (21 °C) = -149°; ^{1}H NMR (CD_2Cl_2, 300 MHz): δ 3.64 (ddd, 1H, J_{HH} = 18.3 Hz, 2.6 Hz, J_{HP} = 7.5 Hz), 4.21 (ddd, 1H, J_{HH} = 18.4 Hz, 9.7 Hz, J_{HP} = 4.3 Hz), 6.11 (ddd, 1H, J_{HH} = 9.7 Hz, 2.7 Hz, J_{HP} = 4.1 Hz), 7.13-7.32 (m,

5H), 7.38-7.48 (m, 3H), 7.50-7.64 (m, 10H), 7.76-7.78 (m, 1H), 7.88-7.90 (m, 2H), 8.00-8.06 (m, 2H), 8.29 (s, 1H); $^{13}C\{^{1}H\}$ NMR (CD_2Cl_2, 100 MHz): δ 38.5, 50.7, 51.4, 111.4, 120.2, 122.4, 123.3, 127.6 (d, J = 2.6 Hz), 128.8 (d, J = 2.2 Hz), 129.0, 129.1, 129.3, 129.7 (d, J = 11.5 Hz), 130.2, 130.4, 130.9 (d, J = 9.4 Hz), 131.7 (d, J = 9.0 Hz), 132.8 (d, J = 2.7 Hz), 133.3 (d, J = 2.8 Hz), 134.2, 134.7, 139.8, 143.0, 143.5, 146.8, 194.8 (d, J = 10.8 Hz); $^{31}P\{^{1}H\}$ NMR (CH_2Cl_2, 121 MHz): δ 30.74; HRMS (+ESI) m/z: (M + H)+ calcd for $C_{34}H_{28}N_2O_2P$, 527.1888; found, 527.1889.

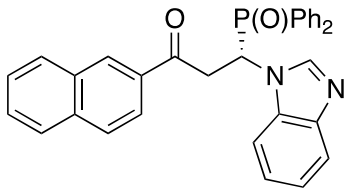

100q. White solid. Yield: 0.0253 g, 0.0506 mmol, 88%. $[\alpha]_D$ (21 °C) = -102°; ^{1}H NMR (CD_2Cl_2, 300 MHz): δ 3.74 (ddd, 1H, J_{HH} = 18.3 Hz, 2.6 Hz, J_{HP} = 7.5 Hz), 4.35 (ddd, 1H, J_{HH} = 18.3 Hz, 9.7 Hz, J_{HP} = 4.2 Hz), 6.15 (ddd, 1H, J_{HH} = 9.6 Hz, 2.7 Hz, J_{HP} = 3.9 Hz), 7.13-7.34 (m, 5H), 7.52-7.60 (m, 8H), 7.79-7.84 (m, 4H), 7.91-7.94 (m, 1H), 8.02-8.08 (m, 2H), 8.32-8.40 (m, 2H); $^{13}C\{^{1}H\}$ NMR (CD_2Cl_2, 100 MHz): δ 38.5, 111.3, 120.2, 122.5, 123.3, 123.7, 127.4, 128.1, 128.8, 128.9 (d, J = 5.1 Hz), 129.2 (d, J = 9.0 Hz), 129.4, 129.7 (d, J = 11.5 Hz), 130.0, 130.1, 130.3, 130.8 (d, J = 7.0 Hz), 130.9, 131.6 (d, J = 10.1 Hz), 131.7 (d, J = 8.8 Hz), 132.7, 132.8 (d, J = 2.8 Hz), 133.3 (d, J = 2.6 Hz), 134.3, 136.2, 143.1, 143.4, 195.1 (d, J = 10.8 Hz); $^{31}P\{^{1}H\}$ NMR (CH_2Cl_2, 121 MHz): δ 30.90; HRMS (+ESI) m/z: (M + H)+ calcd for $C_{32}H_{26}N_2O_2P$, 501.1732; found, 501.1721.

References

(1) Wanzlick, H. W., *Aspects of Nucleophilic Carbene Chemistry, Angew. Chem. Int. Ed.* **1962,** *1*, 75-80.

(2) Lappert, M. F., *The coordination chemistry of electron-rich alkenes (enetetramines), J. Organomet. Chem.* **1988,** *358*, 185-213.

(3) Arduengo, A. J.; Harlow, R. L.; Kline, M., *A stable crystalline carbene, J. Am. Chem. Soc.* **1991,** *113*, 361-363.

(4) (a) Díez-González, S.; Marion, N.; Nolan, S. P., *N-Heterocyclic Carbenes in Late Transition Metal Catalysis, Chem. Rev.* **2009,** *109*, 3612-3676; (b) Herrmann, W. A., *N-Heterocyclic Carbenes: A New Concept in Organometallic Catalysis, Angew. Chem. Int. Ed.* **2002,** *41*, 1290-1309; (c) Herrmann, W. A.; Elison, M.; Fischer, J.; Köcher, C.; Artus, G. R. J., *N-Heterocyclic Carbenes: Generation under Mild Conditions and Formation of Group 8–10 Transition Metal Complexes Relevant to Catalysis, Chem. Eur. J.* **1996,** *2*, 772-780; (d) Vougioukalakis, G. C.; Grubbs, R. H., *Ruthenium-Based Heterocyclic Carbene-Coordinated Olefin Metathesis Catalysts, Chem. Rev.* **2010,** *110*, 1746-1787.

(5) Gaggioli, C. A.; Bistoni, G.; Ciancaleoni, G.; Tarantelli, F.; Belpassi, L.; Belanzoni, P., *Modulating the Bonding Properties of N-Heterocyclic Carbenes (NHCs): A Systematic Charge-Displacement Analysis, Chem. Eur. J.* **2017,** *23*, 7558-7569.

(6) Tereniak, S. J.; Landis, C. R.; Stahl, S. S., *Are Phosphines Viable Ligands for Pd-Catalyzed Aerobic Oxidation Reactions? Contrasting Insights from a Survey of Six Reactions, ACS Catalysis* **2018,** *8*, 3708-3714.

(7) Clavier, H.; Nolan, S. P., *Percent buried volume for phosphine and N-heterocyclic carbene ligands: steric properties in organometallic chemistry, Chem. Commun.* **2010,** *46*, 841-861.

(8) Gaillard, S.; Renaud, J.-L., *When phosphorus and NHC (N-heterocyclic carbene) meet each other, Dalton Trans.* **2013,** *42*, 7255-7270.

(9) (a) Wolf, J.; Labande, A.; Daran, J.-C.; Poli, R., *Nickel(II) complexes with bifunctional phosphine–imidazolium ligands and their catalytic activity in the Kumada–Corriu coupling reaction, J. Organomet. Chem.* **2006,** *691*, 433-443; (b) Tsoureas, N.; Danopoulos, A. A.; Tulloch, A. A. D.; Light, M. E., *(Diphenylphosphino)alkyl-Functionalized Nucleophilic Carbene Complexes of Palladium, Organometallics* **2003,** *22*, 4750-4758.

(10) (a) Shi, J.-C.; Yang, P.-Y.; Tong, Q.; Wu, Y.; Peng, Y., *Highly efficient and stable palladium/imidazolium salt-phosphine catalysts for Suzuki–Miyaura cross-coupling of aryl bromides, J. Mol. Catal. A: Chem.* **2006,** *259*, 7-10; (b) Hahn, F. E.; Jahnke, M. C.; Pape, T., *Synthesis of Palladium and Platinum Complexes with Phosphine-Functionalized Benzimidazolin-2-ylidene Ligands, Organometallics* **2006,** *25*, 5927-5936; (c) Lee, H. M.; Chiu, P. L.; Zeng, J. Y., *A convenient synthesis of phosphine-functionalized N-heterocyclic carbene ligand precursors, structural characterization of their palladium complexes and catalytic application in Suzuki coupling reaction, Inorg. Chim. Acta* **2004,** *357*, 4313-4321; (d) Yang, C.; Lee, H. M.; Nolan, S. P., *Highly Efficient Heck Reactions of Aryl Bromides with n-Butyl Acrylate Mediated by a Palladium/Phosphine−Imidazolium Salt System, Org. Lett.* **2001,** *3*, 1511-1514.

(11) Seo, H.; Park, H.-j.; Kim, B. Y.; Lee, J. H.; Son, S. U.; Chung, Y. K., *Synthesis of P- and S-Functionalized Chiral Imidazolium Salts and Their Rh and Ir Complexes, Organometallics* **2003,** *22*, 618-620.

(12) Nanchen, S.; Pfaltz, A., *Chiral Phosphino- and (Phosphinooxy)-Substituted N-Heterocyclic Carbene Ligands and Their Application in Iridium-Catalyzed Asymmetric Hydrogenation, Helv. Chim. Acta* **2006,** *89*, 1559-1573.

(13) (a) Debono, N.; Labande, A.; Manoury, E.; Daran, J.-C.; Poli, R., *Palladium Complexes of Planar Chiral Ferrocenyl Phosphine-NHC Ligands: New Catalysts for the Asymmetric Suzuki−Miyaura Reaction, Organometallics* **2010,** *29*, 1879-1882; (b) Focken, T.; Raabe, G.; Bolm, C., *Synthesis of iridium complexes with new planar chiral chelating phosphinyl-imidazolylidene ligands and their application in asymmetric hydrogenation, Tetrahedron: Asymmetry* **2004,** *15*, 1693-1706; (c) Labande, A.; Daran, J.-C.; Manoury, E.; Poli, R., *New (1-Phosphanylferrocen-1'- and -2-yl)methyl-Linked Diaminocarbene Ligands: Synthesis and Rhodium(I) Complexes, Eur. J. Inorg. Chem.* **2007,** *2007*, 1205-1209.

(14) Hodgson, R.; Douthwaite, R. E., *Synthesis and asymmetric catalytic application of chiral imidazolium–phosphines derived from (1R,2R)-trans-diaminocyclohexane, J. Organomet. Chem.* **2005,** *690*, 5822-5831.

(15) Willms, H.; Frank, W.; Ganter, C., *Hybrid Ligands with N-Heterocyclic Carbene and Chiral Phosphaferrocene Components, Chem. Eur. J.* **2008,** *14*, 2719-2729.

(16) (a) Gischig, S.; Togni, A., *PdII Complexes of Tridentate PCP N-Heterocyclic Carbene Ligands: Structural Aspects and Application in Asymmetric Hydroamination of Cyano Olefins, Eur. J. Inorg. Chem.* **2005,** *2005*, 4745-4754; (b) Lee, H. M.; Zeng, J. Y.; Hu, C.-H.; Lee, M.-T., *A New Tridentate Pincer Phosphine/N-Heterocyclic Carbene Ligand: Palladium Complexes, Their Structures, and Catalytic Activities, Inorg. Chem.* **2004,** *43*, 6822-6829; (c) Wang, A.-E.; Zhong, J.; Xie, J.-H.; Li, K.; Zhou, Q.-L., *Highly Efficient Suzuki Cross-Coupling Catalyzed by Palladium/Phosphine-Imidazolium Carbene System, Adv. Synth. Catal.* **2004,** *346*, 595-598.

(17) Hoffmann, S.; Hartung, K.-J.; Hanh, N. T.; Mewes, R.; Baluzow, W., *Synthesen vinyloger N-Acyl-azole (Vinazolide), Z. Anorg. Allg. Chem.* **1986,** *26*, 105-106.

Chapter 3

Syntheses of Phosphine-NHC Metal Complexes

3.1 General Introduction to Phosphine-NHC Metal Complexes

Generally, syntheses of organometallic complexes bearing phosphine-NHC moieties are accomplished either *via* an intramolecular reaction between individual phosphine and NHC fragments or through coordination of the ligand to the metal.

3.1.1 Syntheses of Phosphine-NHC Metal Complexes

3.1.1.1 Intramolecular Route

Leung reported the synthesis of a chelating phosphine-NHC palladium(II) complex through an internal *Diels-Alder* reaction between a bound phosphine and an incoming 1-vinylimidazole. The NHC ligand formed in the product labilised the *trans* chiral auxiliary due to its high *trans* effect and dissociated the auxiliary from the palladium centre.[1] (Scheme 3.1)

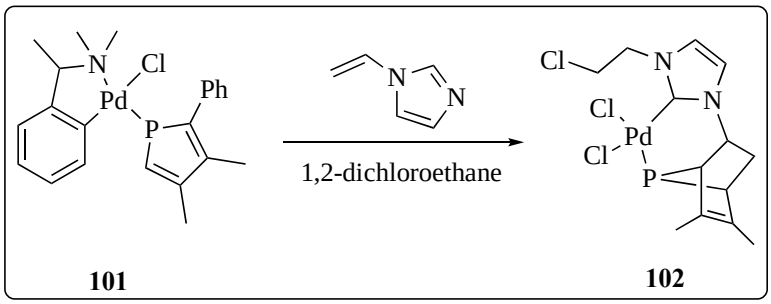

Scheme 3.1 *Diels-Alder* reaction between bound phosphine and 1-vinylimidazole followed by NHC formation and palladium coordination.

Hahn subsequently reported a base-mediated macrocyclization of a bound NHC and the fluorophosphinoaryl ligand to furnish the final tridentate *bis*(phosphine)-NHC metal complexes.[2] This method worked as the ligated imidazoline had two acidic hydrogens on the pendant arms of the nitrogen which could be abstracted by a strong base with a leaving fluoride group on a aryl group situated in close proximity to the NHC precursor. A variety of metals including platinum[2] , rhenium[3] , manganese[4] , ruthenium[5] and iron[6] supported by carbon monoxide and cyclooctadiene ligands incorporating such structural motifs had also been reported. (Scheme 3.2)

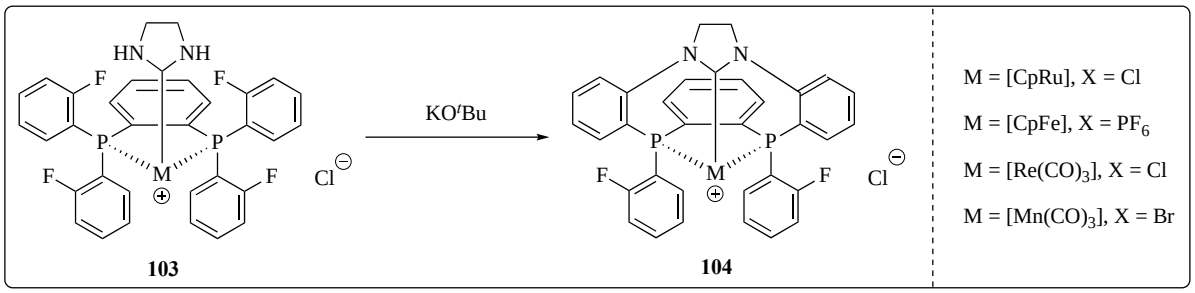

103 **104**

Scheme 3.2 Deprotonation of acidic imidazoline followed by expulsion of fluoride leaving group to give **104** and derivatives.

3.1.1.2 Direct Coordination of Ligand to Metal Route

Coordination of a phosphine-NHC or phosphine-NHC precursor ligand to the metal represents a more commonly utilized class of method as compared to the intramolecular method described in the previous section. In this approach and in the literature, phosphino-azolium salts are commonly prepared using the synthetic protocols described in Chapter 2, other than hydrophosphination. The phosphorus and NHC donors can then be transposed to a metal of choice using the following four methods. In method (a), deprotonation of NHC precursor before coordination of the bidentate phosphine-NHC ligand to a metal[7] ; in (b), coordination of phosphine donor prior to deprotonation and coordination of the azolium

moiety[8]; in (c), transmetallation of a silver(I)-NHC, formed by the acid base reaction between a NHC precursor and a silver(I) base such as silver(I) oxide, silver(I) acetate or silver(I) carbonate, to a metal of choice *in situ*[9] and in (d), oxidative addition by an electron-rich metal to the C-H bond of the NHC precursor followed by coordination.[10] (Scheme 3.3)

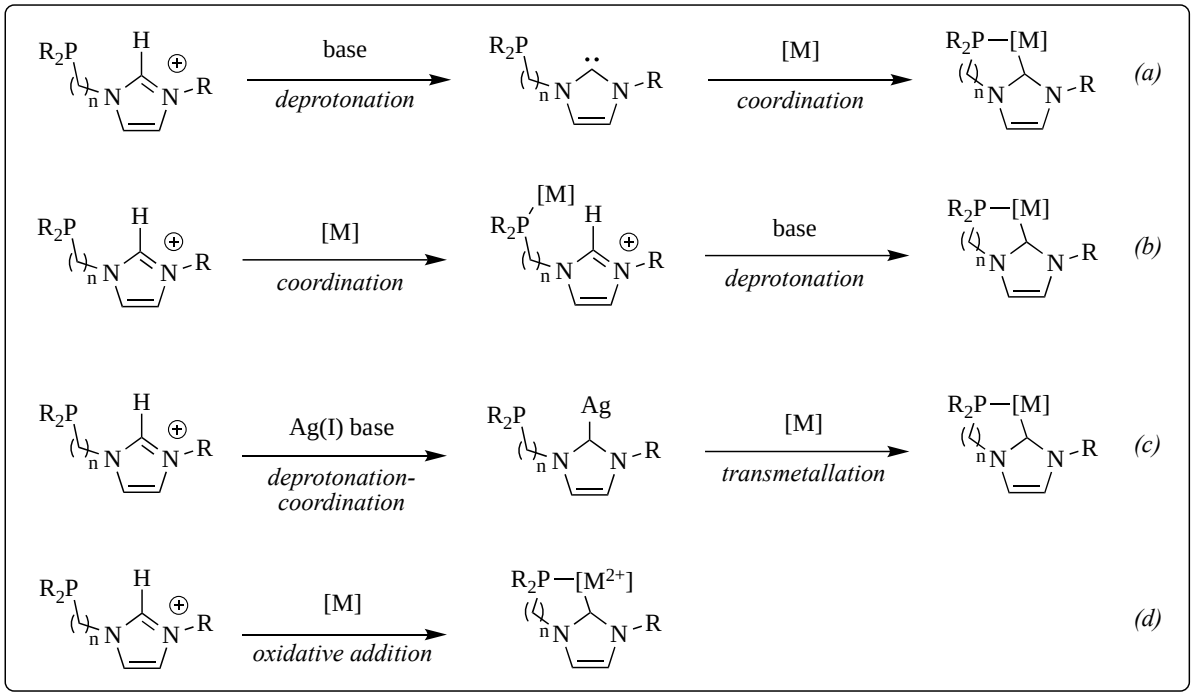

Scheme 3.3 Four general methods of accessing phosphine-NHC metal complexes.

The methods are generally straightforward; however, several groups have reported interesting findings which are worth discussing.

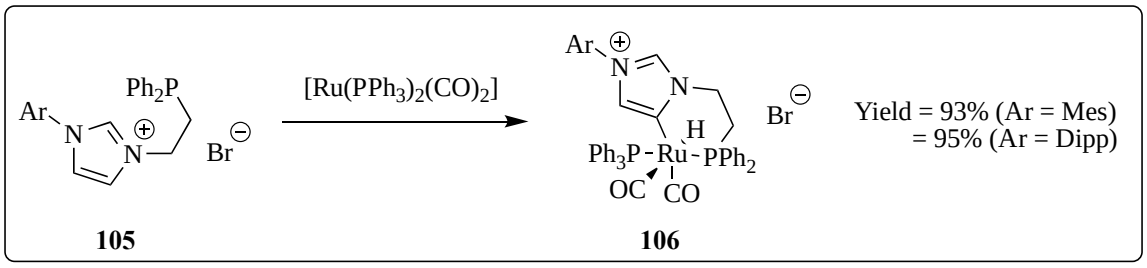

Scheme 3.4 Formation of 'abnormal' carbene in **106**.

In using method (d), Lavign reported the synthesis of an 'abnormal' carbene-ruthenium(II) complex where the coordination of the ruthenium(II) occurred through the insertion into the C-H bond in the C4 position.[11] Similar 'abnormal' carbene-iridium(III) complexes have also been reported[12] and Li explained that this unique mode of coordination depended on the size of the chelating ring.[13] (Scheme 3.4)

Beside the variation in the donocity of carbon in the azole moiety, the phosphine and NHC moieties could also exhibit different modes of coordination depending on the steric bulk of the NHC moiety. Hoffmann reported two related *bis*(phosphine-NHC) dicopper(I) complexes with different coordination modes.[14] As the steric bulk imposed by the mesylate group was more influential than that of the *tert*-butyl group, a single copper(I) was found to coordinate to only one NHC, instead of two, at a time. Since the substituent on the nitrogen in NHC pointed towards the coordination sphere, this steric effect on coordination mode became, expectedly, more pronounced when the steric bulk of the NHC increased. (Scheme 3.5)

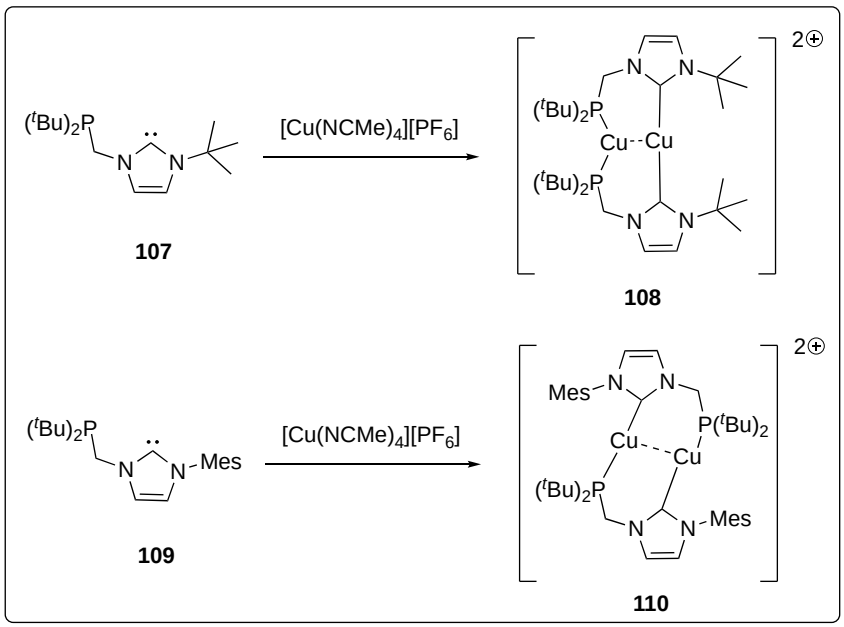

Scheme 3.5 Different modes of coordination depending on steric influence by the *N*-substituents.

According to Togni and Gischig[15], in the presence of strongly bridging soft donors such as iodide, bimetallic copper(I) complexes where an unusual mode of bonding existed between two copper(I) could be also produced. (Scheme 3.6)

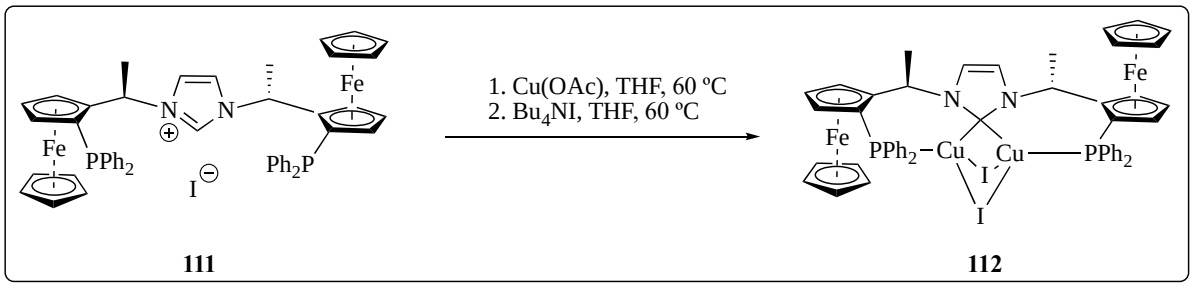

Scheme 3.6 Bimetallic copper(I) complex **112** exhibiting unique modes of bonding with iodide, phosphine and NHC.

Besides copper(I), silver(I) also forms silver(I) NHC complexes with a myriad of structures.[16] A trinuclear silver(I) complex with an unsymmetrically bound chloride ligand was obtained when a *bis*(phosphine)-NHC precursor was deprotonated in the presence of silver(I) oxide.[17] (Scheme 3.7)

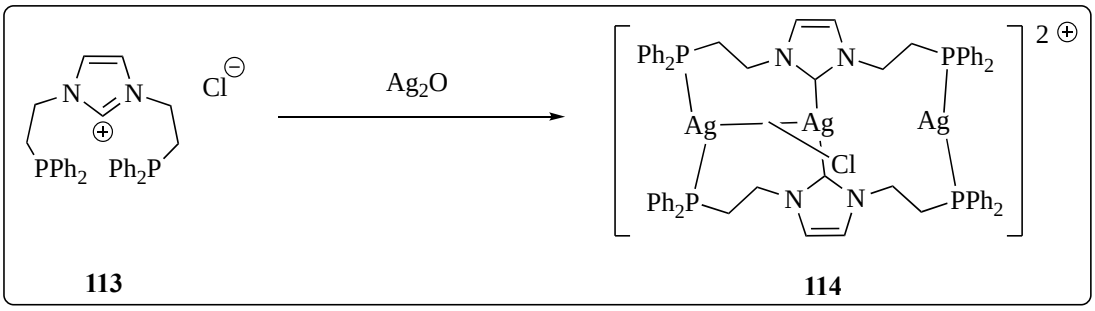

Scheme 3.7 Multinuclear silver(I) complex **114**.

Silver NHC compounds are useful transmetallating agents. When silver NHC was transmetallated to rhodium(I) in the presence of an electrophilic solvent, dichloromethane, oxidative addition into the solvent was observed to give a rhodium(III) product; this

unambiguously illustrated the electron-richness of the phosphine-NHC rhodium(I) chloride intermediate.[17] Another study by Brill had also illustrated the electron-richness of iridium(I) complexes bearing phosphine-NHC; the iridium(I) centre oxidatively added into the C-H bond in the *tert*-butyl group on the nitrogen pendant arm to give a hydrido iridium(III) species. (Scheme 3.8)

Scheme 3.8 Activation of electrophilic dichloromethane by electron-rich phosphine-NHC rhodium(I) to give rhodium(III) complex **115**.

With the uncommon *NH,N*-tethered-phosphino-imidazolylidene, the coordination of the ligand occurred *via* coordination at the C2 position.[18] The condition required for this specific C2 coordination was the presence of a benzimidazole moiety as the backbone or a bulky group such as *tert*-butyl in the backbone of the imidazole.[8, 19] (Figure 3.1)

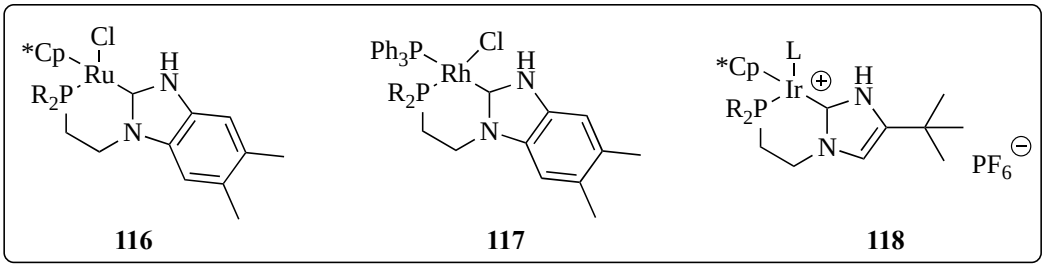

Figure 3.1 Protic phosphine-NHC complexes of ruthenium(II), rhodium(I) and iridium(I) complexes.

Lastly, besides bidentate phosphine-NHC metal complexes, pincer type *bis*(phosphine)-NHC metal complexes had also been synthesized *via* the direct oxidative addition of electron rich nickel(0), palladium(0) and platinum(0) into the C-H bond of the imidazolium moiety.[20] (Scheme 3.9)

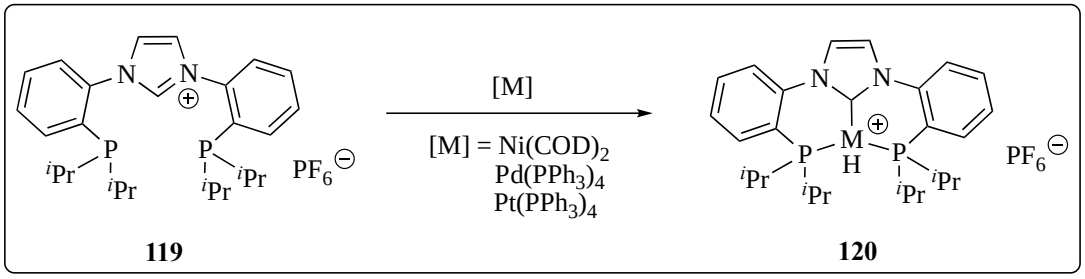

Scheme 3.9 Oxidative addition of electron-rich metals into C-H bond of NHC precursor to give **120** and derivatives.

3.1.2 Catalytic Applications of Phosphine-NHC Metal Complexes

The catalytic activity of phosphine-NHC complexes in coupling reactions has been studied across a limited scope of metals such as nickel, palladium, rhodium and iridium. The phosphine-NHC metal complexes usually contained inert ligand backbones such as alkyl, aryl and ferrocenyl moieties with a strongly ligating NHC which allowed them to be used in a variety of coupling reactions under harsh conditions.

3.1.2.1 Catalysis by Phosphine-NHC Nickel and Palladium Complexes

In Suzuki coupling reactions, well-defined phosphine-NHC palladium complexes exhibited roughly the same activity and efficiency as palladium complexes generated *in situ* from phosphine azolium precursors.[21] While structural variation of the phosphine-NHC ligands affected the yield of the reaction, the yields obtained from some of the better performing

ligands were all well above 90%.[21-22] Suitable aryl halides included bromides and iodide while chloride derivatives displayed lower activity.[22a] In addition, catalytic activity of the palladium complexes in Suzuki coupling reactions could be accelerated using microwave radiation and a high TON of up to 133 h^{-1} could be attained.[23] (Scheme 3.10)

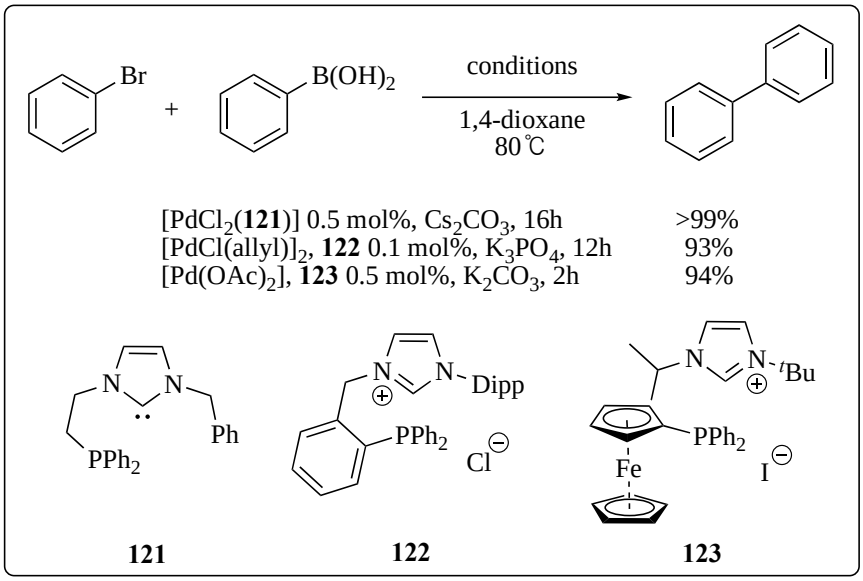

Scheme 3.10 Suzuki coupling mediated by palladium(II) complexes of ligands **121** to **123**.

In 2010, Labande reported the asymmetric Suzuki–Miyaura reaction with a planar chiral phosphine-NHC ligand. Binaphthyl derivatives were obtained in moderate to good yields (30 to 95%) and low to moderate *ee* (10 to 42%).[24] (Scheme 3.11)

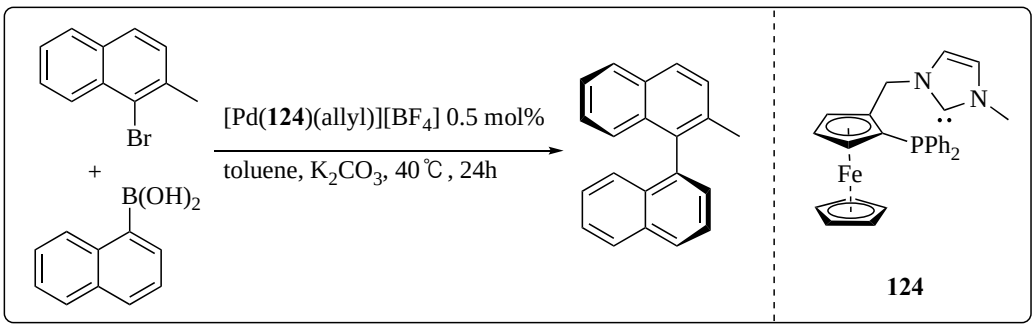

Scheme 3.11 Enantioselective Suzuki coupling mediated by a palladium(II) complex of ligand **124**.

Other than the commonly used palladium, Lee also reported a phosphine-NHC nickel complex capable of coupling aryl chlorides with aryl boronic acids. Using 4-chloroanisole, a comparison amongst nickel complexes containing different *N*-substituted pendant arms revealed that bulkier substituents on imidazole weakened the Ni-P bond, favoured the dissociation of the phosphine ligand and hence facilitated the facile reduction of Ni(II) to Ni(0) which then acted as the active catalyst in the coupling reaction.[25] (Scheme 3.12)

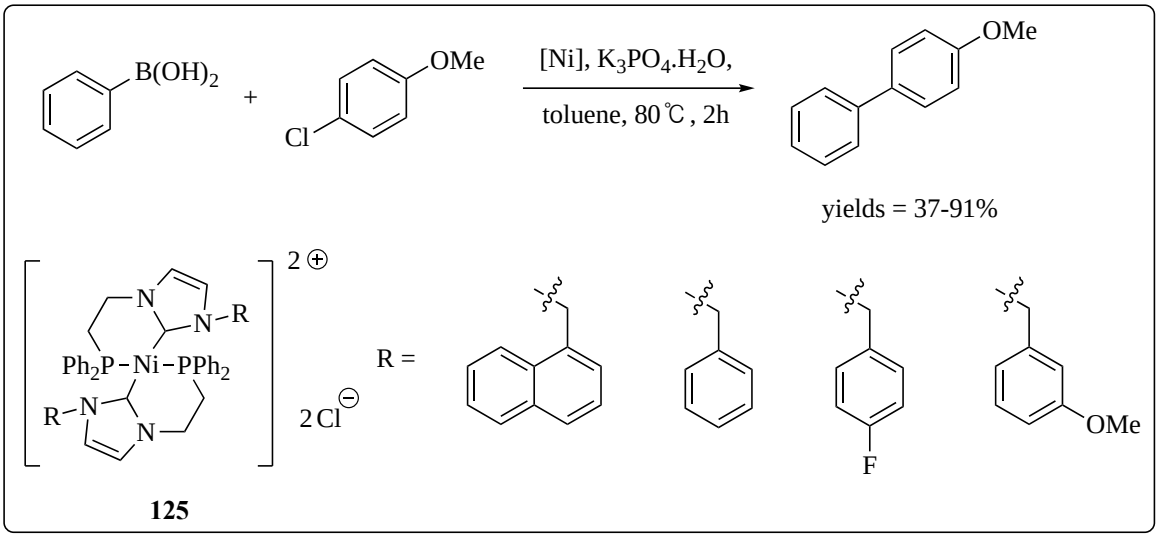

Scheme 3.12 Suzuki coupling mediated by nickel(II) complexes of ligands **125** and derivatives.

Besides C-C coupling reactions, phosphine-NHC palladium complexes have also been used in C-N coupling reactions. Both aryl chlorides and bromides were reported to be active substrates in this transformation and interestingly, the reaction gave a higher yield when the bulk on the nitrogen pendant arm was reduced from the bulkier adamantyl to the sterically unhindered methyl group.[26] (Scheme 3.13)

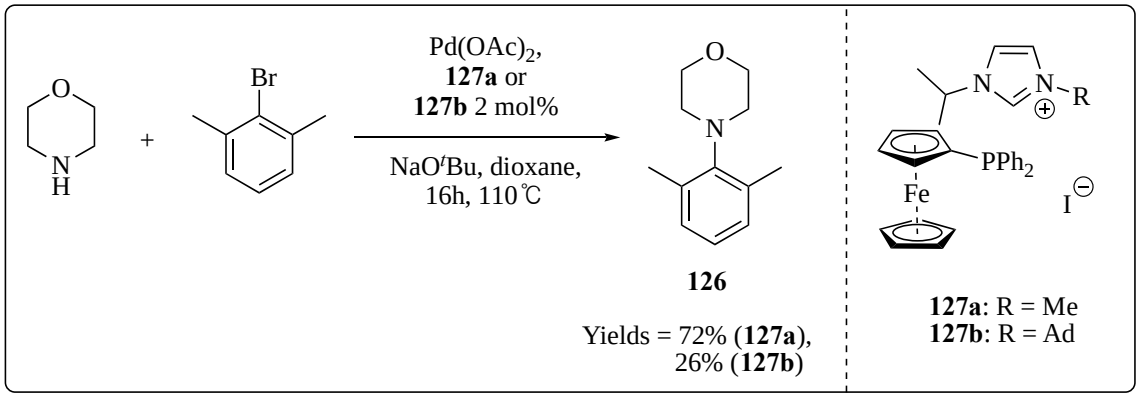

Scheme 3.13 Buchwald-Hartwig coupling by palladium(II) complexes of **127a** and **b**.

3.1.2.2 Catalysis by Phosphine-NHC Rhodium and Iridium Complexes

On the other hand, phosphine-NHC rhodium complexes have found new applications in the field of 1,2-addition, conjugate addition, hydrosilylation, hydroamination and hydrogenation reactions.

Enantioselective addition of boronic acids to aldehydes have been reported using the chiral phosphine oxide-imidazolium precursor in the presence of rhodium(II) acetate dimer and a base to give enantioenriched secondary alcohols with low to modest enantioselectivities.[27] (Scheme 3.14)

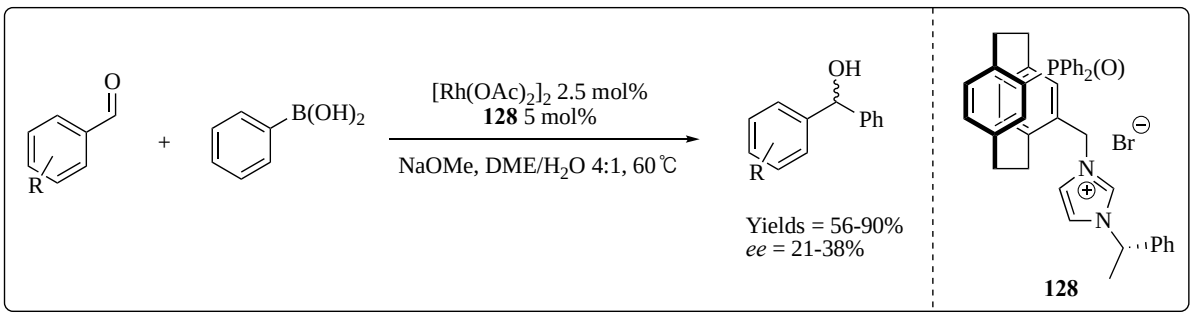

Scheme 3.14 Asymmetric addition of boronic acids to aldehydes catalyzed by rhodium(I) complex of phosphine oxide-NHC ligand.

Nonetheless, some phosphine-NHC rhodium(I) complexes provided encouraging yields and enantioselectivity in 1,4-conjugate addition of boronic acids to enones and α, β-unsaturated esters.[28] (Scheme 3.15)

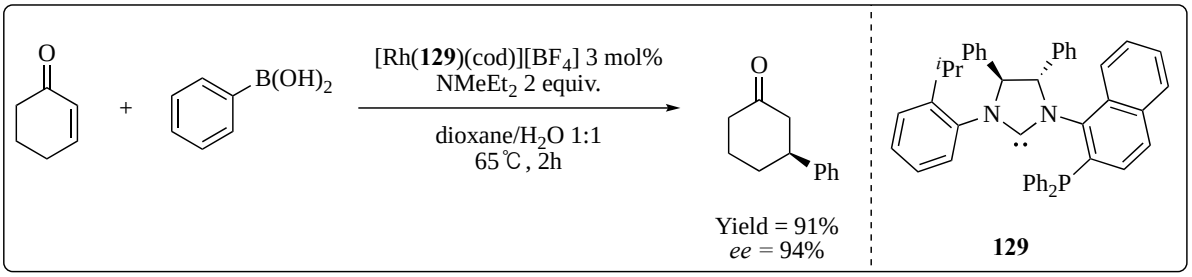

Scheme 3.15 Asymmetric conjugate addition of boronic acid to enone catalyzed by rhodium(I) complex of **129**.

Addition of N-H and Si-H moieties across unsaturated bonds catalyzed by rhodium and iridium catalysts have also been reported by several groups. The advantages of such systems include mild reaction conditions and excellent conversions.[29] (Schemes 3.16 to 3.18)

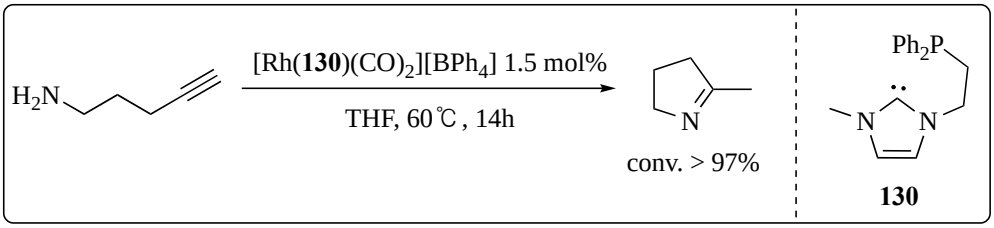

Scheme 3.16 Hydroamination and ring closure catalyzed by rhodium(I) complex of **130**.

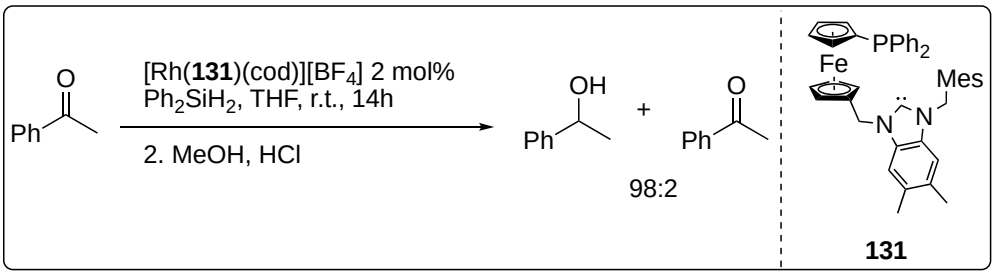

Scheme 3.17 Transfer hydrogenation catalyzed by rhodium(I) complex of **131**.

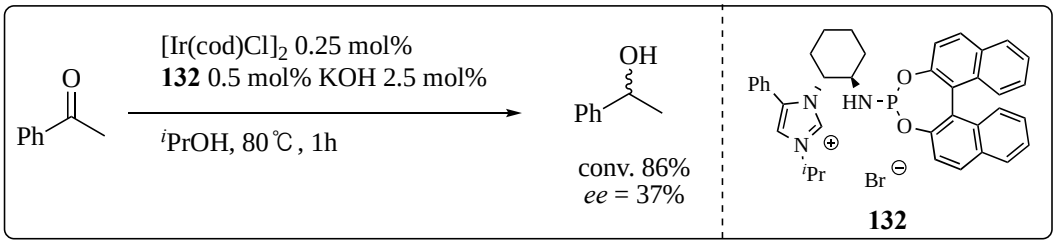

Scheme 3.18 Asymmetric transfer hydrogenation catalyzed by iridium(I) complex of **132**.

Lastly, rhodium and iridium complexes bearing phosphine-NHC ligands have also been shown to exhibit high activity in the hydrogenation of C=C and C=N bonds. With dimethyl itaconate, better activity and enantioselectivity were obtained with rhodium than with iridium complex.[30] (Scheme 3.19) On the other hand, electron-rich styrene gave clean conversion, albeit low enantioselectivity, when hydrogenated with the chiral iridium complex.[30b] (Scheme 3.20)

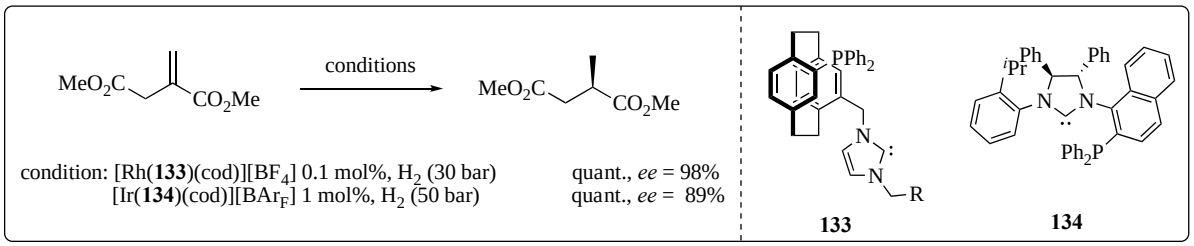

Scheme 3.19 Asymmetric hydrogenation of olefin mediated by rhodium(I) and iridium(I) complexes of **133** and **134**.

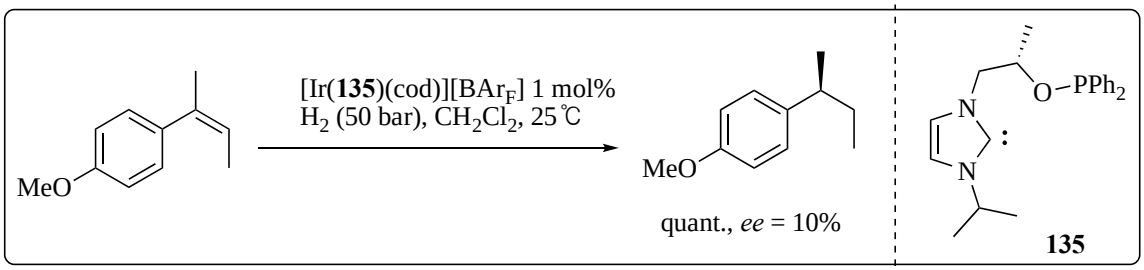

Scheme 3.20 Asymmetric hydrogenation of olefin mediated by iridium(I) complex of **135**.

With the versatile applications of phosphine-NHC ligated metal complexes in a myriad of chemical transformations, the asymmetric hydrophosphination methodology developed in Chapter 2 now provides a fresh and exciting perspective into the synthesis and utility of new metal complexes incorporating novel structures.

3.2 Results and Discussion

3.2.1 Synthesis, Structure and Chemistry of Phosphine-NHC Palladium Complex

3.2.1.1 Initial Attempts and Discovery of Divergent Reaction Pathways

Using the enantioenriched *N*-methylated phosphine azole generated cleanly from the methylation of the phosphine azole obtained from the hydrophosphination, attempts to coordinate the phosphorus donor and deprotonate the azolium salt using a plethora of reaction conditions were made. Most commonly, the azolium salt can be deprotonated using a strong base such as *n*-butyllithium, sodium hydride, potassium *bis*(trimethylsilyl)amide and occasionally potassium *tert*-butoxide in an inert aprotic solvent for substrates of a higher acidity to generate the active free NHC ligand before a metal precursor is added to complete the complexation. Alternatively, the silver NHC transmetallation method using silver(I) bases such as silver(I) oxide, silver(I) acetate and silver(I) carbonate could potentially also be used to transfer the silver(I)-bound NHC moiety onto a metal of choice. In the case of *N*-methylated phosphine azoles, however, the abovementioned methods might not work as expected to furnish the desired phosphine-NHC metal complex due to a few predictable challenges. Firstly, in the event the active NHC ligand was formed, the highly basic nature of the NHC would likely lead to a fast deprotonation of the α-hydrogen adjacent to the electron-withdrawing ketone group and eventually a decomposition of the ligand backbone. Furthermore, the highly nucleophilic active NHC ligand could also attack the electrophilic carbon in the ketone functional group to give unwanted side products. Secondly, the presence of a highly acidic α-

hydrogen precluded the use of strong bases which would otherwise lead to expulsion of the excellent cationic azolium leaving group and in turn trigger a similar ligand backbone decomposition. The choice of base was thought to be highly pertinent as the p*K*a of the chosen base had to be compatible with that of the α-hydrogen and the azolium C-H. To address both challenges, the *N*-methylated phosphine azole was first coordinated to a metal centre bearing a labile ligand, before being deprotonated by a weak base to give the active NHC moiety. The hypothesis is when the highly nucleophilic active NHC moiety is generated, assuming the azolium C-H is more acidic than the α-hydrogen, it will coordinate to the *Lewis*-acidic metal centre rapidly rather than attack other acidic or electrophilic centres within the ligand structure. This hypothesis is supported by the close proximity of the newly formed NHC moiety to the coordination sphere of the metal. It was thought that the NHC would be more likely to react with the metal centre instead of with other farther reactive centres. The conditions for the final coordination-deprotonation step were screened using palladium(II) and platinum(II) as the metals of choice.

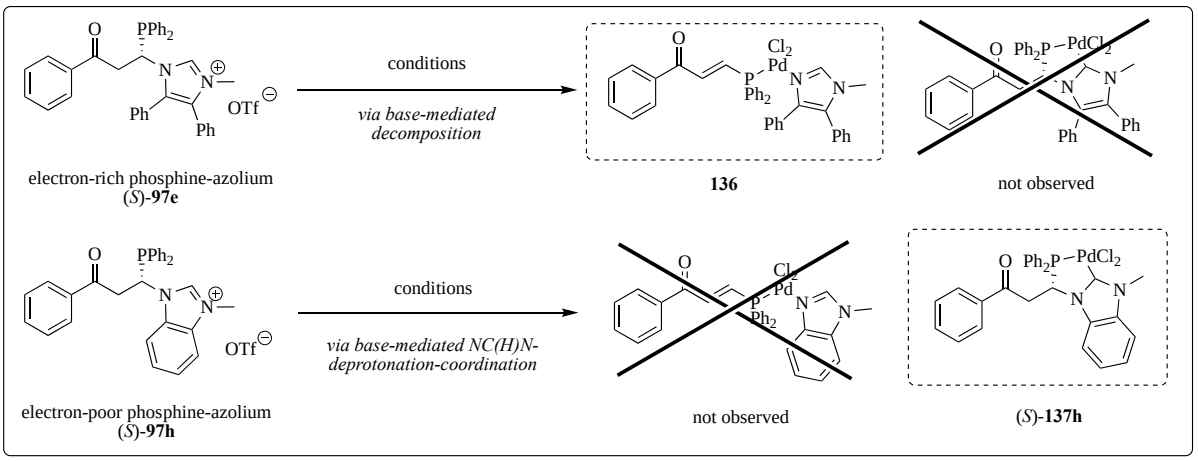

Table 3.1 Different fates of phosphine azolium salts **97e** and **97h**.

S/N	Substrate	Conditions[a]	Product	Yield[b]/%
1	(*S*)-**97e**	1. $PdCl_2(NCMe)_2$, CH_2Cl_2, -40 °C, 2h 2. NEt_3, 25 °C, 12 h	**136**	50
2	(*S*)-**97h**	1. $PdCl_2(NCMe)_2$, CH_2Cl_2, -40 °C, 2h 2. NEt_3, 25 °C, 12 h	(*S*)-**137h**	30
3	(*S*)-**97h**	1. $PdCl_2(NCMe)_2$, DMF, -40 °C, 2h 2. NaOAc, 25 °C, 12 h	(*S*)-**137h**	17
4[c]	(*S*)-**97h**	1. $PdCl_2(NCMe)_2$, CH_2Cl_2, -40 °C, 2h 2. Ag_2O, 25 °C, 12 h	(*S*)-**137h**	50
5[d]	(*S*)-**97h**	1. Li_2PdCl_4, MeOH/CH_2Cl_2, -40 °C, 2h 2. Ag_2O, 25 °C, 12 h	(*S*)-**137h**	0
6	(*S*)-**97h**	1. Li_2PdCl_4, MeOH/CH_2Cl_2, -40 °C, 2h 2. Ag_2O, 25 °C, 12 h	(*S*)-**137h**	49
7	(*S*)-**97h**	1. Li_2PdCl_4, MeOH/CH_2Cl_2, -40 °C, 2h 2. AgOAc, 25 °C, 12 h	(*S*)-**137h**	0
8	(*S*)-**97h**	1. Li_2PdCl_4, MeOH/CH_2Cl_2, -40 °C, 2h 2. NEt_3, 25 °C, 12 h	(*S*)-**137h**	95

[a] Reactions were carried out with the stated substrate (0.0575 mmol), 1 equiv. of [Pd] precursor, 2 equiv. of halide source (if any) and 1 equiv. of base in the listed solvent(s) (total volume 3 mL). [b] Crude $^{31}P\{^1H\}$ NMR yield. [c] 2 equiv. of NEt_4Cl was added. [d] 0.5 equiv. of Ag_2O was used.

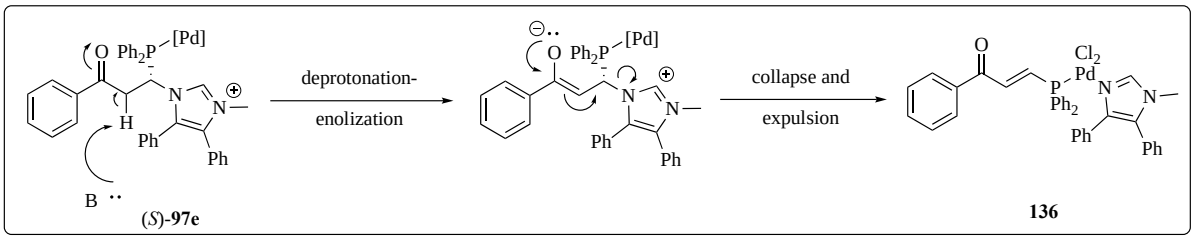

Scheme 3.21 Proposed base-mediated decomposition pathway of (*S*)-**97e**.

Two specific *N*-methylated phosphine azoles were selected for the study on the effects of acidity on the feasibilities of the base-mediated decomposition pathway and the base-mediated NC(H)N-deprotonation-coordination pathway, one bearing an electron-donating diphenyl substituent (diphenylimidazole) and one bearing an electron-withdrawing benzene-fused substituent (benzimidazole). From the initial result obtained using substrate (*S*)-**97e** with diphenylimidazole as the substituent in the *N*-methylated phosphine azole, it can be seen that when the acidity of the α-hydrogen was higher than that of the diphenylimidazolium C-H, decomposition of the ligand backbone, as correctly predicted by the preceding hypothesis, would occur. (entry 1) In the proposed mechanism of the decomposition pathway, the added base would first abstract the more acidic α-hydrogen, leading to an intermediatory enolate which then collapsed spontaneously with the cleavage of the C-N bond, expulsion of a cationic leaving group and the formation of a C=P double bond to give two distinct molecular fragments. Unfortunately, a loss in chirality also occurred. The disintegrated conjugated phosphine ligand and methyldiphenyllimidazole then coordinated to the palladium(II) centre to afford the final decomposition product **136** as the sole product. The two molecular fragments coordinated in a *cis* fashion, featuring a P-Pd and a N-Pd bond in a non-chelating manner. The methyldiphenylimidazole phosphine palladium(II) complex could be recrystallized from a saturated solution of dichloromethane and hexane at room temperature to give air and moisture stable dark orange crystals.

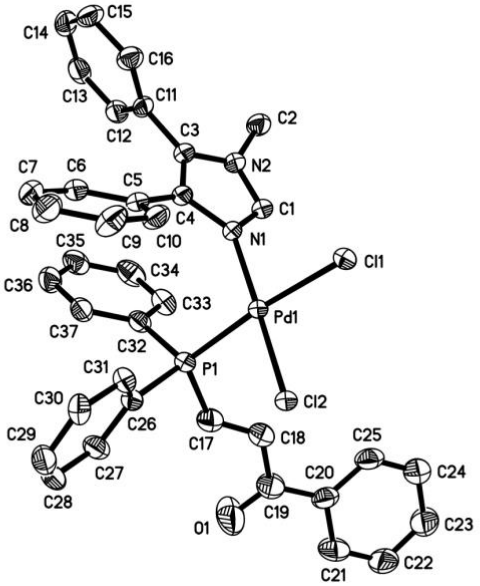

Figure 3.2 Molecular structure of achiral methyldiphenylimidazole phosphine Pd(II) chloride complex **136** with thermal ellipsoids shown at 50% probability.

Structurally, the methyldiphenylimidazole phosphine Pd(II) complex featured a palladium(II) centre in a pseudo square planar geometry, with a N(1)-Pd(1)-P(1) of 94.53(7)°, slighter wider than that of an ideal square planar. The P(1)-Pd(1) bond length was 2.2382(8) Å and the Pd(1)-Cl(1) and Pd(1)-Cl(2) bond lengths were 2.3646(8) and 2.2880(7) Å respectively. The P-Cl bond *trans* to the phosphine was significantly longer than the P-Cl bond *cis* to the phosphine; this disparity in bond length was attributed to the higher *trans* influence of the phosphine as compared to the imidazole moiety. Lastly, the phenyl ring on C4 of the methyldiphenylimidazole seemed to interact with one of the phenyl rings on the phosphine in a π- π stacking manner.

On the other hand, in the benzimidazole-substituted phosphine azolium salt (*S*)-**97h**, the extensive delocalization of π electrons within the two conjugated planar rings in the latter lowers the HOMO of the system and this lower-energy HOMO helps to substantially stabilize the resulting conjugate base of the benzimidazolium moiety. It was thought that an increase in

acidity of the azolium moiety would lower the feasibility or shut down completely the base-mediated decomposition pathway and favor the NC(H)N-deprotonation-coordination pathway.

With the newly amended benzimidazolium backbone in (*S*)-**97h**, the formation of the desired chelating phosphine-NHC palladium(II) complex (*S*)-**137h** was attempted and was eventually proved fruitful after an extensive series of palladium(II) precursors, bases, both organic and inorganic, and solvents was examined. From the results, with the new benzimidazole-substituted substrate (*S*)-**97h**, the yields obtained ranged from modest to excellent except for entries 5 and 7. Solvents were selected based on the solubility of the employed base and it was assumed that the solvents played no significant role in affecting the yield of the final product. Generally, the palladium(II) precursor bearing two highly labile acetonitrile ligands gave comparatively lower yields (entries 2-4) than those obtained from the tetrachloropalladate(II) precursor (entries 6 and 8). In addition, different bases ranging from triethylamine in dichloromethane to sodium acetate in dimethylformamide and silver(I) oxide in dichloromethane were plausible although their yields greatly differed. These differing yields could be explained by the relative basicity of the base used; the stronger the base, the more efficient the deprotonation step and hence the higher the product yield. Lastly, as the reaction solvent for the deprotonation-coordination was protic, it was speculated that the deprotonation and coordination probably occurred in a concerted step without involvement from the methanol molecules although no further experiments were done to ascertain this. Spectroscopically, upon coordination of the phosphine moiety to the tetrachloropalladate(II) anion, a positive coordination shift of 40 ppm was observed for the phosphorus nucleus, indicating a donation of a significant amount of electron density from the phosphorus lone pair to the palladium vacant orbitals. When the five-membered chelate ring formed after the addition of the base, a further 13 ppm-increase in the chemical shift of the phosphorus nucleus was observed. The

chemical shift of the phosphorus centre in the chelating phosphine-NHC palladium(II) complex (*S*)-**137h** was 60.50 ppm.

3.2.1.2 Solid State Structure of Chelating Phosphine-NHC Palladium Complex (*S*)-137h

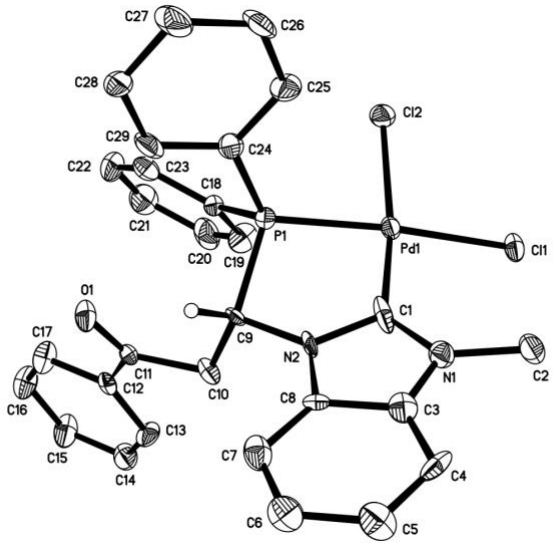

Figure 3.3 Molecular structure of chiral chelating P-NHC Pd(II) chloride complex (*S*)-**137h** with thermal ellipsoids shown at 50% probability (CCDC Ref.: 2035450). Hydrogen atoms except H(C9) are omitted for clarity.

The chiral phosphine-NHC palladium(II) dichloride complex (*S*)-**137h** was obtained *via* slow evaporative crystallization of a saturated solution from dichloromethane and hexane at room temperature to give yellow crystals. Interesting, the corresponding racemic phosphine-NHC palladium(II) dichloride complex could not be obtained using the dichloromethane-hexane solvent system; instead, it was crystallized from a tetrahydrofuran-hexane solvent system. The difference between the energetics of crystal packing of the enantioenriched molecules and the racemic molecules in the solid state might have been the cause for this solvent dependency in the crystallization process. The complex exhibited high solubility in chlorinated solvents such as dichloromethane and chloroform and in tetrahydrofuran and

acetonitrile. It was found to be insoluble in hexane, toluene, methanol, ethanol, water and diethyl ether amongst the common solvents. The absolute stereochemistry at the chiral carbon centre was found to be (*S*) and identical to the same chiral carbon centre in the enantioenriched phosphine azole precursor. This was expected as coordination of the phosphine donor atom to the metal centre should not racemize or invert the chirality at the non-reactive chiral carbon centre.

Structurally, the phosphine and NHC moiety coordinated in a *cis* fashion due to the five-membered chelate ring. The bite angle of this bidentate ligand was 82.0(6)° and the geometry about the palladium centre was approximately square planar. The bond lengths of Pd(1)-Cl(1) and Pd(1)-Cl(2) were 2.368(4) and 2.335(6) Å respectively. Noticeably, the Pd-Cl bond *trans* to the phosphine was longer than that *trans* to the NHC. As NHCs are generally more electron- donating than phosphines, the slightly longer Pd-Cl bond *trans* to the phosphine could be attributed to steric repulsion between the methyl group on C(2) and Cl(1). The Pd(1)-C(1) and Pd(1)-P(1) bonds in the five-membered chelating complex were also slightly shorter as compared to those found in other chelating complexes.[22a]

Between complexes (*S*)-**137h** and **136**, it could be seen that the Pd-P bond in (*S*)-**137h** was 2.206(4) Å, shorter than the Pd-P bond (2.2382(8) Å) in **136**. This difference in bond lengths could be attributed to the higher electron-donating propensity, and hence a stronger σ-donating effect, of the alkyl phosphine in (*S*)-**137h** than the alkenyl phosphine in **136**. In addition, the Pd-Cl bonds *trans* to the phosphine in both complexes had roughly the same length even though the Pd-Cl bond in (*S*)-**137h** was *trans* to a weaker π-acceptor as compared to the Pd-Cl bond in **136**, which was *trans* to a much stronger π-acceptor by virtue of the conjugated enone moiety. This suggests that the π-accepting properties of the phosphine ligands in both complexes had little effect on the *trans* Pd-Cl bonds. Lastly, the Pd-Cl bonds

cis to the phosphine had vastly different lengths- 2.335(6) Å in (*S*)-**137h** versus 2.2880(7) Å in **136**. This observation was again due to the higher *trans* influence of the NHC donor than the imidazole ligand.

3.2.1.3 Chemistry of Chelating Phosphine-NHC Palladium Complex (*S*)-137h

To probe the reactivity of the Pd-Cl bonds in complex (*S*)-**137h**, one equivalent of triphenylphosphine was added to an equimolar of the complex in tetrahydrofuran at room temperature but no ligand substitution occurred. The Pd-Cl bonds in the complex proved to be more inert than one would otherwise expect from the high *trans* influence exerted by both the phosphine and carbon donor atoms; this low lability of the Pd-Cl bond was attributed to the low *trans* effect of the NHC ligand due to its negligible π- accepting property. In support of this explanation, studies from our group have previously shown that in the presence of ligands with a high *trans* effect, such as aryl and quinoline moieties which are strong π- acceptors, substitution of the *trans* chloride ligand takes place readily.[31] (Scheme 3.22)

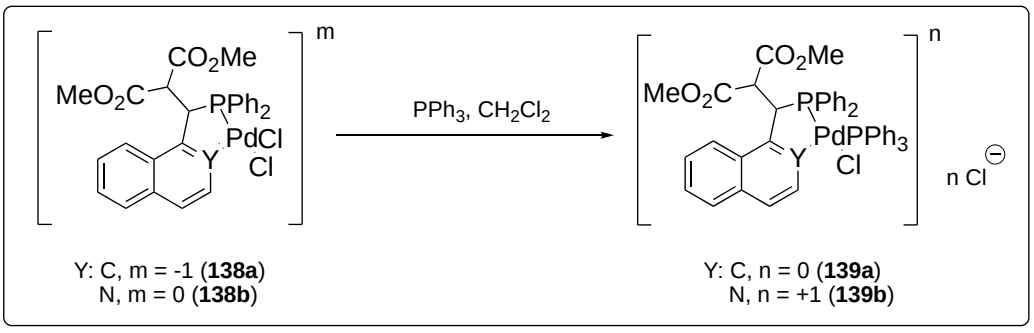

Scheme 3.22 Ligand exchange reaction of complexes **138a** and **b** with π- accepting aryl or quinoline donor.

To probe the reactivity of the stability of the Pd-P bond in (*S*)-**137h**, the phosphine ligand showed no sign of sulfurization *via* ligand dissociation even after the complex was

heated (in a sealed tube) with twenty equivalents of sulfur in dichloromethane at 65 °C for three days. In addition, no sign of oxidation was observed when the complexed was reacted with aqueous hydrogen peroxide in tetrahydrofuran at room temperature overnight. Lastly, the addition of one equivalent of iodobenzene dichloride in dichloromethane at room temperature over 24 h in the dark did not lead to the oxidation of the palladium centre to the +4 state. In short, the phosphine and metal centres were generally stable to oxidants.

3.2.2 Syntheses, Structures and Chemistry of Phosphine-NHC Platinum Complexes

3.2.2.1 Syntheses and Derivatization of Phosphine-NHC Platinum Complexes

Attempts to synthesize phosphine-NHC platinum complexes from *bis*(acetonitrile)platinum(II) chloride were made using the optimized complexation and deprotonation conditions obtained from the palladium analogue.

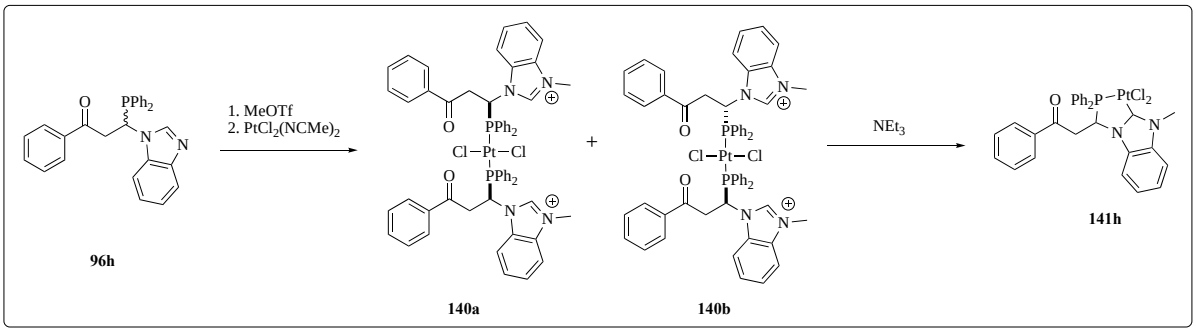

Scheme 3.23 Formation of diastereomeric dimers **140a** and **b**.

Interestingly, the coordination between the phosphine azolium cation derived from **95h** and *bis*(acetonitrile)platinum(II) chloride gave rise to a new pair of resonance singlets at 26.39 and 25.81 ppm with equal intensities in the ^{31}P NMR spectrum. As this phenomenon was not observed when the metal precursor was changed to *bis*(acetonitrile)palladium(II) chloride, it was hypothesized that a facile coordination of two phosphine ligands to a platinum centre might

have occurred due to the highly diffuse 5*d* orbitals and larger atomic radius of platinum. Upon addition of triethylamine, the chelating phosphine-NHC platinum complex **141h** formed and a concomitant downfield shift of 13 ppm in the ^{31}P NMR spectrum was observed. It should be noted that potassium tetrachloroplatinate could also be employed as the source of platinum; the yields were comparable in both cases. Lastly, the complex was purified on silica gel chromatography to give an air- and moisture-stable off-white solid which could then be recrystallised from a saturated solution of dichloromethane and hexane to give enantiopure crystals.

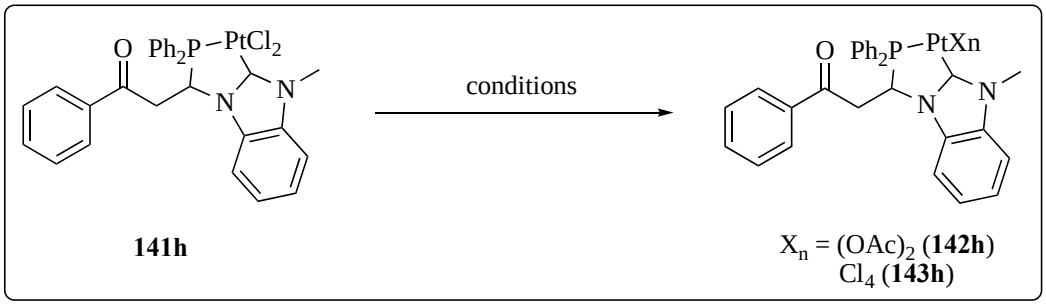

Table 3.2 Derivatisation of complex **141h** *via* ligand exchange and oxidation.

S/N	Conditions[a]	Xn	Yield[b]/%	**δ** ^{31}P[c]	$^{1}J_{P\text{-}Pt}$/Hz	Physical form
ref.[d]	**141h**	Cl_2	-	40.22	3735	Colourless needles
1	AgOAc (2 equiv.), dark CH_2Cl_2, 25 °C, 6 h	$(OAc)_2$ (**142h**)	>99	30.57	4041	Colourless blocks
2	$PhICl_2$ (1 equiv.), dark CH_2Cl_2, 25 °C, 24 h	Cl_4 (**143h**)	>99	36.82	2095	Yellow plates

[a] Reactions were carried out with the starting material (0.0575 mmol) and the stated amount of silver (I) salt or iodobenzene dichloride in the stated solvent (5 mL) in the dark at 25 °C for

the sated duration. [b] Crude $^{31}P\{^{1}H\}$ NMR yield. [c] CD_2Cl_2 as solvent. [d] Starting material was included as reference for ease of comparison.

Phosphine-NHC platinum(II) chloride **141h** underwent ligand exchanges in the presence of a silver(I) salt which acted as a chloride abstractor and oxidation with iodobenzene dichloride to give a series of novel phosphine-NHC platinum complexes with a different supporting anionic ligand and in a higher oxidation state. These reactions readily occurred in the absence of light and the products could be isolated by filtration (entries 1 and 2) and recrystallization to give colourless and yellow crystals.

When the chloride ligand was exchanged for acetate ligands, the chemical shift of the phosphine moved upfield by roughly 10 and the $^{1}J_{P\text{-}Pt}$ increased from 3735 Hz to 4041 Hz.. The less diffuse 2*p* orbitals of oxygen enabled a larger extent of π- donation to platinum and significantly increased the electron density on the platinum centre and as a result, the π-backdonation from the now electron-rich platinum to the vacant orbitals of the *trans* phosphine ligand was enhanced. This synergetic *trans* P-Pt-O orbital arrangement ultimately led to a larger $^{1}J_{P\text{-}Pt}$ coupling constant and a smaller chemical shift of the phosphine in **142h**.

Upon oxidation to Pt(IV), the chemical shift of the phosphine was reduced by 3 ppm while the $^{1}J_{P\text{-}Pt}$ decreased drastically to 2095 Hz. The reduced coupling was due to the lower extent of π- backdonation from the less electron rich Pt(IV). In the solid state, the phosphine-platinum bond was also shown to be longer in **143h** than in **141h**.

3.2.2.2 Solid State Structures of Chelating Phosphine-NHC Platinum Complexes

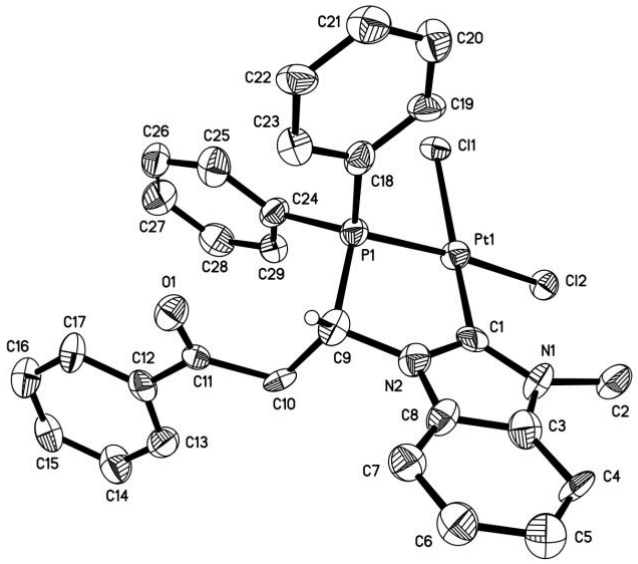

Figure 3.4 Molecular structure of chiral chelating P-NHC Pt(II) chloride complex (*S*)-**141h** with thermal ellipsoids shown at 50% probability (CCDC Ref.: 2090612). Hydrogen atoms except H(C9) are omitted for clarity.

The platinum centre was bonded to a chelating phosphine-NHC moiety and two chloride anions in a slightly distorted square planar geometry. The bite angle of the P(1)-Pt(1)-C(1) chelate was 83.0(5)°, expected of a smaller five-membered constrained ring and the bond lengths of P(1)-Pt(1) and C(1)-Pt(1) were 2.199(4) Å and 1.954(16) Å respectively, considerably shorter and thus stronger than those found in similar reported compounds.[20, 32] Interestingly, the Pt-Cl *trans* to the phosphine was significantly longer, at 2.371(4) Å, than the Pt-Cl *trans* to the NHC, at 2.349(6) Å. Since NHCs are known to exert a stronger *trans* influence than phosphines, this unexpected difference in bond length could be attributed to the steric repulsion induced by the methyl group on the NHC pendant arm since this group pointed directly into the coordination sphere, a unique steric feature of NHCs that has also been observed in the previous palladium analogue (*S*)-**137h**.[33]

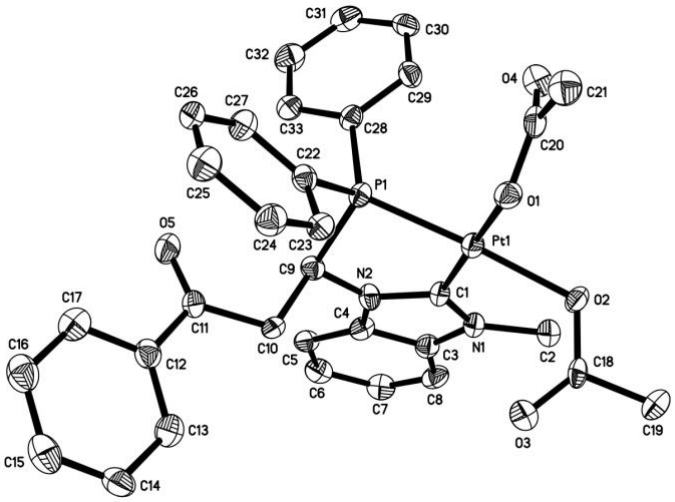

Figure 3.5 Molecular structure of chiral chelating P-NHC Pt(II) acetate complex *rac*-**142h** with thermal ellipsoids shown at 50% probability (CCDC Ref.: 2090610). Hydrogen atoms are omitted for clarity.

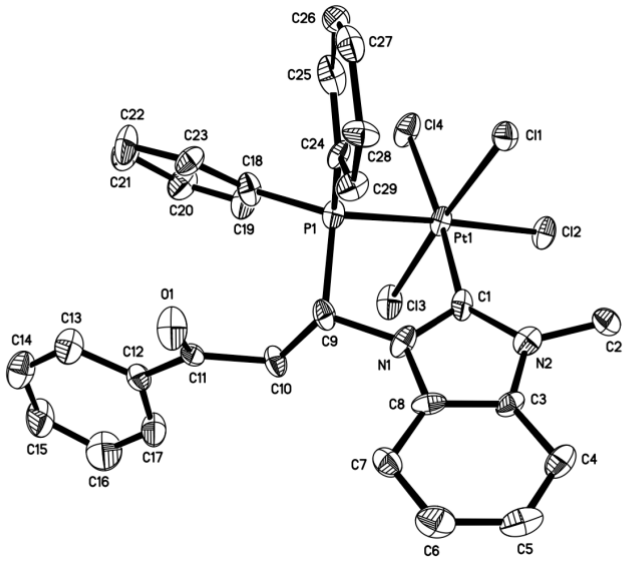

Figure 3.6 Molecular structure of chiral chelating P-NHC Pt(IV) chloride complex *rac*-**143h** with thermal ellipsoids shown at 50% probability (CCDC Ref.: 2095299). Hydrogen atoms are omitted for clarity.

Table 3.3 Structural parameters of platinum complexes **141h**, **142h** and **143h**.

Parameter[a]	**141h**	**142h**	**143h**
Pt(1)-P(1)	2.199	2.2088	2.300
Pt(1)-C(1)	1.954	1.970	2.009
Pt(1)-Cl(2)	2.371	-	2.376
Pt(1)-Cl(1) (**141h**) Pt(1)-Cl(4) (**143h**)	2.349	-	2.366
Pt(1)-O(2) (**142h**) Pt(1)-O(1) (**142h**)	-	2.071 2.067	-
Pt(1)-Cl(1) (**143h**) Pt(1)-Cl(3) (**143h**)	-	-	2.328 2.342
P(1)-Pt(1)-C(1)	83.0	82.1	81.0

[a] Bond lengths and angles are given in units of Å and in degrees respectively. See Appendix for the omitted standard deviations of parameters in this table.

Table 3.3 shows that generally the identity of the *trans* ligand to the phosphine did not affect the Pt-P bond length when the oxidation of platinum remained constant. However, oxidation of the platinum centre to the +4 oxidation state significantly lengthened the Pt-P bond length due to reduced backdonation from the Pt(IV) centre. The same trend was also observed for the Pt-C bond for all three complexes. In terms of the *trans* influence of phosphine against NHC, the ligand *trans* to the former consistently had a longer metal-ligand bond length than that *trans* to the latter; again, this suggested the presence of significant repulsion between the methyl group on the NHC moiety with the ligand *trans* to the phosphine group across all three

complexes. Lastly, the supporting anionic ligand and oxidation state of platinum had a negligible effect on the phosphine-NHC ligand bite angle.

3.2.3 Attempted Catalytic Applications of Phosphine-NHC Palladium and Platinum Complexes

3.2.3.1 C(*sp*)-N coupling

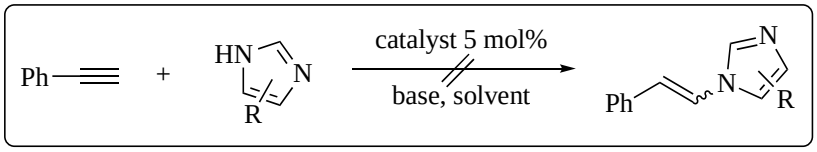

Scheme 3.24 Attempted hydroamination of phenylacetylene.

Nitrogen-containing compounds such as amines, enamines and imines are important motifs in bulk chemicals, specialty chemicals and in pharmaceuticals and the direct formation of amines *via* the highly efficient hydroamination presents a direct, valuable and significant synthetic route.[34] In view of this, phosphine-NHC palladium and platinum complexes **137h**, **141h** and **142h** were initially screened as potential catalysts in the hydroamination of phenylacetylene with imidazole and its derivatives. A range of electron-rich and electron-deficient imidazole derivatives were tested as substrates in this catalytic trial. No reactions were observed for all imidazole derivatives with phenylacetylene in the absence of an external base at 80 °C for 12 h in a sealed tube with solvents such as dichloromethane, tetrahydrofuran and methanol. In addition, addition of silver(I) tosylate to **137h** and **141h**, both one and two equivalents, as chloride abstractor did not improve the feasibility of the reaction.

3.2.3.2 C(sp^2)-C(sp^2) coupling

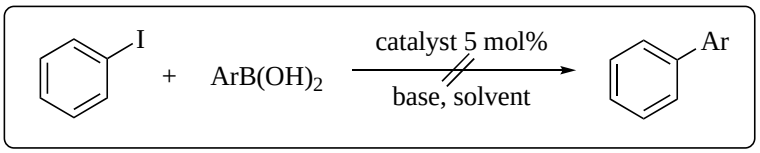

Scheme 3.25 Attempted Suzuki coupling of iodobenzene with arylboronic acids.

Subsequently, to probe the catalytic activity of complexes **137h**, **141h** and **142h** in other coupling reactions, a series of other substrates was employed. Suzuki coupling remains one of the most widely employed C-C bond formation reactions in modern synthetic chemistry as it has found extensive uses in industrial processes ranging from polymer production and fine chemicals synthesis to total synthesis and pharmaceuticals production.[35] In a preliminary trial, the Suzuki coupling of iodobenzene with arylboronic acids was attempted. However, no reactions were observed in a series of bases (NEt_3 and K_3PO_4) and solvents (tetrahydrofuran, dichloromethane and acetonitrile) screened even under a harsh condition of 80 °C for a duration of 12 h. The addition of silver(I) salts ($AgPF_6$ and $AgClO_4$) did not improve the reaction as well.

3.3 Conclusion

In this chapter, the challenges associated with the deprotonation-coordination of phosphine azolium salts bearing electronically different substituents, electron-donating and electron-withdrawing ones, were discussed. The electronically deficient phosphine azolium salt was complexed to palladium and platinum, with two more derivatives of the latter synthesized. The solution- and solid-state structures of the complexes were studied and compared. Lastly, attempted hydroamination and Suzuki coupling as catalytic applications of the palladium and platinum complexes did not work successfully even under improved conditions.

Experimental Section

Unless otherwise stated, all reactions were carried out under a positive pressure of nitrogen using standard Schlenk techniques. Solvents were purchased from their respective companies (MeOH: Fulltime Reagent, DCM, EA: Fisher Chemicals, Toluene, n-hexane: Avantor, THF: Schedelco, Acetone: VWR Chemicals) and used as supplied. Prior to use, all solvents intended for air sensitive reactions were dried and distilled or degassed where necessary. A PSL-1820 Low Temp Pairstirrer was used for conducting low temperature reactions. Thin layer chromatography (TLC) was done using Merck silica gel 60 F254 aluminium supported plates. Flash column chromatography was performed using Merck silica gel 60. NMR spectra were obtained using Bruker AV 300 (^{1}H at 300 MHz, ^{13}C{^{1}H} at 75 MHz, ^{31}P{^{1}H} at 121 MHz); AV 400 (^{1}H at 400 MHz, ^{13}C{^{1}H} at 100 MHz, ^{31}P{^{1}H} at 162 MHz), AV 500 (^{1}H at 500 MHz, ^{13}C{^{1}H} at 125 MHz, ^{31}P{^{1}H} at 202 MHz) and BBFO (^{1}H at 400 MHz, ^{13}C{^{1}H} at 100 MHz, ^{31}P{^{1}H} at 161 MHz) spectrometers. Chemical shifts were reported in ppm and referenced to an internal $SiMe_4$ standard at δ 0 ppm, or to the residual proton signals of the respective deuterated solvents for ^{1}H and ^{13}C{^{1}H} NMR. Melting points were measured using an SRS Optimelt Automated Point System SRS MPA100m machine. Chiral high-performance liquid chromatography (HPLC) data were acquired using an Agilent Technologies 1200 Series HPLC machine with Daicel CHIRALPAK I-series columns. Optical rotations were measured with a JASCO P-1030 Polarimeter in the specified solvent and concentration in a 0.1 dm cell at 25.0^{o}C unless otherwise stated.

General synthesis of palladium complex (*S*)-**137h**

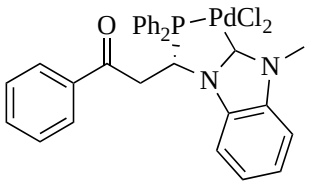

Diphenylphosphine (10 µL, 0.0575 mmol, 1 equiv.), CH_2Cl_2 (1150 µL) and (*R*)-**53** (0.0009 g, 2.5 mol%) were added to an oven-dried 10 mL storage tube and cooled to - 78 °C. Substrate **95h** (0.0575 mmol, 1 equiv.) and tetramethylethylenediamine (8.6 µL, 1 equiv.) were added sequentially into the mixture and the reaction mixture was stirred at - 78 °C for the stipulated time. After which, the reaction mixture was filtered through a short plug of celite to give (*S*)-**96h.** Solvent and base were fully removed by heating the mixture to 50 °C under strong vacuum for 1 hr. CH_2Cl_2 (1150 µL) was then added and the reaction mixture was cooled back to -40 °C. MeOTf (6.5 µL, 0.0590 mmol) was added and the mixture was left to stir for 5 hrs to give (*S*)-**97h** which was not isolated due to difficulty in purifying the air sensitive sticky compound. A methanolic solution of Li_2PdCl_4 (0.0575 mmol, 1 equiv.) was subsequently added and the solution was left to stir for another 2 hrs before triethylamine (8 µL, 1 equiv.) was added. Finally, the mixture was warmed up to room temperature and stirred overnight. Volatiles were removed under reduced pressure and the crude mixture was purified *via* repeated recrystallizations (CH_2Cl_2/hexane) to afford the enantiopure (*S*)-**137h**. Complex (*S*)-**137h** was observed to decompose with significant loss in yield on silica gel and was hence not purified by column chromatography.

General synthesis of platinum complexes **141h**, **142h** and **143h**

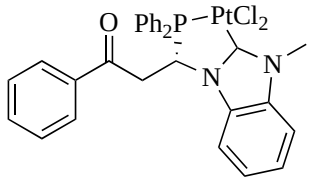

Diphenylphosphine (10 µL, 0.0575 mmol, 1 equiv.), CH_2Cl_2 (1150 µL) and (*R*)-**53** (0.0009 g, 2.5 mol%) were added to an oven-dried 10 mL storage tube and cooled to - 78 °C. Substrate **95h** (0.0575 mmol, 1 equiv.) and tetramethylethylenediamine (8.6 µL, 1 equiv.) were added sequentially into the mixture and the reaction mixture was stirred at - 78 °C for the stipulated time. After which, the reaction mixture was filtered through a short plug of celite to give (*S*)-**96h.** Solvent and base were fully removed by heating the mixture to 50 °C under strong vacuum for 1 hr. CH_2Cl_2 (1150 µL) was then added and the reaction mixture was cooled back to -40 °C. MeOTf (6.5 µL, 0.0590 mmol) was added and the mixture was left to stir for 5 hrs to give (*S*)-**97h** which was not isolated due to difficulty in purifying the air sensitive sticky compound. $PtCl_2(NCMe)_2$ (0.0575 mmol, 1 equiv.) was subsequently added and the solution was left to stir for another 2 hrs before triethylamine (8 µL, 1 equiv.) was added. Finally, the mixture was warmed up to room temperature and stirred overnight. Volatiles were removed under reduced pressure and the crude mixture was purified *via* repeated recrystallizations to afford the enantiopure (*S*)-**141h**.

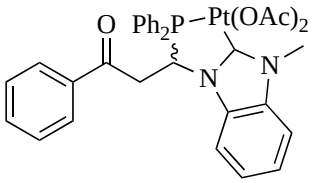

141h (0.0575 mmol, 1 equiv.) was dissolved in NCMe (3 mL) and AgOAc (0.115 mmol, 2 equiv.) was added in the dark and the solution was stirred overnight at room temperature. The mixture was filtered through a short plug of celite and dried to afford **142h**.

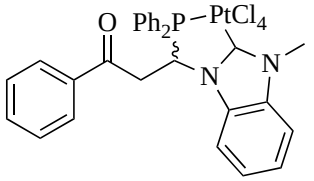

141h (0.0575 mmol, 1 equiv.) was dissolved in CH_2Cl_2 (3 mL) and $PhICl_2$ (0.0575 mmol, 1 equiv.) was added in the dark and the solution was stirred overnight at room temperature. The mixture was filtered through a short plug of celite, washed repeatedly with methanol and then dried to afford **143h**.

Characterisation of **137h**, **141h**, **142h** and **143h**

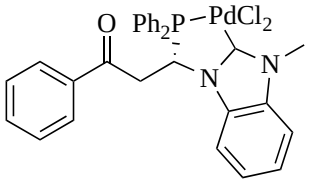

137h. Pale yellow solid. Yield: 0.0065 g, 18%. $[\alpha]_D$ (21 °C) = 209.3°; ^{1}H NMR (CD_2Cl_2, 500 MHz): δ 3.45 (td, 1H, J = 27.9 Hz, 2.9 Hz), 4.02-4.10 (m, 1H), 4.47 (s, 3H), 6.21-6.26 (m, 1H), 7.16 (t, 3H, J_{HH} = 2.4 Hz), 7.35 (t, 2H, J_{HH} = 7.9 Hz), 7.43-7.48 (m, 2H), 7.53-7.62 (m, 8H), 7.83-7.87 (m, 2H), 8.18-8.22 (m, 2H); ^{13}C{^{1}H} NMR (CD_2Cl_2, 75 MHz): δ 36.0, 51.2 (d, J = 6.5 Hz), 111.3, 112.1, 123.8, 124.6 (d, J = 4.8 Hz), 125.1, 125.3, 127.9, 128.2, 128.4, 128.5,

129.6 (d, J = 11.4 Hz), 130.8 (d, J = 11.7 Hz), 132.7 (d, J = 13.0 Hz), 133.7 (d, J = 11.3 Hz), 134.1, 134.8, 135.8, 135.9, 135.9, 172.1, 194.4 (d, J = 1.8 Hz); $^{31}P\{^{1}H\}$ NMR (CD_2Cl_2, 202 MHz): δ 59.20.

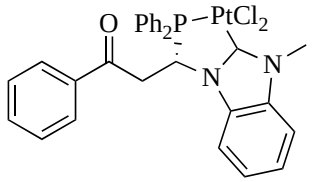

141h. Pale yellow-white solid. Yield: 0.0053 g, 13%. ^{1}H NMR (CD_2Cl_2, 500 MHz): δ 3.37-3.45 (m, 1H), 4.09 (ddd, 1H, J = 18.0 Hz, 11.0 Hz, 11.0 Hz), 4.39 (s, 3H), 6.03 (td, 1H, J = 16.0 Hz, 3.0 Hz), 7.12-7.16 (m, 3H), 7.33-7.43 (m, 4H), 7.47-7.59 (m, 8H), 7.83-7.86 (m, 2H), 8.24-8.28 (m, 2H); $^{13}C\{^{1}H\}$ NMR (CD_2Cl_2, 100 MHz): δ 35.8, 40.8, 40.8, 111.4, 112.2, 125.2, 125.4, 128.2, 128.4, 128.5, 128.6 (d, J = 4.4 Hz), 128.8, 129.2, 129.4, 129.7 (d, J = 11.6 Hz), 130.9 (d, J = 9.5 Hz), 132.8 (d, J = 2.3 Hz), 133.0 (d, J = 3.7 Hz), 134.2 (d, J = 11.4 Hz), 134.4, 135.1, 136.3 (d, J = 11.5 Hz), 195.0; $^{31}P\{^{1}H\}$ NMR (CD_2Cl_2, 202 MHz): δ 40.22.

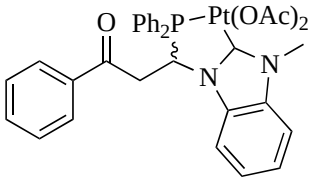

142h. White solid. Yield: 0.0413 g, 99%. ^{1}H NMR (CD_2Cl_2, 400 MHz): δ 2.57 (s, 6H), 3.49-3.54 (m, 1H), 3.95-4.04 (m, 1H), 4.08 (s, 3H), 5.78 (td, 1H, J = 14.0 Hz, 4.0 Hz), 7.18-7.20 (m, 3H), 7.32-7.36 (m, 4H), 7.42-7.44 (m, 2H), 7.49-7.53 (m, 4H), 7.63 (d, 2H, J = 7.0 Hz), 7.87-7.93 (m, 2H), 8.26-8.31 (m, 2H); $^{13}C\{^{1}H\}$ NMR (CD_2Cl_2, 100 MHz): δ 14.3, 22.8, 32.0, 33.2, 41.1 (d, J = 5.4 Hz), 56.2, 56.6, 111.5, 124.8, 125.0, 126.7, 128.3, 128.7, 128.8, 129.0 (d, J = 11.6 Hz), 129.2 (d, J = 6.8 Hz), 131.2 (d, J = 8.6 Hz), 132.3 (d, J = 2.3 Hz), 132.5 (d, J = 2.8

Hz), 133.0, 134.1, 134.2 (d, J = 11.7 Hz), 135.3 (d, J = 11.4 Hz), 135.6, 136.1, 176.0, 195.8 ; $^{31}P\{^{1}H\}$ NMR (CD_2Cl_2, 202 MHz): δ 30.57.

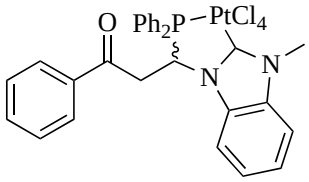

143h. Bright yellow solid. Yield: 0.0426 g, 99%. ^{1}H NMR (CD_2Cl_2, 500 MHz): δ 3.34 (ddd, 1H, J = 19.0 Hz, 16.0 Hz, 2.0 Hz), 4.48 (ddd, 1H, J = 19.0 Hz, 15.0 Hz, 8.0 Hz), 4.60 (s, 3H), 6.34 (ddd, 1H, J = 12.0 Hz, 8.0 Hz, 2.0 Hz), 7.27-7.36 (m, 5H), 7.41-7.48 (m, 4H), 7.52-7.63 (m, 6H), 7.71-7.75 (m, 2H), 8.26-8.29 (m, 2H); $^{13}C\{^{1}H\}$ NMR (CD_2Cl_2, 125 MHz): δ 36.3, 42.7, 112.2, 113.4, 118.6, 119.2, 124.2, 124.7, 126.9, 127.1, 128.4, 129.0 (d, J = 12.3 Hz), 129.1, 129.4 (d, J = 12.6 Hz). 130.8 (d, J = 9.8 Hz), 133.0 (d, J = 8.7 Hz), 134.0 (d, J = 3.4 Hz), 134.5 (d, J = 2.9 Hz), 134.8 (d, J = 8.4 Hz), 136.9, 137.9 (d, J = 9.6 Hz), 145.7, 195.4 (d, J = 1.9 Hz); $^{31}P\{^{1}H\}$ NMR (CD_2Cl_2, 202 MHz): δ 36.82.

References

(1) Lang, H.; J. Vittal, J.; Leung, P.-H., *Metal-template synthesis and co-ordination properties of a palladium complex containing a novel and stable imidazole-substituted phosphine C–P bidentate chelate, J. Chem. Soc., Dalton Trans.* **1998**, 2109-2110.

(2) Edwards, P. G.; Hahn, F. E., *Synthesis and coordination chemistry of macrocyclic ligands featuring NHC donor groups, Dalton Trans.* **2011,** *40*, 10278-10288.

(3) Kaufhold, O.; Stasch, A.; Edwards, P. G.; Hahn, F. E., *Template controlled synthesis of a coordinated [11]ane-P2CNHC macrocycle, Chem. Commun.* **2007**, 1822-1824.

(4) Kaufhold, O.; Stasch, A.; Pape, T.; Hepp, A.; Edwards, P. G.; Newman, P. D.; Hahn, F. E., *Metal Template Controlled Formation of [11]ane-P2CNHC Macrocycles, J. Am. Chem. Soc.* **2009,** *131*, 306-317.

(5) Flores-Figueroa, A.; Kaufhold, O.; Hepp, A.; Fröhlich, R.; Hahn, F. E., *Synthesis of a Ruthenium(II) Complex Containing an [11]ane-P2CNHC (NHC = Imidazolidin-2-ylidene) Macrocycle, Organometallics* **2009,** *28*, 6362-6369.

(6) Flores-Figueroa, A.; Pape, T.; Weigand, J. J.; Hahn, F. E., *Template-Controlled Formation of an [11]ane-P2CNHC Macrocyclic Ligand at an Iron(II) Template, Eur. J. Inorg. Chem.* **2010,** *2010*, 2907-2910.

(7) (a) Danopoulos, A. A.; Winston, S.; Gelbrich, T.; Hursthouse, M. B.; Tooze, R. P., *Synthesis and structural characterisation of stable pyridine- and phosphine-functionalised N-heterocyclic carbenes, Chem. Commun.* **2002**, 482-483; (b) Gu, P.; Xu, Q.; Shi, M., *Synthesis and structural studies on the chiral phosphine-NHC rhodium and palladium complexes for their performances in the metal-catalyzed reactions, Tetrahedron* **2014,** *70*, 7886-7892; (c) Ahmida, A.; Elmagbari, F. M.; Egold, H.; Flörke, U.; Henkel, G., *NHC-phosphane rhodium complexes and their reaction with oxygen, Polyhedron* **2020,** *181*, 114472; (d) Brill, M.; Marrwitz, D.; Rominger, F.; Hofmann, P., *Comparative study of electronic and steric*

properties of bulky, electron-rich bisphosphinoethane, bis-NHC and phosphino-NHC chelating ligands in analogous rhodium(I) and iridium(I) COD and carbonyl complexes, J. Organomet. Chem. **2015,** *775*, 137-151.

(8) Miranda-Soto, V.; Grotjahn, D. B.; DiPasquale, A. G.; Rheingold, A. L., *Imidazol-2-yl Complexes of Cp*Ir as Bifunctional Ambident Reactants, J. Am. Chem. Soc.* **2008,** *130*, 13200-13201.

(9) Wang, H. M. J.; Lin, I. J. B., *Facile Synthesis of Silver(I)−Carbene Complexes. Useful Carbene Transfer Agents, Organometallics* **1998,** *17*, 972-975.

(10) Clement, N. D.; Cavell, K. J., *Transition-Metal-Catalyzed Reactions Involving Imidazolium Salt/N-Heterocyclic Carbene Couples as Substrates, Angew. Chem. Int. Ed.* **2004,** *43*, 3845-3847.

(11) Benhamou, L.; Wolf, J.; César, V.; Labande, A.; Poli, R.; Lugan, N.; Lavigne, G., *Chelation-Assisted Reactions of Phosphine- and Olefin-Tethered Imidazolium Derivatives and Their Affiliated N-Heterocyclic Carbenes with Roper's Complex Ru(CO)2(PPh3)3, Organometallics* **2009,** *28*, 6981-6993.

(12) Wolf, J.; Labande, A.; Daran, J.-C.; Poli, R., *Reactivity of Phosphane–Imidazolium Salts Towards [Ir(COD)Cl]2: Preparation of New Hydridoiridium(III) Complexes Bearing Abnormal Carbenes, Eur. J. Inorg. Chem.* **2008,** *2008*, 3024-3030.

(13) Song, G.; Wang, X.; Li, Y.; Li, X., *Iridium Abnormal N-Heterocyclic Carbene Hydrides via Highly Selective C−H Activation, Organometallics* **2008,** *27*, 1187-1192.

(14) Kühnel, E.; Shishkov, I. V.; Rominger, F.; Oeser, T.; Hofmann, P., *Synthesis and Structures of Copper(I) Complexes with Phosphino-Functionalized N-Heterocyclic Carbenes (NHCP) and Bis-N-Heterocyclic Carbenes (Bis-NHC), Organometallics* **2012,** *31*, 8000-8011.

(15) Gischig, S.; Togni, A., *A Dinuclear Copper(I) Complex Containing a Bridging Chiral Tridentate Carbene Ligand, Organometallics* **2005,** *24*, 203-205.

(16) Garrison, J. C.; Youngs, W. J., *Ag(I) N-Heterocyclic Carbene Complexes: Synthesis, Structure, and Application, Chem. Rev.* **2005,** *105*, 3978-4008.

(17) Zeng, J. Y.; Hsieh, M.-H.; Lee, H. M., *Rhodium complexes of PCNHCP: Oxidative addition of dichloromethane and catalytic hydrosilylation of alkynes affording I-alkenylsilanes, J. Organomet. Chem.* **2005,** *690*, 5662-5671.

(18) (a) Naziruddin, A. R.; Hepp, A.; Pape, T.; Hahn, F. E., *Synthesis of Rhodium(I) Complexes Bearing Bidentate NH,NR-NHC/Phosphine Ligands, Organometallics* **2011,** *30*, 5859-5866; (b) Hahn, F. E.; Naziruddin, A. R.; Hepp, A.; Pape, T., *Synthesis, Characterization, and H-Bonding Abilities of Ruthenium(II) Complexes Bearing Bidentate NR,NH-Carbene/Phosphine Ligands, Organometallics* **2010,** *29*, 5283-5288.

(19) Miranda-Soto, V.; Grotjahn, D. B.; Cooksy, A. L.; Golen, J. A.; Moore, C. E.; Rheingold, A. L., *A Labile and Catalytically Active Imidazol-2-yl Fragment System, Angew. Chem. Int. Ed.* **2011,** *50*, 631-635.

(20) Steinke, T.; Shaw, B. K.; Jong, H.; Patrick, B. O.; Fryzuk, M. D., *Synthesis and Coordination Chemistry of a Tridentate o-Phenylene-Bridged Diphosphine−NHC System, Organometallics* **2009,** *28*, 2830-2836.

(21) Shi, J.-C.; Yang, P.-Y.; Tong, Q.; Wu, Y.; Peng, Y., *Highly efficient and stable palladium/imidazolium salt-phosphine catalysts for Suzuki–Miyaura cross-coupling of aryl bromides, J. Mol. Catal. A: Chem.* **2006,** *259*, 7-10.

(22) (a) Lee, H. M.; Chiu, P. L.; Zeng, J. Y., *A convenient synthesis of phosphine-functionalized N-heterocyclic carbene ligand precursors, structural characterization of their palladium complexes and catalytic application in Suzuki coupling reaction, Inorg. Chim. Acta* **2004,** *357*, 4313-4321; (b) Wang, A.-E.; Zhong, J.; Xie, J.-H.; Li, K.; Zhou, Q.-L., *Highly Efficient Suzuki Cross-Coupling Catalyzed by Palladium/Phosphine-Imidazolium Carbene System, Adv. Synth. Catal.* **2004,** *346*, 595-598.

(23) Ho, C.-C.; Chatterjee, S.; Wu, T.-L.; Chan, K.-T.; Chang, Y.-W.; Hsiao, T.-H.; Lee, H. M., *Direct Arylation Mediated by Palladium Complexes with Rigid Phosphine-Functionalized N-Heterocyclic Carbenes, Organometallics* **2009,** *28*, 2837-2847.

(24) Debono, N.; Labande, A.; Manoury, E.; Daran, J.-C.; Poli, R., *Palladium Complexes of Planar Chiral Ferrocenyl Phosphine-NHC Ligands: New Catalysts for the Asymmetric Suzuki−Miyaura Reaction, Organometallics* **2010,** *29*, 1879-1882.

(25) Lee, C.-C.; Ke, W.-C.; Chan, K.-T.; Lai, C.-L.; Hu, C.-H.; Lee, H. M., *Nickel(II) Complexes of Bidentate N-Heterocyclic Carbene/Phosphine Ligands: Efficient Catalysts for Suzuki Coupling of Aryl Chlorides, Chem. Eur. J.* **2007,** *13*, 582-591.

(26) Shi, J.-c.; Yang, P.; Tong, Q.; Jia, L., *Palladium-catalyzed aminations of aryl halides with phosphine-functionalized imidazolium ligands, Dalton Trans.* **2008**, 938-945.

(27) Ma, Q.; Ma, Y.; Liu, X.; Duan, W.; Qu, B.; Song, C., *ChemInform Abstract: Planar Chiral Imidazolium Salts Based on [2.2]Paracyclophane in the Asymmetric Rhodium-Catalyzed 1,2Addition of Arylboronic Acids to Aldehydes, Cheminform* **2010,** *41*.

(28) Becht, J.-M.; Bappert, E.; Helmchen, G., *Application of Rhodium Complexes of Chiral Diphenylphosphino-Functionalized N-Heterocyclic Carbenes as Catalysts in Enantioselective Conjugate Additions of Arylboronic Acids, Adv. Synth. Catal.* **2005,** *347*, 1495-1498.

(29) (a) Field, L. D.; Messerle, B. A.; Vuong, K. Q.; Turner, P., *Intramolecular Hydroamination with Rhodium(I) and Iridium(I) Complexes Containing a Phosphine−N-Heterocyclic Carbene Ligand, Organometallics* **2005,** *24*, 4241-4250; (b) Gülcemal, S.; Labande, A.; Daran, J.-C.; Çetinkaya, B.; Poli, R., *Rhodium(I) Complexes of New Ferrocenyl Benzimidazol-2-ylidene Ligands: The Importance of the Chelating Effect for Ketone Hydrosilylation Catalysis, Eur. J. Inorg. Chem.* **2009,** *2009*, 1806-1815; (c) Labande, A.; Daran, J.-C.; Manoury, E.; Poli, R., *New (1-Phosphanylferrocen-1'- and -2-yl)methyl-Linked Diaminocarbene Ligands: Synthesis and Rhodium(I) Complexes, Eur. J. Inorg. Chem.* **2007,**

2007, 1205-1209; (d) Hodgson, R.; Douthwaite, R. E., *Synthesis and asymmetric catalytic application of chiral imidazolium–phosphines derived from (1R,2R)-trans-diaminocyclohexane, J. Organomet. Chem.* **2005,** *690*, 5822-5831.

(30) (a) Focken, T.; Raabe, G.; Bolm, C., *Synthesis of iridium complexes with new planar chiral chelating phosphinyl-imidazolylidene ligands and their application in asymmetric hydrogenation, Tetrahedron: Asymmetry* **2004,** *15*, 1693-1706; (b) Nanchen, S.; Pfaltz, A., *Chiral Phosphino- and (Phosphinooxy)-Substituted N-Heterocyclic Carbene Ligands and Their Application in Iridium-Catalyzed Asymmetric Hydrogenation, Helv. Chim. Acta* **2006,** *89*, 1559-1573; (c) Bappert, E.; Helmchen, G., *Synthesis and Application of Complexes of a Novel Chiral Diphenylphosphino-Functionalized N-Heterocyclic Carbene, Cheminform* **2005,** *36*.

(31) Katona, D.; Lu, Y.; Li, Y.; Pullarkat, S. A.; Leung, P.-H., *Catalytic Approach toward Chiral P,N-Chelate Complexes Utilizing the Asymmetric Hydrophosphination Protocol, Inorg. Chem.* **2020,** *59*, 3874-3886.

(32) Flores-Figueroa, A.; Pape, T.; Feldmann, K.-O.; Hahn, F. E., *Template-controlled synthesis of a planar [16]ane-P2CNHC2 macrocycle, Chem. Commun.* **2010,** *46*, 324-326.

(33) Seah, J. W. K.; Li, Y.; Pullarkat, S. A.; Leung, P.-H., *Access to a Chiral Phosphine–NHC Palladium(II) Complex via the Asymmetric Hydrophosphination of Achiral Vinyl Azoles, Organometallics* **2021**.

(34) Müller, T. E.; Hultzsch, K. C.; Yus, M.; Foubelo, F.; Tada, M., *Hydroamination: Direct Addition of Amines to Alkenes and Alkynes, Chem. Rev.* **2008**, *108*, 3795–3892.

(35) Hooshmand, S. E.; Heidari, B.; Sedghi, R.; Varma, R. S., *Recent advances in the Suzuki–Miyaura cross-coupling reaction using efficient catalysts in eco-friendly media, Green Chem.* **2019**, *21*, 381-405.

Chapter 4

Syntheses & Cytotoxicity of Aryl-functionalized Phosphine-NHC Platinum Complexes

4.1 General Introduction to Medicinal Properties of Platinum Complexes

The World Health Organization (WHO) names cancer as one of the leading causes of death globally, responsible for nearly eight millions deaths worldwide in 2008 and is projected to approximately double by 2030.[1] One of the oldest reported metallodrugs employed in the treatment of cancers is cisplatin, diaminedichloroplatinum(II). This complex is a d^8 square planar complex of platinum in the +2 oxidation state with the two ammonia ligands oriented in a *cis* fashion.[2] Cisplatin was first synthesized by Peyrone in 1844 and its medicinal properties were subsequently discovered by Rosenberg in the 1960s.[3] In 1978, the FDA approved cisplatin for use as an anticancer drug, paving the way for the utility of metal-based inorganic compounds in cancer treatments. Cisplatin can be used alone or combined with other drugs in medical treatment for a plethora of cancers and has become one of the most important metallodrugs in terms of its health potency and economic value.[4] Currently, cisplatin is usually administered as a periodic intravenous dose after surgical removal of malignant cancer tissues.

4.1.1 Coordination Chemistry of Cisplatin

Cisplatin movement into the cells occurs either through passive diffusion across the plasma membrane or *via* mediation by a copper-based protein known as the copper transporter CTR1 in mammals.[5] While it has been reported that cisplatin triggers the biodegradation of CTR1, reduces the influx of cisplatin and subsequently increases the level of drug resistance to cisplatin, a small amount of cisplatin still enters the cells successfully.[6] In the cells, cisplatin undergo a chemical activation where the chloride ligands are replaced by water molecules

stepwise through monoaquation and diaquation. These ligand exchanges are facilitated by the low concentration of chloride ions, roughly 2-10 mM, in the cytoplasm of cells and are responsible for the generation of highly *Lewis*-acidic platinum(II) mono and dications such as **144** and **146**. These cations are highly acidic and can in turn undergo further deprotonation as the bound activated aquo ligand loses a proton to water in the cellular environment to give the neutral chlorohydroxoplatinum(II) **145** and monocationic aquahydroxoplatinum(II) **147**. In fact, cisplatin exists as an equilibrium mixture of these neutral and cationic aquated platinum(II) species in the cells. It is important to note that this system of equilibria is dependent on the pH, temperature and chloride concentration of the solution. (Scheme 4.1)

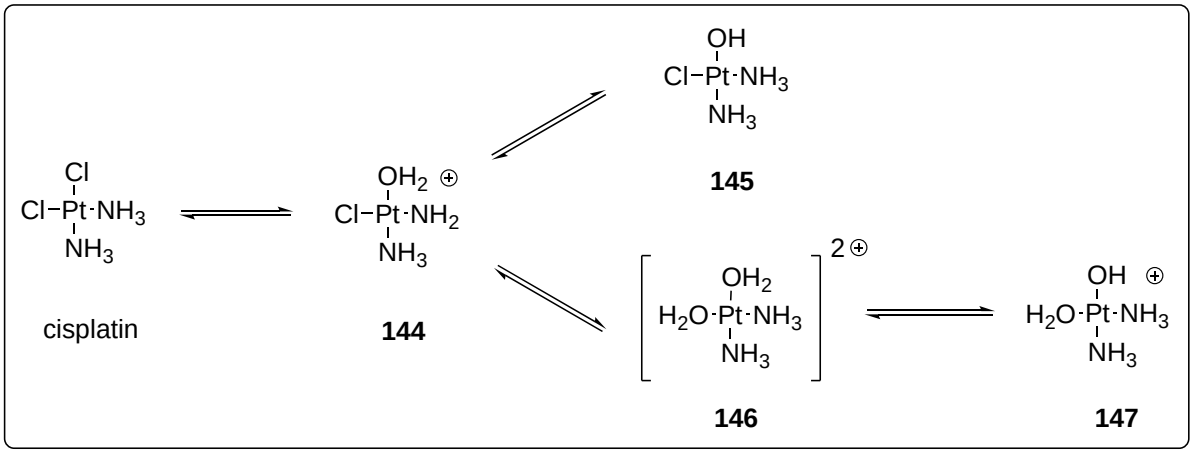

Scheme 4.1 Equilibration of various platinum(II) species **144**-**147** in an aqueous environment.

Formation of the aqua complexes is necessary as these species exhibit higher reactivity to *Lewis* bases by virtue of their increased electrophilicity and the presence of a better leaving group. The aqua complexes also react readily with sulfur-based nucleophiles such as the sulfhydryl functional groups in proteins and nitrogenous bases such as the purine functional groups present in DNA molecules.[6] Specifically, the substrate of cisplatin is the DNA molecule and the interaction between the former and latter form adducts which consequentially inhibit the repair process of cancerous cells.[7] The complexity of this process leads to varied levels of

coordination, forming mono-strands, inter- and intra-strand DNA-Pt adducts and these adducts display different extent of cytotoxicity.[5b, 8] The propensity of the nitrogen donor atoms to coordinate to the diammineplatinum(II) complex is the highest for the imidazole in guanine; Lippard proved that the oxygen from the amide functional group in guanine forms strong hydrogen bonds with the hydrogen atoms on the ammonia ligands on the platinum centre and this interaction helps to stabilise the G-Pt adduct.[9] A computational study on the binding energies of the nitrogen and oxygen donors in the nucleotides to $[Pt(NH_3)_2]^{2+}$ has also been reported and the results showed that the order followed the sequence, G(N7) > C(N3) > C(O2) > G(O6) > A(N3) ≈ A(N1) > A(N7) > G(N3) > T(O4) > T(O2).[6] (Figure 4.1)

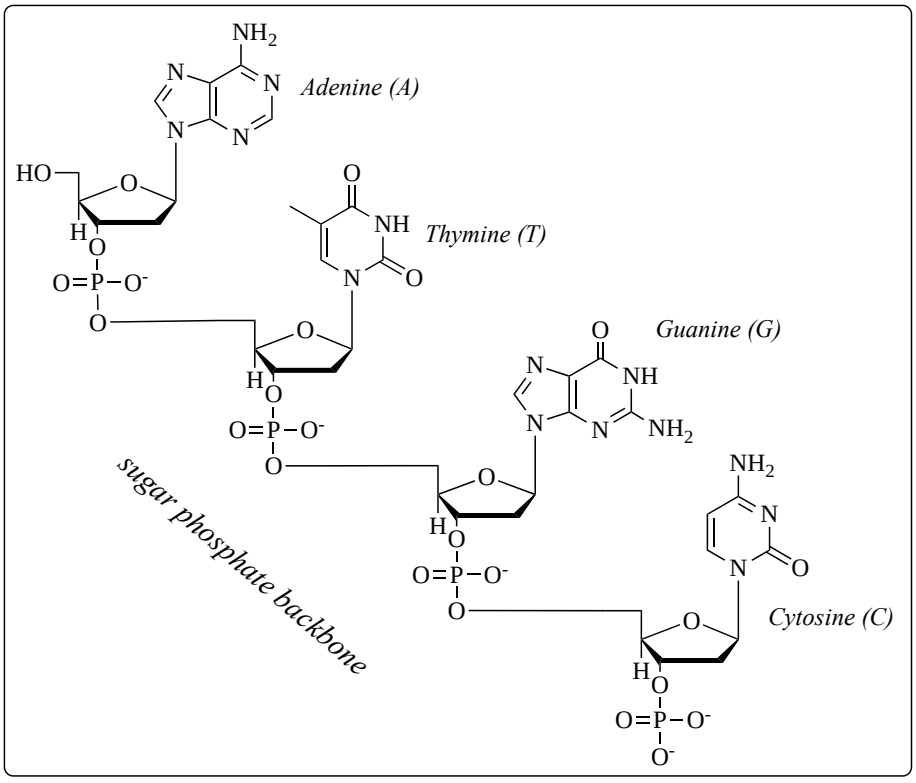

Figure 4.1 Binding affinities of $[Pt(NH_3)_2]^{2+}$ to different *N*- and *O*-donors in DNA.

After platinum coordination, complex structures such inter- and intra-stranded adducts such as 1,2-d(GpG), 1,3-d(GpG), 1,2-d(GpA), 1,3-(GpXpG), Gp and protein-functionalized DNAs form and the structure of the DNAs changes by twisting, bending and rewinding.[10] If

the contorted DNAs do not get repaired by the DNA repair enzymes, the DNAs lose their functions and apoptosis occurs. (Figure 4.2)

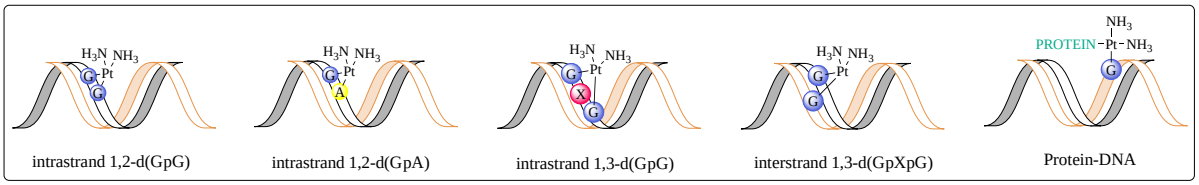

Figure 4.2 Different modes of interaction between DNA and electrophilic Pt(II) species.

While cisplatin remains highly effective in destroying a variety of cancer cells, it becomes highly cytotoxic and induces a large number of side effects when the drug dosage increases.[11] The major side effects include nephrotoxicity, ototoxicity, hepatotoxicity and gastrointestinal toxicity amongst others.[12] Furthermore, cisplatin resistance has been reported for certain cancers such as non-small cell lung cancer and colorectal cancer.[10a, 13] In general, cisplatin resistance may be induced by lowering of the cellular drug uptake, decreasing drug influx or increasing drug efflux, detoxification by thiols, alteration in drug targets and repair of DNAs. These resistance occur at various moments; during bloodstream circulation, during movement across membranes, during time spent in the cytoplasm and after DNA binding.[14] These two significant drawbacks of cisplatin eventually paved the way for the development and testing of novel structurally-different analogue drugs of cisplatin.

4.1.2 Chemical Modifications to Cisplatin

Platinum Drugs	Anticancer Activities	Name/Advantages
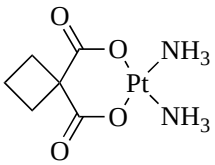	Lung, head, neck, oesophagus *etc*.	• *carboplatin* • Reduced nephrotoxicity

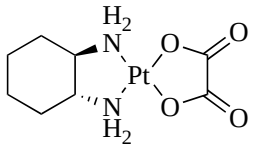	Colon and non-small cell lung cancers *etc*.	• *oxaplatin* • Chiral ligand plays a major role in cytotoxicity • Better safety profile than cisplatin
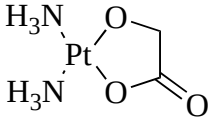	Urological tumours *etc*.	• *nedaplatin* • Reduced nephrotoxicity
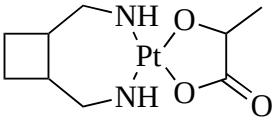	Lung, ovarian and gastric cancers *etc*.	• *lobaplatin* • Displays non-cross-resistance to cisplatin • Clinical trials pertaining to increased dosage showed positive results
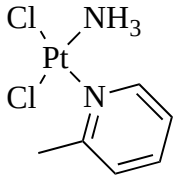	Colorectal and prostate cancers *etc*.	• *picoplatin* • Shields DNA repair pathway
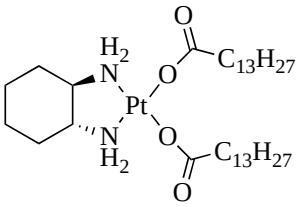	Advanced hepatocellular carcinoma *etc*.	• *miriplatin* • Chiral backbone • Lipophilic platinum-based drug with long retention time in lesions

Table 4.1 Modifications in cisplatin analogues and their projected characteristic properties.

Besides addressing cisplatin resistance and its cytotoxicity, extensive attention have also being paid to DNA-Pt binding, water-versus-lipid solubilities, chemical stability and an increased spectrum of drug activity etc. Firstly, in *carboplatin* and *nedaplatin*, by changing the leaving halide group into an anionic chelate, the rate of ligand dissociation is reduced due to

entropic factor and the rapid formation of highly active complexes which may otherwise initiate undesirable reaction pathways involving other reactive species physiologically is prevented.[15] Similarly, in *oxaliplatin* and *lobaplatin*, the entropic stabilisation provided by the anchor ligand, usually an amine, is enhanced by using bidentate instead of monodentate amines.[15a] Next, in *picoplatin*, the steric bulk provided by the methyl group on the pyridine ligand inhibits DNA enzymes from repairing the damaged DNA and subsequently heightens the drug efficiency.[16] Lastly, in *miriplatin*, the lipophilicity of the drug can be improved by incorporating lengthy alkyl chains which drastically improves the solubility of the drugs in non-polar solvents.[17] The above examples evidently illustrate how chemical modifications on a molecular level can aid in the formulation of drugs with improved efficacies by displaying characteristic properties. The applicability and advantages offered by some of the more common cisplatin analogues bearing modified substituents are summarised in Table 4.1.

4.1.3 Recent Developments in Platinum Drugs as Novel Medicinal Drugs

4.1.3.1 Incorporation of NHC Moieties and Post-functionalisation

Apart from the ubiquitous nitrogen-based ligands such as ammonia, amines and pyridine found in cisplatin and cisplatin analogues, two other categories of important ligands, *N*-heterocyclic carbenes (NHC) and phosphines, have also surfaced as anchor ligands in platinum-based drugs due to their high compatibility with platinum. This affinity originates from the soft-soft interaction between the ligands and platinum. In NHC-platinum bonds, a high degree of covalency develops between the electrically neutral soft carbon donor and polarisable platinum acceptor and this kinetically inert bond inhibits ligand dissociation and slows the formation of highly electrophilic complexes which may otherwise induce undesirable effects as these complexes react indiscriminately with biological molecules. Furthermore, in terms of post-modifications to enhance the structural diversity of the complexes, not only can

these complexes be post-functionalised by direct ligand substitution or by modification of the ligand on the metal through azide-alkyne cycloaddition (**156**, **159** and **160**) and oxime ligation (**153** and **155**), chiral moieties such as amines from enantiopure amino acids (**152**) and alcohols from enantiopure natural sugars (**157**) and steroids (**158**) may also be added to the (including non-NHC ones) complexes to give a wide variety of potentially useful chemical scaffolds.[18]

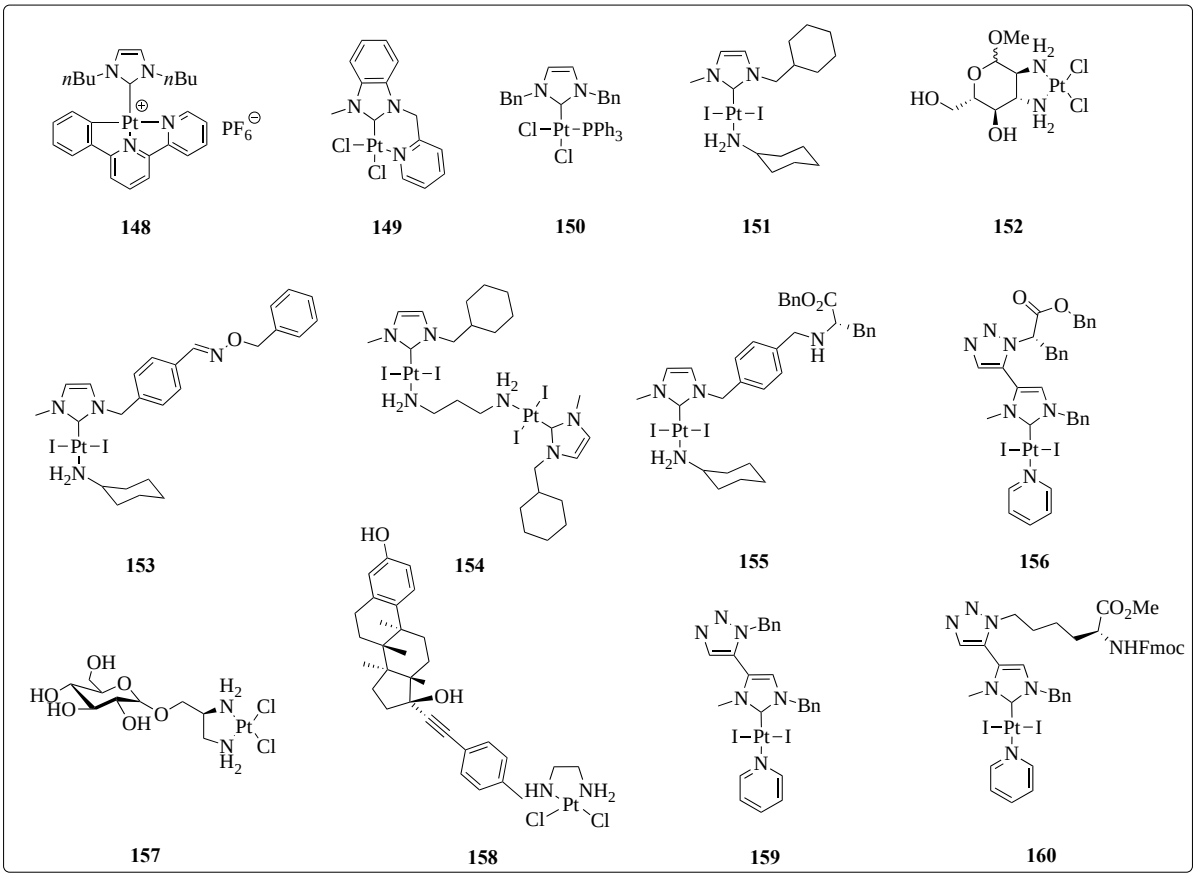

Figure 4.3 NHC- (and post-modified non-NHC-) platinum complexes with medicinal activity.

4.1.3.2 Incorporation of Phosphine Moieties

Similarly, phosphines also form strong σ bonds with a high degree of covalent character to platinum by virtue of their polarisable electron clouds but unlike NHCs, phosphines can also act as π acceptors when their substituents contain electronegative atoms such as halogens or

oxygens or groups such as phenyl and vinyl. This secondary interaction brings about partial double bond character and further stabilises the phosphine-platinum bond.[19]

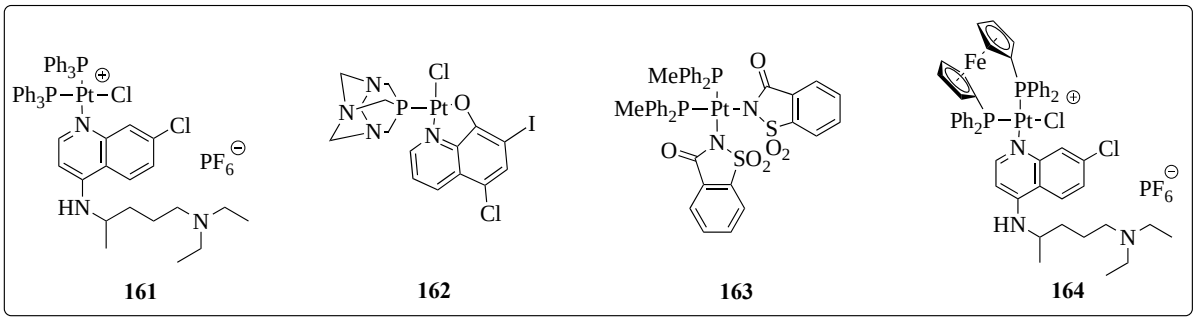

Figure 4.4 Phosphine-platinum complexes that exhibit medicinal activity.

Phosphine-platinum complexes are easily made by the direct complexation of phosphine ligands to a suitable platinum precursor. Electron-rich phosphines are air-sensitive and this complexation may require the use of an inert atmosphere with carefully deoxygenated solvents and reactants. Once the phosphine is coordinated to platinum, the resulting complex is usually not air-sensitive and can be purified under normal atmospheric conditions. Phosphine-platinum complexes showing anticancer properties are not as widely represented as NHC-platinum complexes and this research gap prompts the investigation and application of such complexes in greater details so as to widen the library of knowledge associated with these complexes. (Figure 4.4)

4.1.4 Research Motivation and Aim

With the knowledge from the recent developments in the fields of both NHC- and phosphine-based platinum drugs, it was envisioned that combinational unique hybrid scaffolds featuring both NHCs and phosphines could form a new class of drugs with potential enhanced efficacies in anticancer treatments. Factors of consideration in the design of novel platinum drugs include a) introduction of chelation to increase the entropical stability of complex, b)

incorporation of chirality to enhance recognisability in a chiral cellular environment, c) facile formation of hybrid *C*- and *P*-donors to reinforce thermodynamical stability and d) addition of biologically-active functional groups to potentially increase interactions with DNA and its side chains.

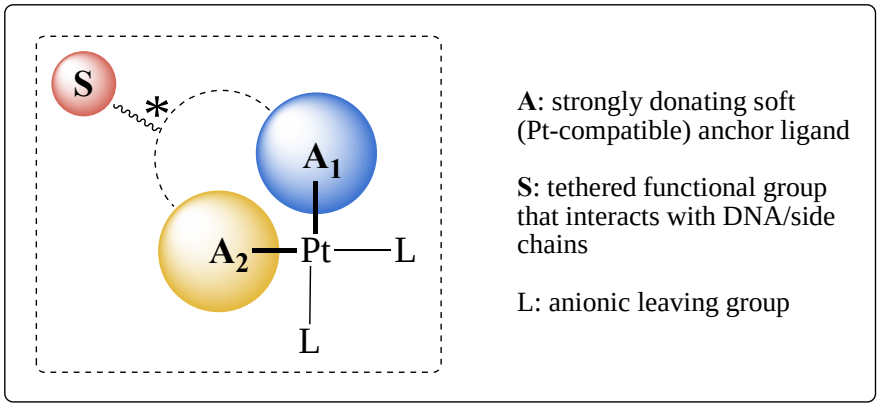

Figure 4.5 Structural design of novel platinum drugs.

In line with the ongoing interests of our group in advancing the utility of asymmetric hydrophosphination, application of this methodology to a specific category of activated vinyl azoles immediately surfaced as a valuable and viable method in the introduction of a chiral centre and a bidentate chelate bearing both NHC (**A_1**) and phosphine (**A_2**) donors into a ligand backbone. In addition, functionalization of the initial substrates for asymmetric hydrophosphination allows the incorporation of biologically active functional groups (**S**) which can potentially engage in non-covalent electronic and steric interactions such as (i) hydrogen bonding, (ii) hydrophobic interaction, (iii) dipole-dipole interaction, (iv) steric repulsion and (v) *van der Waals'* (including π- π stacking) with DNA molecules and their side chains.

4.2 Results and Discussion

4.2.1 Syntheses of Racemic Phosphine-NHC Platinum Complexes

In a preliminary biological study to probe the potential benefits associated with the novel molecular scaffold as anticancer drugs, a series of racemic phosphine-NHC platinum(II) complexes was synthesized from the corresponding vinyl azoles using the racemic form of the palladacycle catalyst in the hydrophosphination step. The choice of racemic complexes was to minimise additional complications which might arise from the stereochemistry of the complexes on the drug efficacy in a chiral biological environment. Details pertaining to the effects of different aryl substituents on the rate, enantioselectivity and yield of the asymmetric hydrophosphination reaction using the enantiopure form of the palladacycle catalyst can be found in Chapter 2 of this thesis and will not be described in this chapter.

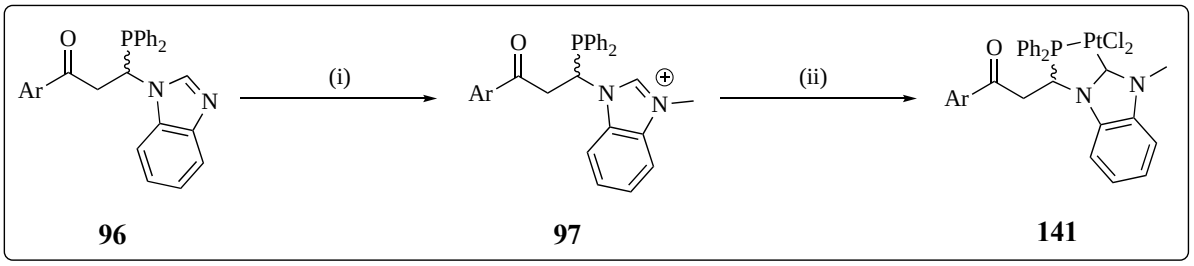

Table 4.2 Transformation of racemic phosphine azoles to phosphine-NHC platinum(II) chloride complexes.[a]

S/N	Product	Ar	Effect of aryl substituent	Yield[b]/%
1	**141h**	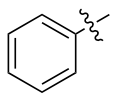	basic structure	13
2	**141i**	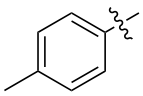	steric repulsion	29

3	**141j**	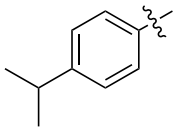	steric repulsion	18
4	**141k**	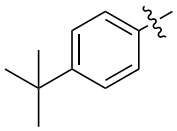	steric repulsion	29
5	**141l**	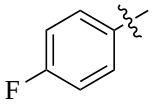	hydrophobic interaction	29
6	**141m**	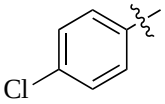	dipole-dipole interaction	20
7	**141n**	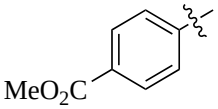	hydrogen bonding	27
8	**141p**	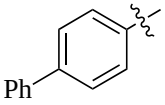	*van der Waals'* interaction	16
9	**141q**	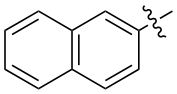	π- π stacking	12

[a] Reactions were carried out with phosphine azole **96** (0.0575 mmol), methyl triflate (0.0575 mmol) in CH_2Cl_2 (2 mL) at -40 °C for 5 h in (i) and with $PtCl_2(NCMe)_2$ (0.0575 mmol) and NEt_3 (0.0575 mmol) respectively at -40 °C for 2 h and 25 °C overnight respectively in (ii). [b] Isolated yield.

The substrate scope consisted of a total of nine functional groups which could be involved in a myriad of chemical interactions with DNA molecules and their side chains. The synthesis of the complexes was simple albeit tedious; the starting materials were hydrophosphinated according to the optimized process and conditions described in Chapter 2 and the resulting air-sensitive phosphine ligands were purified by passing the crude solution through a short plug of celite before the filtrate was subjected to high vacuum at 50 °C for 1 h to remove the solvent and TMEDA base. The solid obtained was then redissolved in

dichloromethane at cooled to -40 °C and methylated using methyl triflate for 5 h. After which, *bis*(acetonitrile)dichloroplatinum(II) was added and the solution was stirred for another 2 h at -40 °C. Lastly, triethylamine was added in the cold and the mixture was warmed to 25 °C and stirred overnight to yield the series of NHC-phosphine platinum(II) chloride complexes. The complexes were purified on silica gel chromatography to give off-white solids. Finally, the solubilities of the complexes in a myriad of organic solvents and water were evaluated so that a satisfactory solvent could be selected for drug screenings in the later phase. These novel complexes exhibited extremely high solubility in dichloromethane, chloroform and dimethyl sulfoxide and moderate solubility in tetrahydrofuran, acetonitrile, acetone and ethanol. They were sparingly soluble in methanol, toluene, diethyl ether, hexane and water.

4.2.2 Efficacies of Phosphine-NHC Platinum Complexes in MKN74 and MCF7 Cell Lines

To elucidate the drug efficacies of selected phosphine-NHC platinum(II) complexes **141h** to **141q** versus cisplatin on cancer cells, MKN74 and MCF7 cancer cells were treated with respective drug complexes, with their overall cell viability determined every 24 hours, normalised to untreated control group. Relative AUCs were calculated for the complexes across time and compared to cisplatin.

In MKN74 cancer cells, drug complexes **141i**, **141h** and **141j** were indicative of being comparable to cisplatin after 24 hours. At the 48-hour timepoint, drug complexes **141h** and **141k** were comparable to cisplatin, while at the 72-hour timepoint, drug complexes **141i** and **141m** were comparable to cisplatin. In MCF7 cancer cells, complex **141h** was consistently comparable to cisplatin at all timepoints of 24, 48 and 72 hours, while complex **141i** only showed comparability to cisplatin at 24 hours.

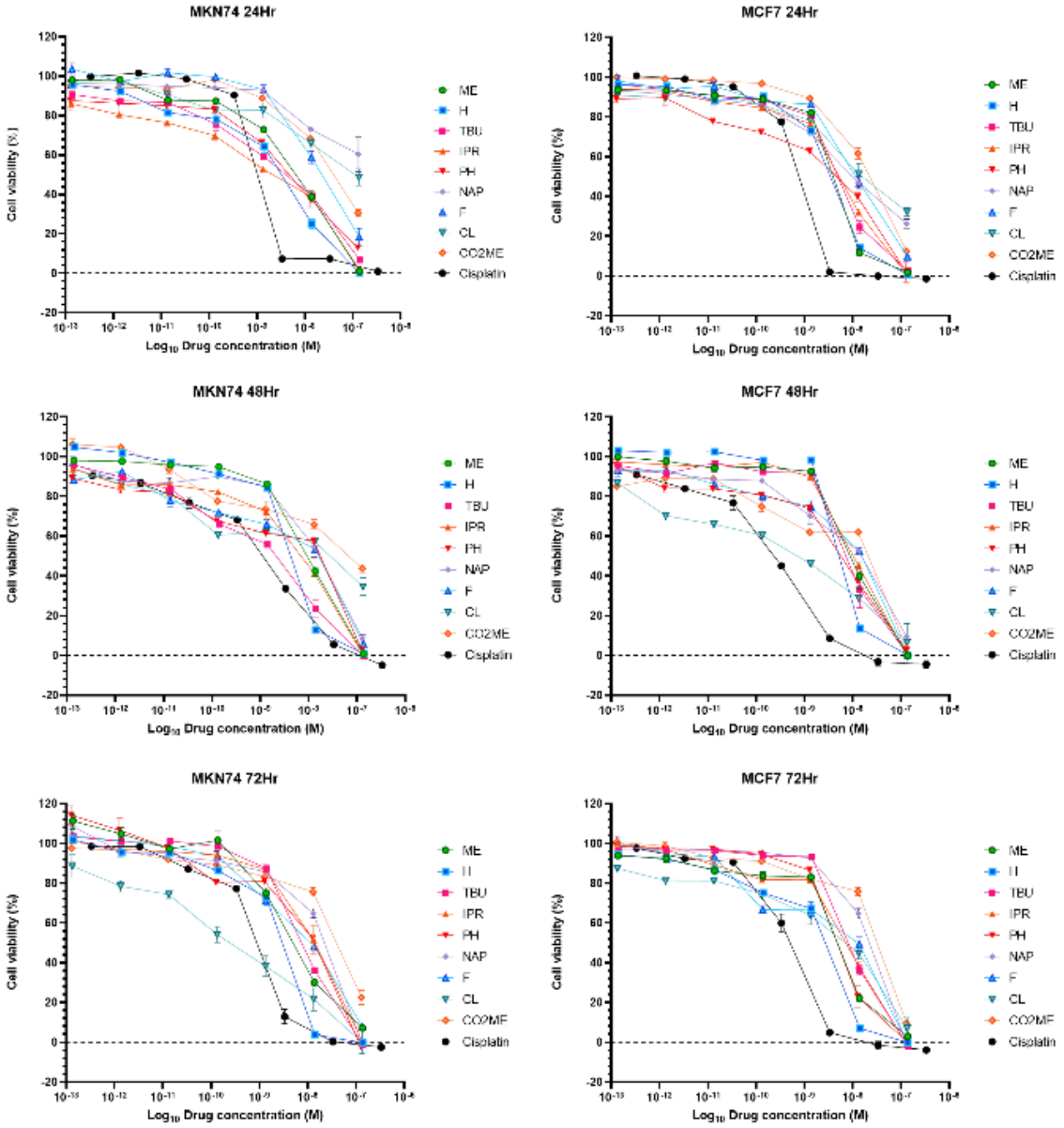

Figure 4.6 Cell viability (%) of MKN74 and MCF7 cultured cancer cells with respective drug treatment every 24 hours. Compound labels read: *ME*(**141i**), *H*(**141h**), *TBU*(**141k**), *IPR*(**141j**), *PH*(**141p**), *NAP*(**141q**), *F*(**141l**), *CL*(**141m**) and *CO2ME*(**141n**).

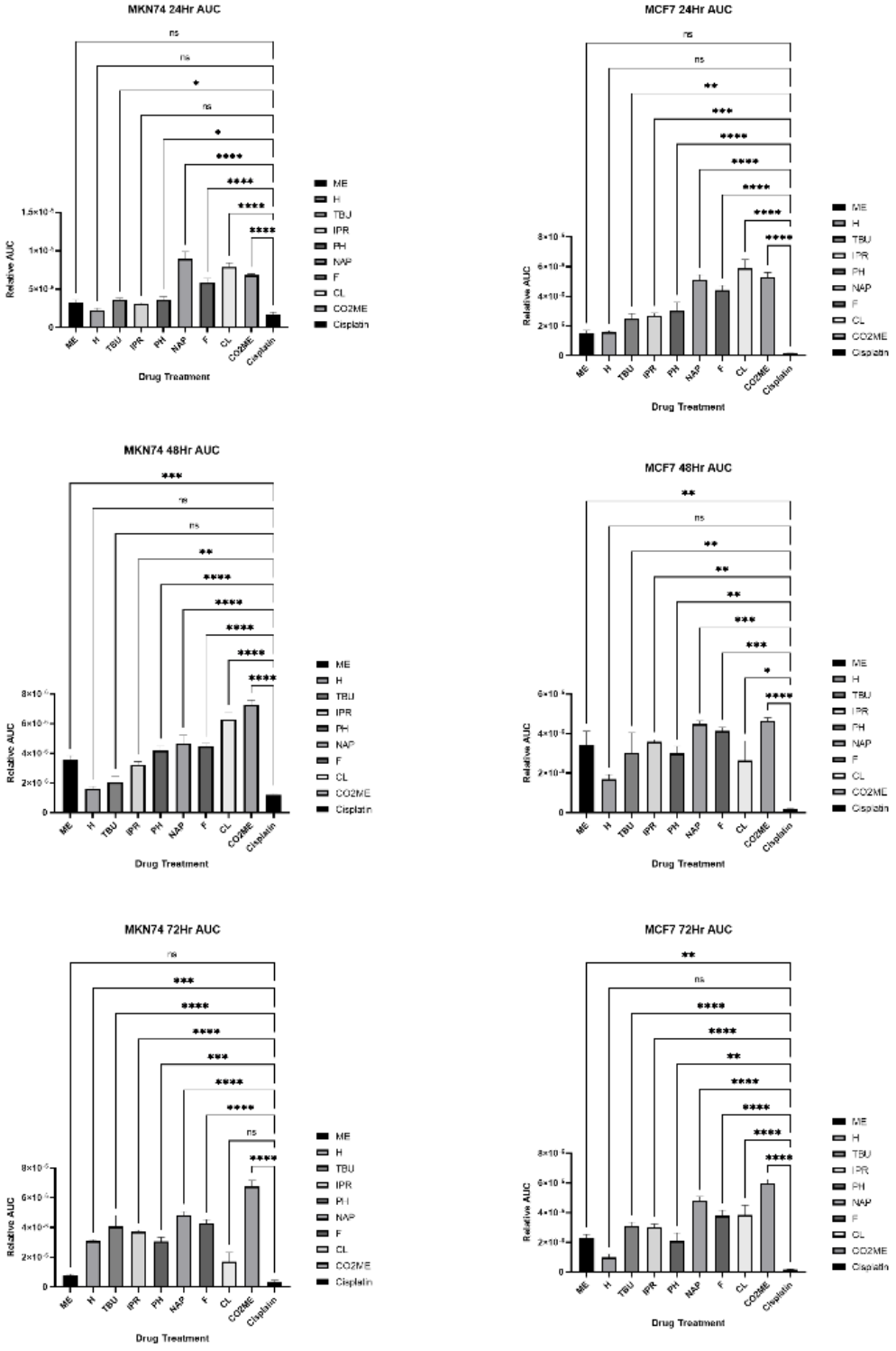

Figure 4.7 Relative area under curve (AUC) of respective drug treatment in comparison to cisplatin. Compound labels read: *ME*(**141i**), *H*(**141h**), *TBU*(**141k**), *IPR*(**141j**), *PH*(**141p**), *NAP*(**141q**), *F*(**141l**), *CL*(**141m**) and *CO2ME*(**141n**).

4.3 Conclusion

In conclusion, catalytic asymmetric hydrophosphination has proven to be a viable method of accessing hybrid phosphine-NHC platinum complexes. The cytotoxic properties of nine phosphine-NHC platinum(II) chloride complexes were evaluated in the MKN74 and MCF7 cancer cell lines. Of which, some of these candidates, **141j** and **141m**, can potentially act as cisplatin-substitutes, given their comparable efficacies to that of cisplatin at various time points. Further studies on drug solubilities under physiological conditions may reveal other potential candidates undiscovered.

Experimental Section

Unless otherwise stated, all reactions were carried out under a positive pressure of nitrogen using standard Schlenk techniques. Solvents were purchased from their respective companies (MeOH: Fulltime Reagent, DCM, EA: Fisher Chemicals, Toluene, n-hexane: Avantor, THF: Schedelco, Acetone: VWR Chemicals) and used as supplied. Prior to use, all solvents intended for air sensitive reactions were dried and distilled or degassed where necessary. A PSL-1820 Low Temp Pairstirrer was used for conducting low temperature reactions. Thin layer chromatography (TLC) was done using Merck silica gel 60 F254 aluminium supported plates. Flash column chromatography was performed using Merck silica gel 60. NMR spectra were obtained using Bruker AV 300 (^{1}H at 300 MHz, ^{13}C{^{1}H} at 75 MHz, ^{31}P{^{1}H} at 121 MHz); AV 400 (^{1}H at 400 MHz, ^{13}C{^{1}H} at 100 MHz, ^{31}P{^{1}H} at 162 MHz), AV 500 (^{1}H at 500 MHz, ^{13}C{^{1}H} at 125 MHz, ^{31}P{^{1}H} at 202 MHz) and BBFO (^{1}H at 400 MHz, ^{13}C{^{1}H} at 100 MHz, ^{31}P{^{1}H} at 161 MHz) spectrometers. Chemical shifts were reported in ppm and referenced to an internal $SiMe_4$ standard at δ 0 ppm, or to the residual proton signals of the respective deuterated solvents for ^{1}H and ^{13}C{^{1}H} NMR. Melting points were measured using an SRS Optimelt Automated Point System SRS MPA100m machine. Chiral high-performance liquid chromatography (HPLC) data were acquired using an Agilent Technologies 1200 Series HPLC machine with Daicel CHIRALPAK I-series columns. Optical rotations were measured with a JASCO P-1030 Polarimeter in the specified solvent and concentration in a 0.1 dm cell at 25.0^{o}C unless otherwise stated.

General synthesis of *rac* platinum complexes **141i** to **q**

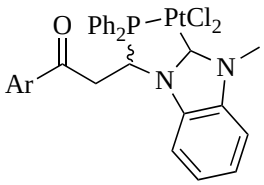

Diphenylphosphine (10 µL, 0.0575 mmol, 1 equiv.), CH_2Cl_2 (1150 µL) and *rac*-**53** (0.0009 g, 2.5 mol%) were added to an oven-dried 10 mL storage tube and cooled to the respective temperature. Substrate **95** (0.0575 mmol, 1 equiv.) and tetramethylethylenediamine (8.6 µL, 1 equiv.) were added sequentially into the mixture and the reaction mixture was stirred at the respective temperature for the stipulated time. After which, the reaction mixture was filtered through a short plug of celite to give **96**. Solvent and base were fully removed by heating the mixture to 50 °C under strong vacuum for 1 hr. CH_2Cl_2 (1150 µL) was then added and the reaction mixture was cooled back to -40 °C. MeOTf (6.5 µL, 0.0590 mmol) was added and the mixture was left to stir for 5 hrs to give **97** which was not isolated due to difficulty in purifying the air sensitive sticky compound. $PtCl_2(NCMe)_2$ (0.0575 mmol, 1 equiv.) was subsequently added and the solution was left to stir for another 2 hrs before triethylamine (8 µL, 1 equiv.) was added. Finally, the mixture was warmed up to room temperature and stirred overnight. Volatiles were removed under reduced pressure and the crude mixture was purified *via* repeated recrystallizations to afford the *rac*-**141**.

Characterisation of **141i** to **q**

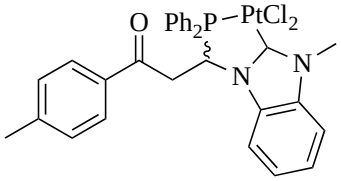

141i. Pale yellow-white solid. Yield: 0.0121 g, 29%. ^{1}H NMR (CD_2Cl_2, 500 MHz): δ 3.39 (ddd, 1H, J = 20.0 Hz, 18.0 Hz, 3.0 Hz), 3.99 (ddd, 1H, J = 18.0 Hz, 11.0 Hz, 11.0 Hz), 4.39 (s, 3H), 6.02 (td, 1H, J = 16.0 Hz, 3.0 Hz), 7.13-7.15 (m, 5H), 7.38-7.44 (m, 5H), 7.47-7.51 (m, 3H), 7.55-7.60 (m, 4H), 7.82-7.87 (m, 2H), 8.24-8.28 (m, 2H); ^{13}C{^{1}H} NMR (CD_2Cl_2, 100 MHz): δ 21.8, 35.8, 40.7, 40.7, 111.4, 112.2, 125.2, 125.4, 128.3, 128.5 (d, J = 12.3 Hz), 129.5, 129.7 (d, J = 11.6 Hz), 130.9, 131.0, 132.7, 132.8 (d, J = 3.0 Hz), 133.0 (d, J = 2.6 Hz), 134.1, 134.2, 136.2, 136.3, 136.7, 145.6, 194.6; ^{31}P{^{1}H} NMR (CD_2Cl_2, 202 MHz): δ 40.16.

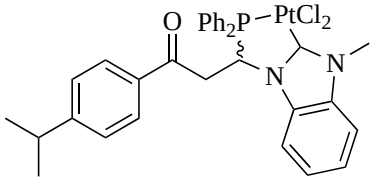

141j. Pale yellow-white solid. Yield: 0.0078 g, 18%. ^{1}H NMR (CD_2Cl_2, 500 MHz): δ 1.23 (d, 6H, J = 7.0 Hz), 2.93 (sep, 1H, J = 7.0 Hz), 3.38 (ddd, 1H, J = 20.0 Hz, 18.0 Hz, 3.0 Hz), 3.99 (ddd, 1H, J = 18.0 Hz, 11.0 Hz, 11.0 Hz), 4.39 (s, 3H), 6.03 (td, 1H, J = 16.0 Hz, 3.0 Hz), 7.09-7.16 (m, 3H), 7.19 (d, 2H, J = 8.0 Hz), 7.38-7.43 (m, 2H), 7.46-7.51 (m, 4H), 7.55-7.60 (m, 3H), 7.82-7.87 (m, 2H), 8.23-8.27 (m, 2H); ^{13}C{^{1}H} NMR (CD_2Cl_2, 100 MHz): δ 23.7 (d, J = 2.6 Hz), 34.7, 35.9, 40.0, 40.7 (d, J = 5.2 Hz), 111.4, 112.2, 122.8, 123.4, 125.2, 125.4, 126.9, 128.4, 128.5, 129.7 (d, J = 11.6 Hz), 131.0 (d, J = 9.6 Hz), 132.8 (d, J = 2.8 Hz), 132.9 (d, J =

2.8 Hz), 133.1, 134.1 (d, J = 11.3 Hz), 136.3 (d, J = 11.4 Hz), 136.7, 156.3, 160.5, 194.7; $^{31}P\{^{1}H\}$ NMR (CD_2Cl_2, 202 MHz): δ 40.14.

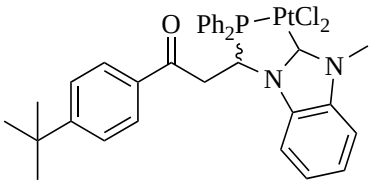

141k. Pale yellow-white solid. Yield: 0.0128 g, 29%. ^{1}H NMR (CD_2Cl_2, 500 MHz): δ 1.31 (s, 9H), 3.39 (ddd, 1H, J = 20.0 Hz, 18.0 Hz, 3.0 Hz), 3.99 (ddd, 1H, J = 18.0 Hz, 11.0 Hz, 11.0 Hz), 4.39 (s, 3H), 6.03 (td, 1H, J = 16.0 Hz, 3.0 Hz), 7.09-7.16 (m, 3H), 7.34-7.42 (m, 4H), 7.47-7.50 (m, 4H), 7.57-7.60 (m, 3H), 7.82-7.86 (m, 2H), 8.23-8.27 (m, 2H); $^{13}C\{^{1}H\}$ NMR (CD_2Cl_2, 100 MHz): δ 31.1, 35.5, 35.8, 40.7 (d, J = 5.1 Hz), 111.5, 112.2, 122.8, 123.4, 124.9, 125.2, 125.4, 125.5, 125.7, 128.2, 128.5 (d, J = 12.2 Hz), 129.7 (d, J = 11.6 Hz), 131.0 (d, J = 9.6 Hz), 132.6, 132.8 (d, J = 2.8 Hz), 132.9 (d, J = 2.8 Hz), 134.1 (d, J = 11.2 Hz), 136.3 (d, J = 11.4 Hz), 136.7, 158.5, 194.7; $^{31}P\{^{1}H\}$ NMR (CD_2Cl_2, 202 MHz): δ 40.13.

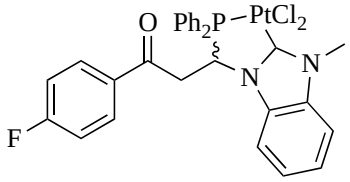

141l. Pale yellow-white solid. Yield: 0.0122 g, 29%. ^{1}H NMR (CD_2Cl_2, 400 MHz): δ 3.32-3.42 (m, 1H), 4.01 (ddd, 1H, J = 18.0 Hz, 11.0 Hz, 11.0 Hz), 4.40 (s, 3H), 6.01 (td, 1H, J = 16.0 Hz, 2.0 Hz), 7.01-7.05 (m, 2H), 7.14-7.16 (m, 3H), 7.39-7.59 (m, 9H), 7.82-7-87 (m, 2H), 8.22-8.27 (m, 2H); $^{13}C\{^{1}H\}$ NMR (CD_2Cl_2, 100 MHz): δ 35.9, 40.7, 111.3, 111.8, 111.9, 112.3, 114.5, 115.9, 116.1, 125.3, 125.4, 126.5, 128.3, 128.5 (d, J = 11.9 Hz), 129.7 (d, J = 11.7 Hz),

131.0 (d, J = 9.7 Hz), 132.6, 132.8, 133.1, 134.1 (d, J = 11.2 Hz), 136.4 (d, J = 11.6 Hz), 136.7, 193.5; $^{31}P\{^{1}H\}$ NMR (CD_2Cl_2, 202 MHz): δ 40.23.

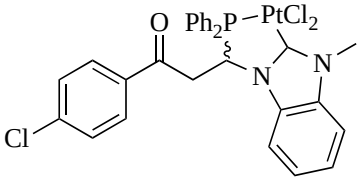

141m. Pale yellow-white solid. Yield: 0.0086 g, 20%. ^{1}H NMR (CD_2Cl_2, 500 MHz): δ 3.38 (ddd, 1H, J = 20.0 Hz, 18.0 Hz, 3.0 Hz), 4.01 (ddd, 1H, J = 19.0 Hz, 11.0 Hz, 11.0 Hz), 4.39 (s, 3H), 6.00 (td, 1H, J = 16.0 Hz, 3.0 Hz), 7.15-7.17 (m, 3H), 7.32-7.34 (m, 2H), 7.39-7.44 (m, 2H), 7.46-7.51 (m, 4H), 7.57-7.61 (m, 3H), 7.82-7.87 (m, 2H), 8.22-8.26 (m, 2H); $^{13}C\{^{1}H\}$ NMR (CD_2Cl_2, 100 MHz): δ 35.9, 40.8 (d, J = 5.2 Hz), 111.3, 112.3, 122.8, 123.1, 123.5, 125.3, 125.5, 128.6 (d, J = 12.2 Hz), 129.2, 129.6, 129.7 (d, J = 11.6 Hz), 130.9 (d, J = 9.7 Hz), 132.9 (d, J = 2.2 Hz), 133.0 (d, J = 2.8 Hz), 133.5, 134.1 (d, J = 11.4 Hz), 136.4 (d, J = 11.5 Hz), 136.7, 140.8, 160.6, 193.9; $^{31}P\{^{1}H\}$ NMR (CD_2Cl_2, 202 MHz): δ 40.25.

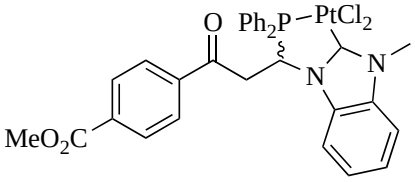

141n. Pale yellow-white solid. Yield: 0.0120 g, 27%. ^{1}H NMR (CD_2Cl_2, 500 MHz): δ 3.43 (ddd, 1H, J = 20.0 Hz, 19.0 Hz, 3.0 Hz), 3.92 (s, 3H), 4.08 (ddd, 1H, J = 19.0 Hz, 11.0 Hz, 11.0 Hz), 4.40 (s, 3H), 6.01 (td, 1H, J = 16.0 Hz, 3.0 Hz), 7.11-7.16 (m, 3H), 7.39-7.59 (m, 9H), 7.82-7.87 (m, 2H), 7.98 (d, 2H, J = 8.0 Hz), 8.23-8.27 (m, 2H); $^{13}C\{^{1}H\}$ NMR ($CDCl_3$, 125 MHz): δ 35.7, 40.8 (d, J = 5.2 Hz), 52.7, 53.4, 110.9, 112.1, 122.2, 122.7, 124.4, 124.9, 125.1, 125.3, 127.9, 128.4 (d, J = 12.5 Hz), 129.5 (d, J = 11.7 Hz), 129.7, 132.6 (d, J = 2.2 Hz),

132.8 (d, J = 3.2 Hz), 133.8 (d, J = 11.5 Hz), 134.8, 136.1 (d, J = 11.6 Hz), 136.3, 137.6, 165.9, 194.5; $^{31}P\{^{1}H\}$ NMR (CD_2Cl_2, 202 MHz): δ 40.23.

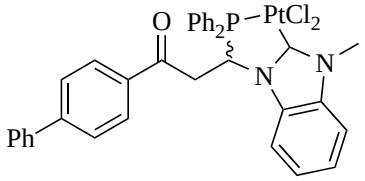

141p. Pale yellow-white solid. Yield: 0.0073 g, 16%. ^{1}H NMR (CD_2Cl_2, 500 MHz): δ 3.44 (ddd, 1H, J = 20.0 Hz, 18.0 Hz, 3.0 Hz), 4.06 (ddd, 1H, J = 18.0 Hz, 11.0 Hz, 11.0 Hz), 4.40 (s, 3H), 6.05 (td, 1H, J = 16.0 Hz, 3.0 Hz), 7.13-7.19 (m, 3H), 7.40-7.44 (m, 3H), 7.47-7.52 (m, 5H), 7.58-7.64 (m, 8H), 7.85-7.90 (m, 2H), 8.25-8.29 (m, 2H); $^{13}C\{^{1}H\}$ NMR (CD_2Cl_2, 100 MHz): δ 35.9, 40.8 (d, J = 5.3 Hz), 58.4, 111.4, 112.2, 113.1, 125.3, 125.4, 127.3, 127.6, 128.6 (d, J = 12.2 Hz), 128.8, 128.9, 129.1, 129.4, 129.7 (d, J = 11.5 Hz), 129.9, 130.9, 131.1, 132.9, 133.0, 133.0, 132.9 (d, J = 9.0 Hz), 133.9, 134.2 (d, J = 11.4 Hz), 136.3 (d, J = 11.2 Hz), 136.5, 136.7, 139.8, 146.9, 194.6; $^{31}P\{^{1}H\}$ NMR (CD_2Cl_2, 202 MHz): δ 40.22.

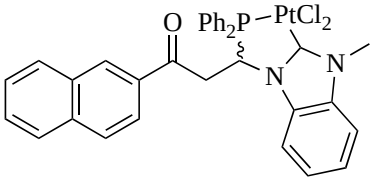

141q. Pale yellow-white solid. Yield: 0.0053 g, 12%. ^{1}H NMR (CD_2Cl_2, 500 MHz): δ 3.54 (ddd, 1H, J = 19.0 Hz, 18.0 Hz, 3.0 Hz), 4.19 (ddd, 1H, J = 18.0 Hz, 11.0 Hz, 11.0 Hz), 4.40 (s, 3H), 6.08 (td, 1H, J = 16.0 Hz, 3.0 Hz), 6.95-6.98 (m, 1H), 7.08 (dt, 2H, J = 12.0 Hz, 3.0 Hz), 7.40-7.43 (m, 2H), 7.49-7.53 (m, 2H), 7.56-7.65 (m, 6H), 7.78 (d, 1H, J = 9.0 Hz), 7.85-7.91 (m, 4H), 8.07 (s, 1H), 8.24-8.28 (m, 2H); $^{13}C\{^{1}H\}$ NMR (CD_2Cl_2, 100 MHz): δ 32.0, 35.1, 40.9 (d, J = 5.3 Hz), 111.5, 112.2, 123.4, 125.3, 125.5, 127.5, 128.1, 128.5 (d, J = 12.2 Hz),

128.7, 129.5, 129.8 (d, J = 11.6 Hz), 130.1, 130.5, 131.0, 131.1, 132.5, 132.6, 132.8 (d, J = 2.6 Hz), 133.0 (d, J = 2.2 Hz), 134.1 (d, J = 11.3 Hz), 136.3, 136.4 (d, J = 11.5 Hz), 136.7, 160.6, 160.7, 195.0; $^{31}P\{^{1}H\}$ NMR (CD_2Cl_2, 202 MHz): δ 40.17.

References

(1) Siegel, R. L.; Miller, K. D.; Jemal, A., *Cancer statistics, 2018, CA Cancer J. Clin.* **2018,** *68*, 7-30.

(2) Barry, N. P. E.; Sadler, P. J., *100 years of metal coordination chemistry: from Alfred Werner to anticancer metallodrugs, Pure and Applied Chemistry* **2014,** *86*, 1897-1910.

(3) (a) Peyrone, M., *Ueber die Einwirkung des Ammoniaks auf Platinchlorür, Justus Liebigs Ann. Chem.* **1844,** *51*, 1-29; (b) Rosenberg, B.; Van Camp, L.; Krigas, T., *Inhibition of Cell Division in Escherichia coli by Electrolysis Products from a Platinum Electrode, Nature* **1965,** *205*, 698-699.

(4) Hambley, T. W., *Platinum binding to DNA: structural controls and consequences, J. Chem. Soc., Dalton Trans.* **2001**, 2711-2718.

(5) (a) Ishida, S.; Lee, J.; Thiele, D. J.; Herskowitz, I., *Uptake of the anticancer drug cisplatin mediated by the copper transporter Ctr1 in yeast and mammals, Proc. Natl. Acad. Sci. U. S. A.* **2002,** *99*, 14298-302; (b) Alderden, R. A.; Hall, M. D.; Hambley, T. W., *The Discovery and Development of Cisplatin, J. Chem. Educ.* **2006,** *83*, 728.

(6) Dasari, S.; Bernard Tchounwou, P., *Cisplatin in cancer therapy: Molecular mechanisms of action, Eur. J. Pharmacol.* **2014,** *740*, 364-378.

(7) (a) Zorbas, H.; Keppler, B. K., *Cisplatin Damage: Are DNA Repair Proteins Saviors or Traitors to the Cell?, ChemBioChem* **2005,** *6*, 1157-1166; (b) Rabik, C. A.; Dolan, M. E., *Molecular mechanisms of resistance and toxicity associated with platinating agents, Cancer Treat. Rev.* **2007,** *33*, 9-23.

(8) Kelland, L., *The resurgence of platinum-based cancer chemotherapy, Nat. Rev. Cancer.* **2007,** *7*, 573-584.

(9) Baik, M. H.; Friesner, R. A.; Lippard, S. J., *Theoretical study of cisplatin binding to purine bases: why does cisplatin prefer guanine over adenine?, J. Am. Chem. Soc.* **2003,** *125*, 14082-92.

(10) (a) Fuertes, M. A.; Alonso, C.; Pérez, J. M., *Biochemical Modulation of Cisplatin Mechanisms of Action: Enhancement of Antitumor Activity and Circumvention of Drug Resistance, Chem. Rev.* **2003,** *103*, 645-662; (b) Malinge, J.-M.; Giraud-Panis, M.-J.; Leng, M., *Interstrand cross-links of cisplatin induce striking distortions in DNA, J. Inorg. Biochem.* **1999,** *77*, 23-29.

(11) Astolfi, L.; Ghiselli, S.; Guaran, V.; Chicca, M.; Simoni, E.; Olivetto, E.; Lelli, G.; Martini, A., *Correlation of adverse effects of cisplatin administration in patients affected by solid tumours: A retrospective evaluation, Oncol. Rep.* **2013,** *29*, 1285-1292.

(12) (a) McKeage, M. J., *Comparative Adverse Effect Profiles of Platinum Drugs, Drug Saf.* **1995,** *13*, 228-244; (b) Sheth, S.; Mukherjea, D.; Rybak, L. P.; Ramkumar, V., *Mechanisms of Cisplatin-Induced Ototoxicity and Otoprotection, Front. Cell. Neurosci.* **2017,** *11*, 338; (c) İşeri, S.; Ercan, F.; Gedik, N.; Yüksel, M.; Alican, İ., *Simvastatin attenuates cisplatin-induced kidney and liver damage in rats, Toxicology* **2007,** *230*, 256-264; (d) Tsang, R. Y.; Al-Fayea, T.; Au, H.-J., *Cisplatin Overdose, Drug Saf.* **2009,** *32*, 1109-1122.

(13) Muggia, F. M.; Los, G., *Platinum resistance: Laboratory findings and clinical implications, Stem Cells* **1993,** *11*, 182-193.

(14) (a) Lempers, E. L. M.; Reedijk, J., Interactions of Platinum Amine Compounds with Sulfur-Containing Biomolecules and Dna Fragments. In *Adv. Inorg. Chem.*, Sykes, A. G., Ed. Academic Press: 1991; Vol. 37, pp 175-217; (b) Lin, X.; Okuda, T.; Holzer, A.; Howell, S. B., *The copper transporter CTR1 regulates cisplatin uptake in Saccharomyces cerevisiae, Mol. Pharmacol.* **2002,** *62*, 1154-9; (c) Wang, W.; Ballatori, N., *Endogenous glutathione conjugates: occurrence and biological functions, Pharmacol. Rev.* **1998,** *50*, 335-56; (d)

Florea, A.-M.; Büsselberg, D., *Cisplatin as an Anti-Tumor Drug: Cellular Mechanisms of Activity, Drug Resistance and Induced Side Effects, Cancers (Basel)* **2011,** *3*, 1351-1371; I Kartalou, M.; Essigmann, J. M., *Mechanisms of resistance to cisplatin, Mutation Research/Fundamental and Molecular Mechanisms of Mutagenesis* **2001,** *478*, 23-43.

(15) (a) Monneret, C., *Platinum anticancer drugs. From serendipity to rational design, Ann. Pharm. Fr.* **2011,** *69*, 286-95; (b) Uehara, T.; Yamate, J.; Torii, M.; Maruyama, T., *Comparative nephrotoxicity of Cisplatin and nedaplatin: mechanisms and histopathological characteristics, J. Toxicol. Pathol.* **2011,** *24*, 87-94.

(16) (a) Chan, B. A.; Coward, J. I., *Chemotherapy advances in small-cell lung cancer, J. Thorac. Dis.* **2013,** *5 Suppl 5*, S565-78; (b) Shah, N.; Dizon, D. S., *New-generation platinum agents for solid tumors, Future Oncol.* **2009,** *5*, 33-42.

(17) Liu, S.; Li, Y.; Wang, X.; Ma, J.; Zhang, L.; Xia, G., *Preparation, Characterization, and Antitumor Activities of Miriplatin-Loaded Liposomes, J. Pharm. Sci.* **2016,** *105*, 78-87.

(18) (a) Wai-Yin Sun, R.; Lok-Fung Chow, A.; Li, X.-H.; Yan, J. J.; Sin-Yin Chui, S.; Che, C.-M., *Luminescent cyclometalated platinum(ii) complexes containing N-heterocyclic carbene ligands with potent in vitro and in vivo anti-cancer properties accumulate in cytoplasmic structures of cancer cells, Chem. Sci.* **2011,** *2*, 728-736; (b) Adhikary, S. D.; Bose, D.; Mitra, P.; Saha, K. D.; Bertolasi, V.; Dinda, J., *Au(i)- and Pt(ii)-N-heterocyclic carbene complexes with picoline functionalized benzimidazolin-2-ylidene ligands; synthesis, structures, electrochemistry and cytotoxicity studies, New J. Chem.* **2012,** *36*, 759-767; (c) Muenzner, J. K.; Rehm, T.; Biersack, B.; Casini, A.; de Graaf, I. A. M.; Worawutputtapong, P.; Noor, A.; Kempe, R.; Brabec, V.; Kasparkova, J.; Schobert, R., *Adjusting the DNA Interaction and Anticancer Activity of Pt(II) N-Heterocyclic Carbene Complexes by Steric Shielding of the Trans Leaving Group, J. Med. Chem.* **2015,** *58*, 6283-6292; (d) Chtchigrovsky, M.; Eloy, L.; Jullien, H.; Saker, L.; Ségal-Bendirdjian, E.; Poupon, J.; Bombard, S.; Cresteil, T.;

Retailleau, P.; Marinetti, A., *Antitumor trans-N-Heterocyclic Carbene–Amine–Pt(II) Complexes: Synthesis of Dinuclear Species and Exploratory Investigations of DNA Binding and Cytotoxicity Mechanisms, J. Med. Chem.* **2013,** *56*, 2074-2086; I Borré, E.; Dahm, G.; Guichard, G.; Bellemin-Laponnaz, S., *Post-functionalization of platinum–NHC complexes by oxime ligation for ligand targeted therapy, New J. Chem.* **2016,** *40*, 3164-3171; (f) Dam, T. K.; Brewer, C. F., *Lectins as pattern recognition molecules: the effects of epitope density in innate immunity, Glycobiology* **2010,** *20*, 270-9; (g) Wang, X.; Guo, Z., *Targeting and delivery of platinum-based anticancer drugs, Chem. Soc. Rev.* **2013,** *42*, 202-24; (h) Gabano, E.; Ravera, M.; Osella, D., *The drug targeting and delivery approach applied to pt-antitumour complexes. A coordination point of view, Curr. Med. Chem.* **2009,** *16*, 4544-80; (i) Chardon, E.; Puleo, G. L.; Dahm, G.; Fournel, S.; Guichard, G.; Bellemin-Laponnaz, S., *Easy Derivatisation of Group 10 N-Heterocyclic Carbene Complexes and In Vitro Evaluation of an Anticancer Oestradiol Conjugate, ChemPlusChem* **2012,** *77*, 1028-1038.

(19) (a) Icsel, C.; Yilmaz, V. T.; Cevatemre, B.; Aygun, M.; Ulukaya, E., *Cytotoxic platinum(II) complexes derived from saccharinate and phosphine ligands: synthesis, structures, DNA cleavage, and oxidative stress-induced apoptosis, J. Biol. Inorg. Chem.* **2020,** *25*, 75-87; (b) Živković, M. D.; Kljun, J.; Ilic-Tomic, T.; Pavic, A.; Veselinović, A.; Manojlović, D. D.; Nikodinovic-Runic, J.; Turel, I., *A new class of platinum(ii) complexes with the phosphine ligand pta which show potent anticancer activity, Inorg. Chem. Front.* **2018,** *5*, 39-53; (c) Villarreal, W.; Colina-Vegas, L.; Rodrigues de Oliveira, C.; Tenorio, J. C.; Ellena, J.; Gozzo, F. C.; Cominetti, M. R.; Ferreira, A. G.; Ferreira, M. A. B.; Navarro, M.; Batista, A. A., *Chiral Platinum(II) Complexes Featuring Phosphine and Chloroquine Ligands as Cytotoxic and Monofunctional DNA-Binding Agents, Inorg. Chem.* **2015,** *54*, 11709-11720.

Chapter 5

Conclusions and Future Work

5.1 Conclusions

5.1.1 Novel Methodology to Access Chiral Phosphine-Azolium Salts

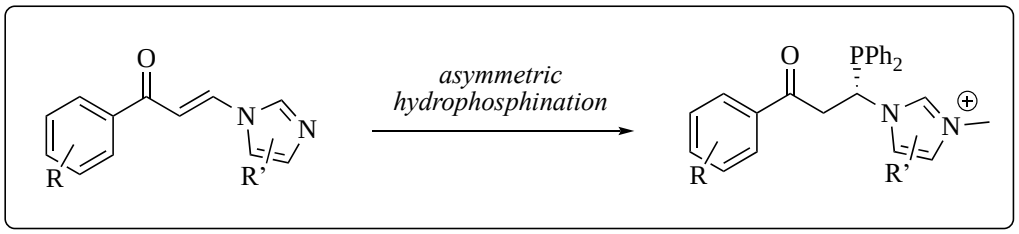

Scheme 5.1 Main idea explored in Chapter 2.

Asymmetric hydrophosphination was devised successfully as a novel methodology to access chiral phosphine-azolium salts, which are direct precursors to privileged phosphine-NHC ligands in homogeneous catalysis. The rate, yield and enantioselectivity of asymmetric hydrophosphination as a function of the electronic and steric attributes of a wide range of functionalized enones were evaluated in depth. The direct use of the chiral phosphine-azolium salts generated *in situ* cleanly was proven possible and was recommended so as to avoid tedious purifications.

5.1.2 Challenges Associated with the Syntheses of Chiral Phosphine-NHC Metal Complexes

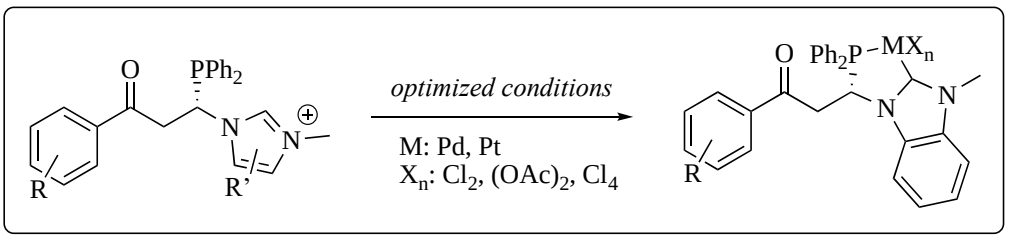

Scheme 5.12 Main idea explored in Chapter 3.

The divergent pathways associated with the formation of phosphine-NHC metal complexes were elucidated by varying the electronic properties of the phosphine azolium salts. The decomposition product and desired phosphine-NHC complexes were isolated and their solution- and solid-state structures were discussed. In addition, derivatization of the platinum analogues was performed to give an unprecedented chiral chelating phosphine-NHC platinum(IV) complex. Applications of these new complexes to C-N and C-C coupling reactions failed however.

5.1.3 Extension to the Biological Applications of Racemic Phosphine-NHC Platinum Complexes

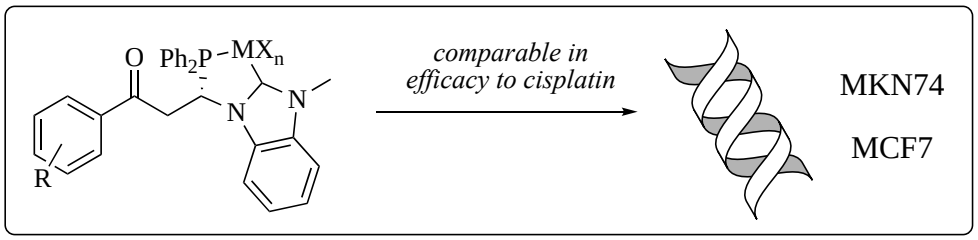

Scheme 5.3 Main idea explored in Chapter 4.

Tapping on the knowledge applied to the modifications of cisplatin by other research groups globally, a series of aryl-functionalized chelating phosphine-NHC platinum complexes were synthesized and evaluated as anti-cancer drugs in two cancer cell lines. The biological results were promising and two of the nine tested complexes exhibited similar efficacies as cisplatin.

5.2 Future Work

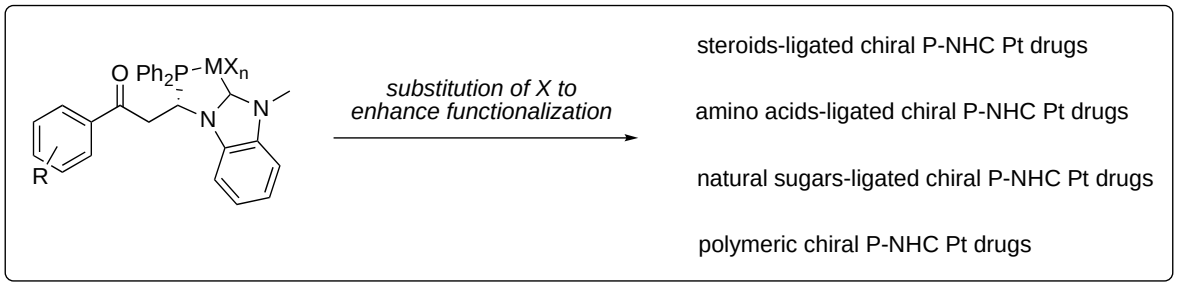

Scheme 5.4 Direction and focus of future work.

To further increase the efficacies and explore the uses of novel chiral chelating phosphine-NHC platinum drugs, incorporation of biological moieties and heterogeneous surfaces into the structural motif of the complexes could present a viable way to improve the delivery, absorption and recognition of the complexes in different chiral cellular environments. Studies have shown that a myriad of biological groups such as steroids[1] , amino acids[2] , sugars[3] and heterogenous phases such as nanoparticles[4] and polymers[5] are able to improve the drug efficacy of the platinum complexes. By replacing the anionic ligand, X, with suitable biologically active groups, new classes of biologically-functionalized platinum drugs could be developed and studied readily.

References

(1) Wang, X.; Guo, Z., *Targeting and delivery of platinum-based anticancer drugs, Chem. Soc. Rev.* **2013,** *42*, 202-224.

(2) (a) Rijal, K.; Bao, X.; Chow, C. S., *Amino acid-linked platinum(II) analogues have altered specificity for RNA compared to cisplatin, Chem Commun (Camb)* **2014,** *50*, 3918-20; (b) Barragán, F.; Moreno, V.; Marchán, V., *Solid-phase synthesis and DNA binding studies of dichloroplatinum(ii) conjugates of dicarba analogues of octreotide as new anticancer drugs, Chem Commun (Camb)* **2009**, 4705-7.

(3) Tsubomura, T.; Yano, S.; Kobayashi, K.; Sakurai, T.; Yoshikawa, S., *First synthesis and characterization of platinum (II) complexes of amino sugars having anti-tumour activity; crystal structure of [ptcl 2 (methyl 2, 3-dideoxy-α-D-mannopyranoside)]· H 2 O, J. Chem. Soc., Chem. Commun.* **1986**, 459-460.

(4) (a) Shi, Y.; Goodisman, J.; Dabrowiak, J. C., *Cyclodextrin capped gold nanoparticles as a delivery vehicle for a prodrug of cisplatin, Inorg. Chem.* **2013,** *52*, 9418-26; (b) Dhar, S.; Liu, Z.; Thomale, J.; Dai, H.; Lippard, S. J., *Targeted single-wall carbon nanotube-mediated Pt(IV) prodrug delivery using folate as a homing device, J. Am. Chem. Soc.* **2008,** *130*, 11467-76.

(5) Rieter, W. J.; Pott, K. M.; Taylor, K. M.; Lin, W., *Nanoscale coordination polymers for platinum-based anticancer drug delivery, J. Am. Chem. Soc.* **2008,** *130*, 11584-5.

Appendix

Crystallographic Data

Crystallographic data for compound 98

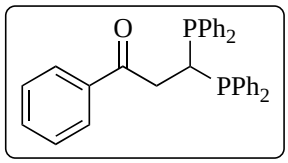

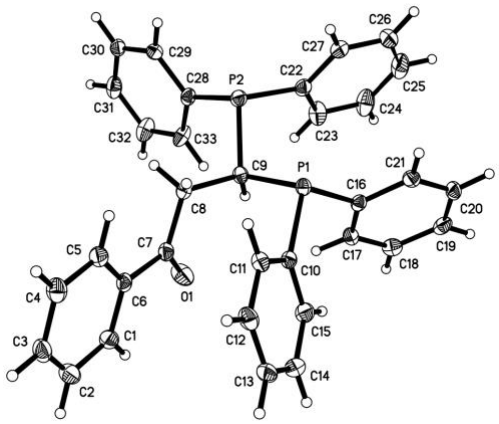

Identification code	leung1086m	
Chemical formula	$C_{33}H_{28}OP_2$	
Formula weight	502.49 g/mol	
Temperature	100(2) K	
Wavelength	0.71073 Å	
Crystal size	0.060 x 0.100 x 0.240 mm	
Crystal habit	colorless needle	
Crystal system	monoclinic	
Space group	P 1 21/c 1	
Unit cell dimensions	a = 6.2303(2) Å	α = 90°
	b = 22.1355(9) Å	β = 93.7357(15)°
	c = 18.7444(7) Å	γ = 90°
Volume	2579.56(16) $Å^3$	
Z	4	
Density (calculated)	1.294 g/cm^3	
Absorption coefficient	0.194 mm^{-1}	
F(000)	1056	

Theta range for data collection	2.36 to 28.73°	
Index ranges	-8<=h<=7, -29<=k<=24, -19<=l<=25	
Reflections collected	17760	
Independent reflections	6538 [R(int) = 0.0631]	
Coverage of independent reflections	97.7%	
Absorption correction	Multi-Scan	
Max. and min. transmission	0.9880 and 0.9550	
Structure solution technique	direct methods	
Structure solution program	XT, VERSION 2014/5	
Refinement method	Full-matrix least-squares on F^2	
Refinement program	SHELXL-2016/6 (Sheldrick, 2016)	
Function minimized	$\Sigma\ w(F_o^2 - F_c^2)^2$	
Data / restraints / parameters	6538 / 0 / 325	
Goodness-of-fit on F^2	1.084	
Final R indices	4652 data; $I>2\sigma(I)$	R1 = 0.0552, wR2 = 0.1188
	all data	R1 = 0.0916, wR2 = 0.1426
Weighting scheme	$w=1/[\sigma^2(F_o^2)+(0.0541P)^2+0.8897P]$ where $P=(F_o^2+2F_c^2)/3$	
Largest diff. peak and hole	0.467 and -0.449 eÅ^{-3}	
R.M.S. deviation from mean	0.112 eÅ^{-3}	

Bond lengths (Å) of compound 98

C1-C2	1.383(3)	C1-C6	1.392(3)
C1-H1	0.95	C2-C3	1.382(4)
C2-H2	0.95	C3-C4	1.382(4)
C3-H3	0.95	C4-C5	1.385(3)
C4-H4	0.95	C5-C6	1.396(3)
C5-H5	0.95	C6-C7	1.499(3)
C7-O1	1.215(3)	C7-C8	1.517(3)
C8-C9	1.539(3)	C8-H8A	0.99
C8-H8B	0.99	C9-P2	1.865(2)

C9-P1	1.872(2)	C9-H9	1.0
C10-C15	1.397(3)	C10-C11	1.398(3)
C10-P1	1.844(2)	C11-C12	1.387(3)
C11-H11	0.95	C12-C13	1.388(4)
C12-H12	0.95	C13-C14	1.385(3)
C13-H13	0.95	C14-C15	1.391(3)
C14-H14	0.95	C15-H15	0.95
C16-C17	1.394(3)	C16-C21	1.395(3)
C16-P1	1.837(2)	C17-C18	1.384(3)
C17-H17	0.95	C18-C19	1.382(4)
C18-H18	0.95	C19-C20	1.385(4)
C19-H19	0.95	C20-C21	1.394(3)
C20-H20	0.95	C21-H21	0.95
C22-C27	1.391(3)	C22-C23	1.395(3)
C22-P2	1.834(2)	C23-C24	1.389(4)
C23-H23	0.95	C24-C25	1.390(4)
C24-H24	0.95	C25-C26	1.376(4)
C25-H25	0.95	C26-C27	1.391(4)
C26-H26	0.95	C27-H27	0.95
C28-C29	1.393(3)	C28-C33	1.403(3)
C28-P2	1.839(2)	C29-C30	1.390(4)
C29-H29	0.95	C30-C31	1.383(4)
C30-H30	0.95	C31-C32	1.378(4)
C31-H31	0.95	C32-C33	1.382(3)
C32-H32	0.95	C33-H33	0.95

Bond angles (°) of compound 98

C2-C1-C6	120.8(2)	C2-C1-H1	119.6
C6-C1-H1	119.6	C3-C2-C1	120.0(2)
C3-C2-H2	120.0	C1-C2-H2	120.0
C2-C3-C4	119.8(2)	C2-C3-H3	120.1
C4-C3-H3	120.1	C5-C4-C3	120.6(2)
C5-C4-H4	119.7	C3-C4-H4	119.7
C4-C5-C6	120.0(2)	C4-C5-H5	120.0
C6-C5-H5	120.0	C1-C6-C5	118.8(2)
C1-C6-C7	117.9(2)	C5-C6-C7	123.3(2)
O1-C7-C6	120.3(2)	O1-C7-C8	120.2(2)
C6-C7-C8	119.35(19)	C7-C8-C9	113.94(18)
C7-C8-H8A	108.8	C9-C8-H8A	108.8

C7-C8-H8B	108.8	C9-C8-H8B	108.8
H8A-C8-H8B	107.7	C8-C9-P2	106.84(16)
C8-C9-P1	110.77(15)	P2-C9-P1	105.52(11)
C8-C9-H9	111.2	P2-C9-H9	111.2
P1-C9-H9	111.2	C15-C10-C11	117.8(2)
C15-C10-P1	125.90(17)	C11-C10-P1	116.20(18)
C12-C11-C10	121.3(2)	C12-C11-H11	119.3
C10-C11-H11	119.3	C11-C12-C13	120.1(2)
C11-C12-H12	119.9	C13-C12-H12	119.9
C14-C13-C12	119.3(2)	C14-C13-H13	120.3
C12-C13-H13	120.3	C13-C14-C15	120.5(2)
C13-C14-H14	119.7	C15-C14-H14	119.7
C14-C15-C10	120.8(2)	C14-C15-H15	119.6
C10-C15-H15	119.6	C17-C16-C21	118.4(2)
C17-C16-P1	124.81(18)	C21-C16-P1	116.76(16)
C18-C17-C16	120.9(2)	C18-C17-H17	119.6
C16-C17-H17	119.6	C19-C18-C17	120.2(2)
C19-C18-H18	119.9	C17-C18-H18	119.9
C18-C19-C20	120.0(2)	C18-C19-H19	120.0
C20-C19-H19	120.0	C19-C20-C21	119.8(2)
C19-C20-H20	120.1	C21-C20-H20	120.1
C20-C21-C16	120.6(2)	C20-C21-H21	119.7
C16-C21-H21	119.7	C27-C22-C23	118.8(2)
C27-C22-P2	114.94(18)	C23-C22-P2	126.25(19)
C24-C23-C22	120.0(3)	C24-C23-H23	120.0
C22-C23-H23	120.0	C25-C24-C23	120.5(3)
C25-C24-H24	119.7	C23-C24-H24	119.7
C26-C25-C24	119.9(3)	C26-C25-H25	120.1
C24-C25-H25	120.1	C25-C26-C27	119.8(3)
C25-C26-H26	120.1	C27-C26-H26	120.1
C26-C27-C22	121.1(2)	C26-C27-H27	119.5
C22-C27-H27	119.5	C29-C28-C33	118.0(2)
C29-C28-P2	116.26(18)	C33-C28-P2	125.72(19)
C30-C29-C28	121.2(2)	C30-C29-H29	119.4
C28-C29-H29	119.4	C31-C30-C29	119.9(2)
C31-C30-H30	120.1	C29-C30-H30	120.1
C32-C31-C30	119.6(2)	C32-C31-H31	120.2
C30-C31-H31	120.2	C31-C32-C33	121.0(2)
C31-C32-H32	119.5	C33-C32-H32	119.5
C32-C33-C28	120.3(2)	C32-C33-H33	119.8
C28-C33-H33	119.8	C16-P1-C10	102.47(10)

C16-P1-C9	103.10(10)	C10-P1-C9	103.57(10)
C22-P2-C28	103.99(10)	C22-P2-C9	103.10(11)
C28-P2-C9	101.39(11)		

Crystallographic data for compound (*S*)-100a

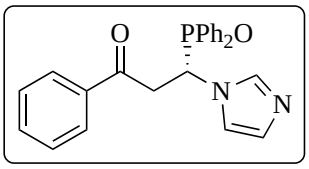

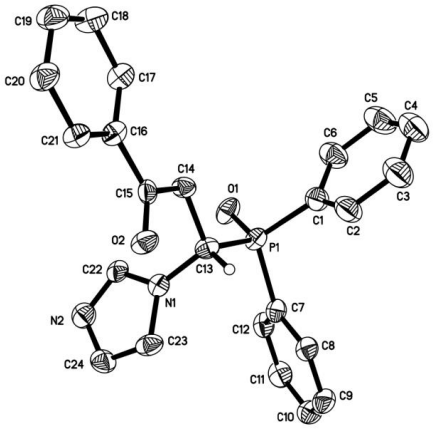

Identification code	leung1172m	
Chemical formula	$C_{25}H_{23}Cl_2N_2O_2P$	
Formula weight	485.32 g/mol	
Temperature	100(2) K	
Wavelength	0.71073 Å	
Crystal size	0.010 x 0.020 x 0.280 mm	
Crystal habit	colorless needle	
Crystal system	orthorhombic	
Space group	P 21 21 21	
Unit cell dimensions	a = 5.5429(7) Å	α = 90°
	b = 19.401(3) Å	β = 90°
	c = 21.533(3) Å	γ = 90°
Volume	2315.6(5) $Å^3$	
Z	4	
Density (calculated)	1.392 g/cm^3	
Absorption coefficient	0.375 mm^{-1}	
F(000)	1008	

Theta range for data collection	2.83 to 25.00°
Index ranges	-6<=h<=6, -23<=k<=23, -25<=l<=25
Reflections collected	14355
Independent reflections	4087 [R(int) = 0.1540]
Coverage of independent reflections	99.6%
Absorption correction	Multi-Scan

Max. and min. transmission	0.9960 and 0.9020	
Structure solution technique	direct methods	
Structure solution program	XT, VERSION 2014/5	
Refinement method	Full-matrix least-squares on F^2	
Refinement program	SHELXL-2018/3 (Sheldrick, 2018)	
Function minimized	$\Sigma\ w(F_o^2 - F_c^2)^2$	
Data / restraints / parameters	4087 / 447 / 359	
Goodness-of-fit on F^2	1.081	
Final R indices	2754 data; $I>2\sigma(I)$	R1 = 0.1033, wR2 = 0.2567
	all data	R1 = 0.1479, wR2 = 0.2892
Weighting scheme	$w=1/[\sigma^2(F_o^2)+(0.1098P)^2+10.8771P]$ where $P=(F_o^2+2F_c^2)/3$	
Absolute structure parameter	-0.07(14)	
Extinction coefficient	0.0140(50)	
Largest diff. peak and hole	0.995 and -0.465 eÅ^{-3}	
R.M.S. deviation from mean	0.123 eÅ^{-3}	

Bond lengths (Å) of compound (*S*)-100a

C1-C2	1.39	C1-C6	1.39
C1-H1	0.95	C2-C3	1.39
C2-H2	0.95	C3-C4	1.39
C3-H3	0.95	C4-C5	1.39
C4-H4	0.95	C5-C6	1.39
C5-H5	0.95	C6-C7	1.483(12)
C7-O1	1.228(13)	C7-C8	1.521(15)
C8-C9	1.522(16)	C8-H8A	0.99
C8-H8B	0.99	C9-N1	1.398(12)
C9-P1	1.848(11)	C9-H9	1.0
N1-C10	1.42	N1-C12	1.42
C10-C11	1.42	C10-H10	0.95
C11-N2	1.42	C11-H11	0.95
N2-C12	1.42	C12-H12	0.95

C13-C14	1.39	C13-C18	1.39
C13-P1	1.791(18)	C14-C15	1.39
C14-H14	0.95	C15-C16	1.39
C15-H15	0.95	C16-C17	1.39
C16-H16	0.95	C17-C18	1.39
C17-H17	0.95	C18-H18	0.95
C13A-C14A	1.39	C13A-C18A	1.39
C13A-P1	1.817(14)	C14A-C15A	1.39
C14A-H14A	0.95	C15A-C16A	1.39
C15A-H15A	0.95	C16A-C17A	1.39
C16A-H16A	0.95	C17A-C18A	1.39
C17A-H17A	0.95	C18A-H18A	0.95
C19-C20	1.39	C19-C24	1.39
C19-P1	1.797(12)	C20-C21	1.39
C20-H20	0.95	C21-C22	1.39
C21-H21	0.95	C22-C23	1.39
C22-H22	0.95	C23-C24	1.39
C23-H23	0.95	C24-H24	0.95
P1-O2	1.500(8)	P1-C19A	1.799(13)
C19A-C20A	1.39	C19A-C24A	1.39
C20A-C21A	1.39	C20A-H20A	0.95
C21A-C22A	1.39	C21A-H21A	0.95
C22A-C23A	1.39	C22A-H22A	0.95
C23A-C24A	1.39	C23A-H23A	0.95
C24A-H24A	0.95	C25-Cl2	1.57(3)
C25-Cl1	1.63(3)	C25-H25A	0.99
C25-H25B	0.99	C25A-Cl2A	1.57(3)
C25A-Cl1A	1.64(3)	C25A-H25C	0.99
C25A-H25D	0.99		

Bond angles (°) of compound (*S*)-100a

C2-C1-C6	120.0	C2-C1-H1	120.0
C6-C1-H1	120.0	C1-C2-C3	120.0
C1-C2-H2	120.0	C3-C2-H2	120.0
C4-C3-C2	120.0	C4-C3-H3	120.0
C2-C3-H3	120.0	C3-C4-C5	120.0
C3-C4-H4	120.0	C5-C4-H4	120.0
C6-C5-C4	120.0	C6-C5-H5	120.0
C4-C5-H5	120.0	C5-C6-C1	120.0

C5-C6-C7	122.2(6)	C1-C6-C7	117.7(6)
O1-C7-C6	120.4(10)	O1-C7-C8	120.7(10)
C6-C7-C8	118.9(9)	C7-C8-C9	111.7(9)
C7-C8-H8A	109.3	C9-C8-H8A	109.3
C7-C8-H8B	109.3	C9-C8-H8B	109.3
H8A-C8-H8B	107.9	N1-C9-C8	112.5(9)
N1-C9-P1	108.1(7)	C8-C9-P1	110.9(8)
N1-C9-H9	108.4	C8-C9-H9	108.4
P1-C9-H9	108.4	C9-N1-C10	126.7(7)
C9-N1-C12	125.2(7)	C10-N1-C12	108.0
N1-C10-C11	108.0	N1-C10-H10	126.0
C11-C10-H10	126.0	N2-C11-C10	108.0
N2-C11-H11	126.0	C10-C11-H11	126.0
C11-N2-C12	108.0	N2-C12-N1	108.0
N2-C12-H12	126.0	N1-C12-H12	126.0
C14-C13-C18	120.0	C14-C13-P1	117.3(14)
C18-C13-P1	122.7(14)	C13-C14-C15	120.0
C13-C14-H14	120.0	C15-C14-H14	120.0
C16-C15-C14	120.0	C16-C15-H15	120.0
C14-C15-H15	120.0	C15-C16-C17	120.0
C15-C16-H16	120.0	C17-C16-H16	120.0
C18-C17-C16	120.0	C18-C17-H17	120.0
C16-C17-H17	120.0	C17-C18-C13	120.0
C17-C18-H18	120.0	C13-C18-H18	120.0
C14A-C13A-C18A	120.0	C14A-C13A-P1	116.0(10)
C18A-C13A-P1	123.9(10)	C15A-C14A-C13A	120.0
C15A-C14A-H14A	120.0	C13A-C14A-H14A	120.0
C16A-C15A-C14A	120.0	C16A-C15A-H15A	120.0
C14A-C15A-H15A	120.0	C17A-C16A-C15A	120.0
C17A-C16A-H16A	120.0	C15A-C16A-H16A	120.0
C16A-C17A-C18A	120.0	C16A-C17A-H17A	120.0
C18A-C17A-H17A	120.0	C17A-C18A-C13A	120.0
C17A-C18A-H18A	120.0	C13A-C18A-H18A	120.0
C20-C19-C24	120.0	C20-C19-P1	123.1(9)
C24-C19-P1	116.9(9)	C19-C20-C21	120.0
C19-C20-H20	120.0	C21-C20-H20	120.0
C22-C21-C20	120.0	C22-C21-H21	120.0
C20-C21-H21	120.0	C21-C22-C23	120.0
C21-C22-H22	120.0	C23-C22-H22	120.0
C24-C23-C22	120.0	C24-C23-H23	120.0
C22-C23-H23	120.0	C23-C24-C19	120.0

C23-C24-H24	120.0	C19-C24-H24	120.0
O2-P1-C13	112.3(9)	O2-P1-C19	110.8(6)
C13-P1-C19	108.6(10)	O2-P1-C19A	111.0(7)
O2-P1-C13A	111.5(7)	C19A-P1-C13A	110.0(9)
O2-P1-C9	113.0(5)	C13-P1-C9	105.9(8)
C19-P1-C9	105.9(7)	C19A-P1-C9	106.6(8)
C13A-P1-C9	104.4(7)	C20A-C19A-C24A	120.0
C20A-C19A-P1	126.6(10)	C24A-C19A-P1	113.4(10)
C19A-C20A-C21A	120.0	C19A-C20A-H20A	120.0
C21A-C20A-H20A	120.0	C22A-C21A-C20A	120.0
C22A-C21A-H21A	120.0	C20A-C21A-H21A	120.0
C21A-C22A-C23A	120.0	C21A-C22A-H22A	120.0
C23A-C22A-H22A	120.0	C24A-C23A-C22A	120.0
C24A-C23A-H23A	120.0	C22A-C23A-H23A	120.0
C23A-C24A-C19A	120.0	C23A-C24A-H24A	120.0
C19A-C24A-H24A	120.0	Cl2-C25-Cl1	123.(2)
Cl2-C25-H25A	106.6	Cl1-C25-H25A	106.6
Cl2-C25-H25B	106.6	Cl1-C25-H25B	106.6
H25A-C25-H25B	106.6	Cl2A-C25A-Cl1A	124.(2)
Cl2A-C25A-H25C	106.4	Cl1A-C25A-H25C	106.4
Cl2A-C25A-H25D	106.4	Cl1A-C25A-H25D	106.4
H25C-C25A-H25D	106.5		

Crystallographic data for compound 136

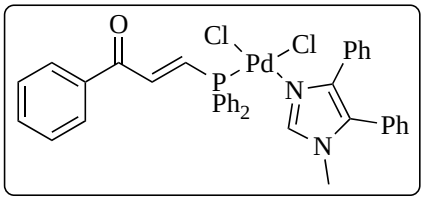

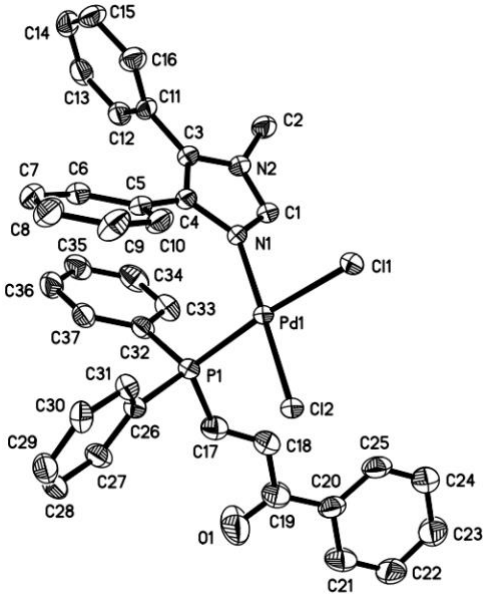

Identification code	leung1155m	
Chemical formula	$C_{37.50}H_{32}Cl_3N_2OPPd$	
Formula weight	770.37 g/mol	
Temperature	100(2) K	
Wavelength	0.71073 Å	
Crystal size	0.120 x 0.240 x 0.280 mm	
Crystal habit	orange block	
Crystal system	triclinic	
Space group	P -1	
Unit cell dimensions	a = 10.8475(4) Å	α = 75.422(2)°
	b = 12.6373(5) Å	β = 87.6220(10)°
	c = 12.6561(5) Å	γ = 83.0370(10)°
Volume	1666.59(11) $Å^3$	
Z	2	
Density (calculated)	1.535 g/cm^3	
Absorption coefficient	0.879 mm^{-1}	
F(000)	782	
Theta range for data collection	2.64 to 33.78°	
Index ranges	-16<=h<=16, -18<=k<=19, -19<=l<=17	
Reflections collected	32765	

Independent reflections	13176 [R(int) = 0.0532]	
Absorption correction	Multi-Scan	
Max. and min. transmission	0.9020 and 0.7910	
Refinement method	Full-matrix least-squares on F2	
Refinement program	SHELXL-2018/3 (Sheldrick, 2018)	
Function minimized	Σ w(Fo2 - Fc2)2	
Data / restraints / parameters	13176 / 16 / 425	
Goodness-of-fit on F2	1.026	
Δ/σmax	0.001	
Final R indices	8581 data; I>2σ(I)	R1 = 0.0567, wR2 = 0.1055
	all data	R1 = 0.1059, wR2 = 0.1286
Weighting scheme	$w=1/[\sigma^2(F_o^2)+(0.0339P)^2+2.6595P]$ where $P=(F_o^2+2F_c^2)/3$	
Largest diff. peak and hole	0.672 and -1.294 eÅ^{-3}	
R.M.S. deviation from mean	0.127 eÅ^{-3}	

Bond lengths (Å) of compound 136

C1-N1	1.325(4)	C1-N2	1.346(4)
C1-H1	0.95	C2-N2	1.464(4)
C2-H2A	0.98	C2-H2B	0.98
C2-H2C	0.98	C3-C4	1.367(4)
C3-N2	1.383(4)	C3-C11	1.486(4)
C4-N1	1.386(4)	C4-C5	1.466(4)
C5-C6	1.396(4)	C5-C10	1.397(5)
C6-C7	1.387(5)	C6-H6	0.95
C7-C8	1.378(5)	C7-H7	0.95
C8-C9	1.380(5)	C8-H8	0.95
C9-C10	1.384(5)	C9-H9	0.95
C10-H10	0.95	C11-C16	1.382(5)
C11-C12	1.391(5)	C12-C13	1.390(5)
C12-H12	0.95	C13-C14	1.384(6)
C13-H13	0.95	C14-C15	1.376(6)
C14-H14	0.95	C15-C16	1.393(5)
C15-H15	0.95	C16-H16	0.95
C17-C18	1.278(5)	C17-P1	1.805(4)

C17-H17	0.95	C18-C19	1.513(5)
C18-H18	0.95	C19-O1	1.226(5)
C19-C20	1.444(5)	C20-C21	1.390(5)
C20-C25	1.413(5)	C21-C22	1.374(6)
C21-H21	0.95	C22-C23	1.389(6)
C22-H22	0.95	C23-C24	1.366(6)
C23-H23	0.95	C24-C25	1.365(6)
C24-H24	0.95	C25-H25	0.95
C26-C31	1.382(5)	C26-C27	1.396(4)
C26-P1	1.821(3)	C27-C28	1.388(5)
C27-H27	0.95	C28-C29	1.376(5)
C28-H28	0.95	C29-C30	1.378(5)
C29-H29	0.95	C30-C31	1.392(5)
C30-H30	0.95	C31-H31	0.95
C32-C37	1.383(5)	C32-C33	1.392(5)
C32-P1	1.814(3)	C33-C34	1.394(5)
C33-H33	0.95	C34-C35	1.374(6)
C34-H34	0.95	C35-C36	1.378(5)
C35-H35	0.95	C36-C37	1.388(5)
C36-H36	0.95	C37-H37	0.95
C38-Cl3	1.740(12)	C38-Cl4	1.740(13)
C38-H38A	0.99	C38-H38B	0.99
Cl1-Pd1	2.3646(8)	Cl2-Pd1	2.2880(7)
N1-Pd1	2.050(2)	P1-Pd1	2.2382(8)

Bond angles (°) of compound 136

N1-C1-N2	109.8(3)	N1-C1-H1	125.1
N2-C1-H1	125.1	N2-C2-H2A	109.5
N2-C2-H2B	109.5	H2A-C2-H2B	109.5
N2-C2-H2C	109.5	H2A-C2-H2C	109.5
H2B-C2-H2C	109.5	C4-C3-N2	106.2(3)
C4-C3-C11	132.1(3)	N2-C3-C11	121.7(3)
C3-C4-N1	108.2(3)	C3-C4-C5	127.9(3)
N1-C4-C5	123.7(3)	C6-C5-C10	118.5(3)
C6-C5-C4	121.0(3)	C10-C5-C4	120.3(3)
C7-C6-C5	120.1(3)	C7-C6-H6	120.0
C5-C6-H6	120.0	C8-C7-C6	120.9(3)
C8-C7-H7	119.6	C6-C7-H7	119.6
C7-C8-C9	119.6(3)	C7-C8-H8	120.2

C9-C8-H8	120.2	C8-C9-C10	120.2(4)
C8-C9-H9	119.9	C10-C9-H9	119.9
C9-C10-C5	120.7(3)	C9-C10-H10	119.6
C5-C10-H10	119.6	C16-C11-C12	119.3(3)
C16-C11-C3	121.3(3)	C12-C11-C3	119.4(3)
C13-C12-C11	120.7(4)	C13-C12-H12	119.7
C11-C12-H12	119.7	C14-C13-C12	119.5(4)
C14-C13-H13	120.3	C12-C13-H13	120.3
C15-C14-C13	120.0(3)	C15-C14-H14	120.0
C13-C14-H14	120.0	C14-C15-C16	120.6(4)
C14-C15-H15	119.7	C16-C15-H15	119.7
C11-C16-C15	119.9(3)	C11-C16-H16	120.1
C15-C16-H16	120.1	C18-C17-P1	129.3(3)
C18-C17-H17	115.4	P1-C17-H17	115.4
C17-C18-C19	120.1(3)	C17-C18-H18	120.0
C19-C18-H18	120.0	O1-C19-C20	121.3(4)
O1-C19-C18	118.2(4)	C20-C19-C18	120.5(3)
C21-C20-C25	118.3(4)	C21-C20-C19	118.5(4)
C25-C20-C19	123.2(3)	C22-C21-C20	120.3(4)
C22-C21-H21	119.9	C20-C21-H21	119.9
C21-C22-C23	120.5(4)	C21-C22-H22	119.8
C23-C22-H22	119.8	C24-C23-C22	119.6(4)
C24-C23-H23	120.2	C22-C23-H23	120.2
C25-C24-C23	120.9(4)	C25-C24-H24	119.5
C23-C24-H24	119.5	C24-C25-C20	120.2(3)
C24-C25-H25	119.9	C20-C25-H25	119.9
C31-C26-C27	119.1(3)	C31-C26-P1	119.7(2)
C27-C26-P1	121.2(3)	C28-C27-C26	119.7(4)
C28-C27-H27	120.2	C26-C27-H27	120.2
C29-C28-C27	120.8(3)	C29-C28-H28	119.6
C27-C28-H28	119.6	C28-C29-C30	119.8(3)
C28-C29-H29	120.1	C30-C29-H29	120.1
C29-C30-C31	119.9(3)	C29-C30-H30	120.0
C31-C30-H30	120.0	C26-C31-C30	120.7(3)
C26-C31-H31	119.7	C30-C31-H31	119.7
C37-C32-C33	119.8(3)	C37-C32-P1	121.1(3)
C33-C32-P1	119.1(3)	C32-C33-C34	119.2(3)
C32-C33-H33	120.4	C34-C33-H33	120.4
C35-C34-C33	120.6(4)	C35-C34-H34	119.7
C33-C34-H34	119.7	C34-C35-C36	120.1(3)
C34-C35-H35	119.9	C36-C35-H35	119.9

C35-C36-C37	120.0(3)	C35-C36-H36	120.0
C37-C36-H36	120.0	C32-C37-C36	120.3(3)
C32-C37-H37	119.9	C36-C37-H37	119.9
Cl3-C38-Cl4	115.0(10)	Cl3-C38-H38A	108.5
Cl4-C38-H38A	108.5	Cl3-C38-H38B	108.5
Cl4-C38-H38B	108.5	H38A-C38-H38B	107.5
C1-N1-C4	107.6(2)	C1-N1-Pd1	121.69(19)
C4-N1-Pd1	130.6(2)	C1-N2-C3	108.3(3)
C1-N2-C2	125.0(3)	C3-N2-C2	125.9(3)
C17-P1-C32	101.77(17)	C17-P1-C26	103.42(16)
C32-P1-C26	104.76(14)	C17-P1-Pd1	115.10(13)
C32-P1-Pd1	115.63(10)	C26-P1-Pd1	114.52(11)
N1-Pd1-P1	94.53(7)	N1-Pd1-Cl2	178.70(7)
P1-Pd1-Cl2	84.90(3)	N1-Pd1-Cl1	89.78(7)
P1-Pd1-Cl1	174.54(3)	Cl2-Pd1-Cl1	90.85(3)

Crystallographic data for compound (*S*)-137h

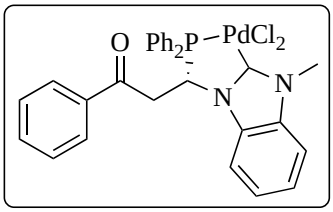

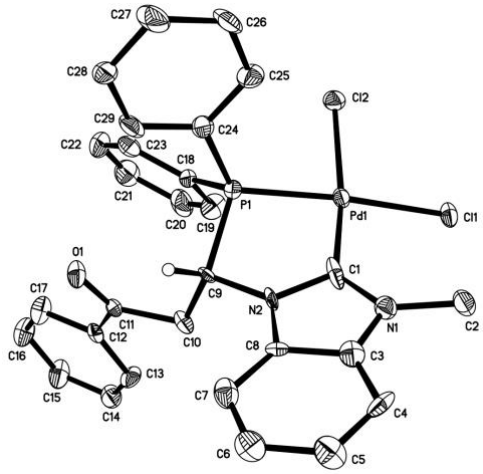

Identification code	leung1177m_tw	
Chemical formula	$C_{29}H_{25}Cl_2N_2OPPd$	
Formula weight	625.78 g/mol	
Temperature	100(2) K	
Wavelength	0.71073 Å	
Crystal size	0.100 x 0.140 x 0.200 mm	
Crystal habit	yellow block	
Crystal system	monoclinic	
Space group	P 1 21 1	
Unit cell dimensions	a = 15.573(2) Å	α = 90°
	b = 12.0833(16) Å	β = 90.106(3)°
	c = 20.842(3) Å	γ = 90°
Volume	3921.9(9) $Å^3$	
Z	6	
Density (calculated)	1.590 g/cm^3	
Absorption coefficient	1.002 mm^{-1}	
F(000)	1896	

Theta range for data collection	2.35 to 29.53°
Index ranges	-21<=h<=21, -16<=k<=16, -28<=l<=28
Reflections collected	63292
Independent reflections	63292 [R(int) = 0.0838]
Coverage of independent reflections	99.1%
Absorption correction	Multi-Scan

Max. and min. transmission	0.9060 and 0.8250	
Structure solution technique	direct methods	
Structure solution program	XT, VERSION 2014/5	
Refinement method	Full-matrix least-squares on F^2	
Refinement program	SHELXL-2018/3 (Sheldrick, 2018)	
Function minimized	$\Sigma\ w(F_o^2 - F_c^2)^2$	
Data / restraints / parameters	63292 / 823 / 975	
Goodness-of-fit on F^2	1.033	
Δ/σ_{max}	0.001	
Final R indices	43772 data; $I>2\sigma(I)$	R1 = 0.0723, wR2 = 0.1445
	all data	R1 = 0.1173, wR2 = 0.1707
Weighting scheme	$w=1/[\sigma^2(F_o^2)+(0.0324P)^2+3.0396P]$ where $P=(F_o^2+2F_c^2)/3$	
Absolute structure parameter	0.04(2)	
Largest diff. peak and hole	1.842 and -1.780 eÅ^{-3}	
R.M.S. deviation from mean	0.216 eÅ^{-3}	

Bond lengths (Å) of compound (*S*)-137h

C1-N2	1.39(2)	C1-N1	1.39(3)
C1-Pd1	1.93(2)	C2-N1	1.45(2)
C2-H2A	0.98	C2-H2B	0.98
C2-H2C	0.98	C3-N1	1.370(18)
C3-C4	1.39	C3-C8	1.39
C4-C5	1.39	C4-H4	0.95
C5-C6	1.39	C5-H5	0.95
C6-C7	1.39	C6-H6	0.95
C7-C8	1.39	C7-H7	0.95
C8-N2	1.364(18)	C9-N2	1.46(2)
C9-C10	1.52(2)	C9-P1	1.864(18)
C9-H9	1.0	C10-C11	1.51(3)
C10-H10A	0.99	C10-H10B	0.99
C11-O1	1.21(2)	C11-C12	1.50(2)

C12-C13	1.39	C12-C17	1.39
C13-C14	1.39	C13-H13	0.95
C14-C15	1.39	C14-H14	0.95
C15-C16	1.39	C15-H15	0.95
C16-C17	1.39	C16-H16	0.95
C17-H17	0.95	C18-C19	1.39
C18-C23	1.39	C18-P1	1.804(11)
C19-C20	1.39	C19-H19	0.95
C20-C21	1.39	C20-H20	0.95
C21-C22	1.39	C21-H21	0.95
C22-C23	1.39	C22-H22	0.95
C23-H23	0.95	C24-C25	1.39
C24-C29	1.39	C24-P1	1.810(9)
C25-C26	1.39	C25-H25	0.95
C26-C27	1.39	C26-H26	0.95
C27-C28	1.39	C27-H27	0.95
C28-C29	1.39	C28-H28	0.95
C29-H29	0.95	C30-N3	1.34(2)
C30-N4	1.35(2)	C30-Pd2	2.011(19)
C31-N3	1.48(2)	C31-H31A	0.98
C31-H31B	0.98	C31-H31C	0.98
C32-C33	1.39	C32-C37	1.39
C32-N3	1.392(17)	C33-C34	1.39
C33-H33	0.95	C34-C35	1.39
C34-H34	0.95	C35-C36	1.39
C35-H35	0.95	C36-C37	1.39
C36-H36	0.95	C37-N4	1.389(16)
C38-N4	1.45(2)	C38-C39	1.51(3)
C38-P2	1.85(2)	C38-H38	1.0
C39-C40	1.52(2)	C39-H39A	0.99
C39-H39B	0.99	C40-O2	1.24(2)
C40-C41	1.51(2)	C41-C42	1.39
C41-C46	1.39	C42-C43	1.39
C42-H42	0.95	C43-C44	1.39
C43-H43	0.95	C44-C45	1.39
C44-H44	0.95	C45-C46	1.39
C45-H45	0.95	C46-H46	0.95
C47-C48	1.39	C47-C52	1.39
C47-P2	1.824(9)	C48-C49	1.39
C48-H48	0.95	C49-C50	1.39
C49-H49	0.95	C50-C51	1.39

C50-H50	0.95	C51-C52	1.39
C51-H51	0.95	C52-H52	0.95
C53-C54	1.39	C53-C58	1.39
C53-P2	1.804(16)	C54-C55	1.39
C54-H54	0.95	C55-C56	1.39
C55-H55	0.95	C56-C57	1.39
C56-H56	0.95	C57-C58	1.39
C57-H57	0.95	C58-H58	0.95
C53A-C54A	1.35(5)	C53A-C58A	1.42(4)
C53A-P2	1.795(17)	C54A-C55A	1.40(5)
C54A-H54A	0.95	C55A-C56A	1.32(5)
C55A-H55A	0.95	C56A-C57A	1.33(5)
C56A-H56A	0.95	C57A-C58A	1.45(5)
C57A-H57A	0.95	C58A-H58A	0.95
C59-N5	1.33(2)	C59-N6	1.36(2)
C59-Pd3	2.023(17)	C60-N5	1.44(2)
C60-H60A	0.98	C60-H60B	0.98
C60-H60C	0.98	C61-N5	1.371(16)
C61-C62	1.39	C61-C66	1.39
C62-C63	1.39	C62-H62	0.95
C63-C64	1.39	C63-H63	0.95
C64-C65	1.39	C64-H64	0.95
C65-C66	1.39	C65-H65	0.95
C66-N6	1.375(17)	C67-N6	1.46(2)
C67-C68	1.51(3)	C67-P3	1.87(2)
C67-H67	1.0	C68-C69	1.53(3)
C68-H68A	0.99	C68-H68B	0.99
C69-O3	1.20(2)	C69-C70	1.46(2)
C70-C71	1.39	C70-C75	1.39
C71-C72	1.39	C71-H71	0.95
C72-C73	1.39	C72-H72	0.95
C73-C74	1.39	C73-H73	0.95
C74-C75	1.39	C74-H74	0.95
C75-H75	0.95	C76-C77	1.39
C76-C81	1.39	C76-P3	1.815(14)
C77-C78	1.39	C77-H77	0.95
C78-C79	1.39	C78-H78	0.95
C79-C80	1.39	C79-H79	0.95
C80-C81	1.39	C80-H80	0.95
C81-H81	0.95	C76A-C77A	1.39
C76A-C81A	1.39	C76A-P3	1.785(15)

C77A-C78A	1.39	C77A-H77A	0.95
C78A-C79A	1.39	C78A-H78A	0.95
C79A-C80A	1.39	C79A-H79A	0.95
C80A-C81A	1.39	C80A-H80A	0.95
C81A-H81A	0.95	C82-C83	1.39
C82-C87	1.39	C82-P3	1.841(12)
C83-C84	1.39	C83-H83	0.95
C84-C85	1.39	C84-H84	0.95
C85-C86	1.39	C85-H85	0.95
C86-C87	1.39	C86-H86	0.95
C87-H87	0.95	C82A-C83A	1.39
C82A-C87A	1.39	C82A-P3	1.757(15)
C83A-C84A	1.39	C83A-H83A	0.95
C84A-C85A	1.39	C84A-H84A	0.95
C85A-C86A	1.39	C85A-H85A	0.95
C86A-C87A	1.39	C86A-H86A	0.95
C87A-H87A	0.95	Cl1-Pd1	2.368(4)
Cl2-Pd1	2.335(6)	Cl3-Pd2	2.364(4)
Cl4-Pd2	2.335(5)	Cl5-Pd3	2.371(5)
Cl6-Pd3	2.357(5)	P1-Pd1	2.206(4)
P2-Pd2	2.203(5)	P3-Pd3	2.216(5)

Bond angles (°) of compound (*S*)-137h

N2-C1-N1	103.7(17)	N2-C1-Pd1	122.1(15)
N1-C1-Pd1	132.8(14)	N1-C2-H2A	109.5
N1-C2-H2B	109.5	H2A-C2-H2B	109.5
N1-C2-H2C	109.5	H2A-C2-H2C	109.5
H2B-C2-H2C	109.5	N1-C3-C4	131.8(10)
N1-C3-C8	108.2(10)	C4-C3-C8	120.0
C3-C4-C5	120.0	C3-C4-H4	120.0
C5-C4-H4	120.0	C4-C5-C6	120.0
C4-C5-H5	120.0	C6-C5-H5	120.0
C7-C6-C5	120.0	C7-C6-H6	120.0
C5-C6-H6	120.0	C6-C7-C8	120.0
C6-C7-H7	120.0	C8-C7-H7	120.0
N2-C8-C7	134.3(10)	N2-C8-C3	105.7(10)
C7-C8-C3	120.0	N2-C9-C10	112.6(15)
N2-C9-P1	101.5(11)	C10-C9-P1	114.5(13)
N2-C9-H9	109.3	C10-C9-H9	109.3

P1-C9-H9	109.3	C11-C10-C9	112.2(16)
C11-C10-H10A	109.2	C9-C10-H10A	109.2
C11-C10-H10B	109.2	C9-C10-H10B	109.2
H10A-C10-H10B	107.9	O1-C11-C12	122.5(17)
O1-C11-C10	119.0(18)	C12-C11-C10	118.5(15)
C13-C12-C17	120.0	C13-C12-C11	122.3(10)
C17-C12-C11	117.7(10)	C14-C13-C12	120.0
C14-C13-H13	120.0	C12-C13-H13	120.0
C13-C14-C15	120.0	C13-C14-H14	120.0
C15-C14-H14	120.0	C14-C15-C16	120.0
C14-C15-H15	120.0	C16-C15-H15	120.0
C17-C16-C15	120.0	C17-C16-H16	120.0
C15-C16-H16	120.0	C16-C17-C12	120.0
C16-C17-H17	120.0	C12-C17-H17	120.0
C19-C18-C23	120.0	C19-C18-P1	117.1(7)
C23-C18-P1	122.8(7)	C20-C19-C18	120.0
C20-C19-H19	120.0	C18-C19-H19	120.0
C21-C20-C19	120.0	C21-C20-H20	120.0
C19-C20-H20	120.0	C20-C21-C22	120.0
C20-C21-H21	120.0	C22-C21-H21	120.0
C21-C22-C23	120.0	C21-C22-H22	120.0
C23-C22-H22	120.0	C22-C23-C18	120.0
C22-C23-H23	120.0	C18-C23-H23	120.0
C25-C24-C29	120.0	C25-C24-P1	119.2(6)
C29-C24-P1	120.8(6)	C24-C25-C26	120.0
C24-C25-H25	120.0	C26-C25-H25	120.0
C27-C26-C25	120.0	C27-C26-H26	120.0
C25-C26-H26	120.0	C26-C27-C28	120.0
C26-C27-H27	120.0	C28-C27-H27	120.0
C29-C28-C27	120.0	C29-C28-H28	120.0
C27-C28-H28	120.0	C28-C29-C24	120.0
C28-C29-H29	120.0	C24-C29-H29	120.0
N3-C30-N4	108.6(16)	N3-C30-Pd2	129.7(14)
N4-C30-Pd2	120.0(13)	N3-C31-H31A	109.5
N3-C31-H31B	109.5	H31A-C31-H31B	109.5
N3-C31-H31C	109.5	H31A-C31-H31C	109.5
H31B-C31-H31C	109.5	C33-C32-C37	120.0
C33-C32-N3	132.9(10)	C37-C32-N3	107.1(10)
C32-C33-C34	120.0	C32-C33-H33	120.0
C34-C33-H33	120.0	C35-C34-C33	120.0
C35-C34-H34	120.0	C33-C34-H34	120.0

C36-C35-C34	120.0	C36-C35-H35	120.0
C34-C35-H35	120.0	C35-C36-C37	120.0
C35-C36-H36	120.0	C37-C36-H36	120.0
N4-C37-C36	133.9(9)	N4-C37-C32	105.9(9)
C36-C37-C32	120.0	N4-C38-C39	112.4(16)
N4-C38-P2	102.6(12)	C39-C38-P2	114.3(13)
N4-C38-H38	109.1	C39-C38-H38	109.1
P2-C38-H38	109.1	C38-C39-C40	112.1(16)
C38-C39-H39A	109.2	C40-C39-H39A	109.2
C38-C39-H39B	109.2	C40-C39-H39B	109.2
H39A-C39-H39B	107.9	O2-C40-C41	119.7(16)
O2-C40-C39	119.0(18)	C41-C40-C39	121.2(15)
C42-C41-C46	120.0	C42-C41-C40	120.2(11)
C46-C41-C40	119.8(11)	C43-C42-C41	120.0
C43-C42-H42	120.0	C41-C42-H42	120.0
C42-C43-C44	120.0	C42-C43-H43	120.0
C44-C43-H43	120.0	C45-C44-C43	120.0
C45-C44-H44	120.0	C43-C44-H44	120.0
C46-C45-C44	120.0	C46-C45-H45	120.0
C44-C45-H45	120.0	C45-C46-C41	120.0
C45-C46-H46	120.0	C41-C46-H46	120.0
C48-C47-C52	120.0	C48-C47-P2	123.6(6)
C52-C47-P2	116.2(6)	C47-C48-C49	120.0
C47-C48-H48	120.0	C49-C48-H48	120.0
C50-C49-C48	120.0	C50-C49-H49	120.0
C48-C49-H49	120.0	C49-C50-C51	120.0
C49-C50-H50	120.0	C51-C50-H50	120.0
C52-C51-C50	120.0	C52-C51-H51	120.0
C50-C51-H51	120.0	C51-C52-C47	120.0
C51-C52-H52	120.0	C47-C52-H52	120.0
C54-C53-C58	120.0	C54-C53-P2	119.(3)
C58-C53-P2	121.(3)	C53-C54-C55	120.0
C53-C54-H54	120.0	C55-C54-H54	120.0
C56-C55-C54	120.0	C56-C55-H55	120.0
C54-C55-H55	120.0	C55-C56-C57	120.0
C55-C56-H56	120.0	C57-C56-H56	120.0
C58-C57-C56	120.0	C58-C57-H57	120.0
C56-C57-H57	120.0	C57-C58-C53	120.0
C57-C58-H58	120.0	C53-C58-H58	120.0
C54A-C53A-C58A	118.(3)	C54A-C53A-P2	119.(4)
C58A-C53A-P2	122.(4)	C53A-C54A-C55A	122.(3)

C53A-C54A-H54A	119.2	C55A-C54A-H54A	119.2
C56A-C55A-C54A	119.(3)	C56A-C55A-H55A	120.5
C54A-C55A-H55A	120.5	C55A-C56A-C57A	124.(4)
C55A-C56A-H56A	117.9	C57A-C56A-H56A	117.9
C56A-C57A-C58A	118.(3)	C56A-C57A-H57A	121.1
C58A-C57A-H57A	121.1	C53A-C58A-C57A	119.(3)
C53A-C58A-H58A	120.7	C57A-C58A-H58A	120.7
N5-C59-N6	107.6(15)	N5-C59-Pd3	132.0(13)
N6-C59-Pd3	118.6(13)	N5-C60-H60A	109.5
N5-C60-H60B	109.5	H60A-C60-H60B	109.5
N5-C60-H60C	109.5	H60A-C60-H60C	109.5
H60B-C60-H60C	109.5	N5-C61-C62	132.8(10)
N5-C61-C66	107.2(10)	C62-C61-C66	120.0
C61-C62-C63	120.0	C61-C62-H62	120.0
C63-C62-H62	120.0	C64-C63-C62	120.0
C64-C63-H63	120.0	C62-C63-H63	120.0
C63-C64-C65	120.0	C63-C64-H64	120.0
C65-C64-H64	120.0	C64-C65-C66	120.0
C64-C65-H65	120.0	C66-C65-H65	120.0
N6-C66-C65	134.3(10)	N6-C66-C61	105.7(10)
C65-C66-C61	120.0	N6-C67-C68	111.0(16)
N6-C67-P3	102.6(12)	C68-C67-P3	115.7(15)
N6-C67-H67	109.1	C68-C67-H67	109.1
P3-C67-H67	109.1	C67-C68-C69	112.5(18)
C67-C68-H68A	109.1	C69-C68-H68A	109.1
C67-C68-H68B	109.1	C69-C68-H68B	109.1
H68A-C68-H68B	107.8	O3-C69-C70	124.1(18)
O3-C69-C68	118.(2)	C70-C69-C68	118.1(17)
C71-C70-C75	120.0	C71-C70-C69	116.0(11)
C75-C70-C69	124.0(11)	C70-C71-C72	120.0
C70-C71-H71	120.0	C72-C71-H71	120.0
C71-C72-C73	120.0	C71-C72-H72	120.0
C73-C72-H72	120.0	C74-C73-C72	120.0
C74-C73-H73	120.0	C72-C73-H73	120.0
C75-C74-C73	120.0	C75-C74-H74	120.0
C73-C74-H74	120.0	C74-C75-C70	120.0
C74-C75-H75	120.0	C70-C75-H75	120.0
C77-C76-C81	120.0	C77-C76-P3	121.3(16)
C81-C76-P3	118.7(16)	C76-C77-C78	120.0
C76-C77-H77	120.0	C78-C77-H77	120.0
C79-C78-C77	120.0	C79-C78-H78	120.0

C77-C78-H78	120.0	C78-C79-C80	120.0
C78-C79-H79	120.0	C80-C79-H79	120.0
C81-C80-C79	120.0	C81-C80-H80	120.0
C79-C80-H80	120.0	C80-C81-C76	120.0
C80-C81-H81	120.0	C76-C81-H81	120.0
C77A-C76A-C81A	120.0	C77A-C76A-P3	125.2(18)
C81A-C76A-P3	114.1(18)	C76A-C77A-C78A	120.0
C76A-C77A-H77A	120.0	C78A-C77A-H77A	120.0
C77A-C78A-C79A	120.0	C77A-C78A-H78A	120.0
C79A-C78A-H78A	120.0	C80A-C79A-C78A	120.0
C80A-C79A-H79A	120.0	C78A-C79A-H79A	120.0
C79A-C80A-C81A	120.0	C79A-C80A-H80A	120.0
C81A-C80A-H80A	120.0	C80A-C81A-C76A	120.0
C80A-C81A-H81A	120.0	C76A-C81A-H81A	120.0
C83-C82-C87	120.0	C83-C82-P3	118.4(12)
C87-C82-P3	121.6(12)	C84-C83-C82	120.0
C84-C83-H83	120.0	C82-C83-H83	120.0
C83-C84-C85	120.0	C83-C84-H84	120.0
C85-C84-H84	120.0	C86-C85-C84	120.0
C86-C85-H85	120.0	C84-C85-H85	120.0
C85-C86-C87	120.0	C85-C86-H86	120.0
C87-C86-H86	120.0	C86-C87-C82	120.0
C86-C87-H87	120.0	C82-C87-H87	120.0
C83A-C82A-C87A	120.0	C83A-C82A-P3	115.(2)
C87A-C82A-P3	125.(2)	C84A-C83A-C82A	120.0
C84A-C83A-H83A	120.0	C82A-C83A-H83A	120.0
C83A-C84A-C85A	120.0	C83A-C84A-H84A	120.0
C85A-C84A-H84A	120.0	C86A-C85A-C84A	120.0
C86A-C85A-H85A	120.0	C84A-C85A-H85A	120.0
C87A-C86A-C85A	120.0	C87A-C86A-H86A	120.0
C85A-C86A-H86A	120.0	C86A-C87A-C82A	120.0
C86A-C87A-H87A	120.0	C82A-C87A-H87A	120.0
C3-N1-C1	110.2(14)	C3-N1-C2	120.2(15)
C1-N1-C2	129.6(16)	C8-N2-C1	112.1(15)
C8-N2-C9	125.8(13)	C1-N2-C9	122.0(16)
C30-N3-C32	108.8(14)	C30-N3-C31	130.9(16)
C32-N3-C31	120.3(14)	C30-N4-C37	109.5(13)
C30-N4-C38	123.3(15)	C37-N4-C38	127.0(14)
C59-N5-C61	109.8(13)	C59-N5-C60	128.5(16)
C61-N5-C60	121.6(15)	C59-N6-C66	109.6(14)
C59-N6-C67	124.6(16)	C66-N6-C67	125.3(14)

C18-P1-C24	109.5(6)	C18-P1-C9	107.1(7)
C24-P1-C9	103.8(8)	C18-P1-Pd1	113.6(4)
C24-P1-Pd1	117.2(4)	C9-P1-Pd1	104.6(6)
C53A-P2-C47	113.(2)	C53-P2-C47	109.(2)
C53A-P2-C38	103.(2)	C53-P2-C38	101.(2)
C47-P2-C38	108.4(7)	C53A-P2-Pd2	114.(2)
C53-P2-Pd2	119.(2)	C47-P2-Pd2	114.0(4)
C38-P2-Pd2	103.9(6)	C82A-P3-C76A	104.1(16)
C76-P3-C82	115.2(13)	C82A-P3-C67	105.6(14)
C76A-P3-C67	108.9(12)	C76-P3-C67	105.6(11)
C82-P3-C67	101.2(10)	C82A-P3-Pd3	116.6(12)
C76A-P3-Pd3	117.3(11)	C76-P3-Pd3	112.9(10)
C82-P3-Pd3	116.2(7)	C67-P3-Pd3	103.6(6)
C1-Pd1-P1	82.0(6)	C1-Pd1-Cl2	166.7(5)
P1-Pd1-Cl2	88.73(18)	C1-Pd1-Cl1	100.2(6)
P1-Pd1-Cl1	170.32(18)	Cl2-Pd1-Cl1	90.53(18)
C30-Pd2-P2	81.8(5)	C30-Pd2-Cl4	164.3(6)
P2-Pd2-Cl4	87.27(18)	C30-Pd2-Cl3	101.0(5)
P2-Pd2-Cl3	172.18(19)	Cl4-Pd2-Cl3	91.38(18)
C59-Pd3-P3	82.7(5)	C59-Pd3-Cl6	166.9(6)
P3-Pd3-Cl6	89.38(19)	C59-Pd3-Cl5	98.8(5)
P3-Pd3-Cl5	171.3(2)	Cl6-Pd3-Cl5	90.55(17)

Crystallographic data for compound (*S*)-141h

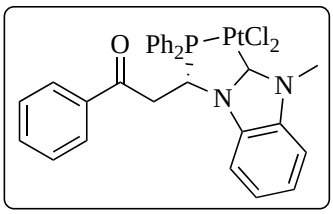

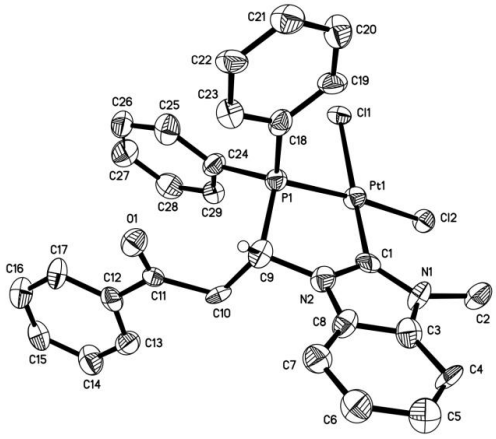

Identification code	leung1192m_tw	
Chemical formula	$C_{29}H_{25}Cl_2N_2OPPt$	
Formula weight	714.47 g/mol	
Temperature	100(2) K	
Wavelength	0.71073 Å	
Crystal size	0.010 x 0.020 x 0.120 mm	
Crystal habit	colorless needle	
Crystal system	monoclinic	
Space group	P 1 21 1	
Unit cell dimensions	a = 15.6042(10) Å	α = 90°
	b = 12.1561(9) Å	β = 90.022(2)°
	c = 20.9652(15) Å	γ = 90°
Volume	3976.8(5) $Å^3$	
Z	6	
Density (calculated)	1.790 g/cm^3	
Absorption coefficient	5.580 mm^{-1}	
F(000)	2088	

Theta range for data collection	1.94 to 30.61°
Index ranges	-22<=h<=22, -17<=k<=17, -25<=l<=29
Reflections collected	21184
Independent reflections	21184 [R(int) = 0.0867]
Coverage of independent reflections	97.4%
Absorption correction	Multi-Scan

Max. and min. transmission	0.9460 and 0.5540	
Structure solution technique	direct methods	
Structure solution program	SHELXT 2014/5 (Sheldrick, 2014)	
Refinement method	Full-matrix least-squares on F^2	
Refinement program	SHELXL-2018/3 (Sheldrick, 2018)	
Function minimized	$\Sigma\ w(F_o^2 - F_c^2)^2$	
Data / restraints / parameters	21184 / 1057 / 834	
Goodness-of-fit on F^2	1.060	
Final R indices	16163 data; $I>2\sigma(I)$	R1 = 0.0601, wR2 = 0.1242
	all data	R1 = 0.0892, wR2 = 0.1388
Weighting scheme	$w=1/[\sigma^2(F_o^2)+(0.0456P)^2+8.9002P]$ where $P=(F_o^2+2F_c^2)/3$	
Absolute structure parameter	0.011(5)	
Largest diff. peak and hole	4.336 and -3.512 eÅ^{-3}	
R.M.S. deviation from mean	0.318 eÅ^{-3}	

Bond lengths (Å) of compound (*S*)-141h

Pt1-C1	1.954(16)	Pt1-P1	2.199(4)
Pt1-Cl1	2.349(6)	Pt1-Cl2	2.371(4)
Pt2-C30	1.967(16)	Pt2-P2	2.208(5)
Pt2-Cl4	2.368(6)	Pt2-Cl3	2.368(5)
Pt3-C59	1.958(15)	Pt3-P3	2.200(5)
Pt3-Cl5	2.355(6)	Pt3-Cl6	2.364(5)
P1-C18	1.816(10)	P1-C24	1.821(12)
P1-C9	1.863(17)	P2-C47	1.803(11)
P2-C53	1.809(12)	P2-C38	1.890(17)
P3-C76	1.817(11)	P3-C82	1.819(11)
P3-C67	1.865(16)	O1-C11	1.23(2)
O2-C40	1.22(2)	O3-C69	1.23(2)
N1-C3	1.37(2)	N1-C1	1.38(2)
N1-C2	1.46(2)	N2-C1	1.37(2)
N2-C8	1.39(2)	N2-C9	1.47(2)

N3-C32	1.367(19)	N3-C30	1.39(2)
N3-C31	1.46(2)	N4-C37	1.37(2)
N4-C30	1.38(2)	N4-C38	1.47(2)
N5-C59	1.35(2)	N5-C61	1.38(2)
N5-C60	1.48(2)	N6-C66	1.35(2)
N6-C59	1.38(2)	N6-C67	1.49(2)
C2-H2A	0.98	C2-H2B	0.98
C2-H2C	0.98	C3-C4	1.39
C3-C8	1.39	C4-C5	1.39
C4-H4	0.95	C5-C6	1.39
C5-H5	0.95	C6-C7	1.39
C6-H6	0.95	C7-C8	1.39
C7-H7	0.95	C9-C10	1.505(15)
C9-H9	1.0	C10-C11	1.500(13)
C10-H10A	0.99	C10-H10B	0.99
C11-C12	1.509(12)	C12-C13	1.39
C12-C17	1.39	C13-C14	1.39
C13-H13	0.95	C14-C15	1.39
C14-H14	0.95	C15-C16	1.39
C15-H15	0.95	C16-C17	1.39
C16-H16	0.95	C17-H17	0.95
C18-C19	1.39	C18-C23	1.39
C19-C20	1.39	C19-H19	0.95
C20-C21	1.39	C20-H20	0.95
C21-C22	1.39	C21-H21	0.95
C22-C23	1.39	C22-H22	0.95
C23-H23	0.95	C24-C25	1.39
C24-C29	1.39	C25-C26	1.39
C25-H25	0.95	C26-C27	1.39
C26-H26	0.95	C27-C28	1.39
C27-H27	0.95	C28-C29	1.39
C28-H28	0.95	C29-H29	0.95
C31-H31A	0.98	C31-H31B	0.98
C31-H31C	0.98	C32-C33	1.39
C32-C37	1.39	C33-C34	1.39
C33-H33	0.95	C34-C35	1.39
C34-H34	0.95	C35-C36	1.39
C35-H35	0.95	C36-C37	1.39
C36-H36	0.95	C38-C39	1.507(15)
C38-H38	1.0	C39-C40	1.503(13)
C39-H39A	0.99	C39-H39B	0.99

C40-C41	1.506(12)	C41-C42	1.39
C41-C46	1.39	C42-C43	1.39
C42-H42	0.95	C43-C44	1.39
C43-H43	0.95	C44-C45	1.39
C44-H44	0.95	C45-C46	1.39
C45-H45	0.95	C46-H46	0.95
C47-C48	1.39	C47-C52	1.39
C48-C49	1.39	C48-H48	0.95
C49-C50	1.39	C49-H49	0.95
C50-C51	1.39	C50-H50	0.95
C51-C52	1.39	C51-H51	0.95
C52-H52	0.95	C53-C54	1.39
C53-C58	1.39	C54-C55	1.39
C54-H54	0.95	C55-C56	1.39
C55-H55	0.95	C56-C57	1.39
C56-H56	0.95	C57-C58	1.39
C57-H57	0.95	C58-H58	0.95
C60-H60A	0.98	C60-H60B	0.98
C60-H60C	0.98	C61-C62	1.39
C61-C66	1.39	C62-C63	1.39
C62-H62	0.95	C63-C64	1.39
C63-H63	0.95	C64-C65	1.39
C64-H64	0.95	C65-C66	1.39
C65-H65	0.95	C67-C68	1.503(15)
C67-H67	1.0	C68-C69	1.505(13)
C68-H68A	0.99	C68-H68B	0.99
C69-C70	1.507(12)	C70-C71	1.39
C70-C75	1.39	C71-C72	1.39
C71-H71	0.95	C72-C73	1.39
C72-H72	0.95	C73-C74	1.39
C73-H73	0.95	C74-C75	1.39
C74-H74	0.95	C75-H75	0.95
C76-C77	1.39	C76-C81	1.39
C77-C78	1.39	C77-H77	0.95
C78-C79	1.39	C78-H78	0.95
C79-C80	1.39	C79-H79	0.95
C80-C81	1.39	C80-H80	0.95
C81-H81	0.95	C82-C83	1.39
C82-C87	1.39	C83-C84	1.39
C83-H83	0.95	C84-C85	1.39
C84-H84	0.95	C85-C86	1.39

C85-H85	0.95	C86-C87	1.39
C86-H86	0.95	C87-H87	0.95

Bond angles (°) of compound (*S*)-141h

C1-Pt1-P1	83.0(5)	C1-Pt1-Cl1	169.4(6)
P1-Pt1-Cl1	90.55(18)	C1-Pt1-Cl2	99.2(5)
P1-Pt1-Cl2	171.5(2)	Cl1-Pt1-Cl2	88.37(19)
C30-Pt2-P2	82.6(4)	C30-Pt2-Cl4	169.4(6)
P2-Pt2-Cl4	90.9(2)	C30-Pt2-Cl3	99.4(5)
P2-Pt2-Cl3	171.8(2)	Cl4-Pt2-Cl3	88.18(19)
C59-Pt3-P3	82.8(4)	C59-Pt3-Cl5	166.5(6)
P3-Pt3-Cl5	88.94(19)	C59-Pt3-Cl6	100.3(4)
P3-Pt3-Cl6	172.9(2)	Cl5-Pt3-Cl6	89.07(19)
C18-P1-C24	109.7(6)	C18-P1-C9	103.6(7)
C24-P1-C9	107.8(7)	C18-P1-Pt1	118.0(5)
C24-P1-Pt1	112.8(5)	C9-P1-Pt1	103.9(5)
C47-P2-C53	110.9(7)	C47-P2-C38	102.3(7)
C53-P2-C38	106.9(7)	C47-P2-Pt2	117.2(5)
C53-P2-Pt2	114.3(5)	C38-P2-Pt2	103.8(5)
C76-P3-C82	110.1(6)	C76-P3-C67	102.6(7)
C82-P3-C67	108.7(6)	C76-P3-Pt3	116.7(5)
C82-P3-Pt3	114.2(5)	C67-P3-Pt3	103.4(5)
C3-N1-C1	110.4(15)	C3-N1-C2	121.2(15)
C1-N1-C2	128.3(17)	C1-N2-C8	110.9(15)
C1-N2-C9	124.3(16)	C8-N2-C9	124.7(15)
C32-N3-C30	109.5(13)	C32-N3-C31	122.5(15)
C30-N3-C31	127.9(16)	C37-N4-C30	112.4(14)
C37-N4-C38	125.3(13)	C30-N4-C38	122.1(16)
C59-N5-C61	110.4(13)	C59-N5-C60	129.8(17)
C61-N5-C60	119.6(16)	C66-N6-C59	112.5(14)
C66-N6-C67	126.7(14)	C59-N6-C67	120.6(15)
N2-C1-N1	105.3(15)	N2-C1-Pt1	119.6(12)
N1-C1-Pt1	134.0(14)	N1-C2-H2A	109.5
N1-C2-H2B	109.5	H2A-C2-H2B	109.5
N1-C2-H2C	109.5	H2A-C2-H2C	109.5
H2B-C2-H2C	109.5	N1-C3-C4	132.1(10)
N1-C3-C8	107.9(10)	C4-C3-C8	120.0
C3-C4-C5	120.0	C3-C4-H4	120.0
C5-C4-H4	120.0	C6-C5-C4	120.0

C6-C5-H5	120.0	C4-C5-H5	120.0
C5-C6-C7	120.0	C5-C6-H6	120.0
C7-C6-H6	120.0	C6-C7-C8	120.0
C6-C7-H7	120.0	C8-C7-H7	120.0
C7-C8-C3	120.0	C7-C8-N2	134.6(10)
C3-C8-N2	105.4(10)	N2-C9-C10	112.8(13)
N2-C9-P1	100.9(12)	C10-C9-P1	115.9(12)
N2-C9-H9	109.0	C10-C9-H9	109.0
P1-C9-H9	109.0	C11-C10-C9	113.2(11)
C11-C10-H10A	108.9	C9-C10-H10A	108.9
C11-C10-H10B	108.9	C9-C10-H10B	108.9
H10A-C10-H10B	107.7	O1-C11-C10	119.6(13)
O1-C11-C12	120.0(13)	C10-C11-C12	120.4(11)
C13-C12-C17	120.0	C13-C12-C11	121.6(8)
C17-C12-C11	118.4(8)	C14-C13-C12	120.0
C14-C13-H13	120.0	C12-C13-H13	120.0
C13-C14-C15	120.0	C13-C14-H14	120.0
C15-C14-H14	120.0	C16-C15-C14	120.0
C16-C15-H15	120.0	C14-C15-H15	120.0
C15-C16-C17	120.0	C15-C16-H16	120.0
C17-C16-H16	120.0	C16-C17-C12	120.0
C16-C17-H17	120.0	C12-C17-H17	120.0
C19-C18-C23	120.0	C19-C18-P1	118.9(7)
C23-C18-P1	121.1(7)	C20-C19-C18	120.0
C20-C19-H19	120.0	C18-C19-H19	120.0
C19-C20-C21	120.0	C19-C20-H20	120.0
C21-C20-H20	120.0	C22-C21-C20	120.0
C22-C21-H21	120.0	C20-C21-H21	120.0
C23-C22-C21	120.0	C23-C22-H22	120.0
C21-C22-H22	120.0	C22-C23-C18	120.0
C22-C23-H23	120.0	C18-C23-H23	120.0
C25-C24-C29	120.0	C25-C24-P1	122.2(8)
C29-C24-P1	117.6(8)	C24-C25-C26	120.0
C24-C25-H25	120.0	C26-C25-H25	120.0
C27-C26-C25	120.0	C27-C26-H26	120.0
C25-C26-H26	120.0	C28-C27-C26	120.0
C28-C27-H27	120.0	C26-C27-H27	120.0
C27-C28-C29	120.0	C27-C28-H28	120.0
C29-C28-H28	120.0	C28-C29-C24	120.0
C28-C29-H29	120.0	C24-C29-H29	120.0
N4-C30-N3	104.1(14)	N4-C30-Pt2	121.5(12)

N3-C30-Pt2	132.8(12)	N3-C31-H31A	109.5
N3-C31-H31B	109.5	H31A-C31-H31B	109.5
N3-C31-H31C	109.5	H31A-C31-H31C	109.5
H31B-C31-H31C	109.5	N3-C32-C33	130.9(10)
N3-C32-C37	109.0(10)	C33-C32-C37	120.0
C32-C33-C34	120.0	C32-C33-H33	120.0
C34-C33-H33	120.0	C35-C34-C33	120.0
C35-C34-H34	120.0	C33-C34-H34	120.0
C36-C35-C34	120.0	C36-C35-H35	120.0
C34-C35-H35	120.0	C35-C36-C37	120.0
C35-C36-H36	120.0	C37-C36-H36	120.0
N4-C37-C36	134.9(9)	N4-C37-C32	104.9(9)
C36-C37-C32	120.0	N4-C38-C39	111.6(13)
N4-C38-P2	102.0(10)	C39-C38-P2	114.7(13)
N4-C38-H38	109.4	C39-C38-H38	109.4
P2-C38-H38	109.4	C40-C39-C38	112.5(11)
C40-C39-H39A	109.1	C38-C39-H39A	109.1
C40-C39-H39B	109.1	C38-C39-H39B	109.1
H39A-C39-H39B	107.8	O2-C40-C39	119.5(14)
O2-C40-C41	120.8(13)	C39-C40-C41	119.6(11)
C42-C41-C46	120.0	C42-C41-C40	118.5(8)
C46-C41-C40	121.3(9)	C41-C42-C43	120.0
C41-C42-H42	120.0	C43-C42-H42	120.0
C42-C43-C44	120.0	C42-C43-H43	120.0
C44-C43-H43	120.0	C43-C44-C45	120.0
C43-C44-H44	120.0	C45-C44-H44	120.0
C46-C45-C44	120.0	C46-C45-H45	120.0
C44-C45-H45	120.0	C45-C46-C41	120.0
C45-C46-H46	120.0	C41-C46-H46	120.0
C48-C47-C52	120.0	C48-C47-P2	117.7(8)
C52-C47-P2	122.2(8)	C49-C48-C47	120.0
C49-C48-H48	120.0	C47-C48-H48	120.0
C50-C49-C48	120.0	C50-C49-H49	120.0
C48-C49-H49	120.0	C49-C50-C51	120.0
C49-C50-H50	120.0	C51-C50-H50	120.0
C50-C51-C52	120.0	C50-C51-H51	120.0
C52-C51-H51	120.0	C51-C52-C47	120.0
C51-C52-H52	120.0	C47-C52-H52	120.0
C54-C53-C58	120.0	C54-C53-P2	117.3(7)
C58-C53-P2	122.5(7)	C53-C54-C55	120.0
C53-C54-H54	120.0	C55-C54-H54	120.0

C56-C55-C54	120.0	C56-C55-H55	120.0
C54-C55-H55	120.0	C55-C56-C57	120.0
C55-C56-H56	120.0	C57-C56-H56	120.0
C56-C57-C58	120.0	C56-C57-H57	120.0
C58-C57-H57	120.0	C57-C58-C53	120.0
C57-C58-H58	120.0	C53-C58-H58	120.0
N5-C59-N6	104.3(14)	N5-C59-Pt3	132.9(11)
N6-C59-Pt3	121.4(11)	N5-C60-H60A	109.5
N5-C60-H60B	109.5	H60A-C60-H60B	109.5
N5-C60-H60C	109.5	H60A-C60-H60C	109.5
H60B-C60-H60C	109.5	N5-C61-C62	132.2(10)
N5-C61-C66	107.8(10)	C62-C61-C66	120.0
C63-C62-C61	120.0	C63-C62-H62	120.0
C61-C62-H62	120.0	C62-C63-C64	120.0
C62-C63-H63	120.0	C64-C63-H63	120.0
C65-C64-C63	120.0	C65-C64-H64	120.0
C63-C64-H64	120.0	C64-C65-C66	120.0
C64-C65-H65	120.0	C66-C65-H65	120.0
N6-C66-C65	135.0(9)	N6-C66-C61	104.8(9)
C65-C66-C61	120.0	N6-C67-C68	114.5(13)
N6-C67-P3	102.3(10)	C68-C67-P3	115.8(13)
N6-C67-H67	108.0	C68-C67-H67	108.0
P3-C67-H67	108.0	C67-C68-C69	112.3(11)
C67-C68-H68A	109.2	C69-C68-H68A	109.2
C67-C68-H68B	109.2	C69-C68-H68B	109.2
H68A-C68-H68B	107.9	O3-C69-C68	119.5(13)
O3-C69-C70	120.6(13)	C68-C69-C70	119.9(11)
C71-C70-C75	120.0	C71-C70-C69	120.6(8)
C75-C70-C69	119.3(8)	C72-C71-C70	120.0
C72-C71-H71	120.0	C70-C71-H71	120.0
C71-C72-C73	120.0	C71-C72-H72	120.0
C73-C72-H72	120.0	C72-C73-C74	120.0
C72-C73-H73	120.0	C74-C73-H73	120.0
C75-C74-C73	120.0	C75-C74-H74	120.0
C73-C74-H74	120.0	C74-C75-C70	120.0
C74-C75-H75	120.0	C70-C75-H75	120.0
C77-C76-C81	120.0	C77-C76-P3	116.7(8)
C81-C76-P3	123.2(8)	C78-C77-C76	120.0
C78-C77-H77	120.0	C76-C77-H77	120.0
C79-C78-C77	120.0	C79-C78-H78	120.0
C77-C78-H78	120.0	C80-C79-C78	120.0

C80-C79-H79	120.0	C78-C79-H79	120.0
C81-C80-C79	120.0	C81-C80-H80	120.0
C79-C80-H80	120.0	C80-C81-C76	120.0
C80-C81-H81	120.0	C76-C81-H81	120.0
C83-C82-C87	120.0	C83-C82-P3	115.7(7)
C87-C82-P3	124.0(7)	C84-C83-C82	120.0
C84-C83-H83	120.0	C82-C83-H83	120.0
C83-C84-C85	120.0	C83-C84-H84	120.0
C85-C84-H84	120.0	C84-C85-C86	120.0
C84-C85-H85	120.0	C86-C85-H85	120.0
C87-C86-C85	120.0	C87-C86-H86	120.0
C85-C86-H86	120.0	C86-C87-C82	120.0
C86-C87-H87	120.0	C82-C87-H87	120.0

Crystallographic data for compound 142h

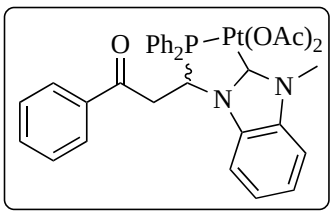

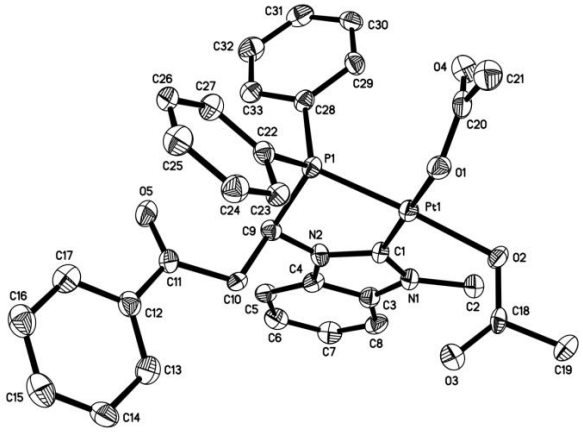

Identification code	leung1213m_0m_5
Chemical formula	$C_{33}H_{33}N_2O_6PPt$
Formula weight	779.67 g/mol
Temperature	100(2) K
Wavelength	0.71073 Å
Crystal size	0.020 x 0.060 x 0.120 mm
Crystal habit	colorless block
Crystal system	triclinic
Space group	P -1
Unit cell dimensions	a = 9.4733(4) Å α = 92.9803(13)°
	b = 10.3270(4) Å β = 95.3637(14)°
	c = 16.6918(7) Å γ = 114.4856(12)°
Volume	1472.17(11) $Å^3$
Z	2
Density (calculated)	1.759 g/cm^3
Absorption coefficient	4.870 mm^{-1}
F(000)	772

Theta range for data collection	2.18 to 31.01°
Reflections collected	9278
Independent reflections	9278 [R(int) = 0.0698]
Coverage of independent reflections	98.6%
Absorption correction	Multi-Scan
Max. and min. transmission	0.9090 and 0.5930

Structure solution technique	direct methods	
Structure solution program	XT, VERSION 2018/2	
Refinement method	Full-matrix least-squares on F^2	
Refinement program	SHELXL-2018/3 (Sheldrick, 2018)	
Function minimized	$\Sigma\ w(F_o^2 - F_c^2)^2$	
Data / restraints / parameters	9278 / 0 / 392	
Goodness-of-fit on F^2	1.031	
Final R indices	7179 data; $I>2\sigma(I)$	R1 = 0.0616, wR2 = 0.1307
	all data	R1 = 0.0923, wR2 = 0.1469
Weighting scheme	$w=1/[\sigma^2(F_o^2)+(0.0573P)^2+6.5008P]$ where $P=(F_o^2+2F_c^2)/3$	
Largest diff. peak and hole	3.292 and -2.039 eÅ^{-3}	
R.M.S. deviation from mean	0.254 eÅ^{-3}	

Bond lengths (Å) of compound 142h

C1-N1	1.353(9)	C1-N2	1.359(9)
C1-Pt1	1.970(7)	C2-N1	1.461(9)
C3-C8	1.388(10)	C3-N1	1.389(9)
C3-C4	1.400(10)	C4-C5	1.380(10)
C4-N2	1.388(9)	C5-C6	1.387(10)
C6-C7	1.399(11)	C7-C8	1.379(11)
C9-N2	1.442(8)	C9-C10	1.525(9)
C9-P1	1.866(7)	C10-C11	1.525(9)
C11-O5	1.215(9)	C11-C12	1.479(10)
C12-C13	1.385(11)	C12-C17	1.423(10)
C13-C14	1.382(11)	C14-C15	1.370(11)
C15-C16	1.372(13)	C16-C17	1.377(11)
C18-O3	1.216(9)	C18-O2	1.297(9)
C18-C19	1.528(10)	C20-O4	1.234(9)
C20-O1	1.304(9)	C20-C21	1.508(10)
C22-C27	1.385(10)	C22-C23	1.402(9)
C22-P1	1.810(7)	C23-C24	1.391(10)
C24-C25	1.374(11)	C25-C26	1.392(11)
C26-C27	1.371(10)	C28-C29	1.384(10)

C28-C33	1.404(10)	C28-P1	1.814(7)
C29-C30	1.392(10)	C30-C31	1.383(11)
C31-C32	1.374(12)	C32-C33	1.378(10)
O1-Pt1	2.067(5)	O2-Pt1	2.071(5)
P1-Pt1	2.2088(17)		

Bond angles (°) of compound 142h

N1-C1-N2	107.0(6)	N1-C1-Pt1	133.5(5)
N2-C1-Pt1	119.6(5)	C8-C3-N1	132.6(7)
C8-C3-C4	120.5(7)	N1-C3-C4	106.9(6)
C5-C4-N2	132.0(7)	C5-C4-C3	122.3(6)
N2-C4-C3	105.7(6)	C4-C5-C6	117.0(7)
C5-C6-C7	121.0(7)	C8-C7-C6	121.8(7)
C7-C8-C3	117.4(7)	N2-C9-C10	112.0(5)
N2-C9-P1	102.9(4)	C10-C9-P1	114.3(5)
C11-C10-C9	111.9(6)	O5-C11-C12	121.9(7)
O5-C11-C10	120.3(6)	C12-C11-C10	117.8(6)
C13-C12-C17	118.8(7)	C13-C12-C11	122.7(7)
C17-C12-C11	118.4(7)	C14-C13-C12	120.1(7)
C15-C14-C13	120.3(7)	C14-C15-C16	121.1(8)
C15-C16-C17	119.8(8)	C16-C17-C12	119.9(7)
O3-C18-O2	126.9(6)	O3-C18-C19	120.8(7)
O2-C18-C19	112.3(6)	O4-C20-O1	124.9(7)
O4-C20-C21	120.5(7)	O1-C20-C21	114.5(7)
C27-C22-C23	119.7(6)	C27-C22-P1	122.7(5)
C23-C22-P1	117.4(5)	C24-C23-C22	119.5(7)
C25-C24-C23	119.4(7)	C24-C25-C26	121.4(7)
C27-C26-C25	119.0(7)	C26-C27-C22	120.9(7)
C29-C28-C33	119.5(6)	C29-C28-P1	118.7(5)
C33-C28-P1	121.5(6)	C28-C29-C30	119.6(7)
C31-C30-C29	120.8(7)	C32-C31-C30	119.2(7)
C31-C32-C33	121.3(8)	C32-C33-C28	119.5(7)
C1-N1-C3	109.9(6)	C1-N1-C2	128.0(6)
C3-N1-C2	122.1(6)	C1-N2-C4	110.5(6)
C1-N2-C9	122.8(6)	C4-N2-C9	126.7(6)
C20-O1-Pt1	121.5(5)	C18-O2-Pt1	117.9(4)
C22-P1-C28	109.6(3)	C22-P1-C9	106.6(3)
C28-P1-C9	102.8(3)	C22-P1-Pt1	116.2(2)
C28-P1-Pt1	118.5(2)	C9-P1-Pt1	101.0(2)

C1-Pt1-O1	176.0(3)	C1-Pt1-O2	95.7(2)
O1-Pt1-O2	84.07(19)	C1-Pt1-P1	82.1(2)
O1-Pt1-P1	97.87(14)	O2-Pt1-P1	176.71(15)

Crystallographic data for compound 143h

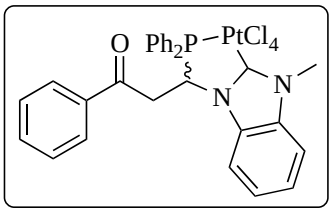

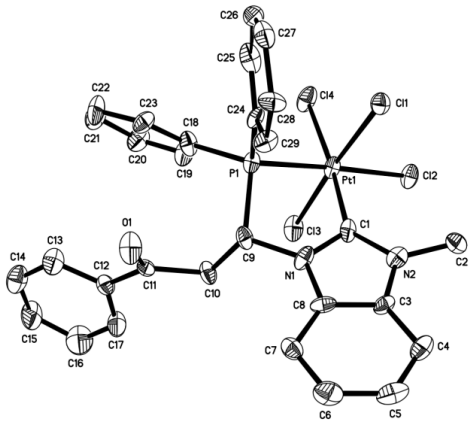

Identification code	leung1223m_0m_5	
Chemical formula	$C_{30}H_{28}Cl_5N_2O_{1.50}PPt$	
Formula weight	843.85 g/mol	
Temperature	100(2) K	
Wavelength	0.71073 Å	
Crystal size	0.010 x 0.100 x 0.140 mm	
Crystal habit	yellow plate	
Crystal system	triclinic	
Space group	P -1	
Unit cell dimensions	a = 8.8283(5) Å	α = 99.7053(19)°
	b = 21.0482(12) Å	β = 96.4985(16)°
	c = 33.6991(17) Å	γ = 90.398(2)°
Volume	6130.5(6) $Å^3$	
Z	8	
Density (calculated)	1.829 g/cm^3	
Absorption coefficient	5.096 mm^{-1}	
F(000)	3296	

Theta range for data collection	1.94 to 29.59°
Reflections collected	35598
Independent reflections	35598 [R(int) = 0.1036]
Coverage of independent reflections	98.2%
Absorption correction	Multi-Scan
Max. and min. transmission	0.9510 and 0.5360
Refinement method	Full-matrix least-squares on F^2

Refinement program	SHELXL-2018/3 (Sheldrick, 2018)	
Function minimized	$\Sigma\ w(F_o^2 - F_c^2)^2$	
Data / restraints / parameters	35598 / 718 / 1521	
Goodness-of-fit on F^2	1.079	
Δ/σ_{max}	0.001	
Final R indices	29335 data; $I>2\sigma(I)$	R1 = 0.0690, wR2 = 0.1309
	all data	R1 = 0.0921, wR2 = 0.1399
Weighting scheme	$w=1/[\sigma^2(F_o^2)+(0.0285P)^2+72.5635P]$ where $P=(F_o^2+2F_c^2)/3$	
Largest diff. peak and hole	3.363 and -4.027 eÅ^{-3}	
R.M.S. deviation from mean	0.272 eÅ^{-3}	

Bond lengths (Å) of compound 143h

C1-N1	1.350(15)	C1-N2	1.359(13)
C1-Pt1	2.009(12)	C2-N2	1.462(15)
C3-C8	1.382(16)	C3-C4	1.382(15)
C3-N2	1.404(14)	C4-C5	1.392(18)
C5-C6	1.387(19)	C6-C7	1.364(17)
C7-C8	1.408(16)	C8-N1	1.391(14)
C9-N1	1.465(13)	C9-C10	1.508(15)
C9-P1	1.867(12)	C10-C11	1.534(15)
C11-O1	1.206(14)	C11-C12	1.483(15)
C12-C17	1.358(18)	C12-C13	1.397(16)
C13-C14	1.403(17)	C14-C15	1.332(19)
C15-C16	1.39(2)	C16-C17	1.39(2)
C18-C23	1.382(16)	C18-C19	1.409(16)
C18-P1	1.812(11)	C19-C20	1.400(16)
C20-C21	1.408(18)	C21-C22	1.380(19)
C22-C23	1.372(16)	C24-C25	1.367(17)
C24-C29	1.392(13)	C24-P1	1.805(11)
C25-C26	1.405(17)	C26-C27	1.379(16)
C27-C28	1.423(17)	C28-C29	1.370(14)
C30-N4	1.353(15)	C30-N3	1.361(14)
C30-Pt2	2.005(12)	C31-N4	1.446(15)
C32-N4	1.373(11)	C32-C33	1.39

C32-C37	1.39	C33-C34	1.39
C34-C35	1.39	C35-C36	1.39
C36-C37	1.39	C37-N3	1.361(10)
C38-N3	1.453(14)	C38-C39A	1.525(17)
C38-C39	1.530(15)	C38-P2	1.877(12)
C39-C40	1.542(19)	C40-O2	1.206(19)
C40-C41	1.497(15)	C41-C42	1.39
C41-C46	1.39	C42-C43	1.39
C43-C44	1.39	C44-C45	1.39
C45-C46	1.39	C39A-C40A	1.54(2)
C40A-O2A	1.204(19)	C40A-C41A	1.498(16)
C41A-C42A	1.39	C41A-C46A	1.39
C42A-C43A	1.39	C43A-C44A	1.39
C44A-C45A	1.39	C45A-C46A	1.39
C47-C48	1.39	C47-C52	1.39
C47-P2	1.806(6)	C48-C49	1.39
C49-C50	1.39	C50-C51	1.39
C51-C52	1.39	C53-C54	1.39
C53-C58	1.39	C53-P2	1.792(10)
C54-C55	1.39	C55-C56	1.39
C56-C57	1.39	C57-C58	1.39
C53A-C54A	1.393(9)	C53A-C58A	1.394(9)
C53A-P2	1.796(9)	C54A-C55A	1.393(9)
C55A-C56A	1.393(9)	C56A-C57A	1.379(9)
C57A-C58A	1.386(9)	C59-N5	1.328(14)
C59-N6	1.354(14)	C59-Pt3	2.051(11)
C60-N6	1.453(14)	C61-C66	1.379(15)
C61-N6	1.395(13)	C61-C62	1.404(14)
C62-C63	1.380(16)	C63-C64	1.413(17)
C64-C65	1.374(15)	C65-C66	1.388(15)
C66-N5	1.409(13)	C67-N5	1.469(12)
C67-C68	1.508(14)	C67-P3	1.858(11)
C68-C69	1.551(15)	C69-O3	1.227(14)
C69-C70	1.484(16)	C70-C75	1.391(17)
C70-C71	1.399(16)	C71-C72	1.390(17)
C72-C73	1.37(2)	C73-C74	1.40(2)
C74-C75	1.389(18)	C76-C77	1.39
C76-C81	1.39	C76-P3	1.791(5)
C77-C78	1.39	C78-C79	1.39
C79-C80	1.39	C80-C81	1.39
C82-C83	1.39	C82-C87	1.39

C82-P3	1.812(5)	C83-C84	1.39
C84-C85	1.39	C85-C86	1.39
C86-C87	1.39	C88-N8	1.336(15)
C88-N7	1.365(14)	C88-Pt4	2.021(11)
C89-N8	1.482(15)	C90-C95	1.350(16)
C90-N8	1.387(14)	C90-C91	1.410(16)
C91-C92	1.391(19)	C92-C93	1.424(18)
C93-C94	1.372(16)	C94-C95	1.389(16)
C95-N7	1.405(14)	C96-N7	1.447(14)
C96-C97	1.536(14)	C96-P4	1.860(10)
C97-C98	1.505(16)	C98-O4	1.209(14)
C98-C99	1.486(16)	C99-C104	1.379(16)
C99-C100	1.407(16)	C100-C101	1.399(15)
C101-C102	1.387(19)	C102-C103	1.37(2)
C103-C104	1.393(19)	C105-C110	1.392(16)
C105-C106	1.400(17)	C105-P4	1.797(11)
C106-C107	1.385(16)	C107-C108	1.40(2)
C108-C109	1.39(2)	C109-C110	1.369(17)
C111-C112	1.382(15)	C111-C116	1.391(16)
C111-P4	1.810(11)	C112-C113	1.362(15)
C113-C114	1.381(18)	C114-C115	1.407(17)
C115-C116	1.387(16)	C117-Cl18	1.746(15)
C117-Cl17	1.767(15)	C118-Cl19	1.744(16)
C118-Cl20	1.774(16)	C119-O5	1.429(17)
C120-O6	1.361(19)	Cl1-Pt1	2.328(3)
Cl2-Pt1	2.376(3)	Cl3-Pt1	2.342(3)
Cl4-Pt1	2.366(3)	Cl5-Pt2	2.318(3)
Cl6-Pt2	2.371(3)	Cl7-Pt2	2.330(3)
Cl8-Pt2	2.391(3)	Cl9-Pt3	2.332(3)
Cl10-Pt3	2.388(3)	Cl11-Pt3	2.376(3)
Cl12-Pt3	2.316(3)	Cl13-Pt4	2.318(3)
Cl14-Pt4	2.372(3)	Cl15-Pt4	2.408(3)
Cl16-Pt4	2.340(3)	P1-Pt1	2.300(3)
P2-Pt2	2.289(3)	P3-Pt3	2.289(3)
P4-Pt4	2.288(3)		

Bond angles (°) of compound 143h

N1-C1-N2	107.2(10)	N1-C1-Pt1	119.0(7)
N2-C1-Pt1	133.8(8)	C8-C3-C4	122.2(11)

C8-C3-N2	107.2(9)	C4-C3-N2	130.6(11)
C3-C4-C5	115.3(11)	C6-C5-C4	122.2(11)
C7-C6-C5	123.0(11)	C6-C7-C8	115.0(11)
C3-C8-N1	106.0(10)	C3-C8-C7	122.3(10)
N1-C8-C7	131.8(11)	N1-C9-C10	114.7(10)
N1-C9-P1	104.2(7)	C10-C9-P1	115.9(8)
C9-C10-C11	110.7(9)	O1-C11-C12	121.3(10)
O1-C11-C10	119.5(10)	C12-C11-C10	119.2(10)
C17-C12-C13	118.7(11)	C17-C12-C11	122.1(11)
C13-C12-C11	119.0(10)	C12-C13-C14	119.6(12)
C15-C14-C13	120.8(12)	C14-C15-C16	119.8(13)
C17-C16-C15	119.7(15)	C12-C17-C16	121.0(13)
C23-C18-C19	120.7(10)	C23-C18-P1	118.4(8)
C19-C18-P1	120.8(9)	C20-C19-C18	118.1(11)
C19-C20-C21	120.5(12)	C22-C21-C20	119.1(11)
C23-C22-C21	121.0(12)	C22-C23-C18	120.2(11)
C25-C24-C29	120.6(10)	C25-C24-P1	117.4(8)
C29-C24-P1	122.0(8)	C24-C25-C26	119.4(10)
C27-C26-C25	120.6(11)	C26-C27-C28	119.3(10)
C29-C28-C27	119.0(10)	C28-C29-C24	121.0(10)
N4-C30-N3	106.8(10)	N4-C30-Pt2	133.8(8)
N3-C30-Pt2	119.2(9)	N4-C32-C33	133.6(6)
N4-C32-C37	106.4(6)	C33-C32-C37	120.0
C34-C33-C32	120.0	C33-C34-C35	120.0
C34-C35-C36	120.0	C37-C36-C35	120.0
N3-C37-C36	132.8(6)	N3-C37-C32	107.0(6)
C36-C37-C32	120.0	N3-C38-C39A	114.4(18)
N3-C38-C39	116.1(11)	N3-C38-P2	103.8(7)
C39A-C38-P2	121.(2)	C39-C38-P2	112.1(10)
C38-C39-C40	111.2(12)	O2-C40-C41	121.5(13)
O2-C40-C39	118.7(13)	C41-C40-C39	119.6(13)
C42-C41-C46	120.0	C42-C41-C40	117.4(9)
C46-C41-C40	122.6(9)	C41-C42-C43	120.0
C42-C43-C44	120.0	C45-C44-C43	120.0
C46-C45-C44	120.0	C45-C46-C41	120.0
C38-C39A-C40A	108.(2)	O2A-C40A-C41A	122.0(17)
O2A-C40A-C39A	119.5(17)	C41A-C40A-C39A	117.7(16)
C42A-C41A-C46A	120.0	C42A-C41A-C40A	118.4(11)
C46A-C41A-C40A	121.6(12)	C41A-C42A-C43A	120.0
C42A-C43A-C44A	120.0	C45A-C44A-C43A	120.0
C44A-C45A-C46A	120.0	C45A-C46A-C41A	120.0

C48-C47-C52	120.0	C48-C47-P2	115.9(4)
C52-C47-P2	123.4(4)	C47-C48-C49	120.0
C50-C49-C48	120.0	C51-C50-C49	120.0
C50-C51-C52	120.0	C51-C52-C47	120.0
C54-C53-C58	120.0	C54-C53-P2	120.9(16)
C58-C53-P2	119.1(16)	C55-C54-C53	120.0
C54-C55-C56	120.0	C57-C56-C55	120.0
C56-C57-C58	120.0	C57-C58-C53	120.0
C54A-C53A-C58A	120.2(9)	C54A-C53A-P2	120.3(12)
C58A-C53A-P2	119.4(12)	C53A-C54A-C55A	120.8(10)
C54A-C55A-C56A	119.0(10)	C57A-C56A-C55A	119.2(10)
C56A-C57A-C58A	122.4(10)	C57A-C58A-C53A	118.0(10)
N5-C59-N6	108.1(9)	N5-C59-Pt3	119.2(8)
N6-C59-Pt3	132.0(8)	C66-C61-N6	108.3(9)
C66-C61-C62	120.9(10)	N6-C61-C62	130.8(10)
C63-C62-C61	115.5(11)	C62-C63-C64	123.2(10)
C65-C64-C63	120.7(11)	C64-C65-C66	116.0(10)
C61-C66-C65	123.7(10)	C61-C66-N5	104.5(9)
C65-C66-N5	131.7(10)	N5-C67-C68	113.1(8)
N5-C67-P3	103.4(7)	C68-C67-P3	115.8(7)
C67-C68-C69	112.5(9)	O3-C69-C70	121.8(10)
O3-C69-C68	118.6(10)	C70-C69-C68	119.6(10)
C75-C70-C71	120.5(11)	C75-C70-C69	121.4(11)
C71-C70-C69	118.0(11)	C72-C71-C70	119.1(12)
C73-C72-C71	119.9(13)	C72-C73-C74	121.4(13)
C75-C74-C73	118.9(14)	C74-C75-C70	119.7(13)
C77-C76-C81	120.0	C77-C76-P3	117.8(4)
C81-C76-P3	121.9(4)	C76-C77-C78	120.0
C79-C78-C77	120.0	C78-C79-C80	120.0
C79-C80-C81	120.0	C80-C81-C76	120.0
C83-C82-C87	120.0	C83-C82-P3	126.2(4)
C87-C82-P3	113.5(4)	C84-C83-C82	120.0
C85-C84-C83	120.0	C84-C85-C86	120.0
C87-C86-C85	120.0	C86-C87-C82	120.0
N8-C88-N7	107.3(10)	N8-C88-Pt4	133.7(9)
N7-C88-Pt4	118.3(8)	C95-C90-N8	109.2(10)
C95-C90-C91	122.9(11)	N8-C90-C91	127.7(11)
C92-C91-C90	113.7(12)	C91-C92-C93	123.4(11)
C94-C93-C92	120.2(11)	C93-C94-C95	116.3(11)
C90-C95-C94	123.4(11)	C90-C95-N7	105.3(10)
C94-C95-N7	131.3(10)	N7-C96-C97	115.7(9)

N7-C96-P4	106.4(7)	C97-C96-P4	116.6(8)
C98-C97-C96	111.5(9)	O4-C98-C99	120.6(10)
O4-C98-C97	119.6(10)	C99-C98-C97	119.7(10)
C104-C99-C100	120.4(11)	C104-C99-C98	122.6(11)
C100-C99-C98	117.0(10)	C101-C100-C99	118.7(11)
C102-C101-C100	120.4(11)	C103-C102-C101	120.1(11)
C102-C103-C104	120.7(13)	C99-C104-C103	119.7(13)
C110-C105-C106	119.4(11)	C110-C105-P4	124.9(10)
C106-C105-P4	115.5(9)	C107-C106-C105	120.3(12)
C106-C107-C108	119.8(13)	C109-C108-C107	119.3(12)
C110-C109-C108	120.8(13)	C109-C110-C105	120.3(13)
C112-C111-C116	121.1(10)	C112-C111-P4	118.8(9)
C116-C111-P4	120.0(9)	C113-C112-C111	119.9(11)
C112-C113-C114	120.9(11)	C113-C114-C115	119.1(11)
C116-C115-C114	120.4(11)	C115-C116-C111	118.4(11)
Cl18-C117-Cl17	111.2(8)	Cl19-C118-Cl20	112.5(7)
C1-N1-C8	110.7(9)	C1-N1-C9	124.7(9)
C8-N1-C9	123.8(10)	C1-N2-C3	108.9(9)
C1-N2-C2	129.1(10)	C3-N2-C2	121.9(9)
C37-N3-C30	109.8(9)	C37-N3-C38	124.4(8)
C30-N3-C38	125.3(9)	C30-N4-C32	109.8(9)
C30-N4-C31	129.0(10)	C32-N4-C31	121.1(9)
C59-N5-C66	110.7(9)	C59-N5-C67	125.2(9)
C66-N5-C67	123.5(9)	C59-N6-C61	108.3(9)
C59-N6-C60	130.3(9)	C61-N6-C60	121.5(9)
C88-N7-C95	109.5(9)	C88-N7-C96	124.7(10)
C95-N7-C96	125.2(9)	C88-N8-C90	108.8(10)
C88-N8-C89	128.8(10)	C90-N8-C89	122.4(10)
C24-P1-C18	105.9(5)	C24-P1-C9	105.9(5)
C18-P1-C9	108.1(5)	C24-P1-Pt1	113.4(4)
C18-P1-Pt1	121.9(4)	C9-P1-Pt1	100.4(4)
C53-P2-C47	111.1(11)	C53A-P2-C47	103.1(9)
C53-P2-C38	102.6(12)	C53A-P2-C38	107.7(9)
C47-P2-C38	106.6(4)	C53-P2-Pt2	109.9(13)
C53A-P2-Pt2	114.3(10)	C47-P2-Pt2	123.0(3)
C38-P2-Pt2	101.1(4)	C76-P3-C82	106.4(3)
C76-P3-C67	106.7(4)	C82-P3-C67	105.0(4)
C76-P3-Pt3	112.1(3)	C82-P3-Pt3	123.4(2)
C67-P3-Pt3	101.8(3)	C105-P4-C111	107.5(5)
C105-P4-C96	106.4(5)	C111-P4-C96	105.4(5)
C105-P4-Pt4	121.2(4)	C111-P4-Pt4	114.2(4)

C96-P4-Pt4	100.5(3)	C1-Pt1-P1	81.0(3)
C1-Pt1-Cl1	90.5(3)	P1-Pt1-Cl1	92.64(10)
C1-Pt1-Cl3	88.2(3)	P1-Pt1-Cl3	90.75(10)
Cl1-Pt1-Cl3	176.15(10)	C1-Pt1-Cl4	174.4(3)
P1-Pt1-Cl4	93.45(10)	Cl1-Pt1-Cl4	90.66(11)
Cl3-Pt1-Cl4	90.95(12)	C1-Pt1-Cl2	97.1(3)
P1-Pt1-Cl2	177.55(11)	Cl1-Pt1-Cl2	88.95(10)
Cl3-Pt1-Cl2	87.60(10)	Cl4-Pt1-Cl2	88.39(10)
C30-Pt2-P2	81.8(4)	C30-Pt2-Cl5	87.6(3)
P2-Pt2-Cl5	94.54(10)	C30-Pt2-Cl7	91.2(3)
P2-Pt2-Cl7	88.61(10)	Cl5-Pt2-Cl7	176.41(11)
C30-Pt2-Cl6	171.4(3)	P2-Pt2-Cl6	91.00(11)
Cl5-Pt2-Cl6	88.38(11)	Cl7-Pt2-Cl6	93.29(11)
C30-Pt2-Cl8	98.5(4)	P2-Pt2-Cl8	175.43(10)
Cl5-Pt2-Cl8	90.03(11)	Cl7-Pt2-Cl8	86.82(11)
Cl6-Pt2-Cl8	89.12(11)	C59-Pt3-P3	80.6(3)
C59-Pt3-Cl12	88.2(3)	P3-Pt3-Cl12	94.43(10)
C59-Pt3-Cl9	92.8(3)	P3-Pt3-Cl9	88.41(10)
Cl12-Pt3-Cl9	177.12(10)	C59-Pt3-Cl11	171.2(3)
P3-Pt3-Cl11	91.58(10)	Cl12-Pt3-Cl11	88.44(10)
Cl9-Pt3-Cl11	90.98(10)	C59-Pt3-Cl10	98.5(3)
P3-Pt3-Cl10	175.97(10)	Cl12-Pt3-Cl10	89.45(10)
Cl9-Pt3-Cl10	87.72(10)	Cl11-Pt3-Cl10	89.59(9)
C88-Pt4-P4	82.9(3)	C88-Pt4-Cl13	87.8(3)
P4-Pt4-Cl13	94.72(10)	C88-Pt4-Cl16	89.0(3)
P4-Pt4-Cl16	87.68(10)	Cl13-Pt4-Cl16	175.75(11)
C88-Pt4-Cl14	170.9(3)	P4-Pt4-Cl14	89.46(11)
Cl13-Pt4-Cl14	87.89(11)	Cl16-Pt4-Cl14	95.64(10)
C88-Pt4-Cl15	98.2(3)	P4-Pt4-Cl15	174.83(10)
Cl13-Pt4-Cl15	90.36(10)	Cl16-Pt4-Cl15	87.30(11)
Cl14-Pt4-Cl15	89.80(11)		